Department of Civil Engineering
University of Strathclyde

A PENALTY-FREE MULTI-OBJECTIVE EVOLUTIONARY OPTIMIZATION APPROACH FOR THE DESIGN AND REHABILITATION OF WATER DISTRIBUTION SYSTEMS

Thesis submitted in accordance with the requirements of
the University of Strathclyde
for the degree of

Doctor in Philosophy

by

CALVIN SIEW YEW MING

December 2011

Signed: CALVIN SIEW YEW MING

Date: 21 DECEMBER 2011

A PENALTY-FREE MULTI-OBJECTIVE EVOLUTIONARY OPTIMIZATION APPROACH FOR THE DESIGN AND REHABILITATION OF WATER DISTRIBUTION SYSTEMS

Calvin Siew Yew Ming

ABSTRACT

As a result of the increasing emphasis placed on water companies to conform to the stringent performance standards in supplying demands within a constrained financial budget, the application of optimization has inevitably become an integral part of managing a water distribution system (WDS) right from the initial phase of designing a new system to the latter stage of the network where rehabilitation and upgrading works are a necessity. This also includes the on-going operation of the WDS in particular the minimization of energy costs related to pumping and storage. This thesis is concerned with the development and application of a new multi-objective genetic algorithm in optimizing the design, operation and long term rehabilitation and upgrading of the WDS.

The novelty and originality of the work done as part of this research are presented next.

A seamless, augmented version of the renowned EPANET 2 with pressure dependent analysis (PDA) functionality has been developed. It integrates within the hydraulic engine a continuous nodal pressure-flow function coupled with a line search and backtracking procedure which greatly enhances the algorithm's overall convergence rate and robustness. The hydraulic simulator is termed "EPANET-PDX" (pressure-dependent extension) herein and is capable of effectively modelling networks under pressure deficient situations which the demand driven analysis based EPANET 2 fails to accurately analyse. In terms of computational efficiency, the performance of EPANET-PDX compares very favourably to EPANET 2. Simulations of real life networks consisting of multiple sources, pipes, valves and pumps were successfully executed with no convergence complications. The simulator depicts excellent modelling performance while analysing both normal and abnormal operating conditions of the WDSs. The accuracy of the generated PDA results has been explicitly validated and verified.

An optimization model for the optimal design and upgrading of WDS involving both the operation of multiple pumps and the sizing and location of multiple tanks is developed. The model couples a new boundary convergent multi-objective genetic algorithm to the highly efficient EPANET-PDX simulator which, inherently, automatically accounts for the node pressure constraints as well as the conservation of mass and energy. With accurate PDA, the direct application of the standard extended period simulation enables pump scheduling and tank sizing and siting to be seamlessly incorporated into the optimization without the need for any extraneous methodology or manual intervention. The significant advantage of this model is that it eliminates the need for ad-hoc penalty functions, additional "boundary search" parameters, or special constraint handling procedures. No operator intervention, parameter calibration and trial runs are required. Conceptually, the approach is straightforward and probably the simplest hitherto. The model is applied to several

benchmark networks yielding superior results in terms of the initial network construction cost and the number of hydraulic simulations required.

The above-mentioned optimization model is extended to form a module for the optimal long term design, upgrading and rehabilitation of WDSs. The multi-criteria problem is set up in a multi-objective frame work i.e. to minimize the capital cost, rehabilitation and upgrading costs, whilst maximizing the network hydraulic performance. A straightforward approach for incorporating reliability measures without further complicating the optimization formulation is utilised and its robustness validated. The effect of deterioration of both the structural integrity and hydraulic capacity of pipes over time is explicitly modelled. The model automatically determines the most cost effective strategy which includes the identification of pipes to be upgraded, the upgrading or rehabilitation options and the timing for the upgrade to be implemented. A real life network in Wobulenzi (Uganda) is used to demonstrate the effectiveness of the model. Results obtained demonstrated major improvements over previous work using the classical linear programming.

ACKNOWLEGEMENT

I am extremely thankful and grateful to God for helping me accomplish my PhD research. Without His help, I would not have made it this far.

I would like to extend my utmost gratitude to my supervisor, Dr. Tiku Tanyimboh, who has patiently and meticulously guided me step by step throughout this study. His passion for research has greatly motivated me to strive for excellence in my work. I am also tremendously thankful to my second supervisor, Dr. James Lim who played a major role in helping me obtain the Overseas Research Students' Award Scheme and Strathclyde university scholarships.

In addition, I would like to thank the British Government (Overseas Research Students' Award Scheme), the University of Strathclyde and the UK Engineering and Physical Sciences Research Council under Grant Number EP/G055564/1 for funding my PhD programme.

My most sincere and heartfelt gratitude goes to my beloved father, Aaron Siew and mother, Ang Saw Hoon who faithfully prayed for me and gave me strong parental support and invaluable advice during difficult times; and to both my dear sister, Adeline Siew and brother, Eugene Siew for their encouragement. Also, I want to thank Henry Eyoh, Su Yin and Daniel Eyoh for showering me with much care and kindness, and treating me as family throughout my stay in Glasgow.

Finally, I would like to thank my friends, Anna Czajkowska, Alemtsehay Seyoum, Euan Barlow, Salah Saleh, and most of all Upaka Rathnayake for always being available and so very helpful in many ways. They created such a conducive working environment in which I could effectively and enjoyably carry out my research.

DEDICATION

This thesis is dedicated to my father, Aaron Siew, mother, Ang Saw Hoon, sister, Adeline Siew and brother, Eugene Siew.

TABLE OF CONTENTS

LIST OF FIGURES

Chapter Five

Chapter Six

Chapter Seven

Chapter Eight

LIST OF TABLES

Chapter Seven

Chapter Eight

Appendix A

Appendix B

Appendix C

Appendix D

Appendix E

NOTATION

α_i	parameter to be calibrated (Logit function)
β_i	parameter to be calibrated (Logit function)
β_τ	product of a discount factor $(1+r)^{-v}$ and price increase factor $(1+c)^{v}$
$\underline{\Delta H}^{(k)}$	vector of the nodal heads corrections
ΔQp	loop-flow corrections
Δt	time step between the current and the next steady state simulation
Δt_h	user defined hydraulic time step
ΔV_m	change of water volume in tank m
∇G	gradient of G
γ	specific weight of water
γ_{br}	empirical break repair coefficient
γ_p	parallel pipe cost constant
γ_r	replaced pipe cost constant
λ	over-relaxation coefficient for the line search and backtracking routine
$\lambda_{\min}$	minimum over-relaxation coefficient line search and backtracking routine
ω	dimensionless conversion factor used in the Hazen-Williams head loss equation (equals to 10.67 in S.I. units)
Φ	empirical break repair exponent
τ	design phase
δHn	full Newton step for the nodal heads
δQp	full Newton step for the pipe flows
ψ	step-length adjustment parameter
age_{ij}	number of years since installation of pipe ij
a_{ij}	roughness growth rate (mm/ year)
a_l	mechanical reliability of link l
a_{o}	pump characteristics curve coefficient
A_{10}	incidence matrix relating the pipes to nodes with known heads

A_{11}	diagonal matrix head loss in links
A_{12}	incidence matrix relating the pipes to nodes with unknown heads
A_{22}	diagonal matrix whose elements are $Qn(Hn)/Hn$
b	annual compound interest rate for the capital borrowed
b_o	pump characteristics curve coefficient
$Benefit(i)$	network benefit resulting from solution i
B_m	set of links connected to tank m
c	inflation rates in construction cost
c_o	pump characteristics curve coefficient
c_p	parallel pipe cost constant
c_r	replaced pipe cost constant
$C_\tau(s_\tau,r_\tau)$	cost of adding capacity r_τ in each design phase τ
CB_{ij}	repair cost per break
CEND	cost-entropy non-dominated
CFND	cost-failure tolerance non-dominated
$C_{ij}(t)$	Hazen-Williams roughness coefficient for pipe ij in year t
C_j	Hazen-Williams roughness coefficient for pipe j
CL	pipe cleaning and lining
C_{net}	network cost
$C_{net}^{\max}$	the maximum network cost in the population
$Cost$	overall cost of a solution in the population
$Cost^{max}$	the highest overall cost in the population
$Cost_i$	cost for pipe i
CR	cost ratio
CRND	cost-reliability non-dominated
$C_{total}(i)$	total cost including energy consumption, pipe rehabilitation and new tanks
dE	pipe head loss conservation equation
dHn	corrective steps of nodal head
d_o	pump characteristics curve coefficient
dq	flow conservation equation
dQp	corrective steps of pipe flow
DDA	demand driven analysis

DF	demand factor
D_{ij}	internal diameter of pipe respectively
D_{11}	derivative of A_{11} and its elements
DGR	percentage annual rate of increase of the base demand
$DF_i(t)$	nodal demand factors
DSR	demand satisfaction ratio
DSR_{crit}	demand satisfaction ratio of the most critical node
DSR_t	network DSR at the t^{th} hydraulic time step
e_{0ij}	initial roughness (mm) at time of installation for pipe ij
EA	evolutionary algorithm
EPS	extended period simulation
E_f	set of links connected to reservoir f
f_{ij}	dimensionless friction factor which is dependent on the pipe roughness and flow rate
$f1$	cost of pipelines including pipe installation, paralleling, replacement and repair costs.
$f2$	indirect cost of setting up construction plant and machinery and is assumed to be incurred at the start of each phase
$f3$	costs that vary depending on the magnitude of the capacity installed
$f1_a$	costs of new pipelines
$f1_b$	costs of parallel pipelines
$f1_c$	cost of pipelines replacement
$\underline{F}$	vector of respective functions of the nodal continuity equations
$FCF(LU_{ij})$	failure cost factor for land use, LU_{ij}, for pipe ij
FT	failure tolerance
F_j	continuity equation for node j
F_1	first objective function
F_2	second objective function
GA	genetic algorithm
GGM	global gradient method
h_{ij}	head loss in pipe ij
h_0	shutoff head of the pump
$\underline{H}$	vector of unknown nodal heads

HDGM	head dependent gradient method
HFT	hydraulic feasibility test
HGL	hydraulic gradient level
Hn	nodal heads
Hn_i	head at node i
H_p	additional head supplied by the pump
Hn_{prv}	pre-set downstream pressure of the pressure reducing valve
Hn_{psv}	pre-set upstream pressure of the pressure sustaining valve
Hn_i^t	pressure threshold above which the nodal flow is independent of the pressure
H_0	known nodal heads
IJ	set of all the links in the network
IJ_{lp}	set of all links in loop lp
J	Jacobian
$J(t)_{ij}$	break rate (breaks/km/year) in year t.
K_{ij}	resistance coefficient for link ij
l_{ij}	length of link ij
lp	loop
lp_{ij}	loops sharing link ij
L_{ij}	length of pipe
LP	linear programming
LPG	linear programming gradient method
LU_{ij}	land use for pipe ij
m_o	pump characteristics curve coefficient
MRI	modified resilience index
nc	flow exponent and takes the value of 1.852
n_p	domination count (the number of solutions that dominate p)
N	population size
ND_i	set of all pipe flows emanating from node i
NDF	non-dominated front
Nl	number of links
Nlp	number of loops in a network
NL	number of loading conditions
NLP	non-linear programming

Nn	number of nodes
NP	installation of new pipes
NR	network resilience
N_s	number of source nodes
NS	number of hydraulic time steps involved in the relevant loading condition
NT	number of tanks
$p(0)$	probability that the network is fully connected and no pipe is out of service
P_i	fraction of the total flow through the network that reaches node i
PC	pipe closure
PDA	pressure dependent analysis
PFMOEA	Penalty-Free Multi-Objective Evolutionary Algorithm
PP	pipe paralleling
PRV	pressure reducing valve
PSV	pressure-sustaining valve
Q_{inst}	installed capacity in a design phase in *l/s*
Qn	total actual flow
$Qn_i^{base}(t)$	base demands for node i at time t
Qn_i^{req}	required supply at node i
Qp	pipe flow
Qp_{ij}	pipe flow in link ij
$Qp_b(t)$	flow rates of links connected to tank m respectively
$Qp_f(t)$	flow rates of links connected to reservoir f
Q_{pu}	flow delivered by the pump
$QR_f(t)$	flow rates of reservoir f
$QT_m(t)$	flow rates of tank m
Q_{0j}^{req}	base demand for node j
r	discount rates in construction cost
r_τ	added network capacity in each phase τ
REP_{ij}	repair costs of these new pipes
RI	resilience index
s_τ	existing network capacity at the beginning of phase τ
S	network entropy value

SHV	source head variation
S_i	entropy of node i
S_p	a set of solutions which is dominated by solution p
SSS	steady state simulation
S_0	entropy of source supplies
v	number of years preceding a design phase
VC	installed capacity cost coefficient
VE	installed capacity exponent
V_f	volume of water from reservoir f
$V_f(t)$	water volumes of reservoirs
$V_m(t)$	water volumes of tanks
t	time
t_b	time from which a pipe starts to incur repair costs
tr	last year of a given design phase
t^r	time at which the status change occurs is recorded
ts	first year of a given design phase
TRR	tank replenishment ratio
TUR	tank utilisation ratio
$T1$	minimum duration (years) for Phase I
$T2$	maximum duration (years) for Phase I

CHAPTER ONE

INTRODUCTION

1.1 BACKGROUND

The design of a water distribution system (WDS) has always been and will undoubtedly remain a field of great interest and challenge to engineers. In reality, designing a cost effective WDS to optimally meet the required performance standard (e.g. sufficient water with adequate pressure for customers with demand uncertainty taken into consideration; maintaining disinfection level of drinking water; adequate water storage for fire-fighting purposes etc) is a multi-criteria problem of high complexity. Given that the decision variables involved are discrete (e.g. commercially available pipe sizes), this combinatorial optimization problem is classified as non-deterministic polynomial-time (NP) hard, which means that it is practically impossible to obtain an optimal design using a rigorous algorithm. The non-linear hydraulic equations along with pump curve characteristics involved make the optimization problem a highly non-linear one. Due to the pressure constraints implemented, the feasible solution space of the problem is highly constrained and discontinuous, setting great limitations to the application of the classical mathematical programming. Stochastic methods such as evolutionary algorithms (EAs) on the other hand are well suited in tackling these types of problems. However, a major disadvantage of these meta-heuristic methods is their inability to directly handle constraints.

An efficient and adequate constraint-handling technique is a key element in the design of competitive EAs to solve the complex and highly constrained WDS optimization problem. The widely used penalty methods have been profoundly criticized for their penalty parameters involved which are ad-hoc and case sensitive. In general, the

effective use of these parameters requires expert experience along with time consuming fine tunings and calibrations. Several researchers have attempted to develop techniques to handle WDS constraints effectively without relying on penalty parameters whilst simultaneously focusing the EA search on boundary solutions (Wu and Walski, 2005; Afshar and Marino, 2007; Farmani and Wright, 2003) to speed up the convergence process. However, though termed as "parameter-free" and "self-adaptive penalty methods", most of these techniques still fall short in effectively eradicating the need for parameters. This thesis proposes a new boundary convergent genetic algorithm which entirely eliminates the reliance on penalty methods in handling constraints.

A well designed WDS is capable of meeting current standards of quantity, quality and pressure in the water supplied to consumers. Nevertheless, as years go by, the network is not likely to cope with the significant increase in demand from population growth and industrial development. Along with this, the structural integrity of the network deteriorates from the years of pipe internal erosion, leading to pipe leaks and bursts. Encrustation build up in pipes causes the network to experience a decline in its hydraulic capacity, resulting in increased head losses, low water supply with insufficient pressure as well as water quality problems. Therefore, periodic rehabilitation and/ or upgrading of the system is crucial to reinforce its structural integrity and maintain a good service performance in meeting both current and future demands.

The rehabilitation and upgrading of a WDS involves a great amount of capital. Hence, the optimization of factors such as the phasing, timing and magnitude of the upgrading with regard to cost is an essential necessity. There are several models developed to address this problem based on diverse approaches. These models can be categorized into three main groups. The first group consists of models based predominantly on network economics that identify optimum water pricing and capacity expansion policies for water supply but do not address the structural and hydraulic integrity (Dandy et al., 1985). The second group are individual asset-based models that impart rehabilitation and upgrading decisions for individual components without considering network hydraulics (Shamir and Howard, 1979; Loganathan et al., 2002). The third group is known as the system-wide models that incorporate

budget constraints and consider network hydraulics and performance explicitly (Halhal et al., 1997; Dandy and Engelhardt, 2001). The models in the third category are rather complex but still lacking in terms of addressing the deterioration of hydraulic capacity of pipes and the timing of rehabilitation explicitly. To achieve an optimal WDS upgrade and rehabilitation in a holistic manner, vital aspects such as the deterioration of the system's structural and hydraulic integrity, network hydraulics, timing of rehabilitation and network performance have to be simultaneously considered, as carried out in this thesis.

Instead of solely focusing on cost minimization, the performance of the network with regards to reliability is also a vital aspect to be considered in the optimization process. This is especially essential for an aging network which is prone to encounter frequent incidences of failure to cope with abnormal operating conditions like fire demands; broken pipes, and pump failures. Such incidences are bound to have a significant impact on the performance of the system. Reliability, in general, measures the performance of the network in the events of mechanical and hydraulic failure. A comprehensive measure of network reliability involves failure simulations for each pipe which will be extremely prohibitive computationally if implemented within an EA optimization procedure which involves numerous solutions. As such, surrogate measures are frequently used to gauge the reliability of the WDS, i.e. resilience index (Todini, 2000), network resilience (Prasad and Park, 2004), statistical entropy (Tanyimboh and Templeman, 1993), etc. To date, entropy has demonstrated to be one of the most robust and consistent surrogate measures for the reliability measure. Its formulation is straightforward and can be easily computed. For these reasons, it has been implemented within the optimization formulation in this research.

The WDS hydraulic analysis has become an extensively used engineering tool for water utilities applications. Engineers are able to expediently model a network and have it analysed from aspects such as performance, water quality, operation etc. In the aspect of network design optimization, the hydraulic model is usually coupled to the EA model to evaluate the solutions obtained. Unfortunately, stochastic natured EAs generate a large number of infeasible solutions which are pressure deficient. An accurate network performance assessment of solutions is essential in guiding the search towards the optimal solution effectively and efficiently. Conventional

hydraulic analysis, known as demand driven analysis (DDA) is incapable of accurately simulating pressure deficient solutions as it assumes that all nodal demands are satisfied in full regardless of the pressure. It produces misleading results that tends to underestimate the performance of pressure deficient networks and as such could misguide the EA search in the wrong direction. The performance of solutions can only be accurately assessed by explicitly taking into account the relationship between nodal flows and pressure. This method of analysis is known as the pressure dependent analysis (PDA).

However, in both fields of research and industry, DDA based hydraulic simulation models (e.g. the public domain EPANET 2) are still highly preferred due to their rapid convergence rate. Many shy away from PDA, having the impression that it is far more expensive computationally and would impose adverse effects on the overall computational time. The development of PDA algorithms that are robust and efficient has thus become a pressing issue. This thesis bursts this false intuition by developing and presenting a highly robust and efficient PDA model.

1.2 SCOPE OF THE PRESENT RESEARCH

The goal of this research is to develop a practical, versatile tool that can be effectively and efficiently utilised for various aspects of WDS optimization. Constraint handling within the EA is addressed in a comprehensive manner. The present work aims to demonstrate the strength and simplicity of handling WDS pressure constraints without penalty parameters within the EA. The study covers two extensively researched aspects of WDS optimization which have been proven to be tremendously well challenging, i.e. 1) the design and rehabilitation optimization considering multiple operating conditions, pump scheduling, tank sizing and siting and 2) the long-term rehabilitation and upgrading of WDS. The research touched on surface the aspect of network reliability and redundancy involving the implementation of statistical entropy as the surrogate measure and has been only applied to the long term upgrading and rehabilitation optimization study.

Another major aspect of the research is to demonstrate the superiority of PDA as opposed to the conventional DDA in analyzing pressure deficient network. The study has been conducted using EPANET-PDX (pressure dependent extension) which is an enhanced version of EPANET 2 capable of PDA. This simulator has been developed here and demonstrated to be virtually as reliable and efficient as the original DDA based EPANET 2. EPANET-PDX has been extensively tested addressing most of the real life features in networks such as the existence of valves, pumps, multiple tanks and reservoirs along with the variation in demands, multiple operating conditions involving the application extended period simulation and has remained highly robust and consistent in performance.

1.3 OBJECTIVES OF THE RESEARCH

1) To effectively develop a robust boundary convergent EA model which effectively handles constraints without the requirement for penalty parameters and apply it to various aspects of the WDS optimization i.e. design, operation and long term rehabilitation and upgrade of WDS.

2) To develop a highly reliable and efficient hydraulic simulator that is capable of PDA and equipped with the full hydraulic and water quality functionality (such as extended period simulation, modelling of other hydraulic components such as pumps, valves and tanks, water age, chlorine decay, etc) with the motivation of embedding it within a EA to enable an accurate performance assessment of solutions generated. It is worth mentioning that the current research does not cover the aspects of water quality. However, a supplementary study (independent from this research) has been carried out to evaluate the difference between PDA and DDA results in analysing the water quality of a pressure deficient network. It demonstrated the capability of the developed PDA simulator to accurately model water quality. Interested readers can refer to Seyoum et al. (2011).

3) To evaluate the robustness, computational performance and practical capability of both the PDA simulator and EA optimization model by applying them to hypothetical and real-life networks.

1.4 A BRIEF DESCRIPTION OF THE METHODOLOGY

This thesis presents a new penalty-free multi-objective evolutionary approach (PFMOEA) for the optimization of WDSs which completely eliminates the need for ad-hoc penalty functions, additional "boundary search" parameters, or special constraint handling procedures. The proposed approach utilizes PDA to develop a multi-objective evolutionary search. PDA accurately simulates both feasible and infeasible networks and provides the actual nodal outflow results which serve as brilliant performance indicators. Formulating the total nodal flows as an objective to be maximized ensures that all nodal demands are satisfied. Hence, the EA search is efficiently guided toward the region of feasible solutions in a "penalty-free" manner.

The PFMOEA model consists of two separate interactive modules which are the Multi-Objective GA (MOGA) and the PDA hydraulic simulator. Both modules are seamlessly coupled together in that data transfer between modules is fully automatic with no manual intervention required. The MOGA is used to obtain the optimal solutions (e.g. the least cost solutions along with the timing and magnitude of the long term upgrading strategy). The hydraulic simulator is used to evaluate the performance and feasibility of the generated solutions which will then be formulated as an objective in the MOGA. Also, it is used to simulate pipe failure conditions which are used as input data for the performance assessment to establish the reliability and failure tolerance measure of each solution.

1.5 LAYOUT OF THESIS

This thesis contains a total of eight chapters. Following the introduction and objectives of the research presented earlier, the thesis is structured as follows:

Chapter 2 addresses the analysis of water distribution systems (WDSs). Fundamentals involved in formulating and modelling the WDSs along with the two different methods of hydraulic analyses namely demand driven analysis and pressure dependent analysis are reviewed in detail.

Chapter 3 presents a review of the application of evolutionary algorithms (EAs), in particular genetic algorithm (GA), in the optimization of WDSs. The highlight of the chapter is the discussion of GA constraint handling methods along with boundary search techniques used in the literature.

Chapter 4 proposes an augmented gradient method for pressure dependent modelling of WDS. The methodology is presented in detail followed by results generated from the simulations of hypothetical and real life networks to demonstrate its robustness and computational efficiency. Pressure dependent results verifications are presented.

Chapter 5 extends the application of the augmented gradient method to form an enhanced version of EPANET 2 capable of pressure dependent analysis (PDA). The developed PDA simulator is applied to hypothetical and real life networks as case studies. Its robustness and computational performance are accessed in a comprehensive manner. Pressure dependent results verifications are also presented.

Chapter 6 presents the application of the proposed penalty-free multi-objective evolutionary approach (PFMOEA) to three well known WDS benchmarks. Comparisons of results to the best solutions obtained in the literature are presented.

Chapter 7 presents a holistic approach to the optimal long-term upgrading of WDSs based on the PFMOEA. The comparisons of results generated by PFMOEA to that of earlier works involving linear programming are presented followed by a concise discussion.

Chapter 8 further demonstrates the robustness of the proposed PFMOEA by applying it to solve for the optimal design and rehabilitation of WDS which includes pump scheduling, tank sizing and siting. The study involves the benchmark “Anytown” network. The many good feasible results which are cheaper than the best result in the literature are presented and discussed.

Chapter 9 winds up with a general summary of the present research and suggestions for further research.

CHAPTER TWO

HYDRAULIC ANALYSIS AND PERFORMANCE ASSESSMENT OF WATER DISTRIBUTION SYSTEMS

2.1 INTRODUCTION

The application of hydraulic simulation models is a crucial part in the design and operation of water distribution systems (WDSs) to meet the current and future water supply demand in a reliable and efficient manner. Hydraulic simulations replicate the operation of a real WDS through the formulations of mathematical equations. They can be utilised to predict system responses and behaviours of events under a wide range of conditions (e.g. peak demands, pipe bursts, pump failures, valve closures, fire flows, etc). Solutions can be evaluated to reveal potential problems that may arise from the proposed or existing systems before time, capital and materials are invested in a WDS project. These are valuable information that will greatly assist engineers in making timely and crucial decisions. With the rapid advancement of the computational technology, sophisticated hydraulic simulation models which are capable of handling realistic WDS features can be realized more fully than ever before.

The WDS can be modelled using either steady-state simulation (SSS) or extended-period simulation (EPS). A SSS essentially analyses the WDS operations under static condition (i.e. nodal demands and water level of storage reservoirs are constant) within a single snapshot in time. A common practice adopted widely is to use SSS in designing the WDS to cope with the worst case situation (e.g. peak hour demands and fire events). However, in reality, the operation of the WDS varies with time and the performance of the WDS can be more realistically depicted by utilizing EPS which

evaluates the performance of the system over a defined duration of time. This form of analysis is capable of modelling the filling and draining of tanks, operation of regulating valves and variable speed pumps and the changes in nodal pressures and pipe flow rates throughout the system in response to the fluctuation in demands.

A typical water distribution system consists of nodes (demand nodes, pipe junctions, service and storage reservoirs) and links (pipes, pumps and valves). In general, a WDS analysis model is developed by firstly defining the layout of the network in terms of the nodal demands, elevations and locations followed by the characteristics of the links (e.g. length, diameter, roughness for pipes) connecting these nodes. The set of WDS constitutive equations (namely mass balance at nodes and energy conservation along hydraulic links) are then formulated and solved numerically to obtain the nodal heads and flow rates in links. These results are compared to the service performance requirements such as the desired minimum nodal pressure to determine the feasibility of the solution.

There are two approaches in analysing the WDS. The conventional approach is formulated based on the assumption that all nodal demands are fully satisfied regardless of the pressure at nodes. This method of analysis is referred to as demand driven analysis (DDA). However, in reality, the nodal flow is pressure dependent and will not be satisfied in full if the network has insufficient pressure. As such, this analysis is incapable of simulating scenarios such as pipe bursts, pump or valve failures which subject the network under pressure deficiency. To accurately model these events require the application of pressure dependent analysis (PDA) which explicitly takes into account the relationship between nodal flows and pressure.

The assessment of the network performance is crucial to gauge the capability of the network in meeting the required and expected goals for which it was designed to fulfil. In addition, it evaluates the robustness of the network in coping with unforeseen abnormal operating conditions. Important performance assessment parameters used include network reliability and failure tolerance (Tanyimboh and Templeman, 1998). Reliability measures the ability of the system to fulfil on average the required nodal demands at adequate pressure whilst considering both normal and abnormal operating conditions where as failure tolerance quantifies the network's redundancy by

assessing its ability to cope with the unavailability of some of its components. Both parameters are essential to ensure a comprehensive performance assessment.

This chapter concisely describes the fundamentals involved in the modelling of WDSs. Section 2.2 presents the governing equations which are the basic blocks of the hydraulic analysis. Emphasis is given to sections 2.5 and 2.6 which cover the concepts of the two types of hydraulic analyses i.e. DDA and PDA. DDA is presented first and it covers the numerical methods and steps involved in the modelling process. The shortcomings of DDA are then discussed which will then lead to the introduction of the pressure dependent analysis. A review of methods for solving PDA has been detailed. The last section of the chapter presents the performance assessment of water distribution systems in a brief manner. The key performance assessment parameters such as reliability and failure tolerance are outlined along with several reliability surrogates which are widely used in the literature.

2.2 CONSTITUTIVE EQUATIONS

2.2.1 Head Loss Equations

Part of the total energy in a pipe flow pipe is lost due to internal friction and turbulence. This energy loss is usually expressed in the form of head and therefore termed head loss. The head loss in a pipe is the sum of frictional head loss and minor head loss. Minor losses do not contribute much to the energy loss and are normally ignored.

The pipe head loss can be expressed in several equations. The primitive pipe resistance equation is the Darcy-Weisbach as stated below.

$$h_{ij} = 4 f_{ij} \frac{L_{ij}}{D_{ij}} \frac{v_{ij}^2}{2g} \qquad \forall ij \in IJ \tag{2.1}$$

where h_{ij} is the head loss in pipe *ij*; f_{ij} is the dimensionless friction factor which is dependent on the pipe roughness and flow rate; L_{ij} and D_{ij} represent the length and internal diameter of pipe respectively; v_{ij} is the mean velocity of the pipe flow; *g* is the gravitational acceleration; *IJ* is the set of all the pipes in the network.

Empirical approximate head loss equations are also broadly used as they are more straight forward and easier to apply in hydraulic simulation models. One of these equations is the Hazen-Williams equation which is described as

$$h_{ij} = \left(\frac{\eta L_{ij}}{C_{ij}^{1.852} D_{ij}^{4.87}} \right) Qp_{ij}^{1.852} \qquad \forall ij \tag{2.2}$$

in which η is a dimensionless conversion factor for units and is equals to 10.67 in S.I. units; Qp_{ij} and C_{ij} are the pipe flow and the Hazen-Williams coefficient respectively. The C_{ij} value varies according to factors such as the material and age of the pipe.

Eq. 2.2 is also often rewritten as

$$h_{ij} = K_{ij} Qp_{ij}^{1.852} \tag{2.3}$$

where K_{ij} is known as the resistance coefficient for link *ij* and can be represented as

$$K_{ij} = \frac{\eta L_{ij}}{C_{ij}^{1.852} D_{ij}^{4.87}} \tag{2.4}$$

The Hazen-Williams equation is used in this research.

Another empirical approximate equations is the Manning's equation as stated below,

$$h_{ij} = \frac{\eta L_{ij} \left(n_{ij} Qp_{ij} \right)^2}{D_{ij}^{5.333}} \qquad \forall ij \in IJ \tag{2.5}$$

where η here equals to 10.29 in S.I. units and n_{ij} represents the Manning's coefficient.

2.2.2 Continuity Equations

In the hydraulic analysis, flow is assumed to be laminar and incompressible. Hence, the sum of nodal inflows and outflows in a network must be zero. The flow continuity equations for node j, j=1,…,Nn, is describe as

$$\sum_{i:Hn_i>Hn_j} Qp_{ij} - \sum_{i:Hn_i<Hn_j} Qp_{ij} = Qn_j \tag{2.6}$$

where Nn is the number of nodes present in the network; Qp_{ij} is the inflow (if $Hn_i>Hn_j$) or outflow (if $Hn_i<Hn_j$) at node j; Qn_j is the demand at node j; Hn_i and Hn_j are heads at nodes i and j respectively. These heads are the sum of the nodal elevation and pressure head and are often referred to as total heads. The velocity head is often negligible.

2.2.3 Equations for Conservation of Energy

2.2.3.1 Loop Equations

In order to fulfil the Conservation of Energy in a network, the sum of head loss in pipes forming a loop must be zero. The equation for each loop can be written as

$$\sum_{ij\in IJ_{lp}} h_{ij} = 0 \qquad lp=1,\ldots,Nlp \tag{2.7}$$

where IJ_{lp} represents the set of all links in loop lp. Nlp is the number of loops in a network and can be obtained using the following equation.

$$Nlp=Nl-Nn+1 \tag{2.8}$$

where *Nn* and *Nl* are the number of nodes and links in the network respectively.

2.2.3.2 Path Equations

The total head loss along a path should be equal to the difference in head between its starting and ending nodes. The equation for a path starting from node *i* with hydraulic gradient level (HGL) Hn_i and ending at node *j* with HGL Hn_j can be written as

$$\sum_{ij \in IJ_p} h_{ij} = Hn_i - Hn_j \qquad \forall ij \in IJ \tag{2.9}$$

where *IJ* is the set of all links in path *p*.

2.2.4 Valves, Pumps and Tanks

2.2.4.1 Valves

In general, there are two categories of valves, i.e. line valves and control valves. Line valves are fitted at pre-specified locations within the network with the purpose of isolating sections of pipes or network zones for scheduled maintenance and repair works. These valves are not usually considered in a design model and their existence can be accounted for as minor head losses.

Control valves are often required in water distribution networks for flow control and pressure regulating purposes. For instance, a non-return valve, or also known as the check valve allows flow through it in one direction only. It is normally fitted at areas prone to back water effect e.g. the downstream end of a pump. A pipe fitted with a non-return valve can be modelled as (Bhave, 1991)

$$Qp_{ij} = \begin{cases} \dfrac{Hn_i - Hn_j}{K_{ij}^{0.54}\left|Hn_i - Hn_j\right|^{0.46}} & Hn_j \le Hn_i \\ 0 & Hn_j > Hn_i \end{cases} \tag{2.10}$$

where Hn_i and Hn_j are the heads for upstream node i and downstream node j respectively.

Another example of a control valve is the Pressure Reducing/ Regulating Valve (PRV). The PRV only allows flow through it below a pre-defined pressure and acts as a maximum pressure limit. It is normally located at high water pressure supply to protect the system (downstream) from excess pressure that may contribute to pipe leakage. The PRV can be mathematically expressed as (Bhave, 1991)

$$Qp_{ij} = \begin{cases} \dfrac{Hn_{prv} - Hn_j}{K_{ij}^{0.54}\left|Hn_{prv} - Hn_j\right|^{0.46}} & Hn_j \le Hn_{prv} \le Hn_i \\ \dfrac{Hn_i - Hn_j}{K_{ij}^{0.54}\left|Hn_i - Hn_j\right|^{0.46}} & Hn_j < Hn_i < Hn_{prv} \\ 0 & Hn_j > Hn_{prv} \end{cases} \tag{2.11}$$

where Hn_{prv} is the pre-set downstream pressure of the PRV which is not to be exceeded.

Conversely, a pressure-sustaining valve (PSV) prevents the upstream pressure from dropping below a set value. The PSV can be represented with the following equation.

$$Qp_{ij} = \begin{cases} \dfrac{Hn_i - Hn_{psv}}{K_{ij}^{0.54}\left|Hn_i - Hn_{psv}\right|^{0.46}} & Hn_i \ge Hn_{psv} \ge Hn_j \\ \dfrac{Hn_i - Hn_j}{K_{ij}^{0.54}\left|Hn_i - Hn_j\right|^{0.46}} & Hn_i > Hn_j > Hn_{psv} \\ 0 & Hn_i < Hn_{psv} \end{cases} \tag{2.12}$$

where Hn_{psv} is the pre-set upstream pressure of the PSV which is to be sustained.

2.2.4.2 Pumps

Nodes with high elevation or downstream end location in a network may require additional head in order for their demands to be fully satisfied. For this purpose, pumps are included at these points to supply additional energy needed to satisfy the minimum required head. In general, the head-flow relationship of a pump can be approximated by a parabolic curve equation as

$$H_p = a_o Q_{pu}^2 + b_o Q_{pu} + c_o \tag{2.13a}$$

where a_o, b_o and c_o are constants specified by the pump manufacturer. These constants can also be obtained by selecting three points from the pump head discharge curve and substituting them into the Eq. 2.13. Q_{pu} is the flow delivered by the pump. H_p is the additional head supplied by the pump or the head difference between nodes located at the upstream and downstream of the pump. Another equation which is commonly used to describe the pump curve is

$$H_p = h_0 - d_o Q_{pu}^{m_o} \tag{2.13b}$$

where h_0 is the shutoff head of the pump (pump head at zero flow). d_o and m_o are the pump curve coefficients.

2.2.4.3 Tanks

A storage tank is a boundary node in a distribution network that supplies water during peak demand hours and acts as a demand node when the demands in the network are low. A tank acts as a buffer to ensure that the network demand can be satisfied during peak demand hours. Including the design of a storage tank into the optimization

procedure involves a combination of decision variables such as the elevation and volume of the tank in terms of the water level. The location of the storage tank can also be considered as another variable though it is usually pre-determined by the designer. A well-optimised tank in terms of design and location would be one that is able to cover the insufficient supply of the network during peak demand hours, and refill back to its original level at the end of the day. More details on the formulation to model tank operation have been presented in subsequent Section 2.4.2.1.

2.3 FORMULATION OF HYDRAULIC EQUATIONS

In the analysis of WDS, the nodal heads and pipe flows are unknown. In general, a system of hydraulic equations is set up and then solved iteratively using suitable numerical approaches. These hydraulic equations can be formulated in several ways.

2.3.1 Pipe flow Rates as Unknown Variables

Hydraulic equations formulated with pipe flows, Qp_{ij} as the unknown variables are referred to as the q-equations (Bhave, 1991). For example, the basic unknowns for Eqs. 2.2 and 2.6 which respectively represent the flow continuity and head loss equations are Qp_{ij}.

2.3.2 Nodal Heads as Unknown Variables

Hydraulic equations formulated with nodal heads as unknown variables are referred to as the H-equations (Bhave, 1991). For example, the flow continuity (Eq. 2.6) can be rewritten as

$$F_j \equiv \sum_{i:Hn_i>Hn_j} \left(\frac{Hn_i - Hn_j}{K_{ij}} \right)^{0.54} - \sum_{i:Hn_i<Hn_j} \left(\frac{Hn_j - Hn_i}{K_{ij}} \right)^{0.54} - Qn_j = 0; \quad \forall j = 1,..., NJ \tag{2.14}$$

where F_j is the continuity equation for node j. As observed, pipe flows are expressed in terms of nodal heads. The H-equation can be conveniently set up and solved without the need for the loop or path equations. To obtain a feasible solution, the number of continuity equation must be equal to the number of unknown nodal heads and the value of one nodal should be known (usually source node of a fixed head).

2.3.3 Loop-Flow Corrections as Unknown Variables

Hydraulic equations formulated with loop-flow corrections as unknown variables are referred to as ΔQp equations (Bhave, 1991). In formulating the ΔQp equations, it is assumed that the node-flow continuity equation (Eq. 2.6) is satisfied. In general, the initial assumed pipe flows will not satisfy the loop-head loss relationship. Hence, pipe flows are adjusted iteratively by applying the loop flow corrections at each loop.

$$Qp_{ij}^{k} = Qp_{ij}^{k-1} + \sum_{lp \in lp_{ij}} \Delta Qp_{lp}^{k} \qquad \forall ij \in Nl \tag{2.15}$$

in which ΔQp_{lp}^{k} is the loop-flow correction applied to the flow for all pipe flows in loop lp; Qp_{ij}^{k-1} is an estimated flow rate and Qp_{ij}^{k} is the corrected flow rate. k represents the iteration number. lp_{ij} represents all the loops sharing link ij. $\sum_{lp \in lp_{ij}} \Delta Qp_{lp}^{k}$ is the summation of the corrections of all loops to which link ij belongs.

The unknowns in Eq. 2.15 are the ΔQp_{lp}. From the loop-head loss relationship (Eq. 2.7), the ΔQp equations can be formulated as

$$\sum_{ij \in IJ_{lp}} K_{ij} \left(Qp_{ij}^{(k-1)} + \sum \Delta Qp_{lp}^{(k)} \right)^{nc} = 0 \qquad \forall ij \in Nl; \qquad lp = 1,\ldots, Nlp \tag{2.16}$$

where Nlp represents the number of loops available. The ΔQp equations can be simultaneously solved using an iterative scheme.

2.4 TYPES OF HYDRAULIC SIMULATIONS

2.4.1 Steady State Simulation

In steady state analysis, the hydraulic simulation model is carried out in a single period of time where network demands and reservoir water levels are treated as constant values. This analysis is only useful in analyzing networks operation at a single time period and cannot be use to portray the network performance throughout the day as neither nodal demands nor water levels in storage reservoirs remain constant in reality.

A common practice adopted widely is to use steady state modeling in designing the WDS to cope with the worst case situation (e.g. peak hour demands and fire events). However, real WDSs operation varies with time and by relying solely on steady state modeling, engineers may miss out certain vital aspects such as tank refilling, operation of valves and variable speed pumps, etc. The application of steady state modeling is therefore limited. Simulating WDSs over time is essentially required.

2.4.2 Extended Period Simulation

Extended period simulation (EPS) is executed over a longer period, e.g. 24 or 48 hours with network demands fluctuating from time to time. The analysis consists of a sequence of steady state analysis performed over several pre-specified hydraulic time steps (intervals). Typical time step values vary from 15 minutes to 1 hour. Solutions obtained at the end of these time intervals which involve the dynamics of tanks (filling-up and depletion), pump scheduling and valve settings are used to update the inputs for the successive steady state analyses. With EPS, a more realistic network analysis can be carried out as the network demands and water levels in tanks are allowed to change throughout the time period. The performance of the network during peak and low demand hours is clearly depicted. Networks with varying speed pumps can also be analysed and the status of valves at each time step can be closely monitored. EPS is an indispensable tool when it comes to optimizing pump scheduling, storage tank design and location. Mathematical formulations on the

volume changes in tanks are presented next followed by the overall procedure of the EPS. These will provide a clear depiction on how steady state simulations are linked together.

2.4.2.1 Volume changes in tanks

A steady state solution is obtained for time t and the tank flow rates are calculated as

$$QT_m(t) = \sum_{b \in B_m} Qp_b(t) \tag{2.17}$$

in which B_m is the set of links connected to tank m. $QT_m(t)$and $Qp_b(t)$, are the flow rates of tank m and links connected to tank m respectively. For reservoirs, the tank flow rates are calculated as

$$QR_f(t) = \sum_{f \in E_f} Qp_f(t) \tag{2.18}$$

in which E_f is the set of links connected to reservoir f. $QR_f(t)$and $Qp_f(t)$, are the flow rates of reservoir f and links connected to reservoir f at time t respectively.

Assuming the flow rate for a tank is constant during the time interval $(t, t+\Delta t)$, the volume change in a tank is obtained as

$$\Delta V_m(t, t+\Delta t) = QT_m(t)\Delta t \tag{2.19}$$

where $\Delta V_m(t, t+\Delta t)$ is the change of water volume in tank m during the time interval $(t, t+\Delta t)$. Δt represents the time step between the current and the next steady state simulation. The changes in water levels are predicted using the tank capacity-elevation curves. The water levels in tanks at time $t+\Delta t$ are determined and are then used to carry out the steady state analysis at time $t+\Delta t$.

Likewise, assuming the flow rate for a reservoir is constant during the time interval *(t, t+Δt)*, the volume of water from the reservoir into the network is calculated as

$$V_f(t, t+\Delta t) = QR_f(t)\Delta t \tag{2.20}$$

where $V_f(t, t+\Delta t)$ is the volume of water from reservoir *f* during the time interval *(t, t+Δt)*. $QR_f(t)$ is the flow rate for reservoir *f* at time *t*. The total flow volume from tanks and reservoirs into the network is then computed as

$$V_{Out}(t, t+\Delta t) = \sum_{m=1}^{M} \Delta V_m(t, t+\Delta t) + \sum_{f=1}^{F} V_f(t, t+\Delta t) \tag{2.21}$$

where *M* is the number of tanks in the network and *F* is the number of reservoirs in the network. $V_{Out}(t, t+\Delta t)$ is the net volume of water from tanks and reservoirs during the time interval *(t, t+Δt)*.

2.4.2.2 Extended Period Simulation Procedure

At time *t*, the following data are available:

1. Water levels (head values) of tanks and reservoirs
2. Water volumes of tanks, $V_m(t)$, and reservoirs, $V_f(t)$
3. Nodal demand factors, $DF_i(t)$, and base demands, $Qn_i^{base}(t)$, for each node *i*.

The extended period simulation of a network can be described with the following general steps:

Step 1. For time *t*, the required nodal demand for each demand node is calculated, as $Qn_i^{req}(t) = Qn_i^{base}(t) \times DF_i(t)$.

Step 2. The pressure dependent steady state hydraulic analysis of the network is obtained for time *t*. The flow rates of the tanks, $QT_m(t)$, are calculated using Eq. 2.17.

Step 3. If no status changes in tanks (e.g. fully depleted or filled), pumps (e.g. variable speed) or valves (e.g. open or closed) occur within the normal time interval, i.e. (t, t^e), where $t^e=t+\Delta t_h$ and Δt_h is the user defined hydraulic time step, then this step is skipped. Else, the time at which the status change occurs is recorded as t^r. The time step from time t to t^r is computed, i.e. $\Delta t_1 = t^r - t$. The time step from t^r to t^e is computed, i.e. $\Delta t_2 = t^e - t^r$. The volume changes in tanks $\Delta V_m(t , t^r)$, are calculated using Eq. 2.19 and the tank water levels are updated. t is then set to t^r, i.e. $t = t^r$ and Step 2 is repeated. This loop (Steps 2 and 3) continues until no further status changes occur.

Step 4. If step 3 was executed, the time step is Δt_2, i.e. $\Delta t=\Delta t_2$. Else, the time step is the user defined hydraulic time step, i.e. $\Delta t =\Delta t_h$. The volume changes in tanks, $\Delta V_m(t, t+\Delta t)$, are calculated using Eq. 2.19. The tank water levels are updated.

Step 5. Time is advanced by the time interval, thus $t = t + \Delta t$.

The procedure is repeated until the entire period of the EPS is analysed.

2.5 DEMAND DRIVEN NETWORK ANALYSIS

The conventional demand driven analysis (DDA) assumes that all nodal demands are fixed and satisfied at all times, disregarding the fact that nodal outflows are pressure dependent. As such, this method of analysis is only capable of analysing water distribution networks under normal operating conditions but yields inaccurate and misleading nodal head results for pressure deficient networks. In reality, the nodal demands will not be satisfied in full if the network has insufficient pressure. A practical depiction of the network performance can only be attained by considering nodal demands to be pressure dependent. Pressure dependent demand analysis has been presented in the subsequent Section 2.6.

To date, DDA still remains as the most widely used form of network analysis in the water industry due to its simple formulation. There are four numerical methods

commonly used for solving the DDA namely the Hardy Cross method, the Newton-Raphson method, the Linear Theory method and the Global Gradient method. In general, these are systematic iterative procedures and require an initial trial solution to begin with. New improved solutions are generated and compared with solutions from the previous iteration. This iterative cycle continues until the difference between consecutive solutions is less than a user specified tolerance and the loop and path equations are satisfied. Brief descriptions of these methods are presented next for completeness.

2.5.1 Hardy-Cross Method

The Hardy-Cross method (Cross, 1936) is based on the loop-flow correction equations. The formulation begins by assuming initial pipe flow rates for a loop to satisfy the flow continuity. This can be mathematically expressed as

$$\sum_{ij \in IJ_{lp}} K_{ij} \left(Qp_{ij}^{(k-1)} + \sum \Delta Qp_{lp}^{(k)} \right)^{nc} = 0 \qquad \forall lp \tag{2.22}$$

where *nc* is the flow exponent and takes the value of 1.852. Applying the first order Taylor's series expansion to Eq. 2.22 yields

$$\sum_{ij \in IJ_{lp}} K_{ij} \left(Qp_{ij}^{(k-1)} \right)^{nc} + \Delta Qp_{lp}^{(k)} \sum_{ij \in IJ_{lp}} \left| nc \cdot K_{ij} \left(Qp_{ij}^{(k)} \right)^{nc-1} \right| = 0 \qquad \forall lp \tag{2.23}$$

Eq. 2.23 is rearranged to give the loop-flow correction values as follow:

$$\Delta Qp_{lp}^{(k)} = - \frac{\sum_{ij \in IJ_{lp}} K_{ij} \left(Qp_{ij}^{(k-1)} \right)^{nc}}{\sum_{ij \in IJ_{lp}} \left| nc \cdot K_{ij} \left(Qp_{ij}^{(k)} \right)^{nc-1} \right|} \qquad \forall lp \tag{2.24}$$

The pipe flows are then updated to give

$$Qp_{ij}^{(k)} = Qp_{ij}^{(k-1)} + \Delta Qp_{lp}^{(k)} \qquad \forall lp\ ; \qquad \forall ij \in IJ_{lp} \tag{2.25}$$

Adjacent loops are assumed to have no effect on the loop-flow correction and therefore each loop-flow correction equation (Eq. 2.24) contains only one variable i.e. the $\Delta Qp_{lp}^{(k)}$ value as unknown. The loop-flow corrections are calculated for all loops and the pipe flows are all updated in one go. This marks the end of an iterative cycle. The next iteration involves using the updated flows as the new estimates for pipe flow rates in Eqs. 2.22 to 2.24. The process is repeated until the loop-flow correction reached an insignificant value and both loop and path equations are satisfied.

2.5.2 Newton-Raphson Method

Martin and Peters (1963) first introduced the Newton-Raphson method to solve the system of non-linear equations. For a single variable non-linear function $F(x)=0$, the Newton-Raphson method can be formulated as

$$x^{(k+1)} = x^k - \frac{F(x^{(k)})}{dF(x^{(k)})/dx} \tag{2.26}$$

where $dF(x^{(k)})/dx$ is the derivative of $F(x)$ evaluated at x^k. For a system of equations, Eq. 2.26 is written as follows:

$$\underline{x}^{(k+1)} = \underline{x}^k - (J_x)^{-1}_{(k)} \underline{F}(\underline{x}^{(k)}) \tag{2.27}$$

where $\underline{x}$ and $\underline{F}$ are the vectors of the variables and function values respectively. J_x is the Jacobian which represents the matrix of the first partial derivatives of each F with respect to each x's. For the application of WDS analysis, the continuity equations at nodes can be written as

$$\underline{F}(\underline{H}) = 0 \tag{2.28}$$

in which $\underline{F}$ here is the vector of respective functions of the nodal continuity equations and $\underline{H}$ is the vector of unknown nodal heads. To begin with, initial estimates for nodal heads are made.

From Eq. 2.27, the Newton-Raphson formulation for the flow continuity can be expressed as

$$\underline{H}^{(k+1)} = \underline{H}^{(k)} - (J_H)^{-1}_{(k)} \underline{F}(\underline{H}^{(k)}) \tag{2.29}$$

in which J_H is the Jacobian matrix for the unknown nodal heads. The inversion Jacobian matrix is computationally expensive. Hence, Eq. 2.29 is rearranged to form

$$(J_H)_{(k)} \underline{\Delta H}^{(k)} = -\underline{F}(\underline{H}^{(k)}) \tag{2.30}$$

where $\underline{\Delta H}^{(k)}$ is the vector of the nodal heads corrections, i.e. $\underline{H}^{(k+1)} - \underline{H}^{(k)}$. Eqs. 2.30 are solved simultaneously (e.g. using the Gaussian elimination algorithm) to obtain $\underline{\Delta H}^{(k)}$ which is then used to update $\underline{H}^{(k+1)}$. The iterative process ends when $\underline{\Delta H}^{(k)}$ or $\underline{F}(\underline{H}^{(k)})$ approaches an insignificant value (normally pre-specified by users).

2.2.3 Linear Theory Method

The Linear Theory method developed by Wood and Charles (1972) suggested that the Hazen-Williams equation can be expressed in a linearized form as follows.

$$h_{ij}^{(k)} = \left(K_{ij}\left[Qp_{ij}^{(k-1)}\right]^{0.852}\right) \cdot Qp_{ij}^{(k)} \qquad \forall ij; \quad k = 1,2 \tag{2.31a}$$

$$h_{ij}^{(k)} = \left(K_{ij}\left[\frac{Qp_{ij}^{(k-1)} + Qp_{ij}^{(k-2)}}{2}\right]^{0.852}\right) \cdot Qp_{ij}^{(k)} \qquad \forall ij; \quad k = 3,4,5,6,... \tag{2.31b}$$

Eqs. 2.31 are used to form a set of loop-head loss and nodal flow continuity equations which are then solved simultaneously in an iterative manner to give an approximated pipe flow rates.

For the first and second iteration, Eq. 2.31a is used and Qp_{ij}^{0} is set to unity. For successive iterations, flows $Qp_{ij}^{(k)}$ are obtained by using the average of the assumed flow values from preceding iterations, i.e. $Qp_{ij}^{(k-1)}$ and $Qp_{ij}^{(k-2)}$ as shown in Eq. 2.31b. This approach was proposed by Wood and Charles (1972) to improve the robustness and convergence rate of the algorithm.

2.5.4 Global Gradient Method

The Global Gradient Method (GGM) proposed by Todini and Pilati (1987) is essentially the application of the Newton-Raphson method to simultaneously obtain both pipe flow and nodal head values.

The conservation laws, namely mass balance at nodes and energy conservation along hydraulic links can be solved simultaneously using the GGM formulation as described below.

$$\begin{bmatrix} A_{11} & \vdots & A_{12} \\ \cdots & \cdots & \cdots \\ A_{21} & \vdots & 0 \end{bmatrix} \begin{bmatrix} Qp \\ \cdots \\ Hn \end{bmatrix} = \begin{bmatrix} -A_{10}H_0 \\ \cdots \\ -Qn^{req} \end{bmatrix} \tag{2.32}$$

where A_{11} represents the diagonal matrix whose elements are $K_j(Qp_j)^{n-1}+m_{loss}Qp_j$ for pipes and $-\omega_{pu}^2(h_0 - K_j(Qp_j/\omega_{pu})^n)/Qp_j$ or $-(a_0\omega_{pu}^2/Qp_j + b_0\omega_{pu} + c_0Qp_j)$ for pumps. K_j and n are the resistance coefficient and flow exponent in the head loss formula respectively. h_0 is the shutoff head for the pump. m_{loss} and ω_{pu} are the minor loss (often neglected) and pump curve coefficients respectively. a_0, b_0 and c_0 are constants specified by the pump manufacturer. Qp_j is the flow rate in pipe j. The

overall incidence matrix relating the pipes to nodes with unknown and known heads is represented by A_{12} and A_{10} respectively. Pipe flow leaving node is defined as -1, pipe flow into node as +1 and 0 if pipe is not connected to node. A_{21} is the transpose of A_{12}. Qp denotes the column vector of unknown pipe flow rates. Hn and H_0 are column vectors for unknown and known nodal heads respectively. Qn^{req} is the column vector for required nodal supply. Eq. 2.32 is differentiated with respect to the pipe discharges and nodal heads to give:

$$\begin{bmatrix} D_{11} & \vdots & A_{12} \\ \cdots & \cdots & \cdots \\ A_{21} & \vdots & 0 \end{bmatrix} \begin{bmatrix} dQp \\ \cdots \\ dHn \end{bmatrix} = \begin{bmatrix} dE \\ \cdots \\ dq \end{bmatrix} \tag{2.33}$$

where diagonal matrix D_{11} can be written as $nK_j\left|Qp_j\right|^{n-1} + 2m_{loss}\left|Qp_j\right|$ for pipes and $nK_j\omega_{pu}^{2-n}\left|Qp_j\right|^{n-1}$ or $-\left(b_0\omega_{pu} + 2c_0Q_j\right)$ for pumps. dQp and dHn represent the corrective steps of Qp and Hn respectively in successive iterations and can be defined as:

$$dQp = Qp^k - Qp^{k+1} \tag{2.34}$$

$$dHn = Hn^k - Hn^{k+1} \tag{2.35}$$

in which k represents the iteration number. dE and dq represent the pipe head loss and flow conservation at each node respectively and from Eq. 2.32 can be written as:

$$dE = A_{11}Qp + A_{12}Hn + A_{10}H_0 \tag{2.36}$$

$$dq = A_{21}Qp + Qn^{req} \tag{2.37}$$

By substituting Eq. 2.36 and Eq. 2.37 into Eq. 2.33, the iterative formulation of the GGM can be described as the following two equations:

$$Hn^{k+1} = A^{-1}F \tag{2.38}$$

$$Qp^{k+1} = Qp^{k} - D_{11}^{-1}(A_{11}Qp^{k} + A_{12}Hn^{k+1} + A_{10}H_{0}) \tag{2.39}$$

where F and A are written as:

$$F = A_{21}Qp^{k} - Qn^{req} - A_{21}D_{11}^{-1}(A_{11}Qp^{k} + A_{10}H_{0}) \tag{2.40}$$

$$A = A_{21}D_{11}^{-1}A_{12} \tag{2.41}$$

Hence the algorithm first solves the equation for *Hn* before solving for *Qp*.

At the first iteration, only the initial guess of pipe flows is required since the corresponding nodal heads are obtained directly from the pipe flows as shown in Eq. 2.38. Initial pipe flow can be taken as unity or any arbitrarily chosen value. As the algorithm converges, the changes in flow and head values approach an insignificant value. The established and widely used hydraulic simulator EPANET 2 (Rossman, 2002) employs the GGM as its network solver. Initial flows in pipes are chosen to be equal the flow corresponding to a velocity of 1 ft/sec (0.3048 m/sec). All computations in EAPANET are made using empirical units, i.e. head in ft and flow in cfs.

2.6 PRESSURE DEPENDENT NETWORK ANALYSIS

Pressure deficient conditions are inevitable in water distribution systems (WDSs) and can be caused by common occurrences such as pump failure, pipe bursts, isolation of major pipes from the system for planned maintenance work and excessive fire fighting demands. Under these circumstances, the WDS may not be able to satisfy all consumer demands. This requires water companies to accurately model and analyse the WDS for crucial decision making. However, the widely used demand driven analysis (DDA) is inappropriate for modelling pressure deficient network. This conventional model is formulated under the assumption that demands are fully

satisfied regardless of the pressure and yields lower or even negative nodal pressure while analysing a pressure deficient network. Hence, DDA is unable to accurately quantify the exact magnitude of deficiency in terms of nodal pressure and outflow. This is critical information that cannot be over-looked during a WDS performance evaluation. The need for an analysis methodology that explicitly takes into account the relationship between nodal flows and pressure cannot be further stressed. This method is known as the pressure dependent analysis (PDA) and models the WDS in a more realistic manner.

There are numerous methods of obtaining the available nodal flow for PDA in the literature. These methods can generally be categorized into two namely methods involving demand driven analysis and methods involving head-flow relationships.

2.6.1 Methods Involving Demand Driven Analysis

Bhave (1991) developed a heuristic approach referred to as the Node Flow Analysis (NFA) in obtaining available nodal flows. The method is essentially a DDA based optimization formulation to maximize the total network outflow subjected to nodal flow constraints derived from the classification of nodes according to two categories in terms nodal flow and hydraulic gradient level (HGL).

In the first NFA iteration, all demand nodes are assumed to be fully satisfied and are therefore categorized (in the aspect of nodal flow) as “adequate flow”. The problem is solved using DDA and these nodes are then categorized (in the aspect of HGL) based on the resulting nodal heads. A check is made on every node to find out whether the assumed nodal flow category is compatible with the resulting HGL category. If node category compatibility is achieved, the assumed node category is retained. Else, nodes with incompatible categories are reassigned to their appropriate node categories. For example, for nodes with heads less than the minimum required and had been assumed to have “adequate flow”, a “critical-flow” category is assigned and the nodal flow constraint of Qn_j=0 is applied to the next NFA iteration. The NFA terminates when all nodes achieve compatibility in both categories. More details of the procedures and categories utilised can be found in Bhave (1991).

Bhave (1991) stated that solution obtained may not be globally optimal. He also observed that the algorithm could converge to infeasible solution wherein one or more constraints are violated. This is somewhat expected since the optimization problem is a highly constrained one, with each demand node contributing a constraint which varies as the NFA progresses. It can be foreseen that the algorithm would face much difficulties in converging while analysing a large network.

Ang and Jowitt (2006) proposed an algorithm which models the network outflows using artificial reservoirs. The algorithm requires executing the DDA solver for multiple times in which artificial reservoirs are added and removed as required at each run before a stable and valid solution is arrived. For a simple 14 pipe network (Ang and Jowitt, 2006), the proposed pressure-deficient network algorithm (PDNA) required 7 separate EPANET 2 runs and a sum of 43 iterations within the hydraulic simulator to converge.

Rossman (2007) showed that the artificial reservoir approach by Ang and Jowitt (2006) is hydraulically equivalent to implementing emitters as orifices at the demand nodes within a DDA framework. The emitter equation used can be expressed as:

$$Qn_e = K_e p^{n_e} \tag{2.42}$$

where Qn_e is the emitter flow; K_e is the emitter coefficient; $p=Hn_i-Hn_i^{elev}$ where Hn_i is the head at node i and Hn_i^{elev} is the elevation of node i; n_e is the emitter exponent. Eq. 2.42 gives unrestricted flow at a node, i.e. nodal flow computed can exceed the required demand or even take a negative value, i.e. $-\infty \le Qn_e \le \infty$ which is totally inappropriate. Rossman (2007) addressed this by modifying the EPANET 2 source code to implement new status variables to emitters, limiting the nodal flow between zero flow and the fully assigned demand. Three different status variables were involved. The status of the emitter is CLOSED when the computed nodal head is below its nodal elevation. The demand at node is set to zero and the effect of the emitter is ignored. In the cases where flow through the emitter exceeds the required demand, the status of the emitter is OPEN. The nodal flow is set to be equal the

required demand and the emitter effect is ignored. The ACTIVE status is employed for the other remaining conditions and the emitter functions in its usual manner. The actual nodal flow is the flow computed through the emitter.

The emitter approach was carried out on the 14-pipe network (Ang and Jowitt, 2006) and the computational efficiency was improved tremendously, i.e. it required one single EPANET 2 run of 9 internal iterations to reach to the same solution. However, it has not been used to simulate large networks. As such, the overall computational efficiency and the algorithm's robustness are unknown. The increase in the number of status changes implemented (due to the increase of demand nodes) when analysing large networks may deteriorate the convergence properties of the algorithm.

Kalungi and Tanyimboh (2003) developed a heuristic in which some aspects of PDA were used in a DDA environment. The technique is based on a systematic algorithm used to identify zero-flow and partial-flow nodes. The algorithm is made up of three parts executed progressively. The first part involved identifying zero-flow nodes. The network is analysed with DDA and nodes with heads less than Hn_i^{min} (the head at node *i* below which the outflow is zero) were identified and their flows fixed to 0. The second and third parts involved the identification of Partial-flow nodes, i.e. nodes with head between Hn_i^{min} and Hn_i^{des} (desired head at node *i* for achieving a full demand). A heuristic is applied to obtain the updated heads of these nodes. The system of head-equations is then converted into a system of head-flow equations (where both nodal heads and pipe flows are unknown basic variables) and nodal flows are obtained. Using the available information (nodal heads and pipe flows), the network analysis is repeated. The algorithm terminates when no pressure deficient (zero flow and partial flow) nodes remain. Interested readers may consult their publications for additional details.

Tanyimboh and Templeman (1995) and Tanyimboh and Tabesh (1997) developed a method based on the relationship between the source head and the network discharge. The basic formulation is expressed as

$$H_s = H_s^{\min} + R_s (Q_s^{avl})^{n_s} \tag{2.43}$$

where H_s is the available head at the source, Q_s^{avl} is the total flow from all demand nodes, R_s is the resistance constant and the exponent n_s was taken as 2. H_s^{min} represents the source head at which the most critical node of the network begins to deliver water. Algebraic manipulation of Eq. 2.43 will give

$$Q_s^{avl} = \left(\frac{H_s - H_s^{\min}}{R_s} \right)^{\frac{1}{n_s}} \tag{2.44}$$

The sum of all available nodal flow is equal to the required demand i.e. $Q_s^{avl} = Q_s^{req}$ when $H_s = H_s^{des}$. H_s^{des} is the desired source head to satisfy all nodal demands in full. It is the sum of head losses (obtained from DDA) in links along a path from the source to the most critical node. Substituting H_s and Q_s^{avl} in Eq. 2.43 with H_s^{des} and Q_s^{req} gives

$$H_s^{des} = H_s^{\min} + R_s (Q_s^{req})^{n_s} \tag{2.45}$$

From Eq. 2.45, an expression for R_s is obtained and applied into Eq. 2.44 to give the source head-discharge relationship for the source head method (SHM).

$$Q_s^{avl} = Q_s^{req} \left(\frac{H_s - H_s^{\min}}{H_s^{des} - H_s^{\min}} \right)^{\frac{1}{n_s}} \qquad H_s^{\min} \le H_s \le H_s^{des} \tag{2.46}$$

This formulation is straight forward and computationally efficient. It provides a fairly good depiction of a pressure deficient network compared to DDA. However, as stated earlier, DDA often underestimates the performance of a pressure deficient network. SHM is based solely on DDA results and consequently, H_s^{des} obtained tends to be higher than its actual value, leading to an underestimation of Q_s^{avl} as observed in Tanyimboh et al. (2001). This method is limited to single source network.

Tabesh (1998) improved the SHM formulation and termed it as the Improved Source Head Method (ISHM). The derivation of the ISHM is essentially the same as the SHM. However, unlike SHM which estimates the network outflow based on the critical node alone, the ISHM considers every demand node individually and calculates its flow as follows

$$Q_j^{avl} \approx Q_j^{req}\left(\frac{H_s - H_s^{\min}}{H_{s,j}^{des} - H_s^{\min}}\right)^{\frac{1}{n_j}} \tag{2.47}$$

where exponent n_j varies between 1.5 and 2 (Gupta and Bhave, 1996). $H_{s,j}^{des}$ is the head required at the source to fully satisfy the demand at node j and is obtained by summing the nodal elevation with the total head losses in pipes (obtained using DDA) connecting node j to the source. Tanyimboh et al. (2001) demonstrated that ISHM generated far more accurate results whilst retaining the computational efficiency of the SHM. Also, the method is applicable to both single and multi-source networks. One major setback of this algorithm is that the exponent, n_j used requires a considerable amount of effort in field data collection in order to be accurately calibrated (Tanyimboh and Tabesh, 1997).

Most of the methods mentioned involve cumbersome algorithms with repetitive use of DDA to successively adjust specific parameters until a sufficient hydraulic consistency is obtained. This can lead to high computational requirement and may present difficulties to be effectively implemented for large networks.

2.6.2 Methods Involving Head-Flow Relationship

Head-flow relationships (HFRs) are functions used to estimate the actual flow at demand nodes based on the nodal pressure e.g. Tanyimboh and Templeman (2010), Udo and Ozawa (2001), Germanopoulos-Gupta-Bhave (Germanopoulos, 1985; Gupta and Bhave, 1996), Wagner et al. (1988), etc. In general, these formulae have been defined on the basis that nodal demand is satisfied in full when the nodal head is equal to or greater than the desired head and zero when the nodal head is equal to or lower

than the minimum head. The HFR is directly embedded in the system of hydraulic equations. As such, the non-linear constitutive equations are solved only once, unlike the former PDA approaches (Section 2.6.1) which involves iterative DDA simulations. A review of HFRs available from the literature is presented next.

Reddy and Elango (1989) suggested a head-dependent flow relationship that can be expressed by

$$Hn_i = Hn_i^{\min} + R_i (Qn_i)^2 \tag{2.48}$$

As observed in Eq. 2.48, flow at node is unrestricted i.e. Qn_i may be greater than Qn_i^{req}.

Wagner et al. (1988) and Chandapillai (1991) developed a parabolic function which is expressed as

$$Hn_i^{des} = H_i^{\min} + R_i (Qn_{i.}^{req})^{n_e} \tag{2.49}$$

where R_i is the resistance constant and n_e is an exponent. Hence

$$Qn_i = Qn_i^{req} \qquad Hn_i \geq Hn_i^{des} \tag{2.50}$$

$$Qn_i = Qn_i^{req} \left(\frac{Hn_i - Hn_i^{\min}}{Hn_i^{des} - Hn_i^{\min}} \right)^{\frac{1}{n_e}} \qquad Hn_i^{\min} \leq Hn_i < Hn_i^{des} \tag{2.51}$$

$$Qn_i = 0 \qquad Hn_i \leq Hn_i^{\min} \tag{2.52}$$

where Qn_i and Qn_i^{req} are the available outflow that can be delivered by the system and the required supply or demand at node i respectively; Hn_i is the actual head at node i; $Hn_i^{\min}$ is the nodal head at node i below which the outflow is zero; Hn_i^{des} is the desired head at node i for achieving a full demand satisfaction, i.e. the outflow is

equal to the demand. The value of the exponent parameter, n_e vary between 1.5 and 2 (Gupta and Bhave, 1996).

Fujiwara and Ganesharaja (1993) considered the pressure dependent outflow and proposed the following function

$$Qn_i = Qn_i^{req} \frac{\int_{Hn_i^{\min}}^{Hn_i} \left(H - Hn_i^{\min}\right)\left(Hn_i^{des} - H\right)dH}{\int_{Hn_i^{\min}}^{Hn_i^{des}} \left(H - Hn_i^{\min}\right)\left(Hn_i^{des} - H\right)dH} \qquad Hn_i^{\min} \le Hn_i < Hn_i^{des} \tag{2.53}$$

The above function is capable of analysing any network. However, it is not straight forward and may be computationally more expensive.

Germanopoulos (1985) approximated the available nodal flow for a pressure deficient network using the following equation.

$$Qn_i = Qn_i^{req}\left(1 - b_i\, e^{-c_i\,[\frac{\Pr_i}{\Pr_i^{\#}}]}\right) \tag{2.54}$$

where b_i and c_i are coefficients to be calibrated for node i. Pr_i is the available pressure at node i and $Pr_i^{\#}$ is the pressure at which a proportion of the required demand of node i is supplied. In the absence of field data, the suggested values of b_i and c_i are 10 and 5 respectively and $Pr_i^{\#}$ is taken as the pressure to satisfy 93.2% of the required nodal demand. Eq. 2.54 contains several weaknesses in that $Qn_i \neq 0$ when $Hn_i = Hn_i^{min}$ and $Qn_i \neq Qn_i^{req}$ when $Hn_i = Hn_i^{req}$. An improvement by Gupta and Bhave (1996) was made to the formulation to cater for the mentioned weaknesses. The modified head-outflow relationship is expressed as

$$Qn_i = Qn_i^{req}\left(1 - 10^{-c_i\left[\frac{Hn_i - Hn_i^{\min}}{Hn_i^{des} - Hn_i^{\min}}\right]}\right) \tag{2.55}$$

Udo and Ozawa (2001) proposed a pressure-nodal flow relationship as follows

$$Qn_i = 0 \qquad \text{if } (Hn_i - Hn_i^{\min}) \le 0 \tag{2.56}$$

$$Qn_i = 0.0189 Qn_i^{req} (Hn_i - Hn_i^{\min})^2 \qquad \text{if } 0 < (Hn_i - Hn_i^{\min}) \le 6.4176m \tag{2.57}$$

$$Qn_i = Qn_i^{req}\left(\frac{\tan^{-1}[1.3(Hn_i - Hn_i^{\min} - 9.5)]}{\pi} + 0.5 \right) \qquad \text{if } 6.4176m < (Hn_i - Hn_i^{\min}) \le 12.582m \tag{2.58}$$

$$Qn_i = Qn_i^{req}[1 - 0.0189(Hn_i - Hn_i^{\min} - 19)]^2 \qquad \text{if } 12.582m < (Hn_i - Hn_i^{\min}) \le 19.0m \tag{2.59}$$

$$Qn_i = Qn_i^{req} \qquad \text{if } (Hn_i - Hn_i^{\min}) > 19.0m \tag{2.60}$$

where Hn_i^{min} corresponds to the nodal elevation. This formulation lacks the flexibility to incorporate different Hn_i^{des} values (Hn_i^{des} is fixed to 19m).

Based on the Logit function, Tanyimboh and Templeman (2004, 2010) suggested a nodal outflow function which is defined as follows

$$Qn_i = Qn_i^{req} \frac{\exp(\alpha_i + \beta_i Hn_i)}{1 + \exp(\alpha_i + \beta_i Hn_i)} \tag{2.61}$$

where both α_i and β_i are parameters to be calibrated with relevant field data. Dividing Eq. 2.61 by Qn_i^{req} would give

$$\frac{Qn_i}{Qn_i^{req}} = \frac{\exp(\alpha_i + \beta_i Hn_i)}{1 + \exp(\alpha_i + \beta_i Hn_i)} \tag{2.62}$$

The term Qn_i/Qn_i^{req} represents the nodal demand satisfaction ratio (DSR). The nodal DSR value is 1.0 when Hn_i is larger or equal to Hn_i^{des}, and zero when Hn_i is less or equals to $Hn_i^{\min}$. In other words, a nodal DSR value of 1.0 means the nodal demand is fully satisfied and a nodal DSR value of 0 means that there is no nodal outflow.

Both parameters α_i and β_i are essential in determining the outflow. Changing these values would alter the gradient or steepness of the function curve. In the event of the no field data, Tanyimboh and Templeman (2010) suggested substituting Eq. 2.62 with DSR values of 0.001 and 0.999, representing scenarios when Hn_i is less than $Hn_i^{\min}$ and when Hn_i achieves Hn_i^{des} respectively to give

$$Qn_i(Hn_i^{req}) = 0.999Qn_i^{req} \tag{2.63}$$

$$Qn_i(Hn_i^{\min}) = 0.001Qn_i^{req} \tag{2.64}$$

Eq. 2.63 and Eq. 2.64 above describe the conditions for virtually full and zero demand satisfaction respectively. Simultaneously solving both equations will give

$$\alpha_i = \frac{-4.595Hn_i^{req} - 6.907Hn_i^{\min}}{Hn_i^{req} - Hn_i^{\min}} \tag{2.65}$$

$$\beta_i = \frac{11.502}{Hn_i^{req} - Hn_i^{\min}} \tag{2.66}$$

One common weakness observed in most of these HFRs is the absence of continuity in the function and/ or their derivatives at the transitions between zero and partial nodal flow and/or between partial and full demand satisfaction. These discontinuities can lead to convergence difficulties in the computational solution of systems of constitutive equations (Tanyimboh and Templeman, 2010). By contrast, the Tanyimboh and Templeman (2004, 2010) HFR and its derivative have no discontinuities and is believed to be a reasonable approximation to the node pressure-flow relationship. Also, the derivative for this function can be easily calculated. These

characteristics make it ideal to be incorporated effectively into the system of equations without much computational complications. For this reason, the Tanyimboh and Templeman (2004, 2010) function has been utilised in this research.

The basic form of the Tanyimboh and Templeman (2004, 2010) function is illustrated in Fig. 2.1. This function obviates the need for the extra conditions $Qn_i(Hn_i \le Hn_i^{\min}) = 0$ and $Qn_i(Hn_i \ge Hn_i^{req}) = Qn_i^{req}$, thus providing a smooth transition between zero and partial nodal outflow and between partial and full demand satisfaction as depicted in Fig. 2.1. Without discontinuities in the function and derivatives, convergence difficulties are evaded in the computational solution of the system of constitutive equations.

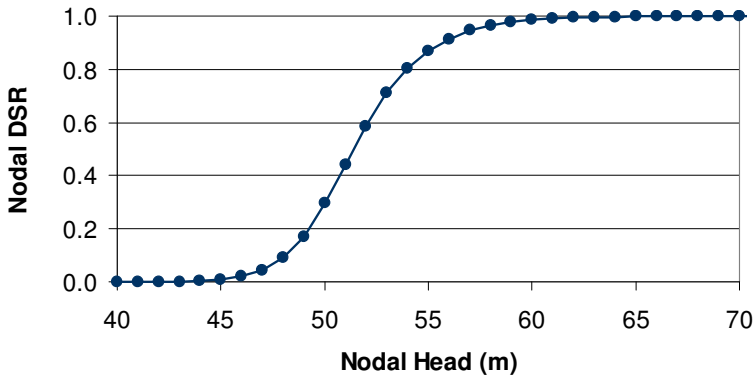

Figure 2.1. Typical nodal performance curve
(Hn_i^{min}=45m, Hn_i^{des}=60m)

Several PDA works have been carried out based on the HFR approach and are presented in the following paragraphs.

Ackley et al. (2001) formulated the pressure-dependent analysis as an optimization model where the sum of nodal outflows was maximized. The Wagner et al. (1988) head-flow relationship was utilised in this work. They also developed a straightforward yet highly robust technique to verify the accuracy of the pressure-dependent results generated since nodal flows computed by the PDA are less and at times vastly different from the corresponding required demands when analyzing pressure deficient networks. They proposed entering the nodal flows obtained from the PDA program into an ordinary DDA program as nodal demands. With all other

parameters remaining unchanged (i.e. nodal elevations, pipe diameter, length and roughness), the DDA program is then executed. Subject to round off error, the resulting set of DDA based nodal heads and pipe flows will be identical to the corresponding nodal heads generated by the PDA program only if the PDA outflows used were accurate. This validation technique works brilliantly in practice and has been incorporated in numerous studies, e.g. Ackley et al. (2001), Tanyimboh et al. (2003), Kalungi and Tanyimboh (2003), Siew and Tanyimboh (2010). This method has been employed in this study and gave excellent results as demonstrated later in Chapter 4.

Tanyimboh and colleagues (i.e. Tanyimboh, 2008; Tanyimboh and Templeman, 2004, 2010; Tanyimboh, Tahar and Templeman, 2003; and Ackley et al., 2001) developed a robust PDA model based on the Newton-Raphson scheme. The prototype FORTRAN computer model is termed as the Program for the Realistic Analysis of the Availability of Water Distribution Systems (PRAAWDS). PRAAWDS offers a choice of four pressure flow relationships to choose from for the PDA analysis, i.e. the Wagner et al. (1988), Germanopoulos-Gupta-Bhave (Gupta and Bhave, 1996), Fujiwara and Ganeshrajah (1993) and Tayimboh and Templeman (2004) functions and also allows users to simulate the network using DDA for comparison purposes. It has a built in feasibility evaluation feature (based on Ackley et al., 2001) to verify the accuracy of the PDA results generated. It has been employed in many studies relating to hydraulic reliability and redundancy e.g. Setiadi et al (2005), Tanyimboh and Setiadi (2008a, b) and has proven to be highly robust and accurate. Many real life networks have been successfully analyzed in Shan (2004). It is user-friendly and simple to utilise. PRAAWDS has been effectively used as one of the tools for validating the accuracy of the results generated by the developed PDA simulator in the current research as presented later in Chapter 4.

Giustolisi et al. (2008b) embedded the Wagner et al. (1988) equation into the Global Gradient Method (GGM) and presented results for two networks which consist of pipes only. The performance of the PDA simulator for analysing networks with pumps and valves was not included. In Giustolisi et al. (2008a), the hydraulic performance of a single source WDS was assessed over 24 hours using PDA with values of the required nodal head (for full demand satisfaction) that varied according

to the diurnal demand pattern. However, at least for water utilities within the UK, the prescribed level of service is fixed and does not vary throughout the day or night (OFWAT, 2004).

Wu et al. (2009) also modified the GGM to incorporate pressure dependent demand. The pressure outflow relationships used were expressed as

$$Qn_i = 0 \qquad Hn_i \le 0 \tag{2.67}$$

$$Qn_i = Qn_i^{req}\left(\frac{Hn_i}{Hn_i^{req}}\right)^{\beta} \qquad Hn_i < Hn_i^t \tag{2.68}$$

$$Qn_i = Qn_i^{req}\left(\frac{Hn_i^t}{Hn_i^{req}}\right)^{\beta} \qquad Hn_i \ge Hn_i^t \tag{2.69}$$

where Hn_i represents the pressure head for node i. Hn_i^t represents the pressure threshold above which the nodal flow is independent of the pressure. Demand nodes with pressure larger than Hn_i^t will have outflow above Qn_i^{req}. β is the exponent of the pressure demand relationship. However, unlike EPANET 2, the PDA model used was commercial software the details of which are not in the public domain.

Tabesh (1998) and Tanyimboh et al. (2001) developed a method based on the Newton-Raphson method to solve for pressure dependent flows and termed it Head-Driven Simulation Method (HDSM). The Wagner et al. (1988) equation was used. A step-length adjustment parameter (SAP) is incorporated into the H-equations to give

$$Hn_i^{k+1} = Hn_i^k + \psi \Delta Hn_i^k \tag{2.70}$$

where ψ represents the SAP. The Newton-Rapson method, though computationally advantageous has the tendency to wander in the wrong search direction if a correction step taken is too big a size resulting in convergence failure. Hence, the SAP ensures that the head correction step taken is suitable, resulting in faster convergence and

eliminates oscillation in the algorithm. However, determining the SAP is not a straightforward task. Values of this step length adjustment parameter are problem (network and node) specific and difficult to ascertain. Their determination required a considerable amount of trial and error.

2.7 PERFORMANCE ASSESSMENT OF WATER DISTRIBUTION SYSTEMS

Abnormal operating conditions caused by scenarios such as pipe bursts, pump failure, planned system maintenance, the need for fire-fighting demands, etc will subject the WDS to pressure deficiency. A well-designed urban WDS should be able to cope with these occurrences while maintaining a satisfactory water supply performance to the customers. The conventional method in the WDS design is often approached as a least cost optimization problem. Head surpluses at demand nodes are seen as wasted network capacity and are generally undesirable. The least-cost approach solely emphasizes on the economic aspects, leading the optimization algorithm to configure layouts with as few pipes as possible. Final solutions obtained are branch like networks in which each demand node is linked to the source via a single path. Suppose an upstream pipe experiences failure and is removed from the system, the water supply to all demand nodes located downstream will be interrupted until the repair is completed. This type of network layout is highly undesirable.

Along with cost savings, the performance assessment of a water distribution system is crucial to determine the capability of the network design in meeting the required expectations during both normal and abnormal operating conditions. A balance between cost and reliability is essential in the WDS design. In recent years, the research interest has shifted to optimize the design of WDS considering the trade-off between cost and performance measure. Most of the studies focused on the optimization of looped networks. Unlike branched networks, a looped configuration has more than one path for water to reach the demand nodes. This provides more flexibility and enables the system to cope better in emergency situations such as fire fighting, failure of pipes or other component. For example, in the event of an

upstream pipe failure, the damaged pipe can be isolated for repair works with little impact on the demand nodes outside that area. Hence, a looped network though higher in cost is viewed to be more cost effective taking into consideration the additional level of reliability and redundancy provided.

Network reliability is probably the most widely used performance measure. It is a performance measure which emphasizes more the hydraulic aspects and less of the network robustness in terms of its layout. However, in practice, there is no universally agreed definition for WDS reliability to date. Herein, the definition of reliability is adopted from Tanyimboh and Templeman (2000), i.e. the statistical measure of the system's ability to fulfil on average the required nodal demands at adequate pressure whilst considering both normal and abnormal operating conditions. Because the reliability is essentially related to the network layout and its calculation requires a series of pipe failure simulations, reliability considerations significantly increases the complexity of the optimization problem.

Another equally important parameter which is often neglected is the network redundancy. Network redundancy assesses the robustness of the network with respect to the layout in a more effective manner. Redundancy exists in layouts with alternative pathways from the source to demand nodes or networks which have surplus capacity during normal operating conditions which can be used to maintain its desirable performance level during critical operating conditions. Similarly to reliability, the redundancy measure is difficult to quantify. Tanyimboh and Templeman (1998) were probably the only researchers who mathematically formulated the redundancy measure in a rigorous manner and termed it failure tolerance. It is essentially a reliability measure which only considers periods in which one or more components are out of service. As such, it has the potential to reveal any faults or weaknesses which may not be obvious from the network reliability parameter alone.

In the subsequent Sections 2.7.1 and 2.7.2, the formulation of key performance assessment parameters implemented in this work i.e. the reliability and failure tolerance are outlined. It will become vivid that the inclusion of performance assessment elevates the optimization problem to another level of difficulty. This is

followed by a brief review on several performance surrogates measures which are widely used in the literature. This thesis will not delve into much details of this aspect as it only makes up a small part of the research carried out herein.

2.7.1 Reliability

Considering only cost minimization (as a single objective) during the optimization of a WDS inherently removes redundancy (spare capacity) which therefore causes the system to be vulnerable when subjected to critical operating conditions. A more practical approach is to consider the WDS reliability as well. There are two major types of failures in WDSs, i.e. mechanical failure and hydraulic failure and hence, a comprehensive reliability assessment should involve both mechanical reliability and hydraulic reliability. The mechanical reliability essentially quantifies the probability that a particular component (such as a pipe, valve or pump) or system is operational at any time whereas the hydraulic reliability is the probability that the system is capable of supplying the adequate amount of water at the desired pressure.

2.7.1.1 Mechanical Reliability Calculation

The probability *p(0)* that the network is fully connected and no pipe is out of service (Tanyimboh and Templeman, 1998) can be calculated as

$$p(0) = \prod_{l=1}^{Nl} a_l \tag{2.71}$$

where a_l represents the mechanical reliability of link l or the probability that link l is available. The pipe availability can be approximated using several formulae from the literature e.g. the formula developed by Cullinane et al. (1992) as follows

$$a_l = \frac{0.21218 D_l^{1.462131}}{0.00074 D_l^{0.285} + 0.21218 D_l^{1.462131}} \qquad \forall l \in Nl \tag{2.72}$$

where D_l is the pipe diameter in inches.

2.7.1.2 Network Reliability Calculation

The hydraulic reliability formulation used is taken as the mean value of the ratio of the available flow to the required flow (Tanyimboh and Templeman, 2000) and is obtained as

$$R = \frac{1}{Qn^{req}}\left(p(0)Qn(0) + \sum_{m_1=1}^{M} p(m_1)Qn(m_1) + \sum_{m_1=1}^{M-1}\sum_{m_2=m_1+1}^{M} p(m_1,m_2)Qn(m_1,m_2) + \ldots \right) + \frac{1}{2}\left(1 - p(0) - \sum_{m_1=1}^{M} p(m_1) - \sum_{m_1=1}^{M-1}\sum_{m_2=m_1+1}^{M} p(m_1,m_2) - \ldots \right) \tag{2.73}$$

where R represents the hydraulic reliability; M is the number of links in the network i.e. pipes, valves and pumps; $p(0)=a_1a_2a_3\ldots a_M$ is the probability that all links are in service; a_{m_1} is the probability that link m_1 is in service and values used herein are based on Cullinane et al. (1992); $p(m_1) = p(0)(u_{m_1} / a_{m_1})$ is the probability that only link m_1 is not in service; $u_{m_1} = 1 - a_{m_1}$ is the probability that link m_1 is unavailable; $p(m_1, m_2) = p(0)(u_{m_1} / a_{m_1})(u_{m_2} / a_{m_2})$ is the probability that only links $m_1$and m_2 are not in service; $Qn(0)$, $Qn(m_1)$, and $Qn(m_1, m_2)$ are, respectively, the total flows supplied with all links in service, only link m_1 out of service, and only links m_1 and m_2 out of service.

The calculation of reliability (Eq. 2.73) consists of two parts. The first represents the proportion of the total demand satisfied on average subjected to multiple component failures. In practice, it is impossible to simulate all possible configurations of component failure due to the expensive computational demand. Hence, the first term tends to under-estimate the actual reliability measure. The second part essentially compensates for the underestimated amount, thus improving the final reliability estimate. An assessment of the terms in the second part shows that its value decreases with the increase of multiple-component failures considered. Including the second

part does not impede the computational efficiency as it only involves pipe availabilities data which do not require any additional hydraulic simulations.

The calculation of reliability used in this thesis only considers single pipe failure scenarios since the probability of more than one pipe being unavailable at any one time is in general very low. PDA has been used to simulate the pipe closures for the reliability calculations herein. Pipe closures subject the WDS to deficiencies in terms of network pressure and flows and PDA simulations are essential to obtain the network performance which would lead to accurate reliability assessments. It is assumed that the pipes can be isolated individually for demonstration purposes. In practice the calculations can be carried out by isolating groups of pipes using information on the actual valve locations. It is worth reiterating that the conventional DDA is unsuitable for pressure deficient operating conditions.

2.7.2 Failure Tolerance

Tanyimboh and Templeman (1998) developed the failure tolerance (*FT*) concept for quantifying the WDS redundancy. They noted the importance of carrying out another separate analysis of the WDS behaviour (in addition to the reliability assessment) that only considers situations at which components are unavailable since most systems are expected to perform to their expected level under normal operating conditions. Doing so reveals weaknesses which may not be evident from the hydraulic reliability parameter alone. The failure tolerance can be calculated as

$$FT = \frac{R - p(0)Qn(0)/Qn^{req}}{1 - p(0)} \tag{2.74}$$

The calculation of *FT* is normally carried out right after the reliability measure is obtained. Its formulation is straightforward and does not involve further hydraulic simulations. As such, no significant computational burden is imposed with the inclusion of this parameter.

Overall, the *FT* measure provides an estimate of the total demand the WDS is capable of delivering when some components are out of service. A low value of *FT* corresponds to a low level of redundancy which directly indicates that the WDS is highly vulnerable when subjected to component failure. The importance of including *FT* in addition to reliability for a better representation of the network performance has been demonstrated in Tanyimboh and Kalungi (2008, 2009).

2.7.3 Surrogate Reliability Measures

Due to the high computational demands required in computing the network reliability, numerous researchers have resorted to using surrogate measures to represent the reliability measure in the optimization problem. Todini (2000) proposed the concept of resilience index as a surrogate reliability measure. The resilience index is the ratio of the sum of the actual power dissipated in the network to the total power dissipated in order to meet the required nodal demands and heads of the network. Hence, the resilience index essentially measures the available surplus (additional) energy that can be used to cope with abnormal operating conditions and is expressed as

$$RI = \frac{\sum_{i=1}^{n_n} Qn_i^{req}\left(Hn_i - Hn_i^{req}\right)}{\sum_{k=1}^{n_r} Qn_k Hn_k + \sum_{j=1}^{n_{pu}} P_j \Big/ \gamma - \sum_{i=1}^{n_n} Qn_i^{req} Hn_i^{req}} \tag{2.75}$$

where *RI* represents the resilience index; Qn_k and Hn_k are the supply and head of reservoir k respectively; P_j is the power introduced by pump j to the network; γ is the specific weight of water; n_{pu}, n_n and n_r are respectively the number of pumps, demand nodes and reservoirs.

Jayaram and Srinivasan (2008) queried the suitability of the resilience index in measuring the performance of a network with multiple sources. They brought out the fact that a high power input (i.e. from reservoirs and pumps) would contribute to more internal surplus power. However, since the power input is part of the denominator of Eq. 2.75, the calculation of resilience index will be low for a multi-sourced network

with lots of surplus power. As such, they suggested a modified resilience index (*MRI*) which was expressed as

$$MRI = \frac{\sum_{i=1}^{n_n} Qn_i^{req}\left(Hn_i - Hn_i^{req}\right)}{\sum_{i=1}^{n_n} Qn_i^{req} Hn_i^{req}} \times 100 \tag{2.76}$$

Prasad and Park (2004) pointed out that the consideration of surplus power alone was not sufficient to represent the network reliability. They extended the resilience index formulation to include the effects of reliable loops. They stated that reliable loops can be ensured if pipes connected to a node are not widely varying in diameter. They introduced a "node uniformity" measure to quantify the uniformity of the pipes connected to the node. The node uniformity was defined as the ratio of the average diameter of the pipes to the maximum pipe diameter. This extension was termed as network resilience (*NR*) and can be expressed as

$$NR = \frac{\sum_{i=1}^{n_n} C_i Qn_i^{req}\left(Hn_i - Hn_i^{req}\right)}{\sum_{k=1}^{n_r} Qn_k Hn_k + \sum_{j=1}^{n_{pu}} P_j \Big/ \gamma - \sum_{i=1}^{n_n} Qn_i^{req} Hn_i^{req}} \tag{2.77}$$

where C_i is the uniformity of node i.

Extensive research has shown that there exists a strong correlation between the statistical entropy and reliability, i.e. hydraulic reliability increases as entropy of pipe flow rates increases (Setiadi et al., 2005; Tanyimboh et al., 2010). Several researchers have effectively applied this reliability surrogate in their WDS optimization model (e.g Prasad and Tanyimboh, 2008). The flow entropy is a measure of the uniformity of the pipe flow rates. Tanyimboh and Templeman (1993) developed the WDS entropy function that enabled pipe flow rates to be interpreted in a probabilistic way. For a network with known pipe flows and directions, the entropy function can be expressed as

$$S = S_0 + \sum_{i=1}^{N_j} P_i S_i \tag{2.78}$$

where S represents the WDS entropy value; S_0 is the entropy of source supplies; S_i is the entropy of node i; and P_i is the fraction of the total flow through the network that reaches node i and is calculated as

$$P_i = \frac{Q_i}{Qn^{req}} \tag{2.79}$$

where Q_i is the total flow reaching node i; and Qn^{req} is the sum of the nodal demands. The entropy of the source supplies is given by

$$S_0 = -\sum_{k=1}^{N_s} \frac{Q_k}{Qn^{req}} \ln\left(\frac{Q_k}{Qn^{req}}\right) \tag{2.80}$$

where Q_k is the flow that source node k contributes; and N_s is the number of source nodes. Similarly the entropy of demand nodes is given by

$$S_i = -\frac{Qn_i}{Q_i} \ln\left(\frac{Qn_i}{Q_i}\right) - \sum_{ij \in ND_i} \frac{Q_{ij}}{Q_i} \ln\left(\frac{Q_{ij}}{Q_i}\right) \tag{2.81}$$

where Qn_i is the demand at node i; Q_{ij} is the pipe flow from node i to node j; and ND_i is the set of all pipe flows emanating from node i.

Tayimboh et al. (2010) assessed the correlation of surrogate reliability measures (i.e. statistical entropy, resilience index, modified resilience index and network resilience index) in relation to the network reliability and failure tolerance. A total of 137 network designs were involved in this study and pressure dependent analysis was used to enable accurate simulations of pressure deficient scenarios. Correlation plots were generated and compared. It was demonstrated that entropy distinctly outperformed the other surrogate reliability measures in terms of consistency of results. As a whole, entropy correlated well with both reliability and failure tolerance. However, plots of

other surrogate measure against reliability and failure tolerance showed a lot more scatter and counterintuitive results were observed, i.e. the increase of reliability and failure tolerance with the decrease of the surrogate measure values

Statistical entropy has been utilised in this research as a means of efficiently incorporating reliability within the optimization. This approach is applied in the optimal long term upgrading and rehabilitation work (presented in Chapter 7). Results generated further reinforced Setiadi et al. (2005) and Tanyimboh et al. (2010), strengthening the evidence that entropy is indeed strongly correlated to reliability and serves as excellent reliability surrogate measure.

2.8 CONCLUSIONS

The hydraulic analysis is a powerful, multi-purpose tool in providing assistance to engineers during the process of designing a water distribution system (WDS). The network model simulates the operations of the system allowing the performance of a proposed network design to be evaluated and anticipated problems solved before the project is implemented in real life.

This chapter has presented the fundamentals of the WDS model which includes the governing equations and the formulation of the system of non-linear hydraulic equations. Along with this, a review of several numerical methods for solving these equations iteratively has been done. Two methods of hydraulic analysis were presented. The limitations of the conventional demand driven analysis (DDA) method in simulating pressure deficient networks along with the importance of pressure dependent analysis (PDA) were clearly highlighted. The various approaches from the literature used to model PDA have been discussed.

The WDS may be subjected to pressure deficiency due to circumstances such as pipe bursts, pump failure and the unavailability of components due to planned system maintenance. Network performance assessments are essential to gauge the capability of the distribution network to supply water under these situations. Two performance

assessment parameters have been detailed, namely network reliability and failure tolerance. Reliability measures the hydraulic performance of the network under both normal and abnormal operating conditions where as failure tolerance assesses the redundancy of the network. The calculation of reliability is highly computationally demanding and prohibitive to be implemented into an EA optimization model. Several reliability surrogates reported in the literature have been presented for completeness.

The following chapter introduces the basic concept together with a concise review of the application of evolutionary algorithms (EAs) in the optimization of the WDS design. Advantages and shortcomings of the EA are discussed.

CHAPTER THREE

WATER DISTRIBUTION SYSTEM DESIGN OPTIMIZATION

3.1 INTRODUCTION

Water distribution systems (WDSs) are built to transport clean water from treatment plants to the community and represent an invaluable element of the infra-structure of the urban population. The construction, operation and maintenance of these systems involve a huge capital investment. Hence, the challenge faced by water companies is to design and manage these systems in the most cost-effective manner whilst ensuring that current regulatory standards of quantity, quality and pressure in the water supplied to consumers are met. This presents a complex optimization problem involving conflicting objectives, making it literally impossible for the most cost-effective design to be efficaciously established just based on engineering experience alone. The necessity and importance of incorporating optimization techniques as a decision support tool to aid practising engineers and planners in these multi-criteria problems cannot be further stressed.

Mathematical programming optimization techniques which are now classified as classical approaches were first used to optimize WDS design. These methods are highly efficient as they approach the optimization problem in a deterministic manner. However, the performances of mathematical programming methods are highly dependent on the continuity of derivatives or gradient information of the optimization problems to be solved. Thus, the formulation of these techniques can become extremely complex due to the many non-linear constraints implemented especially

while analyzing networks with many pipes as well as hydraulic components such as pumps and storage reservoirs.

Evolutionary algorithms (EAs) are stochastic optimization techniques and are formulated in an entirely different manner from classical optimization techniques. These algorithms are frequently based on nature's way of evolving and adapting to the surroundings in order to survive. Their search strategies are based extensively on the defined objective function, hence making them extremely flexible and capable of tackling highly constrained non-linear optimization problems. Also, this allows EAs to handle discrete variables, which is an important feature in the optimization of WDSs. Another striking difference between mathematical programming and EAs is that they deal with a population of solutions in every generation. This feature is advantageous as it allows EAs to be well suited to solve multi-objective optimization problems. Though large numbers of function evaluations are required in EAs, they possess the ability to converge rapidly to an optimal/ near optimal solution whilst only having to analyze a small fraction of the entire solution space, making such algorithms powerful optimization tools.

The WDS is designed to supply adequate water at sufficient pressure to customers. However, as the system ages with time, it inevitably experiences deterioration in terms of its structural and hydraulic integrity due to pipe corrosion and encrustation build-ups. This causes the WDS to be prone to pipe leakages and other problems such as low water supply pressure and water quality problems. As such, they will not be capable of meeting current standards of quantity, quality and pressure in the water supplied to consumers. In addition, the WDS is not likely to cope with the escalation in demand from population and industrial growth. Rehabilitation and upgrading of the system is crucial in meeting both current and future demands at a satisfactory service level.

Accordingly, this chapter presents a literature review of both the classical and evolutionary optimization approaches used for solving WDS problems. The disadvantages and limitations encountered by classical optimization techniques are highlighted. There exist several types of evolutionary algorithms in the literature. Amongst them, genetic algorithms (GAs) are of particular interest and will be

discussed in detail as it is being utilised in this study. An overview of the basic GA process, the nature and advantages of its implementation on WDS design is outlined. A chronology of advancements in the application of GA in water distribution system design is also presented. This includes improvements made to speed up the GA convergence rate and increase its robustness in locating optimal/ near optimal solutions. Various GA constraint handling techniques are reviewed and their short-comings discussed. Lastly, a review of several optimal rehabilitation and upgrading methods is provided. The basic concepts of these models are presented and their short-comings highlighted.

3.2 REVIEW OF OPTIMIZATION MODELS IN WATER DISTRIBUTION SYSTEMS

3.2.1 Classical Optimization Techniques

The computational complexity involved in water distribution systems (WDSs) optimization be it the laying out of a new network configuration or the upgrading and reinforcement of existing networks is exceptionally high. Simply the selection of pipe diameters (from a set of commercially available discrete diameters) to form a water supply system of least capital cost has been demonstrated to be an NP-hard problem, let alone considering multiple loading conditions, operating cost, rehabilitation options and other aspects that affect real-life networks.

Yates et al. (1984) stated that the global optimum solution to WDS design problem can only be guaranteed by means of explicit or implicit enumeration techniques such as dynamic programming. These techniques require an extremely high amount of computational time as they involve searching the entire solution space. For example, a small eight-pipe network with 10 possible pipe sizes has a total of 10^8 feasible and infeasible pipe size combinations. It is clear that the search space increases exponentially with the size of the network. This undoubtedly marks the limitations of exhaustive enumeration techniques in optimizing realistic WDSs.

Gessler (1985) suggested a selective enumeration based on a pruned search space. The technique is carried out based on experience and the global optima may be eliminated in the pruning process. Loubster and Gessler (1990) applied several heuristics to aid the search space reduction. This involved progressively storing the lowest cost feasible solution and eliminating all other solutions with higher cost. Also, pipe combinations that violate the pressure constraints are noted; all combinations that consist of the same (or smaller) pipe sizes are eliminated. Despite the aid of these guidelines, a considerable amount of computational effort was still required and there was still no absolute guarantee that the global optima would be retained.

Several researchers applied mathematical programming techniques in the design optimization of WDSs. Using non-linear programming (NLP), Su et al. (1987) optimized the design of a looped network subjected to reliability constraints while Lansey and Mays (1989) obtained the optimal design and layout for pump-operated network while considering multiple loading cases. The continuity and energy constraints were implicitly solved by a hydraulic simulator coupled to the NLP model. Yates et al. (1984) had shown that the requirement for discrete pipe diameters makes the optimization problem extremely difficult to solve using non-linear programming. Hence, the resulting NLP solutions though feasible were of continuous diameter values which were not directly applicable. Rounding the diameters up or down to the nearest discrete pipe sizes will not necessarily guarantee the optimality of the solution and can often deteriorate the quality of the solution. Moreover, the rounded solution may not even satisfy the pressure constraints and additional simulations are required to evaluate them.

Alperovits and Shamir (1977) solved the highly non-linear WDS design optimization problem by employing linear programming (LP). The problem was linearized by re-writing the pipe head loss equation such that segmental lengths of constant diameter in each link are the decision variables. The formulation is based on a set of assumed pipe flow rates. This method was termed the linear programming gradient (LPG) method .The authors optimized a network containing multiple reservoirs and pumps. However, the design obtained using this sizing methodology consisted of pipes which were made up of two-diameter segments. This type of solution is unfortunately

unsuitable for real-life implementation as the customary engineering practice is to select a single diameter for the entire length of the links.

In the LPG, to reduce the number of constraints, the nodal head constraint (which governs the feasibility of the design) was only applied to selected nodes. The selection of these nodes was carried out by trial and error and required several test runs before the algorithm was able to converge to a feasible solution. No rigorous method was proposed. Though the motivation behind this is to improve the computational efficiency, the test runs could end up being extremely time consuming (especially for large size networks). All in all, the LPG search procedure is not straight forward.

In general, the advantage of mathematical programming methods (i.e. LP and NLP) is that they are computationally very efficient as they approach the optimization problem in a deterministic manner. However, the optimality of these techniques is highly dependent on the chosen initial solution and does not guarantee that the global optimum will be obtained. Often, these search strategies get trapped in local optima, resulting in sub-optimal solutions. In addition, these algorithms are not efficient for solving problems with discrete search spaces. The disjoint feasible spaces due to the presence of constraints make it extremely difficult for these gradient-based techniques to converge to the optimum solution. The performance of these methods deteriorates with the increase in the number of constraints considered, hence limiting the size and scope of the network that can be handled. Lastly, it is difficult to extend these methods to effectively solve practical real-life engineering problems which often involve conflicting objectives. One possible way is to reformulate the multi-objective problem by combining all the objectives using weighting method and solve it as a single objective problem. However, this manner of multiple-objective optimization is rigid and lacks flexibility, yielding only a single final solution per optimization run.

3.2.2 Evolutionary Algorithms

For the past few decades, researchers have extensively applied various types of evolutionary algorithms (EAs) in the area of water resources planning and management. EAs have repeatedly proven to be powerful tools with high flexibility in solving various complex water resources problems which are nonlinear, non-convex, multi-modal and involve discrete variables for which classical optimization methods incur great difficulties or at times fail totally. These stochastic search techniques are easy to implement without mathematical complexity as their search strategy is based on objective functions and does not rely on the continuity of derivatives or gradient information. They operate on a population of solutions and hence effectively explore a vast search space of solutions, significantly increasing the chances of reaching the global optimum solution.

In reality, the optimization of WDSs involves multiple objectives which are often conflicting in nature. For example, minimizing the WDS construction cost and maximizing its reliability are both contradicting objectives to be solved simultaneously. The least-cost WDS is normally a branched network which is low in redundancy (with few or no loops) whereas a highly reliable design is well looped but expensive. The concept of the least cost network being the solely desired optimal solution is slowly fading as engineers realise the need to strike a balance between cost savings and WDS performances (e.g. network reliability and redundancy). EAs have been recognised to be well suited to solve multi-objective optimization problems. Being a population-based approach, EAs possess the ability to simultaneously search different regions of a solution space making it possible to find a diverse set of solutions for difficult problems involving non-convex, discontinuous and multi-modal solution spaces. Unlike single objective optimization, the multi-objective optimization (MOO) does not yield only a single best solution but rather a set of compromised solutions between objectives known as the Pareto-optimal set. These solutions are all of equal optimality and no solution can be deemed superior to the others. Engineers are provided with the option and flexibility to evaluate the trade-offs between different designs and decide according to the performance requirements and budget constraints.

There are various EAs applied in the optimization of WDS design. Loganathan et al. (1995) and Cunha and Sousa (1999) implemented a heuristic based on simulated annealing. Geem et al. (2002) proposed the harmony search methodology while Eusuff and Lansey (2003) developed a model based on the shuffled frog leaping algorithm. Maier et al. (2003) applied the ant colony optimization approach. Cunha and Ribeiro (2004) constructed a tabu search algorithm to obtain the least cost design of WDSs. Genetic algorithms (GAs) were used by Murphy and Simpson (1993), Dandy et al. (1996), Savic and Walters (1997), Wu et al. (2001) and Vairavamoorthy and Ali (2000, 2005). Vasan and Simonovic (2010) used an improved version of GA known as the differential evolution technique.

Amongst stochastic optimization techniques, GAs are best known for their robustness and capability in yielding optimal or near optimal solutions. GAs have been extensively applied within the WDS optimization literature. This includes pump operation scheduling (Goldberg and Kuo, 1987), network design and rehabilitation (Savic and Walters, 1997; Dandy and Engelhardt, 2001) network calibration (Vitkovsky and Simpson, 1997), water quality optimization (Munavalli and Kumar, 2003; Farmani et al., 2006) and the siting and sizing of storage reservoirs (Vamvakeridou-Lyroudia et al., 2005; Prasad, 2010). The research carried out herein involves the implementation of a GA and hence, the thesis will only focus on the development of this EA technique. Interested readers may refer to the mentioned publications for more details on the other EA techniques.

3.3 GENETIC ALGORITHMS

3.3.1 Standard Genetic Algorithm Procedure

The GA mimics the nature of biological organisms evolving genetically throughout generations to adapt to their environment and its concept is strongly based on the survival of the fittest. This search technique begins by randomly generating a population of individuals which represent potential solutions to the optimization problem. These individuals are encoded as chromosomes, each consisting of a set of

genes which are design variables (e.g. pipe sizes) that completely describe a solution. Using operators such as selection, crossover and mutation, the population is evolved for generations towards improved solutions.

During each generation, the chromosomes are evaluated with respect to the objective functions. Objective functions are aims defined at the very beginning of the GA to guide the search toward the desirable solution, e.g. cost minimization. Based on the performance exhibited, the chromosomes are each allocated a fitness value, which is a figure of merit representing how near it is to achieving the aims set.

Next, individuals are selected from the population to create a mating pool. This selection phase is facilitated by a selection operator which selects individuals based on their fitness values. Fitter individuals will be chosen over weaker ones. The reproduction phase follows next where the crossover operator is applied to combine genetic materials from the selected parent individuals (from the mating pool) to produce offspring which represent new solutions. A very small fraction of these off-spring will then be subjected to mutation.

The final phase involves selecting individuals to be brought forth to the next generation. Individuals with high fitness values will have a higher probability of being selected while weaker ones will be discarded. This in general results in the new generation having a higher fitness level on average compared the previous population. The cycle continues until a termination criterion (which in most cases is a pre-specified number of generations) is reached. The operation of the basic GA is illustrated in Fig. 3.1.

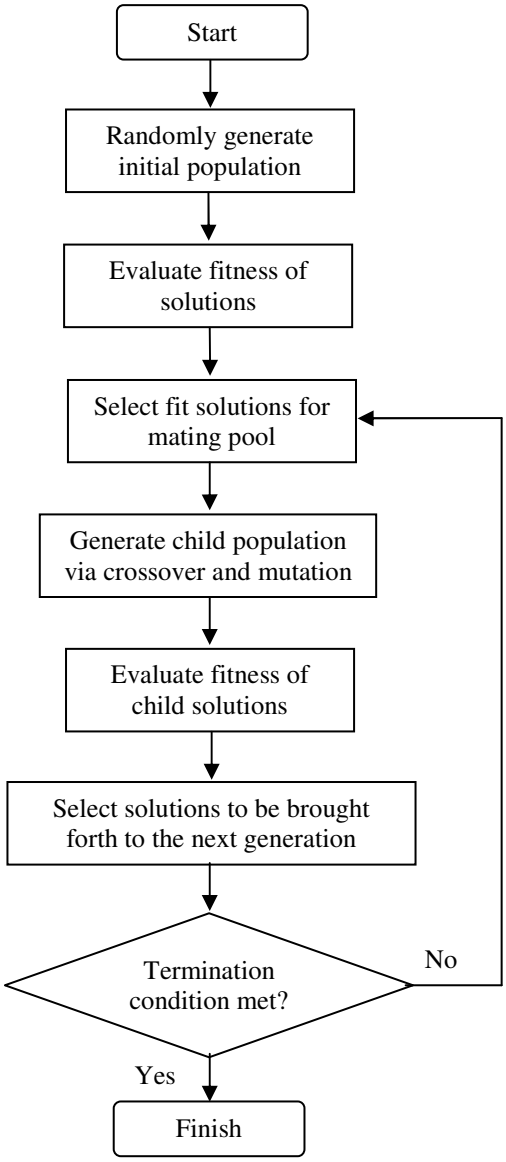

Figure 3.1 Flowchart of the basic GA operation

3.3.2 Selection Operator

There are two selection schemes commonly used in the literature namely the roulette wheel selection and the tournament selection. The roulette-wheel, also known as proportional selection was introduced by Holland (1975). Each individual in the population is represented by a slot on the roulette-wheel. The width of the slot is proportional to the fitness value of the individual. Thus, fitter individuals will tend to be favoured in the selection as the 'ball' is more likely to end up in wider slots.

Goldberg and Deb (1991) observed several drawbacks in this selection scheme such as the loss of diversity and directionless search which causes the GA to converge prematurely.

In the tournament selection proposed by Goldberg and Deb (1991), a specified number of individuals are selected from the population and their fitness compared. A common tournament size is 2. The fittest individual is the winner and will be selected to be part of the mating pool. The tournament is repeated with different individuals until the mating pool is sufficiently filled. The tournament selection is flexible in that the selection pressure can be easily tuned by adjusting the tournament size (i.e. number of competitors involved in the tournament). A large tournament, say involving 4 competitors will result in a mating pool consisting of a higher number of fitter solutions on average as compared to a smaller tournament of 2.

3.3.3 Crossover Operator

One of the key traits in the GA is the crossover operator. The crossover plays a dominant role in the reproduction phase and is usually set to have a very high probability of occurrence during the evolution process. The basic function of a crossover operator is to facilitate the exploitation of the GA search. Exploitation in this aspect essentially means making the best use of good existing solutions to reproduce even better and improved solutions. The search is thus evolved in a certain direction which not only causes the algorithm to converge more rapidly but also progressively confines the search space considered.

The basic crossover (single point crossover) takes place between two parent individuals selected from the mating pool to produce two offspring individuals. A crossover point is randomly picked and genetic materials are interchanged at the crossover point between both parents to produce two offspring as illustrated in Fig. 3.2.

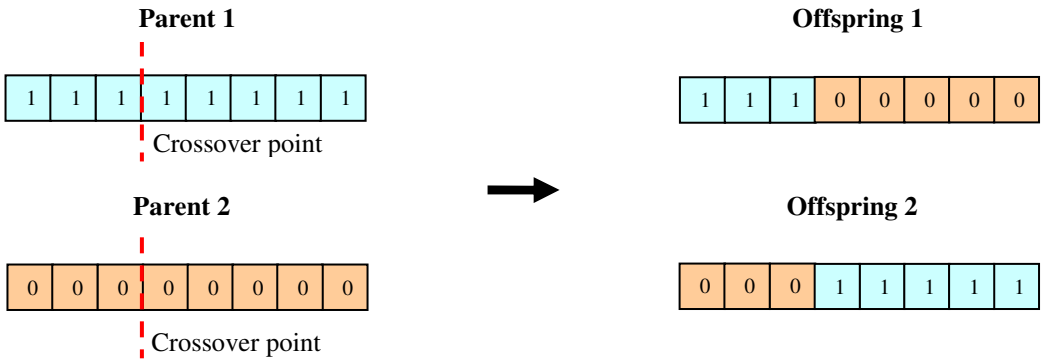

Figure 3.2 Operation of the basic GA crossover

Given that both parents are prevailing candidates from the selection process and have high fitness values, there is a good chance that the offspring may inherit the good genetic material from both sides and end up being potentially fitter than the parent solutions. There are many crossover operator variations devised such as the multi-point crossover, uniform crossover, multi-parent crossover, simulated binary crossover etc. The single point crossover is used in this research.

3.3.4 Mutation Operator

Mutation is essential to facilitate the exploration of new areas of the search space, avoiding the GA to from getting trapped at local optima. Unlike exploitation, exploration seeks to locate improved solutions by searching the solution space more extensively, evolving the algorithm in different search directions. A low mutation probability is usually used to prevent the algorithm from degenerating into a random process. There are various forms of mutation such as the displacement mutation, inversion mutation, greedy mutation etc. The basic single point mutation has been used in this work and is implemented by randomly flipping a bit within the chromosome as illustrated in Fig. 3.3.

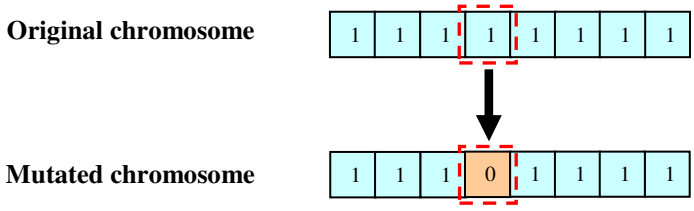

Figure 3.3 Operation of the basic GA mutation

3.3.5 Solution Representation

3.3.5.1 Binary Coding

Originally, binary coding has been used to represent solutions in GAs. Binary coding is probably the most straight-forward representation scheme where decision variables (e.g. pipe sizes) are represented by bit combinations of 0 and 1. For example, consider using 3-bit binary scheme to represent pipe sizes. This allows the representation of 8 (2^3) different pipe sizes as shown in Table 3.1.

Table 3.1. Available pipe sizes and corresponding binary code representation

Pipe sizes (in)	Binary representation
1	0 0 0
2	0 0 1
3	0 1 0
4	0 1 1
5	1 0 0
6	1 0 1
7	1 1 0
8	1 1 1

Hence, a network consisting of 4 pipes with different sizes can be represented as a chromosome with a length of 12 bits as shown in Fig. 3.4.

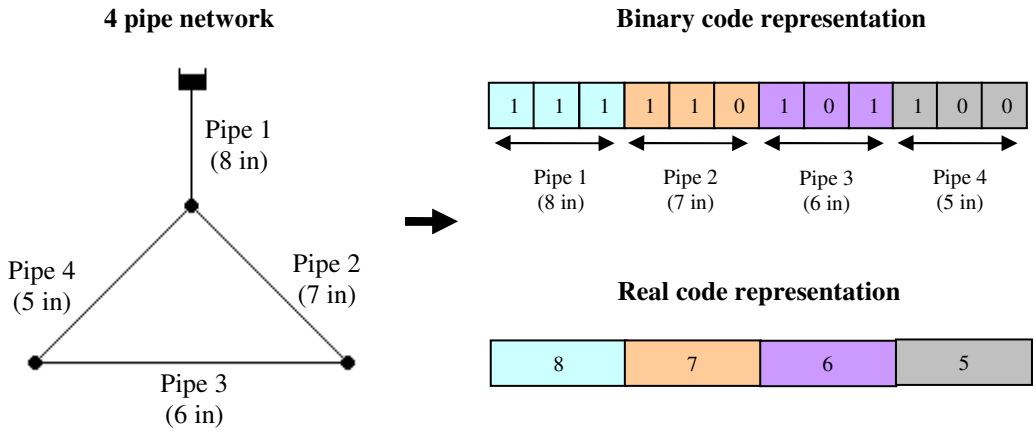

Figure 3.4 Binary and real code representation of a network solution

Binary coding is well suited for the purpose of WDS design optimization given that decision variables such as pipe sizes are of discrete values. Also, this coding method allows the mechanisms of crossover and mutation to be applied with much simplicity as demonstrated in the previous sub-section. One disadvantage associated with binary coding is the possibility of redundant codes existing. For example, if there are 14 available pipe sizes to choose from, a 4-bit representation scheme which has 16 (2^4) possible bit combination has to be used. As such, there exist two redundant bit combinations which will not correspond to any available pipe diameters. However, this problem can be easily solved by randomly remapping these two redundant substrings to any of the 14 available pipe sizes. Binary coding has been used in this research.

3.3.5.2 Gray coding

A general hypothesis is that good solutions have the tendency to lie close to each other in the solution space. However, the Hamming Cliff problem is often encountered while using conventional binary coding. The Hamming Cliff describes the effect whereby neighbouring phenotypes (pipe sizes) are represented by completely different genotypes (binary code) i.e. Hamming distance between the

genotypes is much larger than 1. The Hamming distance represents the number of positions for which the corresponding binary bits are different and is used to measure the distance between genotypes. Consider pipe sizes 4 in and 5 in which are binary coded as (0 1 1) and (1 0 0) respectively as illustrated in Table 3.1. They are neighbours in the phenotype domain but not so in the genotype domain. The Hamming distance between these pipes is 3, i.e. to mutate (0 1 1) to (1 0 0) would require three bit flips successively. Generally, the mutation probability is rather low and hence the probability of pipe size 4 in becoming 5 in is very low.

Using Gray code is an effective way to solve the Hamming Cliff problem. This coding method is essentially a rearrangement of the order of binary codes such that adjacent phenotypes would be given code combinations that differ in only one bit. For instance, the binary code representation in Table 3.1 when Gray coded will become as follows in Table 3.2.

Table 3.2. Available pipe sizes and corresponding grey code representation

Pipe sizes (in)	Binary representation
1	0 0 0
2	0 0 1
3	0 1 1
4	0 1 0
5	1 1 0
6	1 1 1
7	1 0 1
8	1 0 0

Observe that the step from the 2 in pipe to the 3 in pipe only requires the flipping of a single bit (i.e. the second bit). This goes the same for subsequent pipe sizes. In other words, the Hamming distance between every two neighbours is only 1. As such, the Hamming Cliff problem is overcome.

3.3.5.3 Real Coding

In real coding, the variables in solutions are represented by the actual value itself. In other words, the structure of the genotype space is identical to the phenotype space (solution space). Hence, the 4-pipe network can be represented as shown in Fig. 3.4. No decoding is required. This is advantageous when a large number of design variables are to be considered in an optimization problem. A bit-string representation scheme will be prohibitive to the computational efficiency as solutions will be represented by extremely lengthy chromosomes.

In addition, real coding allows the crossover and mutation mechanisms to be applied in new ways. For example, crossover can be carried out by averaging the value of both parents or weighting each child such that its genetic make-up is biased toward a particular parent, etc. As for the mutation operator, it is possible to add or subtract from an existing value of a gene (parameter) or average its value with a random number.

3.3.6 Advancements in WDS Optimization Using Genetic Algorithms

Many developments and enhancements have been carried out to improve the effectiveness and efficiency of GAs in the optimization of WDSs. These developments can be divided into several categories. The discussions and reviews are presented as follows.

3.3.6.1 Application of different coding schemes

Savic and Walters (1997) proposed the use of Gray coding as opposed to binary coding to overcome convergence problems related to the hamming cliff effect. Vairavamoorthy and Ali (2000) avoided the encoding and decoding of variables by implementing real coding. Unlike in the binary coded GAs, real coded decision variables can directly be used to compute the fitness values offering reduction in the

computational burden. Also, the problem of dealing with redundant binary codes was eliminated.

3.3.6.2 Modification to GA Operators

In later generations of the GA where the population is highly dense with good solutions, mutation plays an important role in encouraging further exploration of the search space to increase probability of finding better solutions. Instead of a fixed mutation rate throughout the search process, Kadu et al. (2008) implemented a non-uniform mutation rate where the mutation probability increases from 1% to 10% as the search proceeds.

Based on the hypothesis that good solutions have the tendency to lie close to each other, Dandy et al. (1996) proposed the use of an adjacency mutation operator along with the implementation of Gray coding. This improved mutation operator varies from the conventional bitwise mutation in that it mutates a complete decision variable substring to an adjacent decision variable substring located up or down the list of the design variable candidates, rather than randomly flipping bits from the solution string.

3.3.6.3 Reduction in Computational Effort Related to the Use of the Hydraulic Solver

A large proportion of the execution time required by the EA optimization process is contributed by the hydraulic analyses. Vairavamoorthy and Ali (2000) demonstrated a reduction in the computational time of the GA process by approximating the hydraulic behaviour of the WDS using a linear transformation function (LTF). The LTF in general is a simplified function of the non-linear hydraulic equations (derived from regression analysis of several network samples) which is much easier to solve and less computationally demanding. Since nodal pressures obtained using LTF were merely estimates of the actual results, they were checked against the continuity equations. If violation occurs, the network is solved again using a hydraulic simulator, taking the LTF results as starting solutions for the analysis. It was reported that doing so

significantly improved the convergence rate of the hydraulic simulator i.e. only one to three iterations at average were required for convergence.

3.3.6.4 Solution Space Reduction

The size of the network and the number of candidate pipes considered are factors which directly influence the effectiveness and efficiency of the GA search. The larger the size of the network and the more candidates pipes included, the wider the search space becomes leading to a delayed convergence. The computational time required is increased and the possibility of obtaining the global optimum solution is greatly reduced. Limiting the number of candidate pipe diameters involved could considerably reduce the size of the solution space. However, this has to be done in an intelligent manner as inappropriate selection of candidate pipe sizes may result in a final solution which is sub-optimal. Consider comparing two different cases where a network with 12 pipes is being optimized using 9 and 8 candidate pipe sizes respectively. The total search spaces consist of 2.81×10^{11} and 6.87×10^{10} different solutions for the former and latter cases respectively. Hence, just by eliminating one candidate diameter, the solution space is substantially reduced by 75%.

Search space reduction was attempted by Vairavamoorthy and Ali (2005) by limiting the candidate diameter for each link based on the pipe index (PI). The PI is a measure of the importance of a pipe in terms of their impact on the hydraulic performance of the network as a whole and is used to select appropriate pipe candidate sizes which would yield good feasible solutions. The PI was repeatedly updated during the GA run, gradually reducing the search space by imposing tighter bound constraints on the pipe sizes. The calculation of the PI is highly complex and involves the solution of a system of linear equations with multiple right hand terms. Hence, to calculate the PI regularly during a GA will be extremely burdensome computationally especially for a network of huge size. Noting this fact, the authors adopted a surrogate measure proposed by Arulraj and Rao (1995) which is termed as the significance index (SI). It was proposed that the PI is only used for the initial stage of the GA and is replaced by the SI as the evolution progresses.

Kadu et al. (2008) proposed a heuristic based on the critical path method to limit the number of candidate pipe sizes for each pipe. The fundamental of this concept is built on the assumption that the cheapest mode of delivering water from the source to a demand node is through the shortest available path. The approach requires determining the shortest path connecting each node to the source and using several heuristics, a continuous diameter is obtained for each link. Five commercial available pipe sizes are then selected as candidate diameters for that particular link, i.e. one being the closest discrete pipe size to the obtained continuous diameter; two are of the next smaller sizes; and the remaining two are of the next larger sizes. Indeed, the approach succeeded in obtaining the optimal solution within a great reduction of execution time. However, the examples applied to demonstrate the efficacy of this concept were small networks of 7 and 34 links. Determining the shortest path may not be as straightforward as it appears and can actually be treated as an optimization problem itself if the network considered is huge, highly looped and contain multiple sources. In addition, the critical path concept is not applicable to practical aspects of real world problems such as the rehabilitation of existing networks, networks operating under multiple operating conditions and variation in diurnal demands, the inclusion of pumps and storage reservoirs etc.

3.3.6.5 Seeding GA with Good Initial Solutions

Studies have shown that seeding the GA with good initial solutions could improve its search performance, leading to optimal solutions within a faster convergence rate (Harik and Goldberg, 2000; Hopper and Turton, 2001). With that being said, the seeding mechanism must be sufficiently efficient such that it does not incur any significant computational burden to the GA. Keedwell and Khu (2006) seeded the initial GA population with solutions generated from a computational model known as the Cellular Automaton for Network Design Algorithm (CANDA). The generated results demonstrated that the approach out-performed the basic fast non-dominated sorting genetic algorithm (NSGA II). Unlike EAs which are objective-function driven, the operation of CANDA is based on a set of rules applied to iteratively change the pipe diameters until the desired network pressure is achieved. CANDA was demonstrated to provide good solutions within a very small amount of network

simulations. However, due to its deterministic nature, the solution space explored by the algorithm is somewhat confined and the exact same solutions are repeatedly generated after a short period of execution. As such, CANDA is more suited for generating initial solutions to be fed to the GA rather than being used as a "complete" optimization model itself. Interested readers can refer to Keedwell and Khu (2006) for a detailed description of CANDA.

3.3.6.6 Modification to the GA Formulation

There exists several forms of improved GA whose basic concept remain the same but vary only in the way their operators are employed, e.g. the way the mating pool is created, how parent solutions are chosen and children population generated, the procedure for sorting and ranking of solutions, etc. For example, Halhal et al. (1997) and Wu and Simpson (2001) used messy GAs (MGAs) with variable length string representation. The algorithm is based on progressively building up the complexity of an individual by firstly identifying short strings with high fitness level (potential building blocks) and then concatenating (combining) them together to form individual solutions. MGAs were demonstrated to perform better than the standard GA.

Another type of MOGA which has been successfully applied to many aspects of the WDS optimization studies is the elitism preserving fast non-dominated sorting genetic algorithm (NSGA II) by Deb et al. (2002). The NSGA II is complimented for its efficient non-dominated sorting procedure and strong global elitist approach implemented. Both parent and child populations are combined before being sorted and ranked into several non-dominated fronts based on their non-dominance status. This ensures that all elites (from both parent and child populations) are preserved, enhancing the algorithm's ability to produce much better spread of solutions and better convergence near the optimal solutions.

The NSGA II is one of the widely used multi-objective GA in the area of WDS optimization. Jayaram and Srinivasan (2008) applied the NSGA II to solve the optimal performance based WDS rehabilitation and design problem. In the area of drinking WDS security, Preis and Ostfeld (2008) employed the NSGA II to minimize

two objectives, i.e. the consumed contaminant mass and the number of operational activity required to contain and flush the contaminant out of the system. Prasad (2010) optimized the design and upgrading of a complex WDS ("Anytown" network) involving multi-operating conditions, pump scheduling, tank siting and sizing using the NSGA II. Farmani et al. (2006) further demonstrated the effectiveness of the NSGA II by simultaneously considering two additional aspects, i.e. network reliability and water quality in solving the "Anytown" problem. Due to its proven robustness and effectiveness in locating optimal/ near optimal solutions, the NSGA II was chosen as the multi-objective optimization method for this research.

3.3.6.7 Constraint Handling and Boundary Search Methods

A major disadvantage of EAs is their inability to directly handle constraints since they were originally designed to deal with unconstrained search spaces. The implementation of constraints complicates the topology of the search spaces. Constrained decision spaces are generally multi-modal and discontinuous. This makes it more difficult for EAs to efficiently locate near optimal or optimal solutions.

The handling of constraints within the EA is not an easy task and can have a negative impact on the GA's search performance if formulated inappropriately. There exists various constraint handling methods in the literature. Rather than blindly discarding all infeasible solutions, many of the constraint handling methods have built-in mechanisms to retain near-feasible solutions (or solutions with slight infeasibility) since they usually contain majority of the good genes which are potential building blocks for the optimal solution. In other words, the search is focused at the active constraint boundaries dividing the feasible and non-feasible solution regions where the optimal/ near optimal solutions are most likely to be situated. The formulation of constraint-handling and boundary search mechanisms is an active area of research within the WDS optimization and since it is a major part of the research carried out herein, a whole section (Section 3.3.7) is dedicated to the review and discussion of these methods along with their shortcomings and is presented next.

3.3.7 Constraint Handling and Boundary Search Methods

In general, trial solutions (WDS designs) generated by an EA are simulated using a hydraulic simulator and the resulting nodal heads are evaluated based on the pressure constraint requirements. Solutions that violate the pressure constraints are considered as infeasible. However, a major disadvantage of EAs is that they are unable to directly handle constraints. In other words, EAs are incapable of differentiating feasible solutions from non-feasible ones. The majority of the WDS EA optimization work in the literature use the penalty function approach to handle pressure constraints (e.g. Savic and Walters, 1997). In this method, an additional penalty cost is applied to the actual WDS cost of the infeasible solution. The penalty cost is usually calculated using penalty parameters which are formulated such that greater constraint violations incur higher penalty costs. In this way, the probability of solutions being discarded in the next generation will depend on their degree of constraint violation.

The optimal solution heavily depends on the penalty structure. A large penalty cost inherently restricts the EA search to the feasible region of the solution space potentially resulting in very expensive and highly redundant solutions. On the other hand, a small penalty cost will misguide the EA into ranking the fitness of an infeasible solution to be of similar value as a feasible one, causing its search to revolve around the infeasible region. Choosing suitable penalty functions and their parameters is not a straightforward task. Users usually have to, by trial and error, find the best parameters that would guide the search towards the feasible region. This requires extensive and exhaustive fine-tuning before the penalty function can be effectively incorporated into the EA framework. Moreover, the effectiveness of the penalty parameters is often case sensitive in that the performance varies from one optimization problem to another. If poorly chosen, the penalty parameter can severely distort the objective function and impair the EA in terms of the optimality of the final solution and rate of convergence. Furthermore, the unconstrained optimization problems generated by the penalty functions have larger objective function spaces compared to the original problems which, therefore, decrease the probability of the search to locate the optimum solution.

Several researchers have attempted to address this problem. Khu and Keedwell (2005) avoided the use of penalty functions by formulating each nodal pressure constraint as an objective function within a multi-objective evolutionary algorithm framework. The approach requires enormous computational effort as the number of objective functions to be considered is proportionate to the size of the network optimized. A large network would inherently require the formulation of numerous objective functions and would consequently involve a huge population of candidate solutions whose hydraulic analyses would be too burdensome computationally. As such, the proposed method lacks the practicality to be applied to real-life WDSs which may contain hundreds or even thousands of nodes.

Following Deb (2000), Prasad and Park (2004) adopted a constraint handling method that does not require a penalty coefficient. This method uses a tournament selection operator where 1) feasible solutions are preferred over infeasible solutions; 2) between two infeasible solutions, the one with smaller constraint violation is preferred; and 3) between two feasible solutions, the one with better fitness value is preferred. A closer examination of the approach reveals that it can lead to anomalies. For example, the most expensive feasible solution will be preferred to a cost-effective borderline infeasible solution which may still be acceptable in practice and carry the overwhelming majority of the good genes.

Following Bäck et al. (1991), Wu and Simpson (2002) and Wu and Walski (2005) developed a self-adaptive penalty method based on a heuristic boundary search technique. The approach involved an evolving penalty factor that aimed to focus the GA search around the boundary of the feasible solution region. However, the implementation of this self-adaptive heuristic technique requires the prior calibration of several additional parameters. Essentially, two boundary rules were introduced to alter the penalty factor based on the ratio of the number of feasible solutions to the number of total solutions (feasibility ratio) over a certain pre-specified number of generations. When the feasibility ratio increases to a preset limit, the penalty factor is relaxed hence allowing infeasible solutions to be selected for reproduction. When the feasibility ratio falls below a preset threshold, the penalty parameter is made more stringent and most of the infeasible solutions will be discarded and more feasible solutions will be reproduced.

The regular fluctuations of the solution feasibility ratio encountered clearly indicate that the varying penalty parameter repeatedly stray the search algorithm well away from the boundary. Constantly altering the penalty factor bounds drastically changes the types of solutions present within the population. This can be seen as constantly seeding the search with different solutions or randomly scattering the search around the solution space. As such, the search direction is radically diverted and prevented from converging toward a particular direction or area (which could well be where the optimal solution lies). The algorithm becomes highly stochastic (random) and may severely deteriorate the quality of the search.

Afshar and Marino (2007) proposed a parameter-free self-adapting boundary search method. Though termed parameter-free, the approach essentially involves a self-adaptive penalty factor. The penalty parameter is adapted using a heuristic such that the best infeasible solution (solution which has the lowest infeasibility value, i.e. an infeasible solution nearest to the boundary of the feasible region) will have the same cost as the best feasible solution. The motivation behind this is to provide good solutions with minor violation of constraints a fair chance to compete in the evolution process. The procedure requires an initial value of the penalty parameter to be defined at the start of the optimization process. Two strategies were proposed. The exterior method begins with an initial relaxed penalty parameter which gradually tightens with the generations. As such, the search begins within the infeasible region progressively moving towards the feasible. The interior method is just the opposite where an initial stringent penalty parameter is set and then gradually relaxed such that the search begins within the feasible region, gradually heading toward the boundary of the feasible region.

Studies have shown that the initial population and early stages of a GA do influence its search path and hence, the optimality of the final solution obtained (Keedwell and Khu, 2006). Heavily penalizing infeasible solutions at the very early stages of the evolution process may potentially discard near-feasible solutions that contain good building blocks. Doing so leaves the initial population with very expensive feasible solutions and would most likely cause the search to converge to sub-optimal solutions which are costly. In addition, for most real-world networks which are complicated

(consisting of pumps, tanks, multiple operating conditions, etc), it is very difficult to locate feasible solutions, let alone optimal ones. Applying the exterior method will result in a large amount of infeasible solutions dominating the population and may trap the GA search within the infeasible region. The main point to be stressed here is that determining the penalty parameter is never a straight forward task.

Farmani et al. (2005b) introduced a self-adaptive fitness formulation which does not require any parameter calibration. The approach involves the implementation of a two-stage penalty. The first penalty is applied such that the worst infeasible solution has a cost which is higher or at least equal to the cost of the cheapest feasible solution in the population. The second penalty implementation ensures that the penalised cost objective function of the worst infeasible solution is equal to the most expensive solution. The remaining infeasible solutions are penalised exponentially in proportion to their infeasibility. The researchers demonstrated that this approach enabled solutions which are slightly infeasible to be selected for reproduction. However, even after the two stages of penalization, there will still remain infeasible solutions which are of lower cost than some feasible solutions. The robustness of the suggested scheme is therefore questionable as it allows these low-cost infeasible solutions to be selected over feasible solutions with higher costs. There is a possibility that the population will be over-dominated by infeasible solutions and the search may converge to infeasible solutions.

The constraint handling problem is further complicated by the fact that GAs by nature are heuristic and generate enormous quantities of infeasible solutions which are pressure deficient. A good search strategy is not only limited to the feasible solution space but also focuses on infeasible solutions at the active constraint boundaries. This gives rise to the need to accurately gauge the performance of infeasible solutions. A boundary search technique will not be able to perform at its fullest potential without an accurate evaluation of the solutions. Unfortunately, conventional demand driven WDS simulation methods are incapable of simulating pressure deficient networks. Due to the assumption that nodal demands are fully satisfied regardless of whether the system's pressure is sufficient or deficient, demand driven analysis (DDA) is incapable of depicting the actual performance of a pressure deficient network, i.e. the exact nodal outflow cannot be quantified. The DDA pressure heads do not accurately

represent the actual deficiency of the network. In fact, resulting pressure heads are often lower or even unrealistically large negative values, leading to an exaggeration of the network pressure deficiency. For example, a nodal demand that is approximately 90% satisfied may still have a negative pressure head (Siew and Tanyimboh, 2011), giving a false impression that the nodal flow is zero. This once again highlights the complication and complexity involved in calibrating the penalty parameter. It is clear that the EA search can be easily misled if penalty parameters are not chosen properly.

3.4 REVIEW OF LONG-TERM NETWORK REHABILITATION AND UPGRADING MODELS

A water distribution system (WDS) is designed to meet current regulatory standards of quantity, quality and pressure in the water supplied to consumers. However, as time goes by, the network is not likely to cope with the significant increase in demand from population growth and industrial development. Subjected to continuous environmental and operational stresses, an aging network will inevitably experience a declining ability to transport water due to its diminishing hydraulic capacity as encrustation builds up in pipes. The structural integrity of the network would also deteriorate from years of pipe corrosion, making it prone to bursts and leakage. The implementation of a planned rehabilitation and upgrading strategy is crucial to meet both current and future demands. Failure to do so would lead to adverse effects such as water quality problems, increase in operation cost due to high head losses, pipe leakage, low water supply pressure and unforeseen disruption of water supply to consumers.

Given that the rehabilitation and upgrading of a WDS involves a great amount of capital, the optimization of factors such as the phasing, timing and magnitude of the upgrading with regard to cost is a necessity. There are several models developed to address this problem based on diverse approaches. Kalungi (2003) generalised these rehabilitation and upgrading models into three main categories. The following paragraphs present an overview of these models and their shortcomings.

3.4.1 Network Economics Based Models

The first category focuses exclusively on network economics, e.g. the model by Dandy et al. (1985). Dandy et al. (1985) stated that price elasticity of water demand although small, is usually not zero. As such, an increase in the price of water may result in a reduction of water demand and hence delaying the need for future expansion of the WDS capacity. The main objective of their model was to identify the optimum water pricing and capacity expansion policies for water supply based on the price elasticity of demand. This was done by maximizing the present value of net economic benefits subjected to a series of constraints which included 1) the peak demand cannot exceed the network capacity, 2) no obsolescence of plant components, 3) bounds on water prices, 4) bounds on annual water price changes and 5) bounds on revenue in relation to system costs.

The economic benefits were measured by the revenue generated by the water company from direct water sales. The model determined the required funds, timing and magnitude of upgrading but did not directly identify the components to be upgraded and the structural and hydraulic integrity of the network were not addressed. Important WDS performance parameters e.g. network reliability were not considered as well.

3.4.2 Individual Asset Based Models

The second category consists of individual asset-based models that impart rehabilitation and upgrading decisions for individual components. Shamir and Howard (1979) determined the optimal time for pipe replacement based on an exponential relationship (obtained using regression analysis) between pipe breakage rate and its age. The pipe break prediction model they developed utilised the history of main breaks to forecast the variation of pipe break occurrences with time. The model was based on the assumption that pipes with the same characteristics (e.g. pipe material and age, environmental factors such as soil and temperature, etc) will experience the same rate of deterioration. The work was focused on developing an

analytical approach to forecast water main breaks and using this information to determine the appropriate time to carry out pipe replacement.

Walski and Pelliccia (1982) presented the idea of threshold break rate. They adopted the break rate prediction model by Shamir and Howard (1979) and further introduced two additional pipe break factors relating to the size of pipe and previous failure history. A pipe is to be replaced if its failure rate exceeds a critical value. Whereas the model by Shamir and Howard (1979) is useful for deciding whether to replace the entire group of pipes, the model by Walski and Pelliccia (1982) is more practical in that it analyses the economic replacement on a pipe-by-pipe basis.

Loganathan et al. (2002) derived an economically sustainable threshold break rate by which a pipe should be replaced if its failure rate exceeds the defined critical value. Unlike previous models, it does not incorporate a break rate equation; rather it only involves the discount rate, repair and replacement costs. The model used a time-truncated probability function to project the future pipe break rate without requiring the full failure history of the pipe.

Giustolisi and Berardi (2009) proposed an approach for pipe replacement based on the ranking of pipes with regard to their frequency of selection among all replacement schemes generated by a multi-objective genetic algorithm. The time horizon taken was only one year. They stated several advantages from using a one-year time horizon, i.e. any assumption about discount rate can be disregarded since it is constant and does not affect pipe selection for replacement; and the pipe deterioration process can be assumed to be strictly monotone as there are no other interventions on pipes to be accounted for during one year.

The above-mentioned individual asset-based models do not incorporate hydraulic analysis of the network. In addition, no regard is given to the effect of hydraulic integrity deterioration on the network performance such as network reliability.

3.4.3 System Wide Models

The third category is the system-wide models. These models consider the hydraulic performance of the entire network explicitly. Lansey et al. (1992) developed a non-linear programming model for the scheduling of WDS maintenance. This was carried out by utilizing the segmental approach in which each link is sub-divided into sections to form decision variables. The model was linked to a hydraulic simulator to evaluate the hydraulic feasibility of the solutions. Rehabilitation and/ or expansion options include pipe replacement and cleaning and relining. They suggested dividing the planning horizon into two phases and in doing so provide added flexibility in dealing with any changes that arise during the first phase such as population and demand changes in assumed pipe failure rates. For example, a planning horizon of 12 years could be divided into two phases, e.g. a 5-year first phase followed by a 7-year second phase.

Kleiner et al. (2001) used dynamic programming combined with partial and implicit enumeration to determine the most cost-effective rehabilitation plan. The deterioration of both hydraulic capacity and structural integrity of pipes were explicitly considered in determining the timing of rehabilitation.

Halhal et al. (1997) proposed a multi-objective rehabilitation formulation and solved it using the structured messy genetic algorithm (SMGA). The model minimizes the rehabilitation cost whilst maximizing the benefits to the system which include aspects such as hydraulic performance, water quality, pipe structural integrity and flexibility of the system. The formulation produces a trade-off curve between benefit and cost, providing flexibility to choose the final solution based on the total funds available and the resulting benefit from the rehabilitation scheme. However, the model did not include the timing of rehabilitation. Furthermore, the deterioration of the pipe carrying capacity was not taken into regard.

Dandy and Engelhardt (2001) further demonstrated the effectiveness of GA in solving WDS rehabilitation problems. The model considers direct and indirect costs associated with pipe failure. Indirect costs (e.g. traffic disruption and damage to third parties) were modelled through the use of failure cost factors. The pipe failure model

is based on diameter and age. Only pipe replacement was considered as the rehabilitation option. Though models in the third category (i.e. system wide models) are rather complex, they usually do not explicitly address the influence of the deterioration of hydraulic capacity of pipes on network performance and the timing of rehabilitation.

3.4.4 Models that Incorporate Reliability Measures

Considering only cost minimization (as a single objective) during the optimization of a WDS inherently removes redundancy (spare capacity) which therefore causes the system to be vulnerable when subjected to critical operating conditions. A more practical approach is to consider the WDS reliability as well. The reliability evaluation provides the modeller/ engineer with a greater degree of certainty regarding the capability of the WDS in coping with unforeseen abnormal operating conditions.

In the literature, models for the design of WDSs generally do not explicitly optimize the reliability measure, let alone upgrading and rehabilitation models which are far more complicated and challenging to formulate. The main reason stems from the fact that reliability formulations available in the literature are highly complex and generally involve numerous hydraulic simulations which are computationally laborious and impractical to be directly incorporated in the solution of NP hard WDS optimization problems. Hence, researchers turn to different measures to account for the WDS reliability. For example, in their work to minimize pipe replacement cost and maximize the WDS reliability, Dandy and Engelhardt (2006) used the total expected number of customer interruptions to quantify the reliability of the network. This measure was calculated using a mathematical formulation which involved multiplying the probability of pipe failure by the number of customer interruptions arising from the pipe failure.

Tanyimboh and Kalungi (2008, 2009) were probably the only researchers that incorporated the reliability measure in a comprehensive manner while solving the WDS long-term upgrading and rehabilitation optimization problem in a holistic way.

They considered both the hydraulic reliability and redundancy and demonstrated the importance of assessing the latter in addition to the former. Their model also considered hydraulic performance of the network, economic, social and environmental issues and demand management based on the price elasticity of demand. They explicitly modelled pipe deterioration over time in terms of the reduction in structural integrity and hydraulic capacity and allowed for the direct and indirect failure costs.

Tanyimboh and Kalungi (2008, 2009) used a pre-specified pipe flow distribution based on the maximum entropy flows as the basis of the design. Doing so yields several advantages. Firstly, designing the network to carry maximum entropy flows reduces the size and complexity of the optimization problem as the flows are first calculated and then the pipes sized. The complexity of pipe sizing for WDS is simplified when the pipe flow rates are fixed in advance and this enables the pipes to be sized using linear programming (Alperovits and Shamir, 1977). Secondly, as mentioned in Chapter 2, there is evidence in the literature suggesting that there exists a strong positive correlation between the statistical entropy of WDSs and their hydraulic reliability. Hence, WDSs designed to carry maximum entropy flows would be more reliable as compared to traditional minimum-cost designs (Tanyimboh and Templeman, 2000) and in terms of costs, maximum entropy designs appear not to be unduly expensive (Setiadi et al., 2005).

However, there exist several potential disadvantages and limitations in adopting this LP-based approach. Final results obtained have the property that a pipe may contain more than one constant-diameter pipe segment. This type of solution is unfortunately undesirable for practical implementation. In addition, the developed LP model is limited to networks with pipes only since the presence of pumps and valves further complicates the non-linearity of the main hydraulic constraints. As such, the model is incapable of optimizing all aspects of WDS design and operation.

3.5 CONCLUSIONS

The design, rehabilitation and operation of WDSs are complex multi-criteria problems that require optimization models to be effectively solved. A review on both classical optimization and evolutionary algorithm (genetic algorithms (GAs) in particular) was presented. Classical optimization techniques though computational efficient have great limitations when it comes to solving highly constrained non-linear problems. These optimization techniques are incapable of solving multi-objective problems effectively. GAs on the other hand are well suited for complex combinatory problems with non-convex, multi-modal and discontinuous solution space. They are well suited to solve multi-objective optimization problems as they are able to simultaneously search different regions of a solution space since they deal with a population of solutions.

The general procedure and operators involved in the standard GA have been detailed. Improvements within the GA to make it more robust for the optimization of WDSs have been presented. Special attention was paid to several methods of constraint handling and boundary search employed in the literature. The limitations of these techniques were highlighted and discussed.

The last section of the chapter provides a review of three generalised categories of optimal long-term rehabilitation and upgrading models. The concepts of these models along with their shortcomings were briefly discussed and highlighted. Models based predominantly on network economics do not directly identify components to be upgraded. The appropriate timing for implementing the upgrade is not considered as well. Individual asset based models do not incorporate hydraulic analysis of the network and gives no regard to the effect of hydraulic integrity deterioration on the network performance such as network reliability. System wide models are generally very complex in formulation and computationally demanding.

CHAPTER FOUR

AUGMENTED GRADIENT METHOD FOR PRESSURE DEPENDENT MODELLING OF WATER DISTRIBUTION SYSTEM

4.1 INTRODUCTION

When predicting the behaviour of a pressure-deficient water distribution system (WDS), researchers have acknowledged the fact that results produced by the conventional Demand Driven Analysis (DDA) model are highly unreliable and misleading in depicting the actual deficient state of the network. As explained in Chapter 2, DDA is formulated based on the assumption that demands at nodes are fixed and satisfied in full regardless of the system's state of pressure and is thus incapable of simulating networks under abnormal operating conditions. Conversely, the Pressure Dependent Analysis (PDA) takes into explicit consideration the pressure-dependent nature of outflows, entailing a realistic representation of the network deficiency.

This chapter demonstrates the effectiveness of combining a new continuous pressure dependent demand function, an efficient and robust over-relaxation procedure (i.e. the line search and backtracking routine) and the Global Gradient Method (GGM) by Todini and Pilati (1988) to form a model capable of handling real networks involving both normal and pressure deficient conditions. The algorithm will be referred to as the head dependent gradient method (HDGM) herein (Note: the terms head and pressure are used interchangeably). The Tanyimboh and Templeman (2004, 2010) function has been used as the head-flow relationship (HFR) in this study. This HFR stands out in the literature for the reason that the function and derivative have no discontinuities

which therefore allows a smooth transition between zero and partial nodal outflow and between partial and full demand satisfaction, avoiding convergence difficulties in the computational solution of the system of constitutive equations. As for the GGM, computation effort is minimized by exploiting the structure of the systems of equations in the Newton-Raphson iterative solution, leading to an extremely rapid algorithm. Therefore, integrating the Tanyimboh and Templeman function within the GGM would be extremely advantageous from the computational standpoint.

The developed HDGM is capable of realistically simulating networks for all pressure regimes (low, moderate and high) as demonstrated later in the examples (Section 4.6). The accuracy of the PDA result produced has been tested with a technique known as the Hydraulic Feasibility Test (Ackley et al., 2001; Tanyimboh et al, 2003). PRAAWDS, which is a well established PDA model (see e.g. Tanyimboh and Templeman, 2010) was used to further verify the PDA results generated by the proposed algorithm. In addition, the PDA results generated are compared with DDA results produced by EPANET 2 (Rossman, 2002) to demonstrate the superiority of the former in analysing pressure deficient networks.

The HDGM can analyse networks with multiple reservoirs. However, it is unable to handle pumps, valves and tanks and is only limited to steady state analyses. The main motivation behind the development of the HDGM is to verify and validate the feasibility of integrating the Tanyimboh and Templeman (2004, 2010) function into the GGM. The success of the HDGM has enabled the research to move forward to the next stage, i.e. extending the renowned DDA based EPANET 2 to handle pressure dependent demands as presented in Chapter 5.

4.2 HEAD DEPENDENT GRADIENT METHOD

This section describes the extension of the Global Gradient Method (GGM) to include demands that are pressure dependent. The equations involved in the GGM formulation have been described in detail in Chapter 2. As shown in Chapter 2, the energy conservation and mass balance equations can be written as

$$\begin{bmatrix} A_{11} & \vdots & A_{12} \\ \cdots & \cdots & \cdots \\ A_{21} & \vdots & 0 \end{bmatrix} \begin{bmatrix} Qp \\ \cdots \\ Hn \end{bmatrix} = \begin{bmatrix} -A_{10}H_0 \\ \cdots \\ -Qn^{req} \end{bmatrix} \tag{4.1}$$

The mass balance equation from Eq. 4.1, i.e.

$$A_{21}Qp = -Qn^{req} \tag{4.2}$$

shows that the sum of flows flowing in and out of the demand node (i.e. $A_{21}Qp$) is always equal to the required supply (i.e. Qn^{req}). In other words, the nodal demand is assumed to be fully satisfied at all times. In pressure dependent analysis, the nodal outflow is pressure dependent and will not be fully satisfied if the available pressure is insufficient. This also means that the sum of pipe flows in and out of the demand node will not always be equal to the required supply. To incorporate pressure dependent demand, Qn^{req} is replaced with $Qn(Hn)$ where $Qn(Hn)$ represents the pressure dependent nodal flow function (which is the Tanyimboh and Templeman (2004) function in this research). A diagonal matrix A_{22} is introduced into Eq. 4.1 to form

$$\begin{bmatrix} A_{11} & \vdots & A_{12} \\ \cdots & \cdots & \cdots \\ A_{21} & \vdots & A_{22} \end{bmatrix} \begin{bmatrix} Qp \\ \cdots \\ Hn \end{bmatrix} = \begin{bmatrix} -A_{10}H_0 \\ \cdots \\ 0 \end{bmatrix} \tag{4.3}$$

where the elements of the diagonal matrix A_{22} are $Qn(Hn)/Hn$. Eq. 4.3 is differentiated with respect to the pipe discharges and nodal heads to give

$$\begin{bmatrix} D_{11} & \vdots & A_{12} \\ \cdots & \cdots & \cdots \\ A_{21} & \vdots & D_{22} \end{bmatrix} \begin{bmatrix} dQp \\ \cdots \\ dHn \end{bmatrix} = \begin{bmatrix} dE \\ \cdots \\ dq \end{bmatrix} \tag{4.4}$$

where diagonal matrix D_{11} is the derivative of A_{11} and its elements can be written as $nK_j\left|Qp_j\right|^{n-1} + 2m\left|Qp_j\right|$ for pipes and $n\omega^2 K_j (Qp_j/\omega)^{n-1}$ for pumps. D_{22} is the

derivative of A_{22}. *dQp* and *dHn* represent the corrective steps for *Qp* and *Hn* respectively in successive iterations and can be defined as

$$dQp = Qp^{k} - Qp^{k+1} \tag{4.5}$$

$$dHn = Hn^{k} - Hn^{k+1} \tag{4.6}$$

in which *k* represents the iteration number. *dE* and *dq* represent the pipe head loss and flow conservation at each node respectively and can be written as

$$dE = A_{11}Qp + A_{12}Hn + A_{10}H_0 \tag{4.7}$$

$$dq = A_{21}Qp + A_{22}Hn \tag{4.8}$$

By substituting Eq. 4.7 and Eq. 4.8 into Eq. 4.4, the iterative formulation of the head dependent gradient method (HDGM) can be described as the following two equations:

$$Hn^{k+1} = A^{-1}F \tag{4.9}$$

in which

$$F = A_{21}Qp^{k} + Qn\ (Hn^{k}) - D_{22}Hn^{k} - A_{21}D_{11}^{-1}A_{11}Qp^{k} - A_{21}D_{11}^{-1}A_{10}H_0 \tag{4.10}$$

$$A = A_{21}D_{11}^{-1}A_{12} - D_{22} \tag{4.11}$$

$$Qp^{k+1} = Qp^{k} - D_{11}^{-1}(A_{11}Qp^{k} + A_{12}Hn^{k+1} + A_{10}H_0) \tag{4.12}$$

Hence the algorithm first updates the nodal heads *Hn* by calculating Hn^{k+1} (Eqs. 4.9-4.11) before updating the pipe flow rates *Qp* by calculating Qp^{k+1} (Eq. 4.12).

4.3 LINE SEARCH AND BACKTRACKING PROCEDURE

The integration of the HFR into the system of hydraulic equations is really a complicated task. One major challenge encountered in doing so is the deterioration of the GGM algorithm's convergence property. To include a HFR into the mass balance equations would further increase the overall non-linearity of the system of equations and render it more complex and difficult to be solved. Directly applying the corrective steps obtained from the iterative solution methods for non-linear systems of equations would not be sufficient. For example, Newton's method often fails to converge if the starting point (i.e. the initial estimate) is not close to a solution. A globally convergent strategy that yields a solution from almost any starting point is essentially required.

Giustolisi et al. (2008b) adopted a heuristic approach in their pressure-driven network simulation model whereby an over-relaxation parameter that adjusts the Newton step consisting of both pipe-flow and nodal-head corrections is increased or decreased depending on the errors in the mass and energy balance equations. In the Head-Driven Simulation Model developed by Tabesh et al. (2002), convergence is ensured by using a step length adjustment parameter. However, its value is obtained by means of trial and error. Tanyimboh and Templeman (2010) utilized the line search and backtracking routine in their PDA program PRAAWDS to guide the Newton search in the right direction and ensure global convergence for the systems of non-linear equations. It determines the appropriate Newton step size in a deterministic manner, ensuring both the head loss and flow continuity functions are sufficiently improved in successive iterations. No trial runs or parameter calibrations were required. Experience with PRAAWDS has shown that the line search and backtracking routine is efficient and reliable. For this reason, the HDGM has utilised this technique in enhancing its convergence properties.

The line search and backtracking routine used herein has been adapted from Press et al. (1992). The following section describes the implementation of the line search and backtracking procedure in integration of the Tanyimboh and Templeman (2004) nodal head-flow function within the GGM. The equations for conservation of energy along hydraulic links and mass balance at nodes can be describe as

$$dE(Hn,Qp) = A_{11}Qp + A_{12}Hn + A_{10}H_0 \tag{4.13}$$

$$dq(Hn,Qp) = A_{21}Qp + A_{22}Hn \tag{4.14}$$

The details and derivation of Eq. 4.13 and Eq. 4.14 have been described in the earlier section. The nodal heads are updated iteratively as,

$$Hn^{k+1} = Hn^{k} + \lambda \cdot \delta Hn \tag{4.15}$$

where the scalar parameter λ is an over-relaxation coefficient that satisfies $0 < \lambda \leq 1$ and *k* represents the iteration number. δHn is the full Newton step for the nodal heads *Hn*. Upon substituting the newly obtained nodal heads Hn^{k+1} into Eq. 4.12, the new flows Qp^{k+1} are obtained. Together, Eq. 4.13 and Eq. 4.14 form a single system of simultaneous non-linear equations that hereinafter is referred to as *G(Hn,Qp)*. The aim of the line search and backtracking procedure is to find a suitable λ value so that $G(Hn,Qp)$ decreases sufficiently at each iteration and ultimately approaches zero. The acceptance criterion for this step is described as

$$G(Hn^{k+1},Qp^{k+1}) \leq G(Hn^{k},Qp^{k}) + \alpha \cdot \nabla G \cdot \delta \tag{4.16}$$

where the scalar parameter α satisfies $0 < \alpha < 1$; $\alpha = 10^{-4}$ is used here (value taken from Press et al. (1992)). ∇G is the gradient of *G(Hn,Qp)* whereas $\delta = [\delta Hn, \delta Qp]$ is the Newton step. Both these terms are defined in Press et al. (1992) as

$$\nabla G = G \cdot J \tag{4.17a}$$

$$\delta = -G \cdot J^{-1} \tag{4.17b}$$

where *J* represents the Jacobian matrix. Observe that the Newton step is a decent direction (as represented by "–" in Eq. 4.17b) for *G*. The multiplication of Eqs. 4.17a and 4.17b, i.e. $\nabla G \cdot \delta$, represents the initial rate of decrease for *G(Hn,Qp)* and is effectively calculated as

$$\nabla G \cdot \delta = -G(Hn^k, Qp^k)^2 \tag{4.17c}$$

The criterion of Eq. 4.16 ensures enough progress is made in each iteration.

In HDGM, the first step taken is always the full Newton step, i.e. $\lambda = 1$. A minimum value of $\lambda_{\min} = 0.2$ is also set to stop the algorithm from taking a Newton step that is too small which would result in a longer computational time. However, if the full Newton step is unsatisfactory, i.e. $G(Hn^{k+1}, Qp^{k+1})$ does not meet the acceptance criterion, that is to say $G(Hn^k, Qp^k) - G(Hn^{k+1}, Qp^{k+1})$ is not large enough and thus G has not decreased sufficiently, the procedure will backtrack along the Newton direction, trying a smaller value of λ. For the first iteration, $G(Hn^{k+1}, Qp^{k+1})$ is modelled as a quadratic function of λ by substituting Hn^{k+1} with $Hn^k + \lambda \cdot \delta H$. The minimum of the function is then obtained and represents the new λ value. The procedure is similar for the second and subsequent iterations except that $G(Hn^{k+1}, Qp^{k+1})$ is modelled as a cubic function of λ. This iterative algorithm continues until either Eq. 4.16 is fulfilled or λ has reached the minimum set value. Interested readers can refer to Press et al. (1992) for more details of the line search and backtracking algorithm.

The line search and backtracking procedure can be summarized with the following flow chart presented in Fig. 4.1.

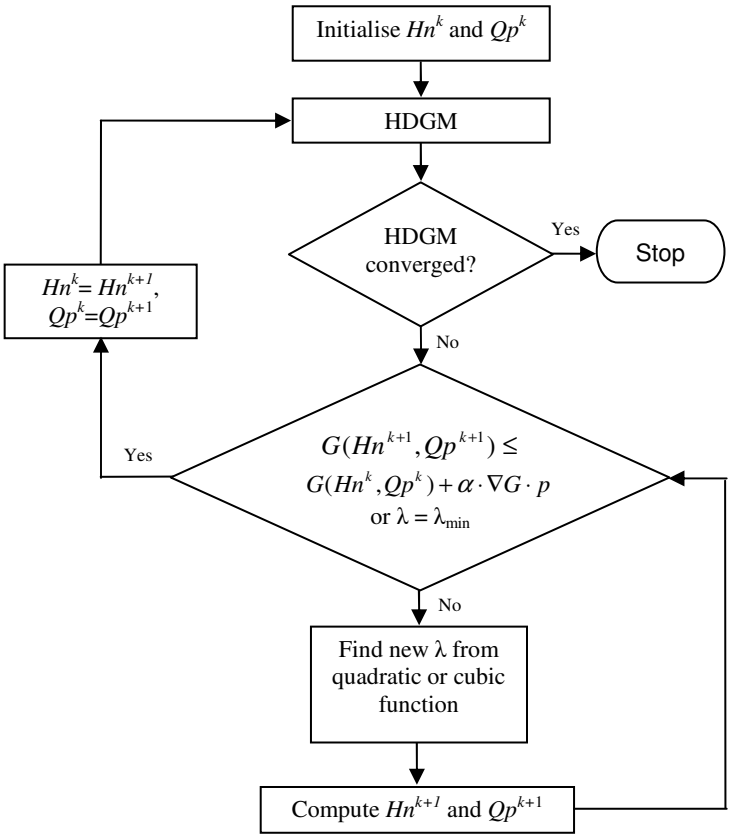

Figure. 4.1 Line search procedure

4.4 HEAD DEPENDENT GRADIENT METHOD EXECUTABLE HYDRAULIC MODEL

A prototype FORTRAN 90 implementation of the HDGM was developed in the present research and the results presented in the next section were generated using the program. The HDGM program by default sets the initial guess of the nodal head to the nodal elevation and the pipe flow rate based on an assumed velocity of 0.3048ms^{-1}. The convergence criterion was chosen such that the absolute value of the maximum change in both the nodal head and pipe flow was less than 0.001m and 0.0001m^{3}s^{-1} respectively.

4.5 METHODS FOR VERIFICATION OF PRESSURE DEPENDENT RESULTS

When analyzing a pressure deficient operating condition, unlike DDA, nodal flows computed by the PDA are less and at times vastly different from the corresponding required demands. Consequently, the feasibility and correctness of the generated PDA results are often questioned. Two approaches were used here to address this as explained below.

4.5.1 Hydraulic Feasibility Test

To monitor the accuracy and consistency of a PDA, Ackley et al. (2001) developed a verification technique which is powerful yet straightforward and simple to implement. In this approach, the nodal flows from the PDA solution are entered into an ordinary DDA program as nodal demands. With all other parameters remaining unchanged, the DDA program is executed. Subject to round off error, the resulting set of DDA based nodal heads and pipe flows will be identical to the corresponding nodal heads generated by the PDA program only if the PDA outflows used were accurate. This test works brilliantly in practice and has been implemented in many studies (e.g. Ackley et al., 2001; Tanyimboh et al., 2003; Kalungi and Tanyimboh, 2003; Siew and Tanyimboh, 2010). Herein, the hydraulic feasibility test has been used to verify the HDGM results and gave excellent results as demonstrated later in the examples (Section 4.6).

4.5.2 PRAAWDS

PRAAWDS (Program for the Realistic Analysis of the Availability of Water in Distribution Systems) is a prototype FORTRAN computer program developed by Tanyimboh and Templeman (2004). Based on the head dependent analysis approach, PRAAWDS generates simulations that are realistic for all pressure regimes. Amongst the unique features of PRAAWDS is the choice of four head-outflow relationships including the new Tanyimboh and Templeman (2004) function. The user is also given

an option to run a conventional (demand-driven) simulation. It is very easy to use, robust and gives accurate results.

PRAAWDS has been effectively incorporated in several studies on hydraulic reliability/ redundancy (e.g. Setiadi et al, 2005; Tanyimboh and Setiadi, 2008a, b). Numerous examples based on real life networks have been analyzed in Shan (2004) with excellent results. Hence, PRAAWDS would make a superior validation tool for the HDGM. Comparing the generated PDA results to that of PRAAWDS will give a clear indication of the accuracy of the proposed algorithm.

4.6 APPLICATION OF HEAD DEPENDENT GRRADIENT METHOD

The HDGM was applied to six networks of different complexity. The main aim of the case study is to validate the accuracy, robustness and efficiency of HDGM. The networks were subjected to a full range of demand satisfaction ratios (DSRs) to observe and analyse their performance behaviour. Comparisons of results produced by HDGM and PRAAWDS in addition to the hydraulic feasibility test (using EPANET 2 as the DDA program) were carried out and the outcome presented and discussed. Aspects of comparison include nodal heads, outflows and the DSR for nodes and network.

4.6.1 Example 1

The first example, shown in Fig. 4.2, is based on a simple network taken from Alperovits and Shamir (1977). This single source network consists of 8 pipes of length 1000 m and 6 demand nodes with the desired pressure heads of 60 m. Details of nodes and pipes are listed in Table 4.1. The HDGM was carried out with a variation of source heads from 40 m to 80 m. Performance of each node and network are illustrated in Fig. 4.3 and Fig. 4.4 respectively.

Table 4.1. Node and pipe data for Example 1

Node	Elevation (m)	Demand (m^3/s)
1	50	0.0417
2	50	0.0417
3	45	0.0778
4	45	0.0417
5	55	0.0556
6	55	0.0889

Pipe	Diameter (mm)	HW roughness
1	500	140
2	400	140
3	400	140
4	400	140
5	250	140
6	250	140
7	250	140
8	250	140

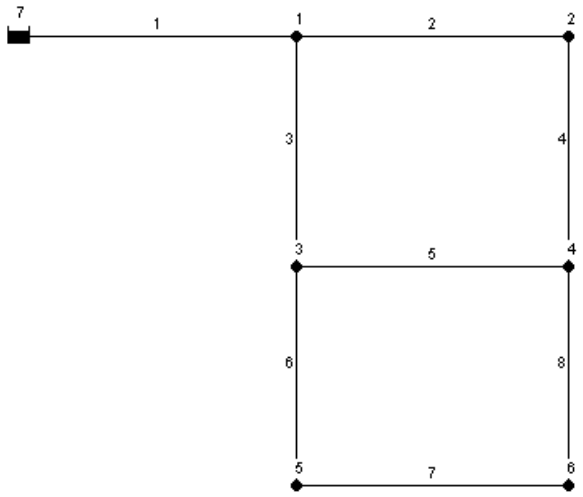

Figure 4.2. Layout of Example 1

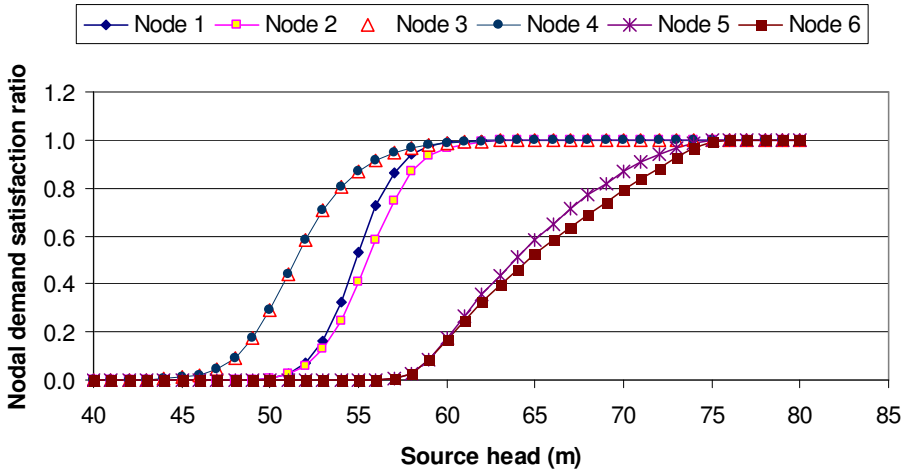

Figure 4.3. Nodal performance of Example 1

The demand nodes each have a unique head-outflow curve depending on their elevations, demands and relative distances from the source. The curves vividly show the magnitude of each nodal outflow at various source heads. For example, at source head 70 m, the demand satisfaction ratio (DSR) of nodes 5 and 6 are 0.87 and 0.79 respectively whereas demands at nodes 1 to 4 are fully satisfied. In addition, the sequence of each node being fully satisfied (with the increment of source head) and the required source head for all demands to be satisfied can be easily deduced. In this case, node 3 and 4 are satisfied simultaneously followed by nodes 1, 2, 5 and 6. A source head above 76 m is required for all demand nodes to be fully satisfied. It is worth noticing that the curves depict a smooth transition from no outflow at minimum head to a full outflow stage, exhibiting no discontinuities. The network performance is illustrated in Fig. 4.4.

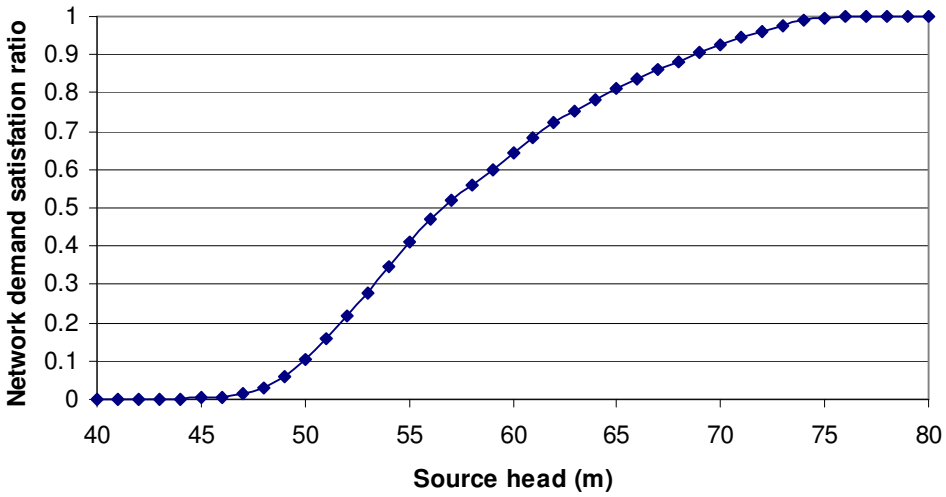

Figure 4.4. Network performance of Example 1

Result verification was carried out using the hydraulic feasibility test (Ackley et al. 2001) where the nodal outflows obtained from the HDGM are applied in EPANET 2 as nodal demands. Simulations for source heads ranging from 40 m to 80 m were performed. Nodal heads generated by EPANET 2 were then compared with those of the proposed algorithm. Fig. 4.5 shows a correlation of $R^2 = 0.9999995$ or $1 - R^2 = 5 \times 10^{-7}$ between the heads produced by both methods. This clearly confirms that the HDGM is producing results which are accurate and reliable.

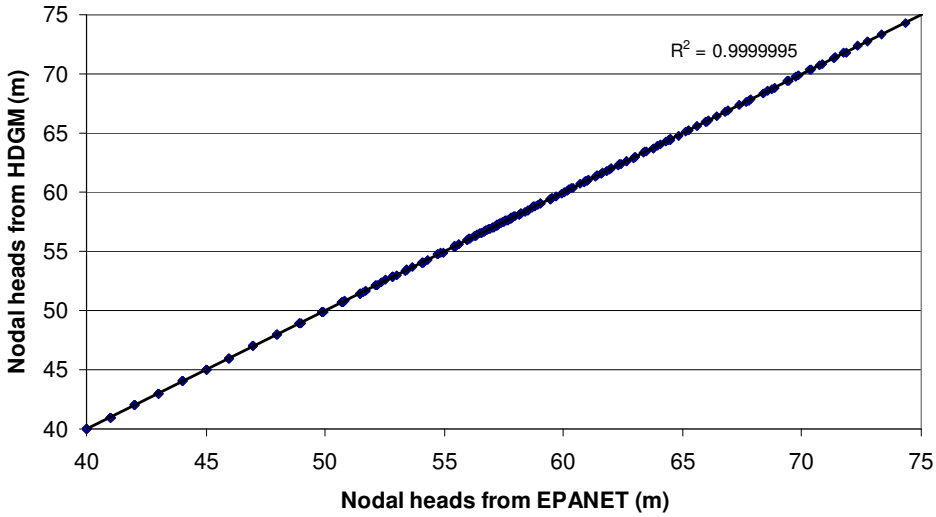

Figure 4.5. Hydraulic feasibility test for Example 1 for source heads between 40m and 80m

4.6.2 Example 2

The second example (Fig. 4.6) is a simple network taken from the literature (Ang and Jowitt, 2006) consisting two reservoirs and fourteen 1000 m long pipes with the Hazen-Williams roughness coefficient of 130. The diameters were 0.3 m for pipe 1 to pipe 7, 0.25 m for pipe 8 to pipe 14 and 0.2 m for pipe 13 and pipe 14. A demand of 0.025 m^3 was used for all the nine demand nodes. Details of nodal elevation and required heads are listed in Table 4.2. The desired head is the nodal head required for a demand node to achieve a DSR of 1. Both HDGM and PRAAWDS were executed for a series of source heads between 85 m & 115 m. It should be noted that the heads for both reservoir 11 and 12 were set to have the same value and rate of increase.

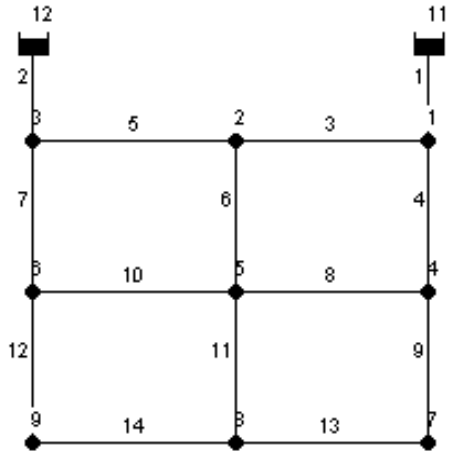

Figure 4.6. Network layout for Example 2

Table 4.2. Nodal elevation and required heads for Example 2

Node	Elevation (m)	Desired Head (m)
1	90	105
2	90	105
3	90	105
4	88	103
5	88	103
6	88	103
7	85	100
8	85	100
9	85	100

Fig. 4.7 illustrates the nodal performance obtained by HDGM and PRAAWDS. Nodes exhibiting similar performances (e.g. node 4, node 5 and node 6) were represented by one curve to provide a better comparison view of both methods. All nodal outflows computed by HDGM are identical to PRAAWDS. This goes the same for the network DSR as shown in Fig. 4.8. Fig. 4.9 illustrates an excellent correlation of $R^2 = 0.999998$ or $1 - R^2 = 2 \times 10^{-6}$ between nodal heads generated by both methods for the entire range of demand satisfaction ratios (DSR).

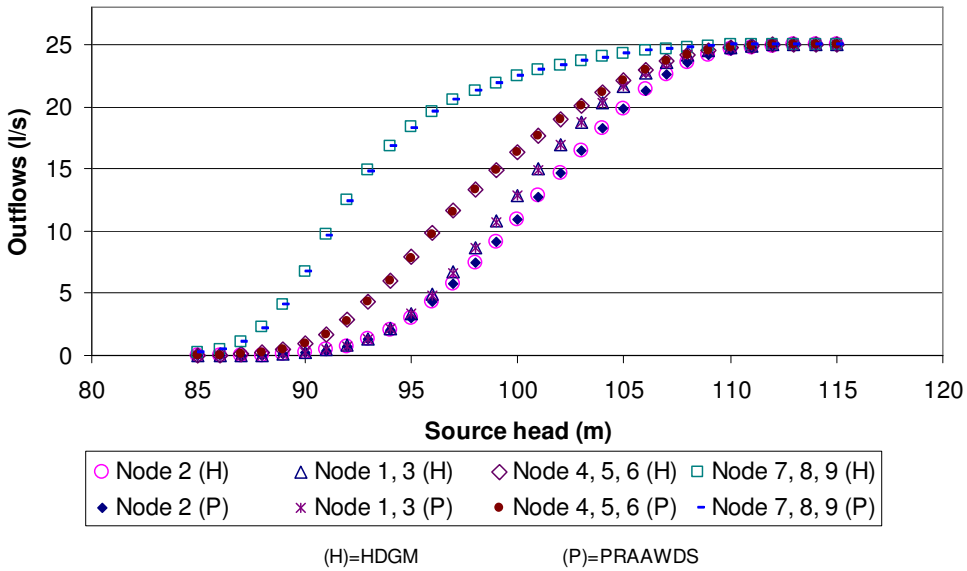

Figure 4.7. Nodal performance of Example 2

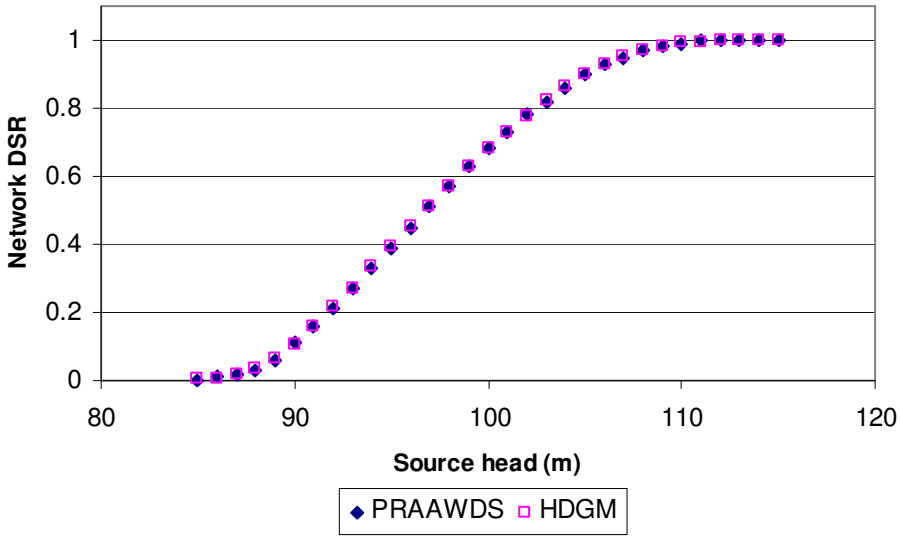

Figure 4.8. Network performance of Example 2

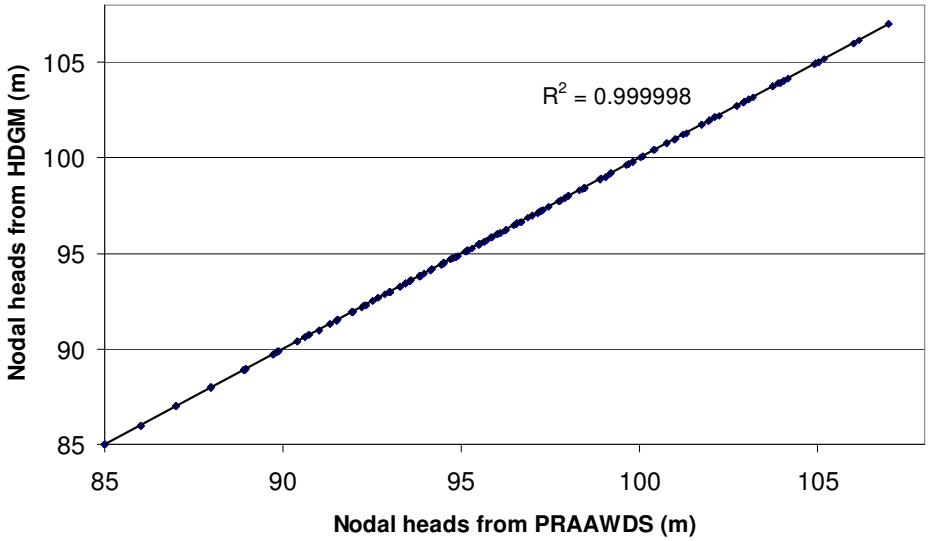

Figure 4.9. Nodal heads generated by HDGM and PRAAWDS for source head between 85 m to 105 m

The efficiency of both methods can be summarized in Fig. 4.10. It is observed that the number of iterations needed by HDGM to converge began to increase significantly when source heads were raised above 97m (network DSR of 0.51) and stabilized after 105m (network DSR of 0.9). Iterations required by PRAAWDS were in a narrower range of 6 to 10. The average convergence rate was 11.5 iterations for HDGM and 9.43 iterations for PRAAWDS.

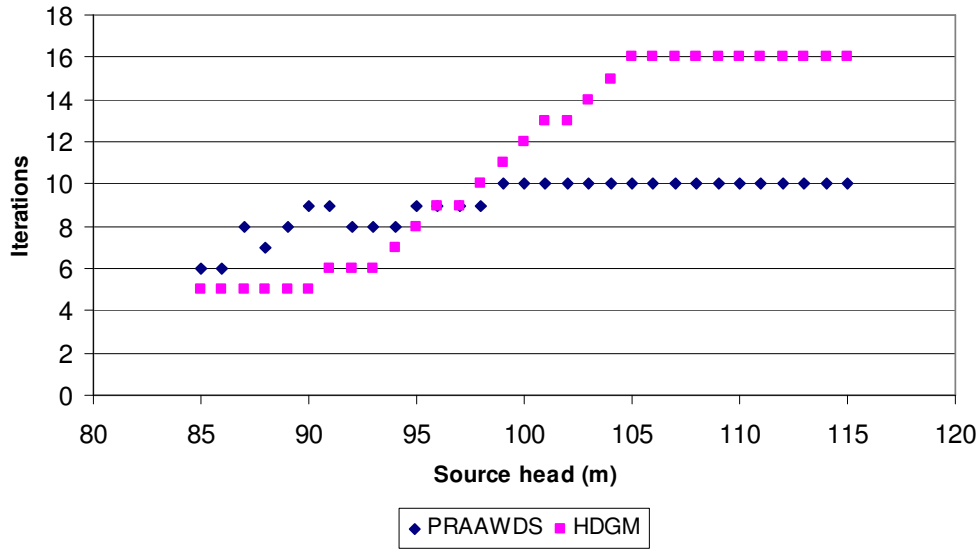

Figure 4.10. Number of iterations required to achieve convergence for Example 2

4.6.3 Example 3

Example 3 (Fig. 4.11) is based on a real network supplying water to approximately 9000 residents in a relatively hilly terrain. The desired residual head for all nodes were 15m. Data for the network pipes and nodes can be found to in Appendix A (section A-1). Both the pumps were removed from the network during the analysis to create a pressure deficient condition. The non-return valve connecting node 33 and node 32 was also excluded for the purpose of simplicity. The overall network demand satisfaction ratio was 0.82.

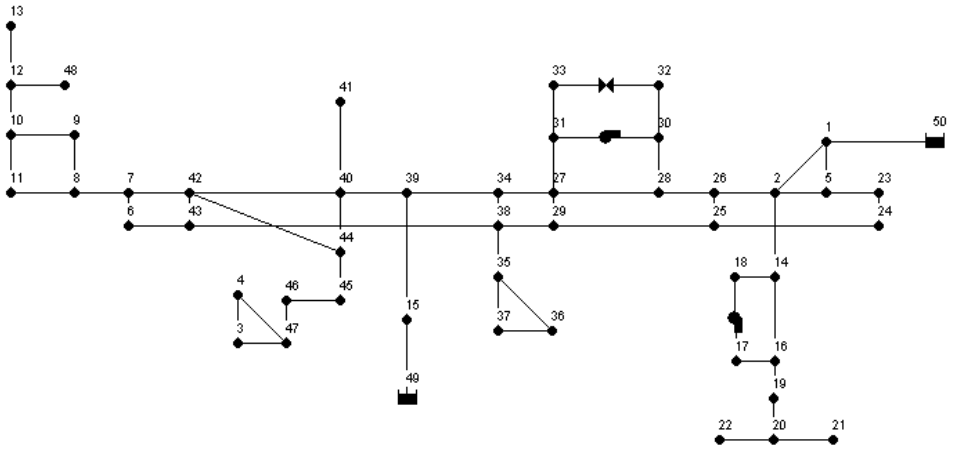

Figure 4.11. Network layout for Example 3

Fig. 4.12 and Fig. 4.13 confirm the consistency in accuracy for HDGM nodal heads and pipe flows respectively. HDGM nodal heads and DSRs perfectly matched those of PRAAWDS. The DDA (EPANET 2) simulation was carried out to be compared to the PDA. It is worth observing that the DDA heads were lower. For example, Fig. 4.14 shows node 19, node 20 and node 22 having a DSR value of 0. In order to fulfil the assumption that all nodal demands are met in full regardless of the deficiency in pressure, the DDA heads of these particular nodes and their surrounding nodes are computed to be lower, hence the obvious dissimilarity in heads within the region of nodes 16 to 22 as seen in Fig. 4.12. This proves the fact that DDA yields inaccurate result during subnormal pressure conditions.

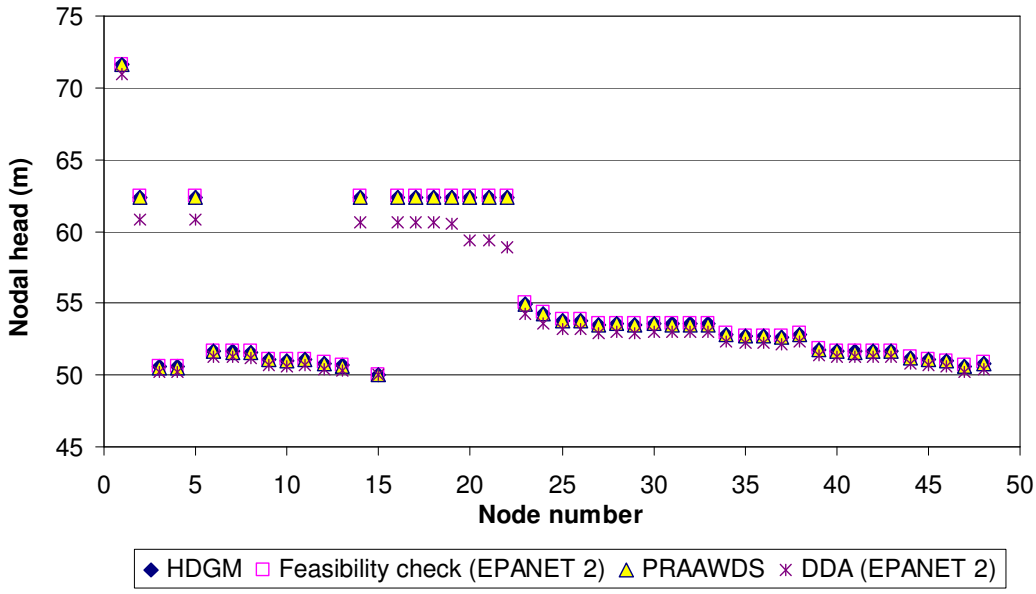

Figure 4.12. Nodal heads for Example 3

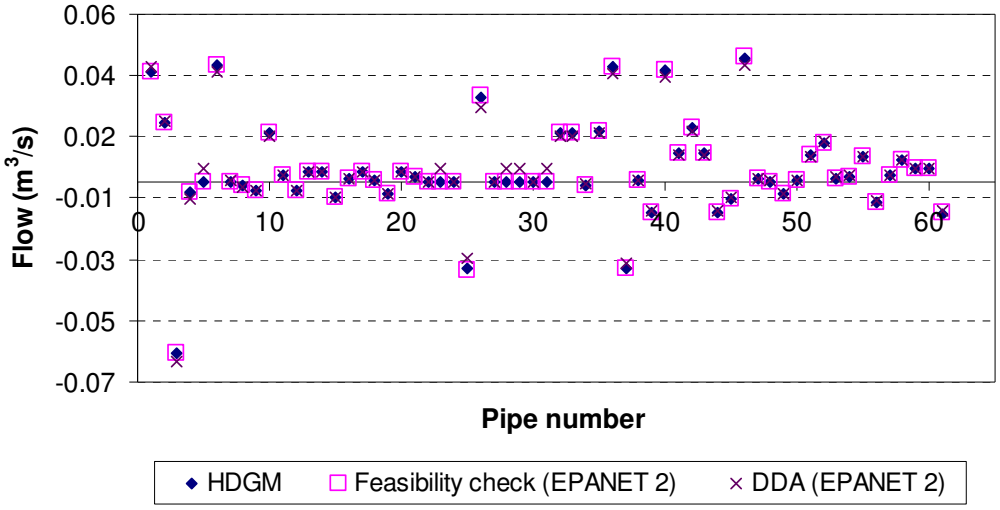

Figure 4.13. Pipe flows for Example 3

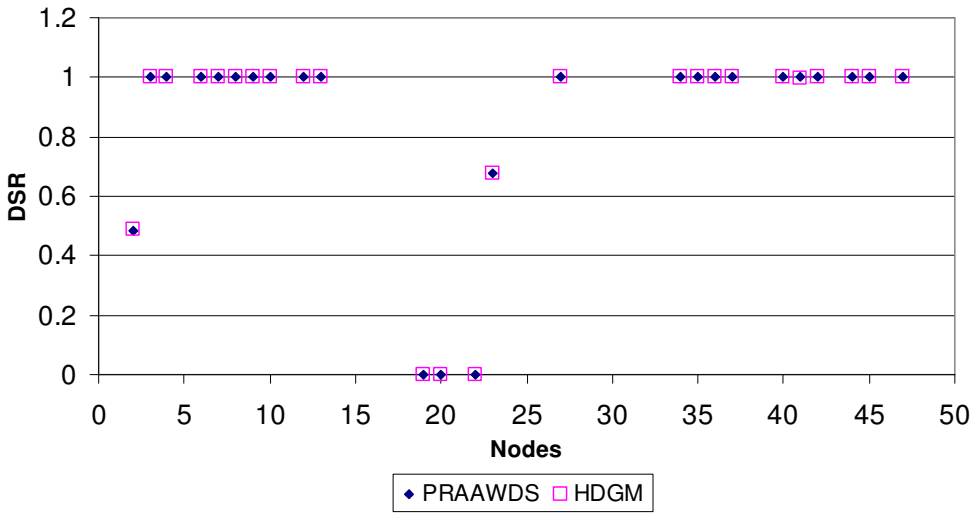

Figure 4.14. Nodal DSRs for Example 3

The HDGM and PRAAWDS simulations were then carried out for this network with a variation of source heads from 5 m to 105 m which enabled the network to experience a full range of network DSR, i.e. from 0 to 1.0. Similarly to Example 2, both the reservoirs were set to have the same heads and rate of increase. The pumps and valve were omitted in this analysis as well for the purpose of simplicity. Fig. 4.15 vividly shows the total outflows yielded were virtually identical. This is further confirmed by the high correlation values of $R^2 = 0.99992$ or $1 - R^2 = 8 \times 10^{-5}$ between the total outflows by both methods as illustrated in Fig. 4.16.

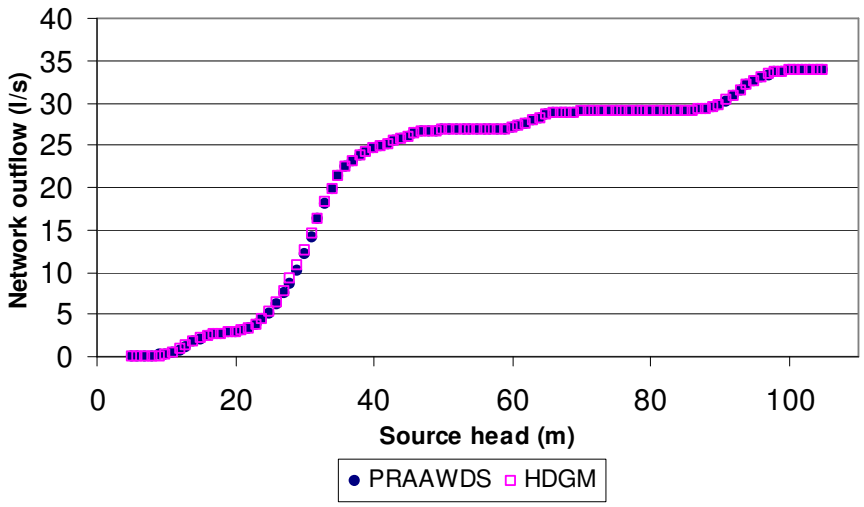

Figure 4.15. Total outflow for Example 3

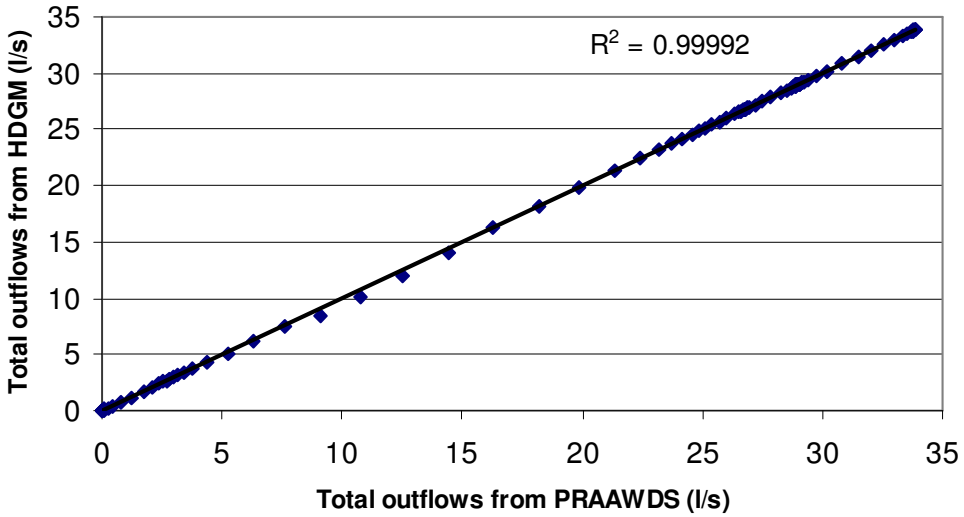

Figure 4.16. Comparison of total outflow between HDGM and PRAAWDS for source heads 5 m to 105 m

Iterations for HDGM were maintained within a consistent range of 5 to 7 throughout the series of source heads as shown in Fig. 4.17. The average convergence rate for HDGM was 5.7 iterations.

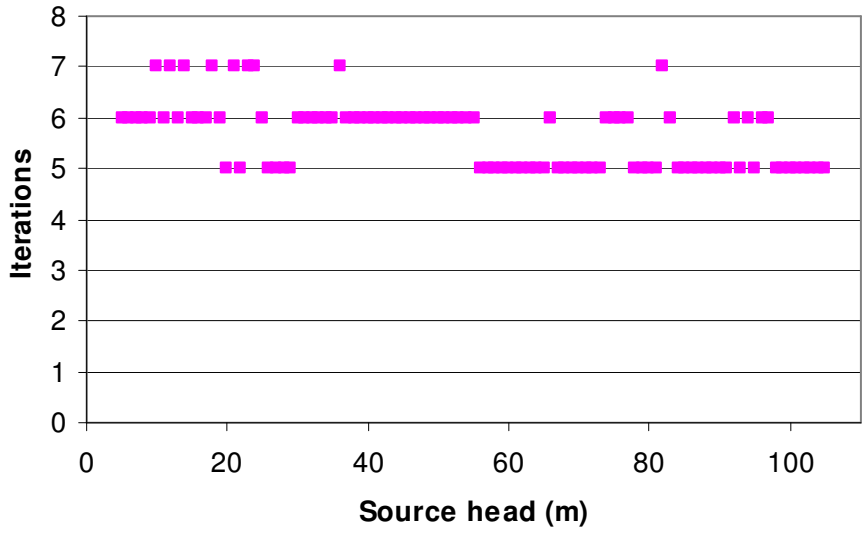

Figure 4.17. Number of iterations required for the HDGM to achieve convergence for Example 3

4.6.4 Example 4

The network in Example 4 consists of 48 nodes, 74 pipes and 2 reservoirs (Nodes 47 and 48) as shown in Fig. 4.18. Data for the nodes and pipes can be found in Appendix A (section A-2). Both source heads were varied at the same rate within a range of 100 m.

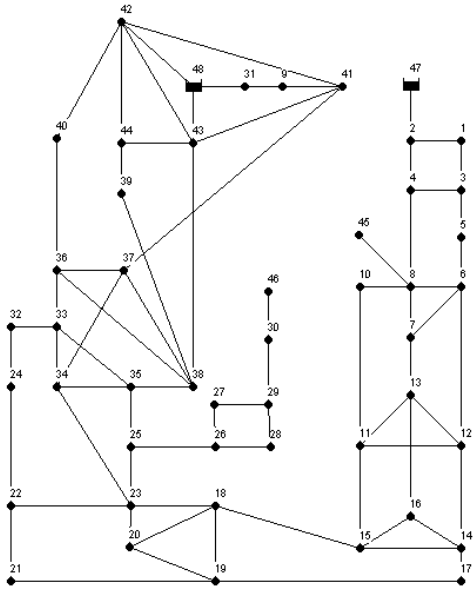

Figure 4.18. Layout of Network 4

Fig. 4.19a shows the network performance of Example 4 for the full range of DSRs. The fact that results were obtained without convergence problems suggests the HDGM is robust. The network head outflow curve consists of two steps. All 13 demand nodes have elevation of 100 m and desired head of 115 m where demands are satisfied in full. The first step corresponds to the scenario where demand nodes 1, 14 and 17 have been fully satisfied with the head of source 47 and 48 rising above 115m and 65 m respectively as shown in Fig. 4.19b. The remaining demand nodes only experienced a negligible increase in outflows. As soon as the head of sources 47 and 48 exceeded 150 m and 100 m respectively, outflows of demand nodes 9, 10, 21, 25, 30, 31, 32, 37, 45 and 46 began to increase significantly. This time, it is ten demand nodes achieving a DSR of 1.0 and hence the network experiences a leap in performance. This clearly explains why the latter step is steeper than the former.

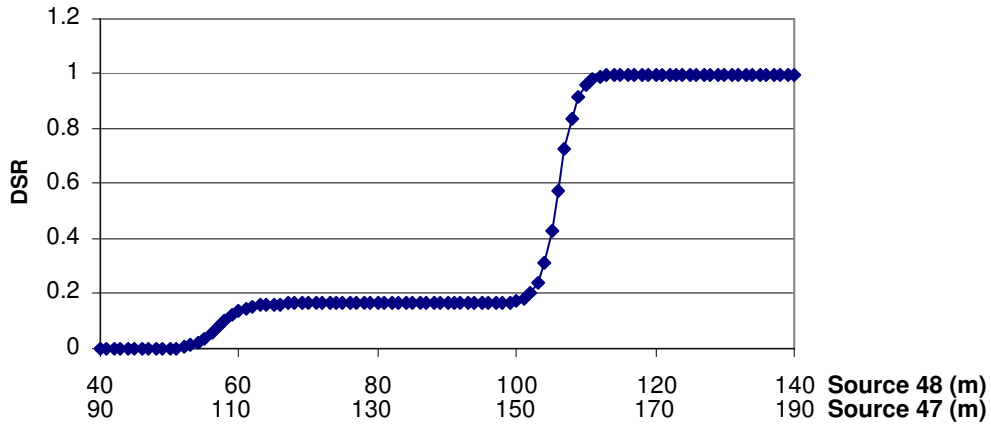

Figure 4.19a. Network performance of Example 4

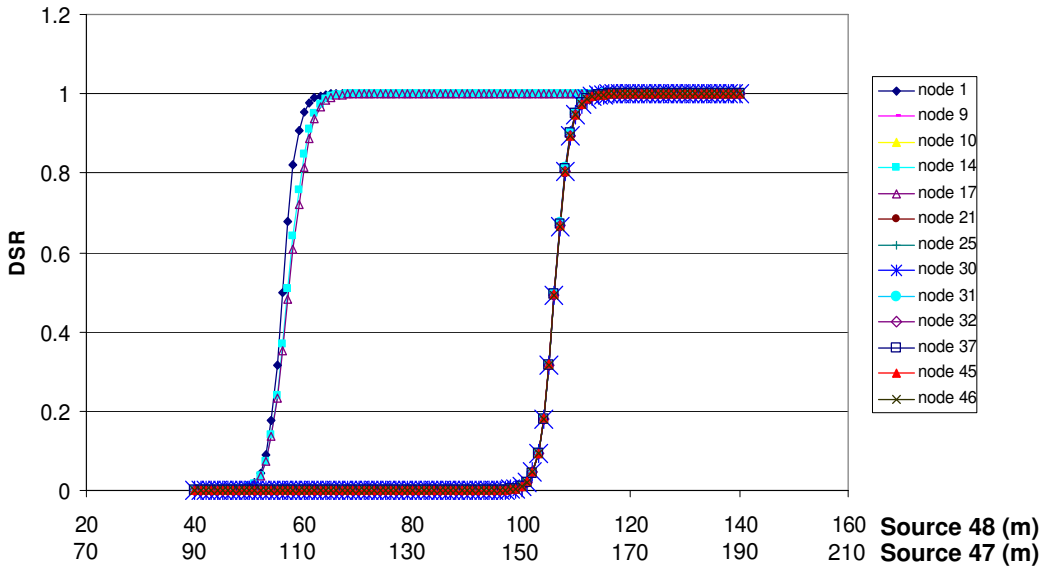

Figure 4.19b. Nodal performance of Example 4

Fig. 4.20 shows the number of iterations needed to achieve convergence. An average convergence rate of 8.68 iterations for this relatively large network suggests the HDGM converges rapidly and is efficient in simulating both normal and deficient operating conditions. To ensure the algorithm did not converge spuriously and the real solution had been found, the norm of the right hand side of Eq. 4.4 (the energy and mass balance) was evaluated. At solution, the norm should approach a value of 0 as an indication of the progress and accuracy of the algorithm. Fig. 4.21 shows a consistent decrease of the norm value for several network operating conditions. The hydraulic feasibility test described above gave a correlation coefficient of $R^2 = 0.9997$ which

confirms the accuracy of the HDGM. This verification was further strengthened by the identical results produced from the modelling of this network using PRAAWDS (Tanyimboh, 2008).

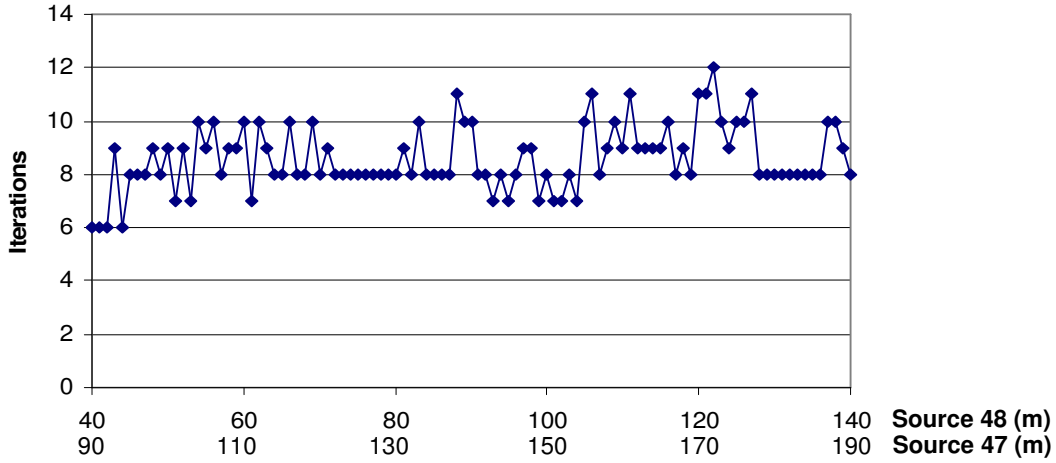

Figure 4.20. Iterations required to achieve convergence for Example 4

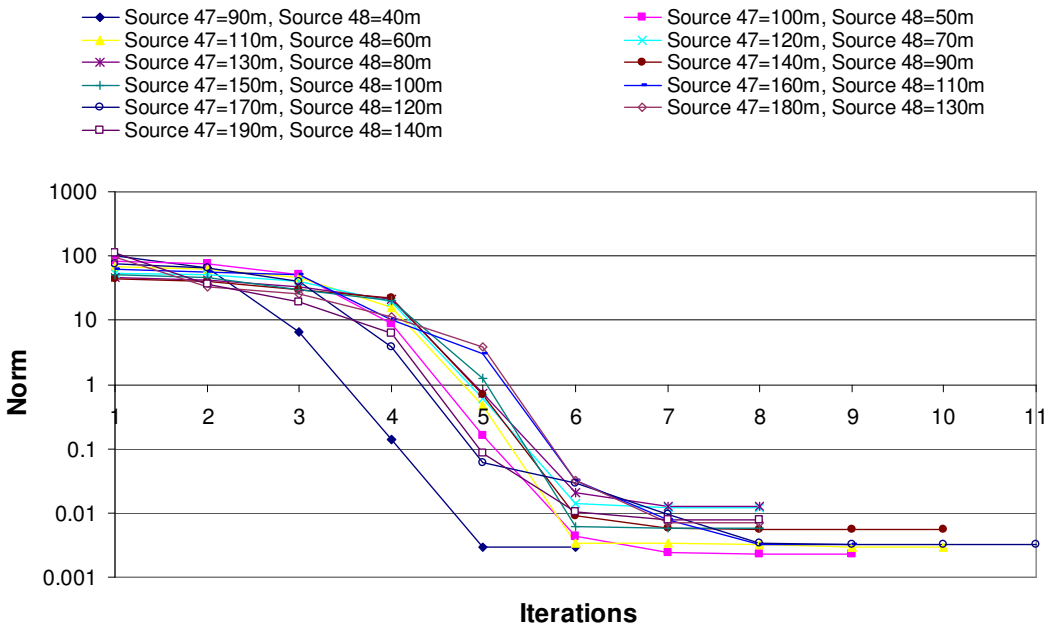

Figure 4.21. Value of norm at each iteration for Example 4

4.6.5 Example 5

The fifth example illustrated in Fig. 4.22 is taken from Shan (2004). The network supplies water to a mixed rural and suburban area with an approximate population of 15,000. The system consists of 164 nodes, 200 pipes, 5 reservoirs, 4 pumps and 2 flow control valves (FCV). For the purpose of simplicity, the pumps and valves were replaced with pipes. Further details of the network can be found in Appendix A (section A-3). For all nodes, the desired residual head was set to 15 m. Removing the pumps created a pressure-deficient condition that resulted in a network demand satisfaction ratio (DSR) of 0.645. A comparison of the nodal heads is shown in Fig. 4.23 where it can be observed that the DDA heads are lower for some nodes especially those with a DSR that is lower than 1.0 as shown in Fig. 4.23. The HDGM heads were compared to the heads generated by PRAAWDS (Tanyimboh, 2008) and an excellent correlation of R^2=0.9999998 was achieved.

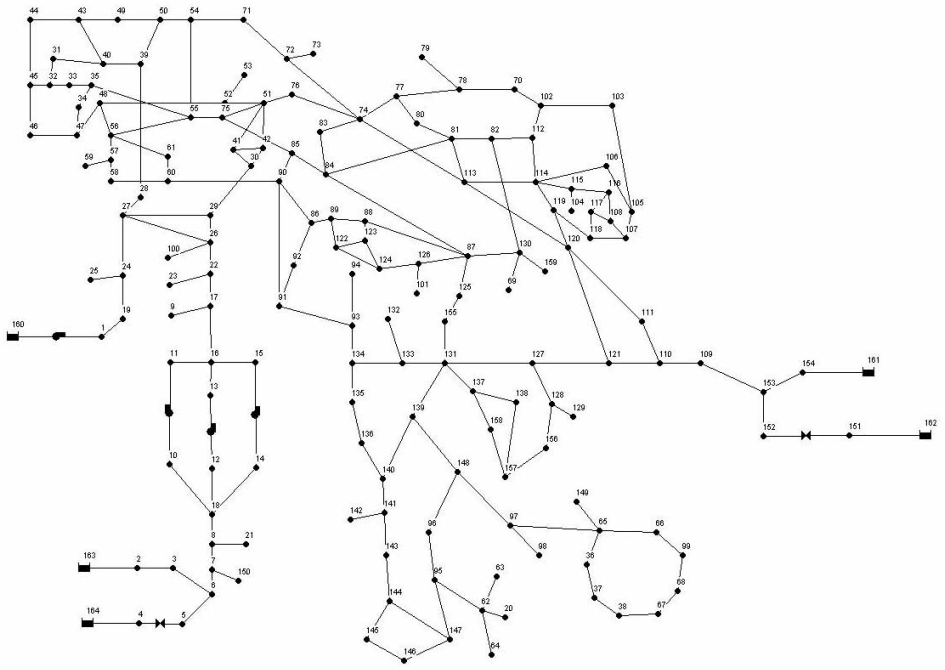

Figure 4.22 Layout of Network 5

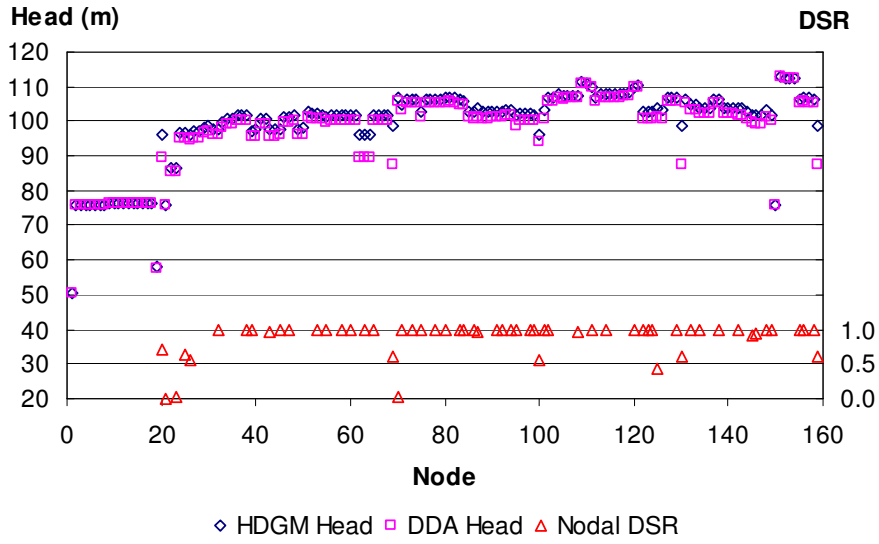

Figure 4.23 Nodal head and DSR results

The HDGM simulation was executed for a series of reservoir heads to enable the network to experience both normal and abnormal operating conditions. The heads of the reservoirs were reduced intensely to simulate an extremely low network DSR. The head of each reservoir was then increased consistently by 1 m for every subsequent simulation until a DSR of 1.0 was achieved. Fig. 4.24 shows the network performance with respect to each reservoir. One can clearly determine the reservoir heads corresponding to any network DSR value. A total of 70 simulations were carried out in this way without convergence complications. This suggests that the HDGM is robust and is capable of analysing the hydraulic network at any pressure operating condition.

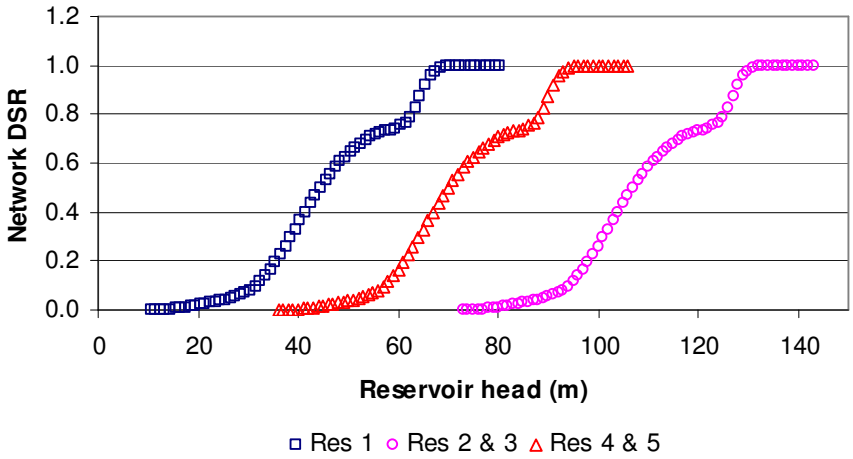

Figure 4.24 Performance of Network 5 with respect to reservoirs

The norm of the right hand side of Eq. 4.4 was evaluated to check for spurious convergence. Fig. 4.25 shows a consistent decrease of the norm value at successive iterations for all 70 simulations executed. It is worth observing that by the 8th iteration, the norm for all simulations was well below 0.01.

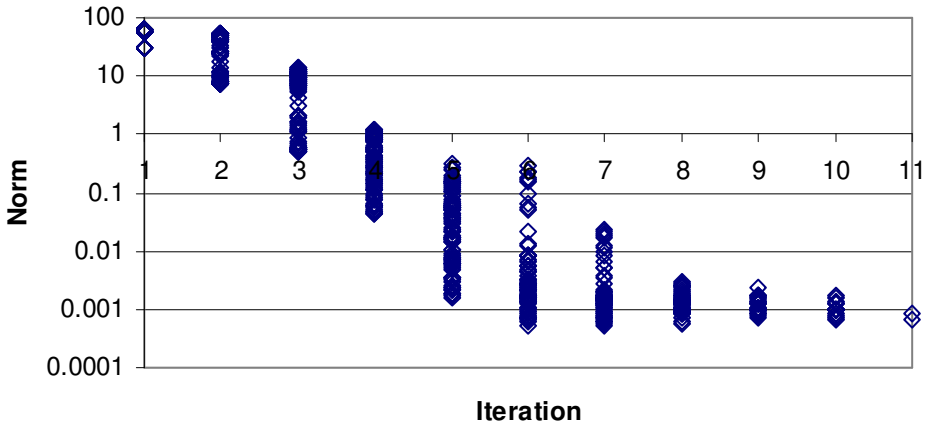

Figure 4.25 Norm at each iteration

The average numbers of iterations required for HDGM and EPANET 2 to converge were 8.15 and 5 respectively. The extra iterations by HDGM were largely due to the differences in the convergence criteria between the two models. However, if the HDGM were to adopt the EPANET 2 convergence criteria (i.e. the ratio of the sum of the absolute values of pipe flow changes to the total flow in all pipes which should be less than 0.001), the average number of iterations would reduce to 6.55 (Fig. 4.26). HDGM nodal head results for both stopping criteria were compared and it was observed that the average difference between the two sets was 3.145×10^{-4} m which is very small and insignificant. In other words, both sets of results were virtually identical. Hence, it is demonstrated that the PDA model compares favourably to EPANET 2 in terms of computational efficiency. The Hydraulic Feasibility Tests for seven simulations evenly chosen out of the 70 were carried out. Fig. 4.27a and 4.27b show the perfect agreement in results.

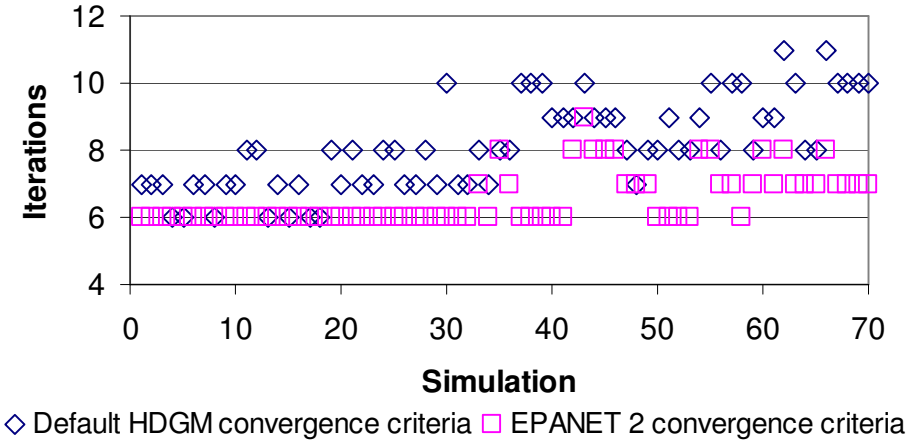

Figure 4.26 Iterations required by HDGM to achieve convergence

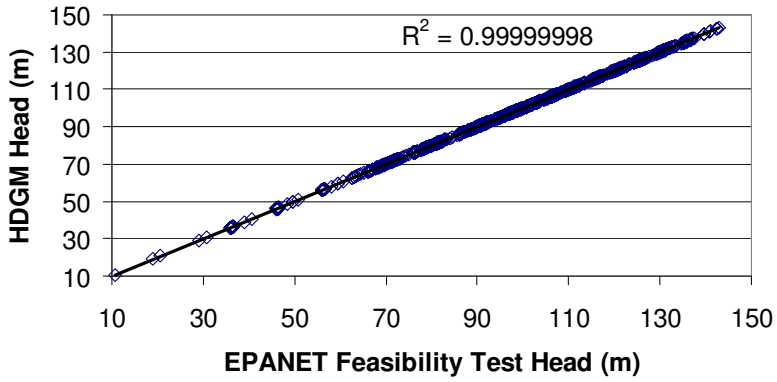

Figure 4.27a Hydraulic Feasibility Test for Network 5 (Nodal Head)

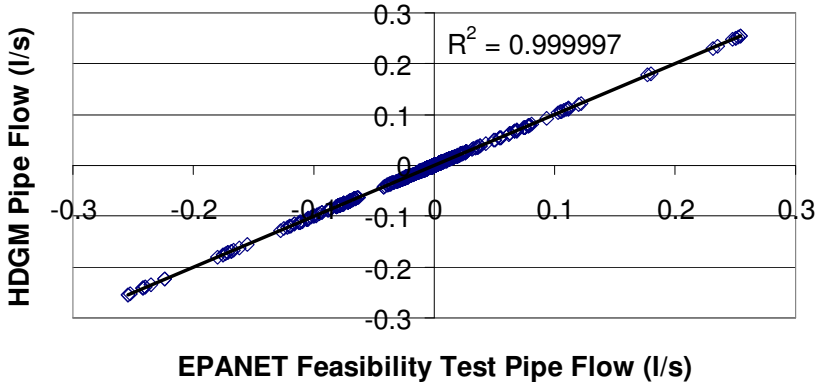

Figure 4.27b Hydraulic Feasibility Test for Network 5 (Pipe Flow)

4.6.6 Example 6

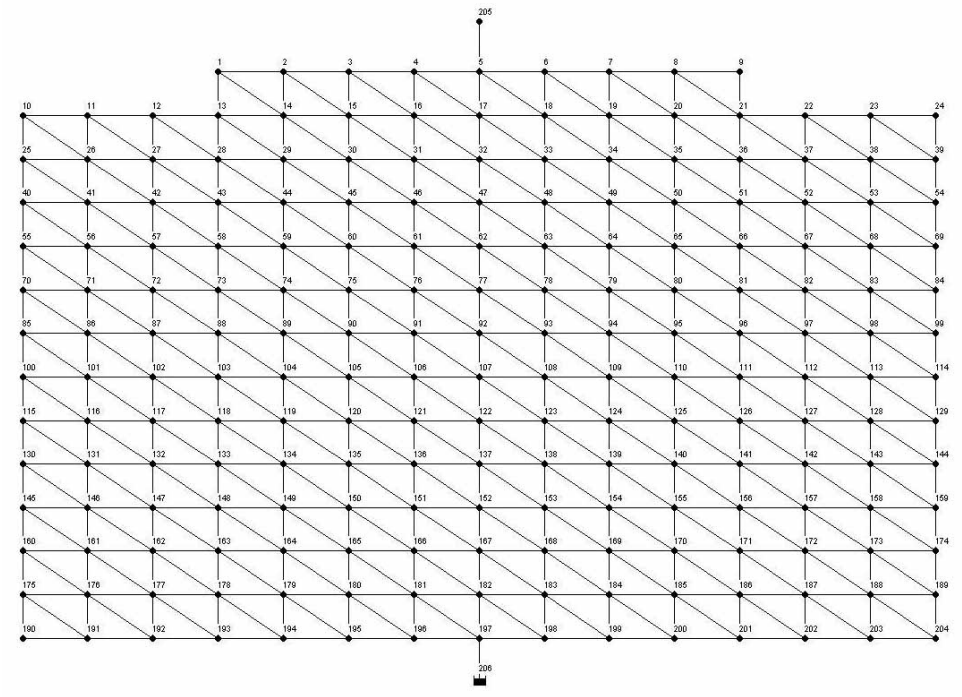

Figure 4.28 Layout for Network 6

The last example (Fig. 4.28) is a hypothetical layout generated by Shan (2004) which consists of 206 nodes, 557 pipes and 1 reservoir. All nodal elevations, required head (to achieve a DSR of 1.0) and demands were 75m, 90m and 10 l/s respectively. The reservoir head was set to 102m to create a pressure deficient condition. All pipe lengths, diameters and Hazen-Williams roughness coefficients were 100m, 450mm and 130 respectively. The results are summarised in Fig. 4.29. The identical heads of both the HDGM and Hydraulic Feasibility Test demonstrate that the program is capable of analysing large networks accurately. It is worth observing that nodal heads computed by EPANET 2 are comparatively lower. This shows that DDA underestimates the capacity of a pressure deficient network. The HDGM simulation was carried out again on this network with the presence of a second reservoir with a head 102m replacing node 205. Fig. 4.30 shows the HDGM and EPANET 2 results. Both HDGM and EPANET heads were identical in this case because the network DSR was 1.

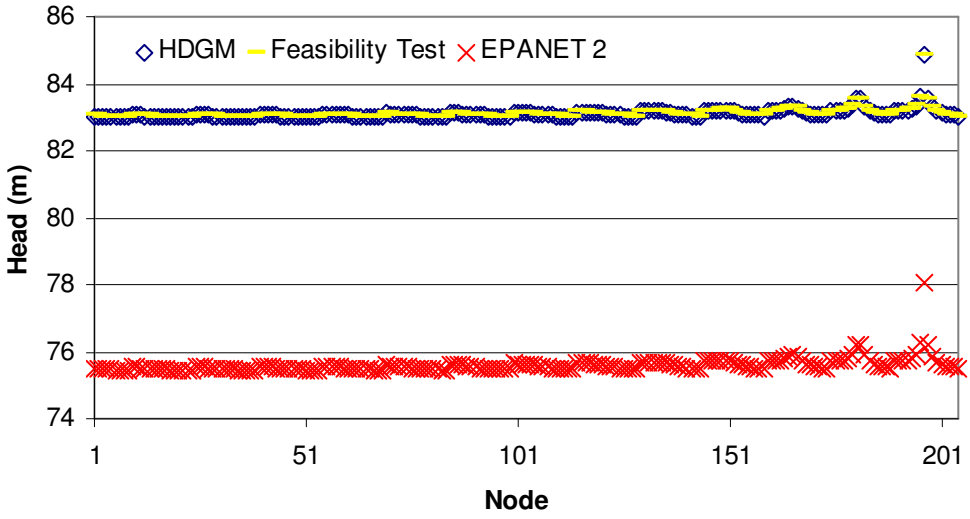

Figure 4.29 Nodal heads for Network 6

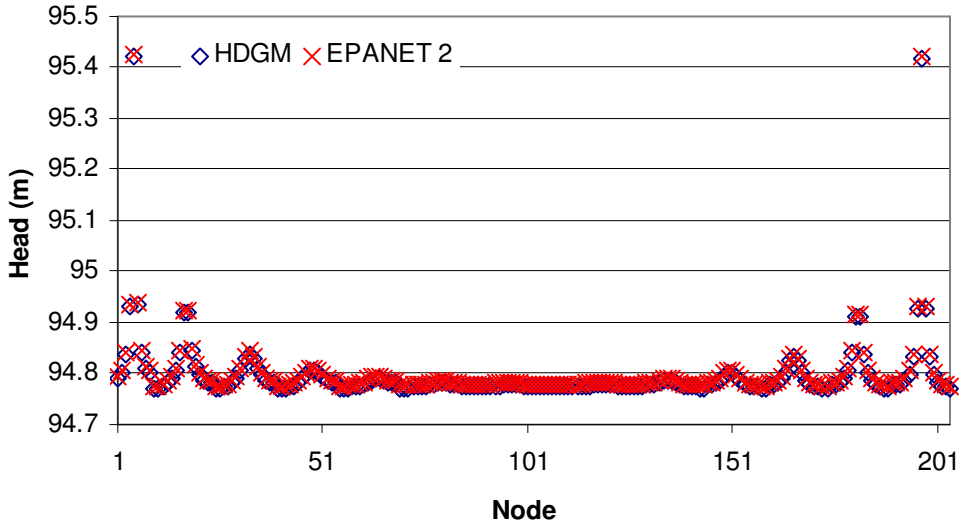

Figure 4.30 Nodal heads for Network 6 (2 reservoirs)

4.7 CONCLUSIONS

A new hydraulic model which incorporates the Tanyimboh and Templeman (2004) pressure-dependent demand function within the Global Gradient Method has been presented. A FORTRAN prototype program based on this model has been developed and tested extensively. Six case studies were performed and the performance of the networks subjected to various states of pressure deficiency were analysed. It was demonstrated that the HDGM was proficient in producing realistic results for both abnormal and normal operating. The ability of the model to analyse the networks under the entire range of DSR without encountering convergence difficulties vividly implies that the algorithm is highly robust. The HDGM was also demonstrated to be capable of handling relatively large networks efficiently and accurately.

Comparison between results generated by PDA and DDA demonstrated that the latter is liable to exaggerate the network deficiency and produce unreliable results in terms of nodal outflows and heads. On the other hand, PDA enables a realistic representation of the pressure deficiency for each demand node. PDA provides a quick and accurate means of gauging the performance of demand nodes and the network as a whole.

Result verification using the hydraulic feasibility test of Ackley et al. (2001) shows that the algorithm generates results that are reliable and accurate. Furthermore, the networks were also modelled using PRAAWDS which gave identical results. The algorithm is demonstrated to be efficient and performs consistently while analysing networks of different complexity and sizes. The integration of the line-search and backtracking procedure has proven to be effective in facilitating the selection of the Newton step size to ensure fast convergence.

The HDGM is limited in scope in that it is unable to handle pumps, valves and tanks. As mentioned at the beginning of the chapter, the HDGM work is merely a tool for verifying and validating the feasibility of integrating the Tanyimboh and Templeman (2004, 2010) function into the Global Gradient Method. As such, no further development and improvements were carried out on the HDGM. However, the

success of this work has set a solid foundation for the research to progress to the next phase, i.e. to extend the renowned DDA based EPANET 2 to incorporate PDA functionality and ultimately, to integrate it into a multi-objective optimization model for the design and long term rehabilitation and upgrading of WDSs as will be presented in the following chapters.

CHAPTER FIVE

A NEW ENHANCED PRESSURE DEPENDENT ANALYSIS EXTENSION OF EPANET 2

5.1 INTRODUCTION

The methodology of the head dependent gradient method (HDGM) was presented in the previous chapter. The study involved simulations of non-trivial real world networks and extensive verification of the formulation using a FORTRAN 90 implementation of the HDGM. Excellent results were achieved and the algorithm has proven to be computationally efficient and robust. However, analyses were limited to networks with pipes only. The HDGM prototype program was incapable of analysing networks with pumps, valves and tanks. In this chapter, this work has been further advanced in a comprehensive way by successfully implementing the HDGM within the EPANET 2 (Rossman, 2002) framework, extending the renowned demand driven analysis (DDA) hydraulic simulator to be able to handle pressure dependent analysis (PDA).

The enhanced version of the EPANET 2 simulator is termed EPANET-PDX (pressure-dependent extension) and is presented herein. EPANET-PDX is capable of simulating real world networks and is able to provide a fully equipped extended period simulation. This chapter delves straight into the application of EPANET-PDX. Similarly, the accuracy of the simulator is verified using the hydraulic feasibility test detailed in the previous chapter (section 4.5.1). In addition, the comparison of computational efficiency between EPANET 2 and EPANET-PDX is presented. Interestingly, it was observed that the efficiency and robustness for EPANET-PDX

simulations is on par with EPANET 2. The computational time and iterations required by both models were very similar in most of the test cases considered.

5.2 EPANET-PDX (PRESSURE DEPENDENT EXTENSION)

EPANET 2 (Rossman, 2002) is a well-renowned hydraulic simulator developed by the Water Supply and Water Resources Division of Environmental Protection Agency, United States. This simulator provides a wide range of hydraulic functionality which includes the modelling of

a) Extended period simulation
b) Constant or variable speed pumps
c) Various types of valves e.g. pressure regulating valve, flow control valve, shutoff valve, check valve etc
d) Storage tanks
e) Variation in nodal demands
f) Water quality e.g. water age, reactions in bulk flow and at pipe wall, etc

It is also equipped with graphic user interface which aids the process of constructing the pipe network and greatly assists in the interpretation of the network analysis results.

EPANET 2 software is used widely in both the research and industrial communities because of its highly robust and efficient performance. However, this hydraulic simulator is based on the conventional DDA and is thus incapable of accurately simulating pressure deficient networks as highlighted in the previous chapter. This sets a great limitation in its practicality in terms of analysing networks under abnormal operating conditions which are often encountered in reality. Extending this hydraulic model to cater for pressure dependent analysis (PDA) would appear to be greatly advantageous. In addition, since it is public domain software which many researchers are familiar with and have free access to, this extension presents a significant contribution to the WDS engineering community and will act as an

effective means of directly promoting the application of PDA to practising engineers. EPANET-PDX is an extension to EPANET 2 to enable it to model pressure dependent flows. This chapter focuses on its application in efficiently producing realistic and accurate PDA results.

The PDA enhancement was implemented directly within the EPANET 2 source code without involving any program interface or toolkit. The implementation of the Tanyimboh and Templeman (2004) head flow relationship (HFR) has been directly coded in subroutine "*netsolve ( )*" which is located in the "hydraul.cpp" source file where the hydraulic solver engine i.e. the Global Gradient Method (Todini and Pilati, 1988) algorithm is written. The incorporation of this HFR into the Global Gradient Method has been detailed in Chapter 4. An additional input file was created to accommodate the desired nodal head data. The minimum required head was taken as the nodal elevation which is already available in the EPANET 2 input file. A new subroutine for the line search and backtracking procedure named "*linesearch ( )*" has been created as well in "hydraul.cpp". It is worth mentioning that the full hydraulic and water quality functionality of EPANET 2 is still preserved with all the modifications implemented.

Initial values for flows in pipes and nodal heads were set to the flow corresponding to a velocity of 1 ft/s and nodal elevation respectively. The convergence criteria were chosen such that the absolute values of the maximum changes in both the nodal heads and pipe flows were less than 0.001 ft (3.048×10^{-4} m) and 0.001 cfs (2.832×10^{-5} m^3s^{-1}) respectively. These criteria may be more stringent compared to the default one used in EPANET 2 (the criterion used in EPANET 2 is the ratio of the sum of the absolute values of pipe flow changes to the total flow in all pipes which should be less than 0.001). However, computational experience has shown that the above mentioned criteria (all $\delta Q \leq 0.001$cfs and all $\delta H \leq 0.001$ ft) prevent spurious convergence and enable the algorithm to perform more consistently. Similarly to EPANET 2, a maximum of 200 iterations is also used as a further threshold control for convergence

EPANET-PDX is capable of accurately modelling a WDS operating over an extended period simulation (EPS) as will be demonstrated in Section 5.3. Aside from the pressure dependent demand aspect, the EPS approach for EPANET-PDX is

essentially identical to that of EPANET 2. The detail description of the overall EPS procedure which includes the operation of tanks, hydraulic data and result management (to link subsequent steady state simulations to form an EPS) has been presented in Chapter 2.

5.3 APPLICATION OF EPANET-PDX

To illustrate the application of EPANET-PDX, a total of 420 steady state simulations (SSSs) and 30 EPS (with duration of 24 hours and 1 hour hydraulic time step) were performed over six networks of different sizes (Table 5.1). Simulations executed involved

1) Varying the source heads thus subjecting the networks to the entire range of DSRs; and
2) Randomly closing pipes to create stress within the networks

as shown in Table 5.1. Under the pipe closure (PC) simulation column in Table 5.1, values in parentheses represent the number of pipes closed. For example, the number of pipes closed for network 2 ranged from 1 pipe to 8 pipes. Details of the PC simulations (i.e. the pipes chosen to be closed) can be referred to in Appendix B (section B-2). Also, EPANET 2 was run concurrently for each simulation to serve as comparison for both PDA and DDA. Thus overall, 840 SSSs and 60 EPSs (which comprised a total of 1,440 or more SSSs) were involved in this assessment. Additional EPANET 2 simulations were carried out to verify the accuracy of the PDA results as detailed later in the "results verification" in Section 5.5.

It is worth mentioning that aside from the simulations presented herein, approximately 46.1 million simulations have been carried out satisfactorily so far within the proposed Penalty-Free Multi-Objective Evolutionary Algorithm framework to solve the WDS benchmarks of Alperovits and Shamir (1977), Hanoi, New York tunnels, Anytown and real life WDS such as the Wobulenzi and North London systems which will be presented in following Chapters 6, 7 and 8.

Table 5.1 Network details and number of simulations

Number of network elements indicated						Number of simulations	
Network number	Nodes	Pipes	Pumps	Valves	Sources	SHV	PC
1	6	8	0	0	1	48	7 (1)
2	36	70	0	0	1	36	57 (1 - 8)
3	9	9	2	1	2	72	15 (1 - 3)
4	164	200	4	2	5	50	50 (2 - 10)
5	204	557	0	0	2	45	43 (5 - 10)
6	22	43	3	0	3	20*	10* (2 – 5)

Values in ( ) represent the range of the number of pipes closed in the pipe closure simulations
* Extended Period Simulation
SHV - Source head variation simulations
PC - Pipe closure simulations

Overall, the performances of EPANET-PDX and EPANET 2 were very similar as will be shown later herein. Consequently, not all aspects of results will be presented for every network. However, comprehensive results for all the networks are presented in Appendix B (section B-2). Detailed results of the simulators' performance on the whole in terms of robustness, average CPU time and number of iterations are presented and discussed at the end of the chapter.

It is essential to clarify two key terms which will be extensively used in the following section of the chapter. The term "demand satisfaction ratio" (DSR) represents the ratio of the available nodal flow to the nodal demand and takes values between 0 and 1. A network DSR value of 0.5 means only 50% of the total network demand is satisfied. It is also worth mentioning that DSRs for nodes and networks are only presented for EPANET-PDX and not EPANET 2. The reason is EPANET 2 is a DDA based hydraulic simulator and hence the nodal demands are implicitly assumed to be satisfied in full regardless of whether the pressure is sufficient or not. The second term, nodal residual pressure head refers to the pressure head of the node excluding the elevation.

5.3.1 Example 1

The first example is the two-loop benchmark network taken from the literature (Alperovits and Shamir, 1977) which was also used in the HDGM analysis in previous chapter (Fig. 4.2). This single source network consists of 8 pipes of length 1000m and 6 demand nodes with the desired pressure heads of 60m. Other details of the nodes and pipes have been presented in Chapter 4 (Table 4.1). EPANET-PDX was carried out with a variation of source heads from 37 m to 84 m. The performance of each node is illustrated in Fig. 5.1 and is observed to be identical to the head dependent gradient method (HDGM) results in section 4.6.1.1. For the SHV simulations carried out, an average of 5 iterations was required for both EPANET-PDX and EPANET 2 to converge to the final solution. In terms of computational time, both models required similar average execution time, i.e. 0.048s and 0.049s for EPANET-PDX and EPANET 2 respectively.

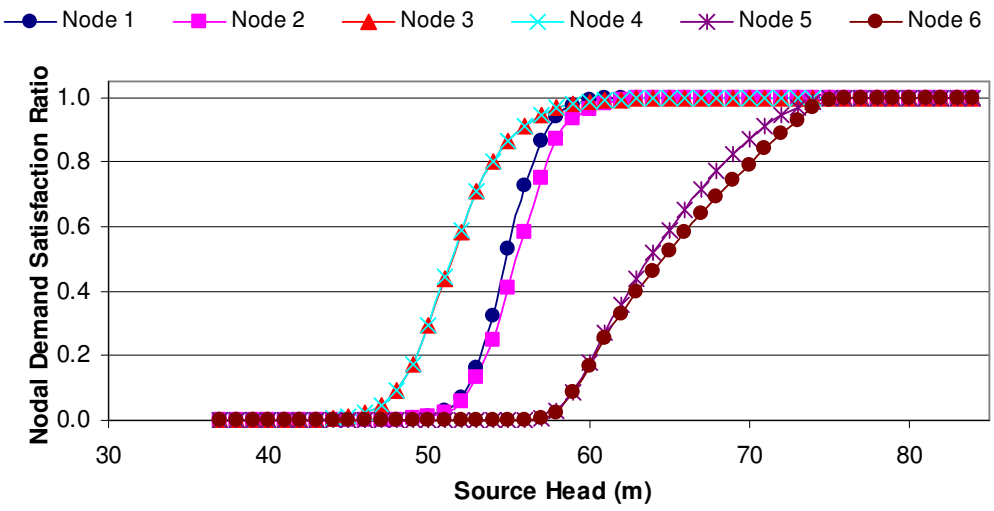

Figure 5.1 Nodal performance of the Two-Loop network (SHV simulations)

PC simulations were executed on this network by closing different individual pipes at a time. The source head was set to79m. Based on the PDA results, the exact shortfall in network performance due to the pipe closures can be accurately quantified as

shown in Fig. 5.2. It can be observed that closing pipes nearer to the source has greater effect on the entire network performance as expected.

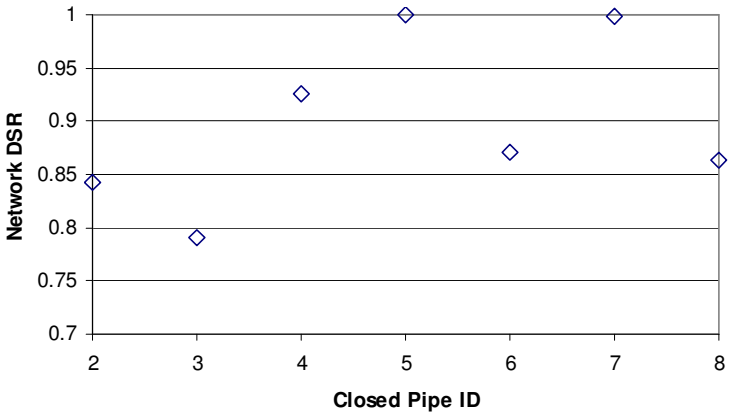

Figure 5.2 Network performances (PC simulations)

For PC simulations, the average computational time required by EPANET-PDX was slightly higher, i.e. 0.054s as opposed to 0.042s by EPANET 2. The average iterations required for convergence were 5.429 and 4.413 for EPANET-PDX and EPANET 2 respectively.

5.3.2 Example 2

The second example is a generic WDS network was taken from Reddy and Elango (1989) and its layout is shown in Fig. 5.3. This network consists of a reservoir, 70 pipes and 36 demand nodes. Further details of pipes and nodes can be found in Appendix B (section B-1). The effective source head was varied from 5m to 40m. This network was chosen to demonstrate the robustness of EPANET-PDX in analysing highly looped networks.

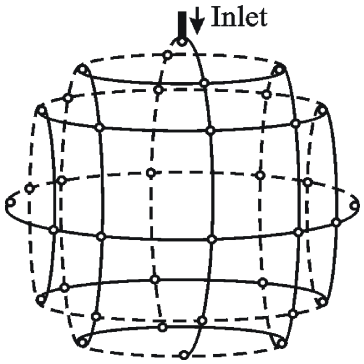

Figure 5.3 Layout of Network 2

A total of 36 SHV simulations were carried out by varying the head of the reservoir from 5m to 40m, subjecting the network to the entire range of DSRs as shown in Fig. 5.4. A comparison of computational performance achieved using EPANET-PDX and EPANET 2 for SHV simulations is summarized in Fig. 5.5. Both simulators achieved an identical average of 4.306 iterations per simulation. In the aspect of CPU time, EPANET-PDX achieved a slightly lower average value of 0.064s per simulation as compared to 0.067s by EPANET 2 (Fig. 5.6).

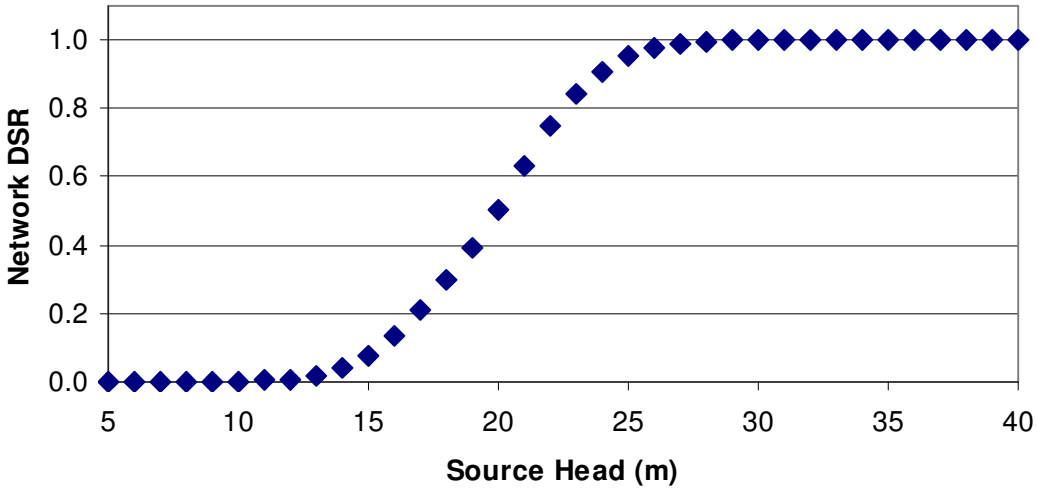

Figure 5.4 Performance of Network 2 (SHV simulations)

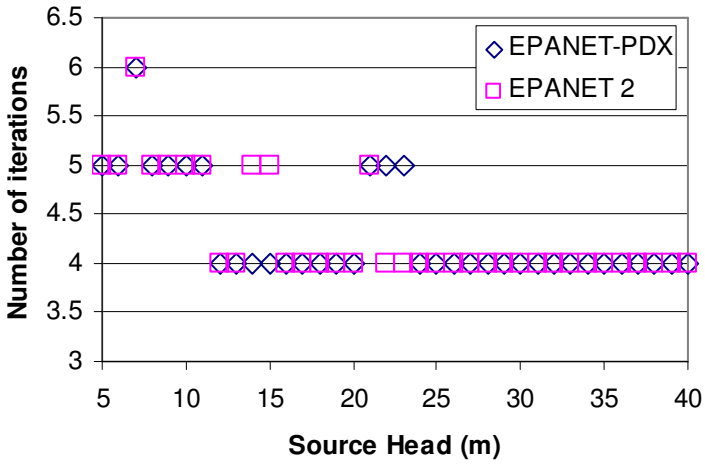

Figure 5.5 Number of iterations required by EPANET-PDX and EPANET 2 (SHV simulations)

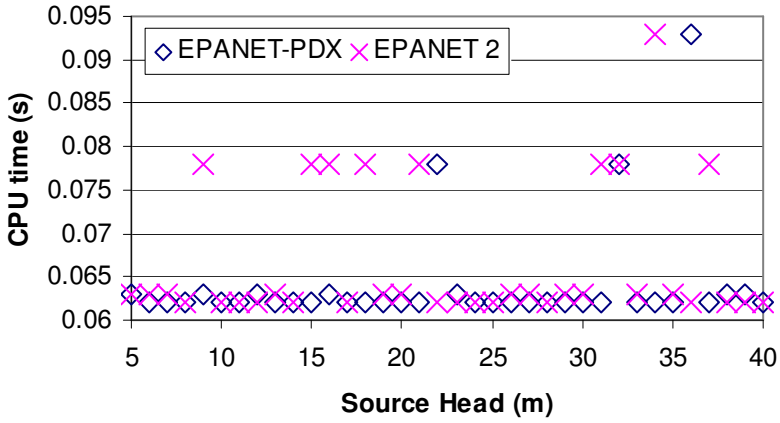

Figure 5.6 CPU time required by EPANET-PDX and EPANET 2 (SHV simulations)

A total of 57 PC simulations were carried out on this network. The number of pipes closed for ranged from 1 pipe to 8 pipes. On average, the performances of both simulators were comparable, i.e. EPANET-PDX required 4.38 iterations (CPU time: 0.069s) to converge where as EPANET 2 required 4.2 iterations (CPU time: 0.058s). More comprehensive results on the performances of the hydraulic simulators for both SHV and PC simulations are presented in Appendix B (section B-2).

5.3.3 Example 3

The third network is based on Jeppson and Davis (1976). The network has two sources, two pumps and one pressure reducing valve as shown in Fig. 5.7. Pipe and node data are given in Fig. 5.7 and Table 5.2 respectively. The hydraulic characteristics of pumps 10 and 11 were represented by H_p=26.67-1042Q_{pu}^2 and H_p=33.33-1029Q_{pu}^2 respectively where H_p is the head supplied by the pump in m and Q_{pu} is the pump discharge in l/s. The pressure-reducing valve (PRV) was set to 140m. The desired residual heads of the demand nodes were each set to 20m. Nodes 1, 3, 7 and 8 are dummy nodes. A total of 72 SHV simulations with different network conditions were performed by simultaneously decreasing the head at both sources 10 and 11 from 158m to 14m and from 238 to 94m respectively.

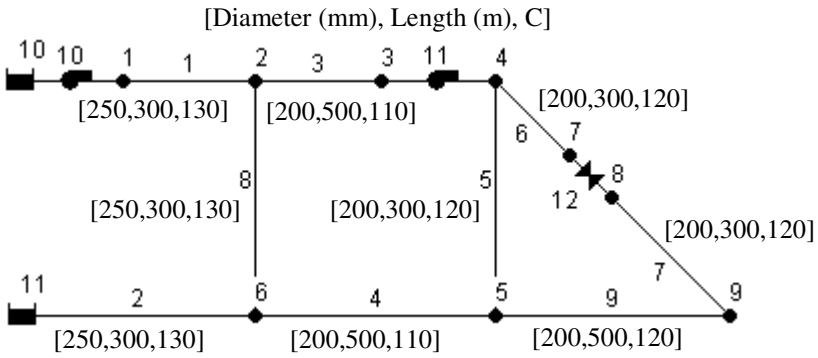

Figure 5.7 Layout of Network 3

Table 5.2 Node data for Network 3

Node	1	2	3	4	5	6	7-8	9
Elevation (m)	150	150	100	130	130	150	120	120
Demand (l/s)	-	30	-	80	50	30	-	80

A closer examination of node 4 was carried out as depicted in Fig. 5.8. It is important to restate that the DSR results presented in this figure correspond to the heads generated by EPANET-PDX, and not EPANET 2. Based on the results in Fig. 5.8, DDA generates significantly lower nodal heads during pressure deficient scenarios, i.e. when nodal residual head is below 20m, giving a very false depiction of the nodal performance. For example, when the head of source 10 was within the range of 90 to

100m, the DSR of node 4 is approximately in the range of 0.7 to 0.8, meaning that there is actually substantial flow emitting from the node. However, based on the negative pressure computed by DDA, one might have the impression that there is no flow at all from node 4 within this source head range. Also, it is shown that the gap between DDA and PDA results gradually closes and finally merges as the nodal DSR approaches one. This clearly demonstrates that the more pressure deficient a network is, the more DDA results underestimate its performance. This also shows that during normal operating conditions, results generated by both analyses are identical.

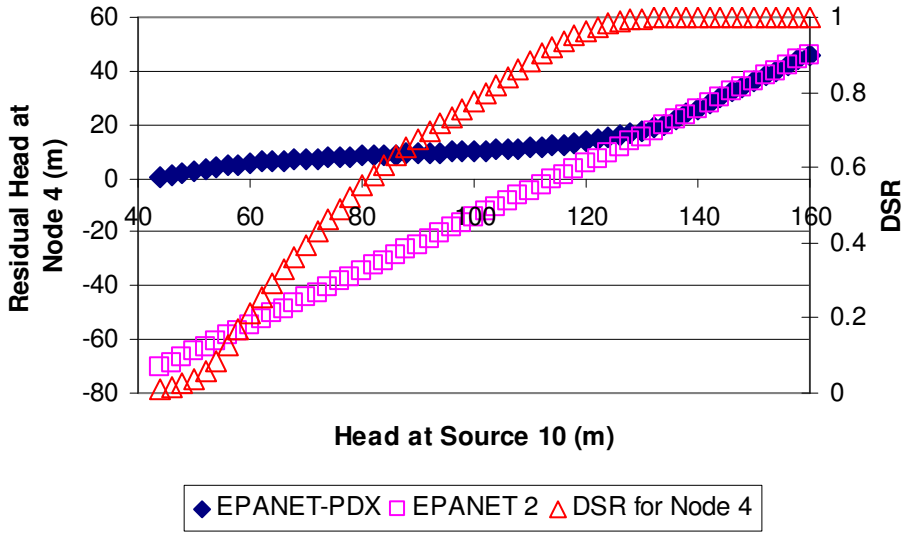

Figure 5.8 Residual Head and DSR of Node 4

Similarly, Fig. 5.9 once again shows how DDA vastly underestimates the nodal performance of node 9 during pressure deficient scenario. When the head at source 10 is 90m, the demand at node 9 is close to being fully satisfied (i.e. DSR of 0.9722). However, DDA users would not even be close to thinking so based on the high negative residual head generated by DDA (i.e. -19.7m). Another interesting observation is when the increment of DDA residual pressure at node 9 somewhat levels off at 20m for a range of pressure, disrupting the continuity of the linear relationship between the DDA nodal head and source head. This is due to the presence of the PRV which was set to halt the flow in pipe 7 to node 9 when its pressure exceeds 140m (which includes the nodal elevation i.e. 120m). However, as pressure in the network continues to increase (to approximately 144m at source 10), the demand

in node 5 gets fully satisfied and additional flow is supplied to node 9 via pipe 9. This explains the further increment in residual pressure above 20m for node 9.

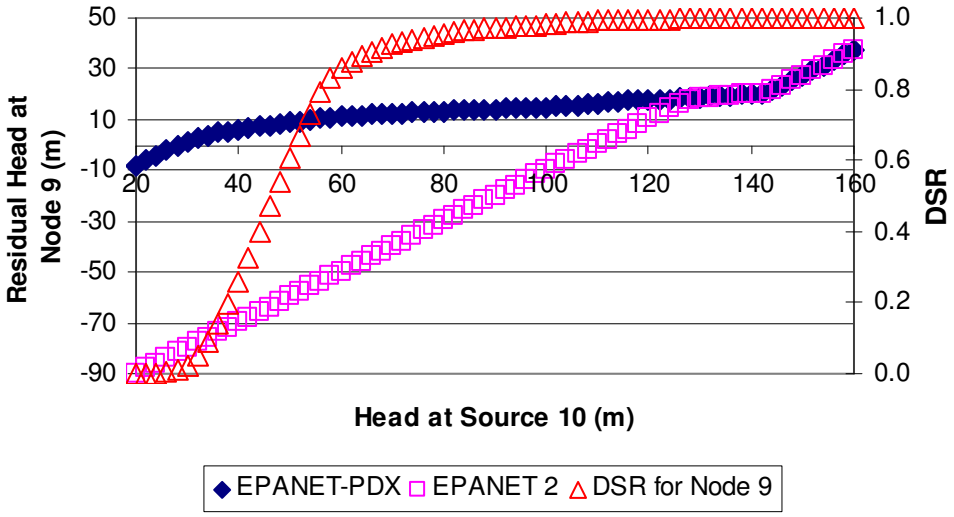

Figure 5.9 Residual Head and DSR of Node 9

For PC simulations, both hydraulic simulators achieved an identical average iteration count of 5.056. The average computational time required by both simulators were very similar, i.e. 0.055s and 0.052s for EPANET-PDX and EPANET 2 respectively. As for SHV simulations, the performances of both hydraulic simulators were virtually identical as summarised in Fig. 5.10 and Fig. 5.11. To achieve convergence, EPANET-PDX took on average 5.575 iterations (average CPU time: 0.059s) while EPANET 2 took 5.562 iterations (average CPU time: 0.054s). Results of the network performances for all SHV and PC simulations can be found in Appendix B (section B-2).

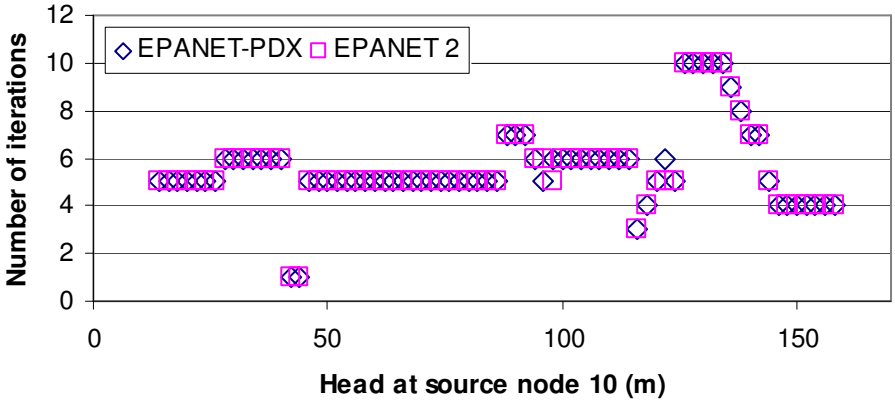

Figure 5.10 Number of iterations required by EPANET-PDX and EPANET 2 (SHV simulations)

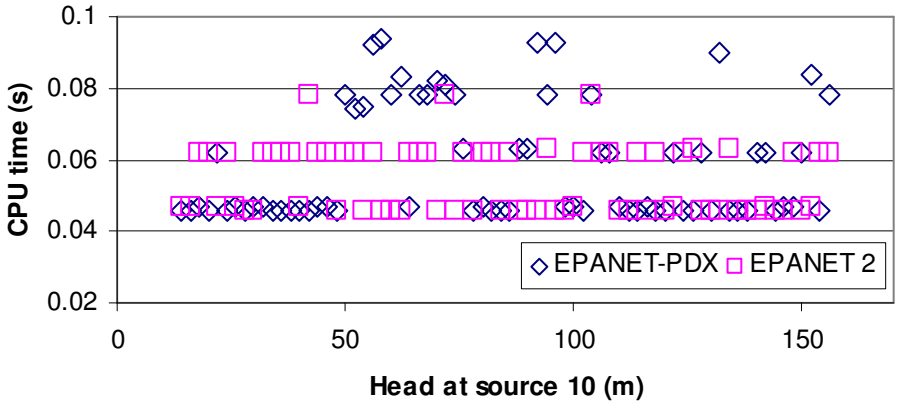

Figure 5.11 CPU time required by EPANET-PDX and EPANET 2 (SHV simulations)

5.3.4 Example 4

The 4th case study involves a real life WDS (Shan, 2004) used in Chapter 4 which consists of 164 nodes, 200 pipes, 5 reservoirs, 4 pumps and 2 flow control valves (FCVs) as shown in Fig. 4.22. Unlike the previous study using the HDGM Fortran 90 program (in Chapter 4), the analysis herein using EPANET-PDX involved the operation of all the pumps and FCVs. The node and pipe input data, hydraulic characteristics of the pumps and FCVs can be found in Appendix A (section A-3).

In this case study, a pressure deficient condition was created by introducing a pressure shortage (with a water level of 100m) for each reservoir such that only 22% of the total demand was satisfied. It is worth observing in Fig. 5.12 that DDA nodal heads computed by EPANET 2 are comparatively much lower to that generated by EPANET-PDX when the network is subjected to pressure deficiency.

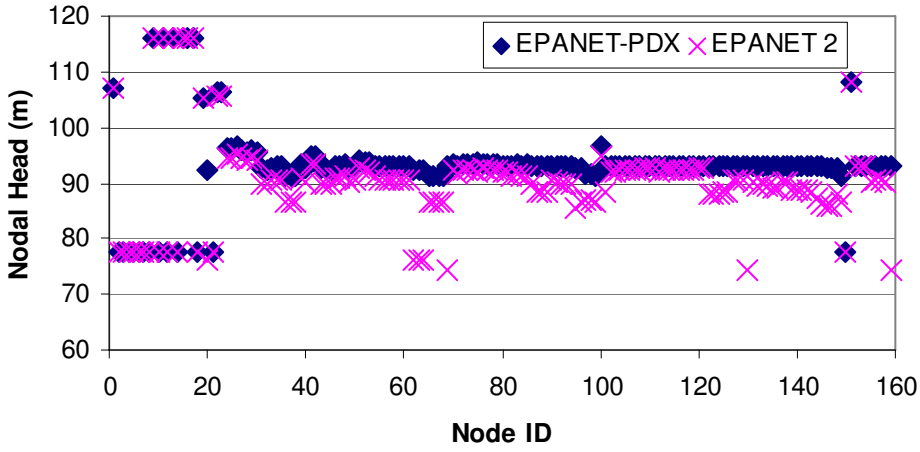

Figure 5.12. Nodal heads generated by EPANET-PDX and EPANET 2 (Network DSR=0.22)

Fig. 5.13 shows the residual head of each demand node generated by both simulators. Based on EPANET 2 (DDA) results, one might have the impression that only one demand node meets the desired residual head requirement, i.e. 15 m. However, based on EPANET-PDX (PDA) results, a total of seven demand nodes have residual pressures above the desired value and are satisfied in full. These seven nodes correspond to a DSR of one as shown in Fig. 5.14. This reinforces the fact that DDA underestimates the capacity of a pressure deficient network. The performance of each demand node can be accurately assessed based on the nodal demand satisfaction ratio (DSR) shown in Fig. 5.14.

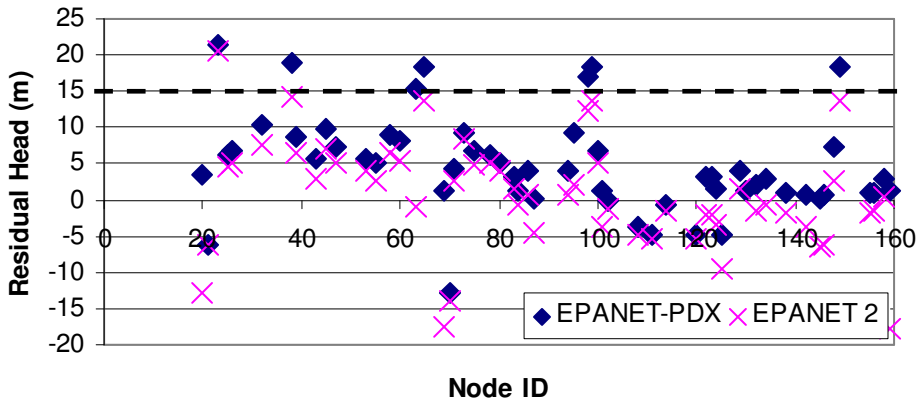

Figure 5.13 Residual nodal heads generated by EPANET-PDX and EPANET 2 (Network DSR=0.22)

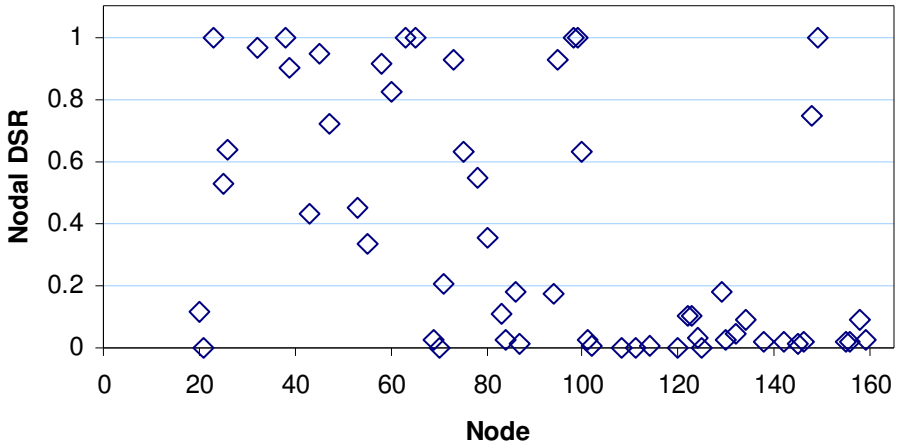

Figure 5.14 Nodal DSR for Network 4 (Network DSR=0.22)

For this network analysis, the performances of both EPANET-PDX and EPANET 2 were very similar. 50 SHV simulations were executed for this network. Both simulators required on average 5.52 iterations to converge. 50 PC simulations involving the closure of up to ten pipes were carried out. The numbers of iterations required for convergence were 5.96 and 5.94 for EPANET-PDX and EPANET 2 respectively. More results which include the required computational time and performances of this network for SHV and PC simulations are presented in Appendix B (section B-2).

5.3.5 Example 5

The fifth example (Fig. 4.28) is the 557 pipe generic network (Shan, 2004) used in the previous chapter. A total of 45 SHV simulations were executed with heads at both reservoir 205 and 206 varying uniformly from 66m to 110m. The network performance is summarised in Fig. 5.15. Fig. 5.16 and Fig. 5.17 show the CPU time required by both EPANET-PDX and EPANET 2 to achieve convergence for each SHV and PC simulation. The average CPU time required by EPANET-PDX and EPANET 2 were 0.157s and 0.158s respectively for SHV simulations. For PC simulations, the required computational time was slightly higher on average for EPANET-PDX, i.e. 0.035s as opposed to 0.022s by EPANET 2. More results on the simulator performance can be found in Appendix B (section B-2).

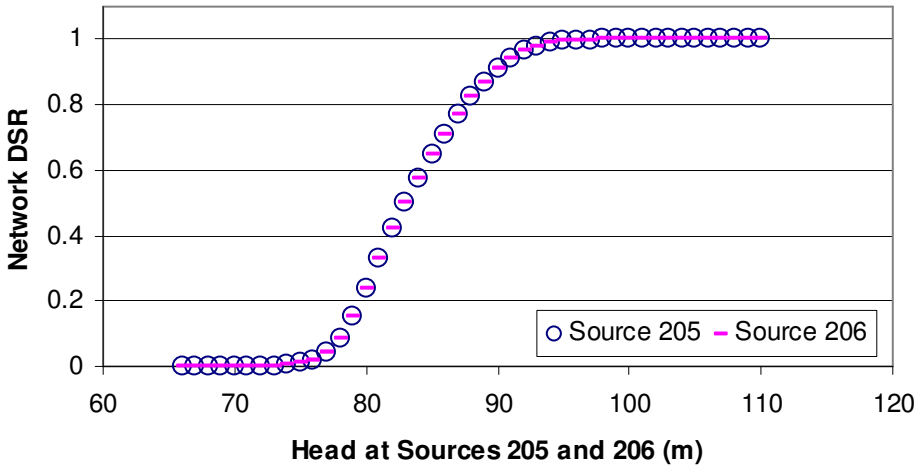

Figure 5.15 Performance of Network 5 (SHV simulations)

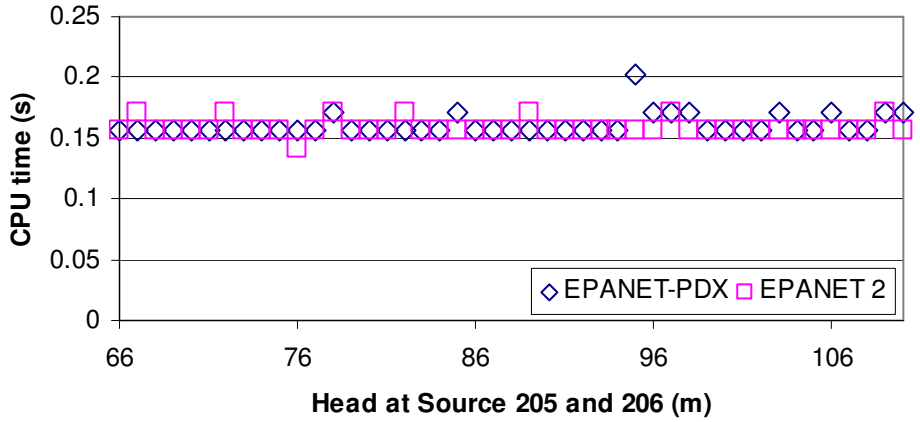

Figure 5.16 Performance of EPANET-PDX and EPANET 2 (SHV simulations)

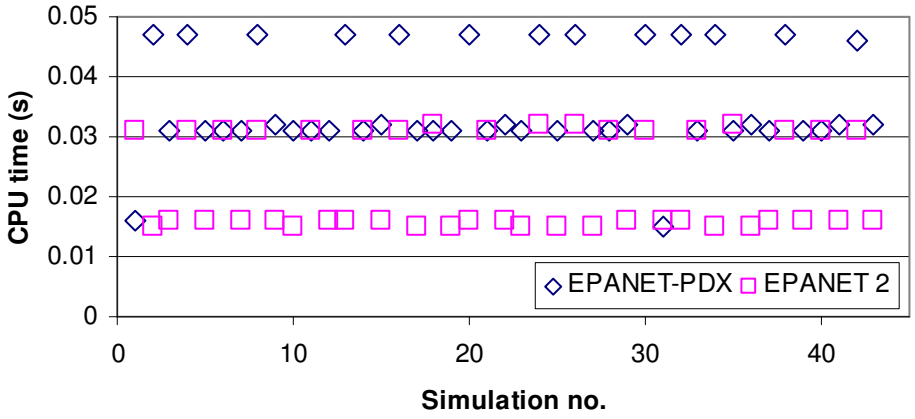

Figure 5.17 Performance of EPANET-PDX and EPANET 2 (PC simulations)

5.3.6 Example 6

Network 6 is the benchmark “Anytown" network (Fig. 5.18) and was chosen to demonstrate the capability of the pressure dependent EPS. The “Anytown” network originally presented an optimization problem involving the upgrading of the system to meet future demands with options including new pipes, cleaning and lining of existing pipes, construction of new pumping stations and tanks. Hence, several modifications to the original (un-optimized network) input data were made here with the sole purpose of enabling an effective EPS to be demonstrated. The diameters of the six new pipes (10, 13, 14, 15, 16 and 25) were set to be 0.3048m (12 in). Demands for nodes 2, 4, 5, 9, 10, 12, 15 were reduced to 3.155 l/s (50 GPM). The modified demand factors (DFs) are presented in Fig. 5.19. The DFs represent the variation in water demand throughout the day. For example, a DF value of 0.6 for the 8th and 9th hour means that the water consumption during both these hours is 0.6 times the average water use. The rest of the network data remain the same as used in Walski et al. (1987) and can be referred to in Appendix E.

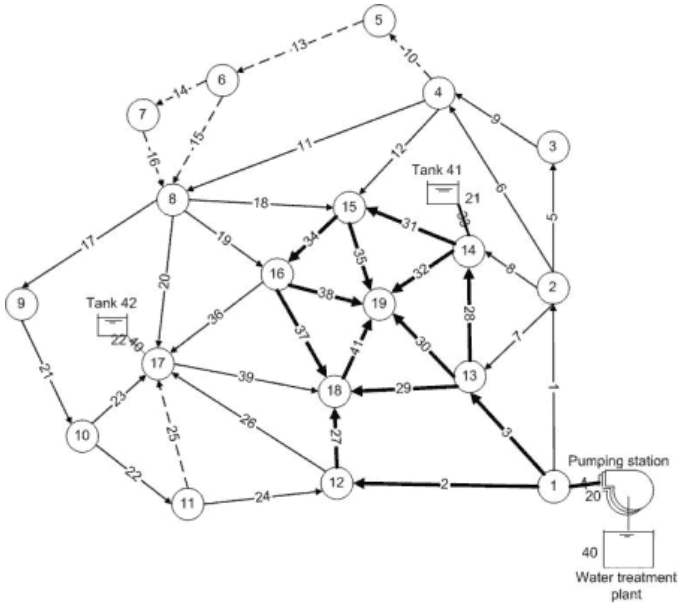

Figure 5.18 Layout of Network 6

The two tanks were operated with water levels between elevations 68.58m (225 ft) and 76.2m (250 ft). A minimum pressure of at least 28.12 m (40psi) must be provided at all nodes. Both tanks were emptied and filled completely over their operational ranges during the day. The network was pressure deficient during the peak demand hours when both tanks were fully depleted. The hydraulic time step used was 1 hour. Observing the plots in Fig. 5.19, the intermediate results for tank heads and network DSR between successive hydraulic time steps indicate that the tanks are either completely filled or emptied.

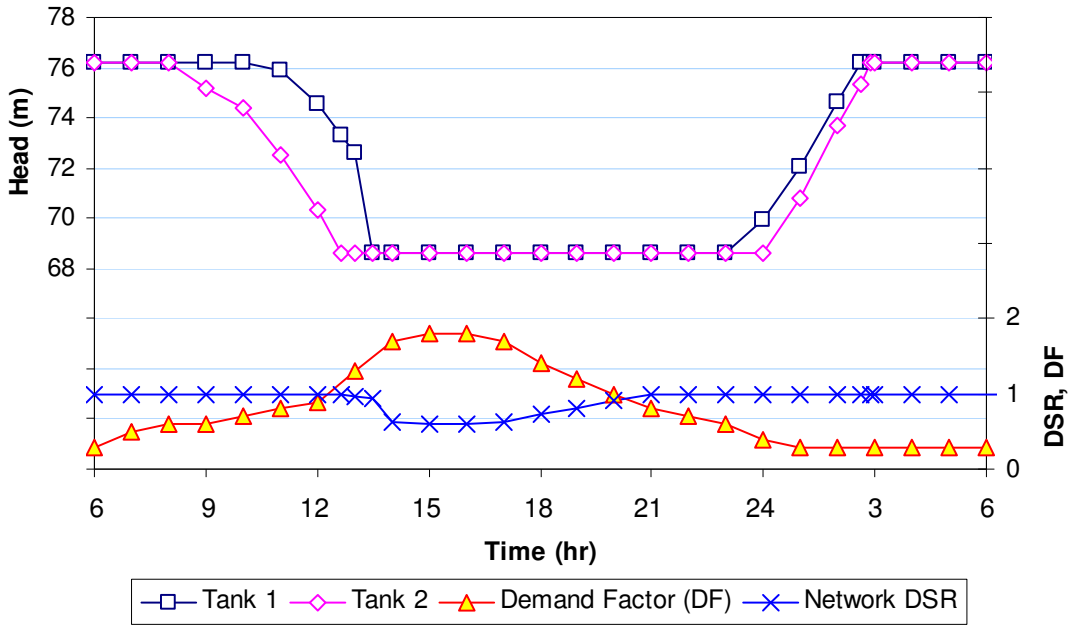

Figure 5.19 Tank heads and network DSR results

Tank 1 and Tank 2 were completely depleted at time 13:27 and 12:37 respectively causing the network to experience a significant drop in DSR as the demand continued peaking with time. Comparing the magnitude of difference in nodal pressure generated by both analyses at time 16:00 and 19:00 (Fig. 5.20 and Fig. 5.21), it is once again shown that the more pressure deficient the network is, the more DDA underestimates its performance. It is worth mentioning that node 1 is connected directly to the source via dummy node 20 and 3 pumps operating in parallel. Hence both these nodes are supplied with constant high pressure throughout the day without being affected much by the variation in demand.

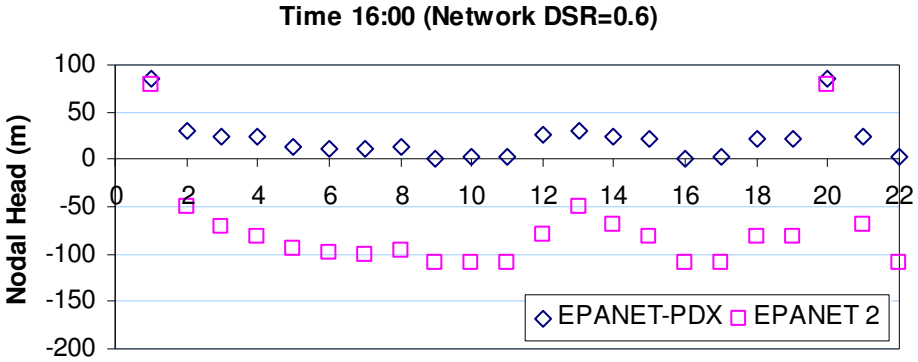

Figure 5.20 Nodal heads for time 16:00

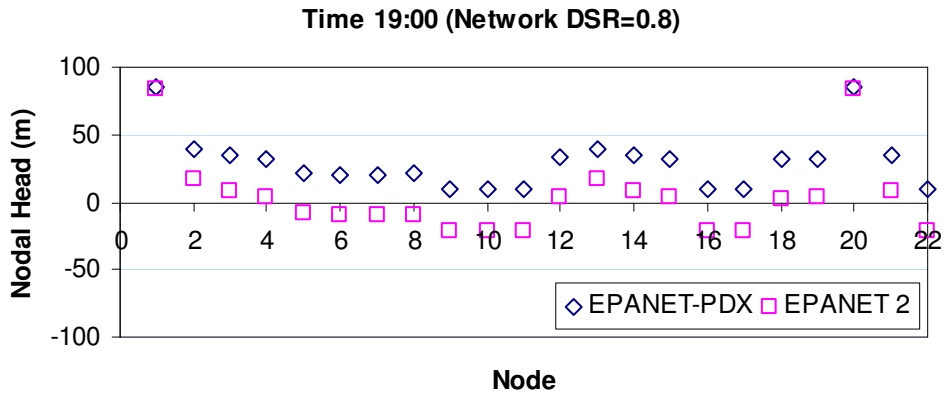

Figure 5.21 Nodal heads for time 19:00

For SHV simulations, a total of 20 EPSs with duration of 24 hours and a hydraulic time step of 1 hour were carried out by varying the heads of both tanks simultaneously from 56.388m (150 ft) to 85.344m (245 ft). On average, EPANET-PDX required 4.102 iterations (CPU time: 0.046s) where as EPANET 2 required 3.171 iterations (CPU time: 0.033s) to achieve convergence. As for PC simulations, 10 EPSs with various pipes closed were executed. EPANET-PDX required 4.26 iterations (CPU time: 0.048s) where as EPANET 2 only required 2.792 iterations (CPU time: 0.033s). In total, approximately 720 (or more) steady state analyses were performed for this network.

5.4 COMPARISON OF PERFORMANCE OF EPANET-PDX AND EPANET 2

Tables 5.3 and 5.4 summarize the performances for both EPANET-PDX and EPANET 2 for all six networks simulated. It is worth mentioning that for Network 6, the average CPU time recorded is the duration of a 24 hour EPS. All steady state simulations were carried out with an Intel single core CPU 3.2GHz, 2GB RAM desktop except for the PC simulations in Network 5. PC simulations of Network 5 along with the EPSs of Network 6 were executed using a more efficient Intel Core 2 Duo CPU 2.66 GHz, 3.23 GB RAM.

The similarity between the mean and median values shows that there are no anomalous data present that may artificially distort the mean values. This appears to suggest that EPANET-PDX, like EPANET 2 performs consistently. As a whole, the computational efficiency of EPANET-PDX compares very favourably to EPANET 2. The performance of the PDA model remains efficient and does not deteriorate with the increase in network size and the presence of other hydraulic elements such as pumps and valves. In cases where EPANET-PDX required higher CPU time such as those reported during pipe closure simulations, the differences were rather trivial. From a numerical and computational efficiency standpoint, this comparison shows that the effort required to incorporate pressure dependent demands is rather insignificant.

Finally, similar to the conclusion arrived by Tanyimboh and Templeman (2004 and 2010), the study herein shows that there is no clear trend suggesting that PDA requires more computational effort when analysing networks under pressure deficiency. The results herein would appear to reinforce the idea that, for well designed PDA and DDA algorithms, any differences are probably insignificant in practical terms.

Table 5.3 Performance of simulators for Source Head Variation simulations

Network	Average number of iterations		Average CPU time (s)	
	EPANET-PDX	EPANET 2	EPANET-PDX	EPANET 2
1	5 (4)	5 (4)	0.048 (0.046)	0.049 (0.046)
2	4.306 (4)	4.306 (4)	0.064 (0.062)	0.067 (0.063)
3	5.575 (5)	5.562 (5)	0.059 (0.047)	0.054 (0.047)
4	5.52 (5)	5.52 (5)	0.169 (0.164)	0.167 (0.164)
5	5.289 (5)	5.289 (5)	0.157 (0.156)	0.158 (0.156)
6	4.102 (4.111)	3.171 (3.148)	0.046 (0.046)	0.033 (0.031)

Values in ( ) represent the median

Table 5.4 Performance of simulators for Pipe Closure simulations

Network	Average number of iterations		Average CPU time (s)	
	EPANET-PDX	EPANET 2	EPANET-PDX	EPANET 2
1	5.429 (6)	4.143 (5)	0.054 (0.047)	0.042 (0.046)
2	4.38 (4)	4.20 (4)	0.069 (0.062)	0.058 (0.047)
3	5.056 (4)	5.056 (4)	0.055 (0.047)	0.052 (0.047)
4	5.960 (6)	5.940 (6)	0.173 (0.125)	0.139 (0.109)
5	4.860 (5)	5.837 (6)	0.035 (0.031)	0.022 (0.016)
6	4.260 (4.226)	2.792 (2.695)	0.048 (0.047)	0.033 (0.031)

Values in ( ) represent the median

5.5 EPANET-PDX RESULT VERIFICATION

The hydraulic feasibility test (HFT) by Ackley et al. (2001) is utilized as a means of verifying the PDA results generated by EPANET-PDX. To avoid any potential confusion, the DDA program used for the HFT which in this case is EPANET 2 is termed as EPANET 2 HFT. The HFT was carried out on a representative sample of simulations for all the network simulations. A graph of correlation between nodal

heads for Network 2 is shown in Fig. 5.22, where R^2 is the statistical correlation coefficient. The agreement between the actual PDA heads (generated by EPANET-PDX) and the DDA heads for PDA nodal flows (generated by EPANET 2 HFT) was excellent. Results for the other networks are reported in Table 5.5. For easier reading, the correlation values are presented in the form of $1\text{-}R^2$. Both sets of nodal heads for each network were essentially identical. The accuracy of the EPANET-PDX PDA results is thus confirmed.

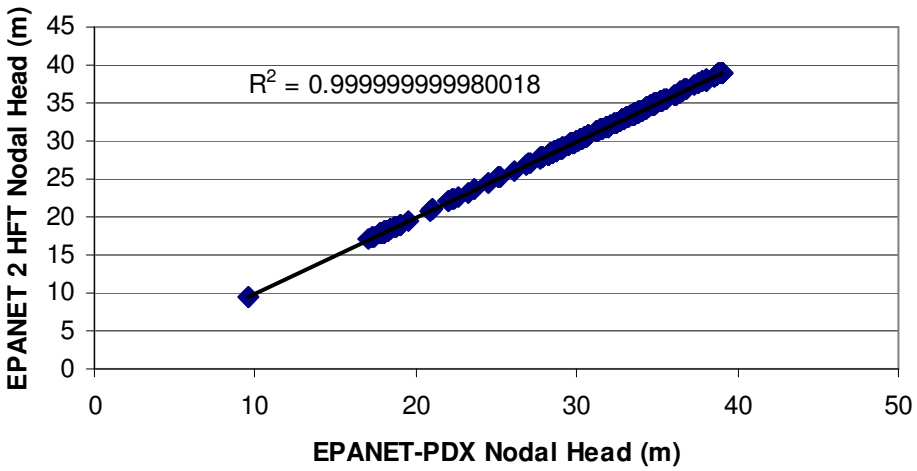

Figure 5.22 Correlation between nodal heads of EPANET-PDX and EPANET 2 HFT (PC simulations for Network 2)

Table 5.5 Correlation between nodal head of EPANET-PDX and EPANET 2 HFT

Network	Source Head Variation		Pipe Closure	
	No. of simulations sampled	$1\text{-}R^2$	No. of simulations sampled	$1\text{-}R^2$
1	22	1.56625×10^{-5}	7	5.2537×10^{-11}
2	18	1.1389×10^{-10}	9	1.9982×10^{-11}
3	15	5.801×10^{-12}	9	1.6335×10^{-11}
4	11	2.6176×10^{-6}	10	8.4723×10^{-8}
5	10	1.3121×10^{-9}	8	2.2984×10^{-6}
6	5*	2.0624×10^{-9}	5*	1.2656×10^{-10}

* Extended Period Simulation

Another verification means is to evaluate the norm of the right hand side of Eq. 4.4 which represents the mass and energy balance. At the solution, the norm should approach a value of 0 as an indication of the progress and accuracy of the algorithm. This ensures that the convergence of EPANET-PDX simulations is not spurious and the real solution has been found. Fig. 5.23 shows a consistent decrease of the norm value at successive iterations for 120 unbiased sampled simulations (from all 6 networks). It is worth observing that the norm reduces very rapidly in the early iterations and by the 4th iteration, majority all of the norm values for these simulations have decreased significantly. These results strongly demonstrate that the line search and backtracking technique effectively optimizes the algorithm's search for the *Hn* and *Qp* vectors, leading to a smooth and rapid convergence.

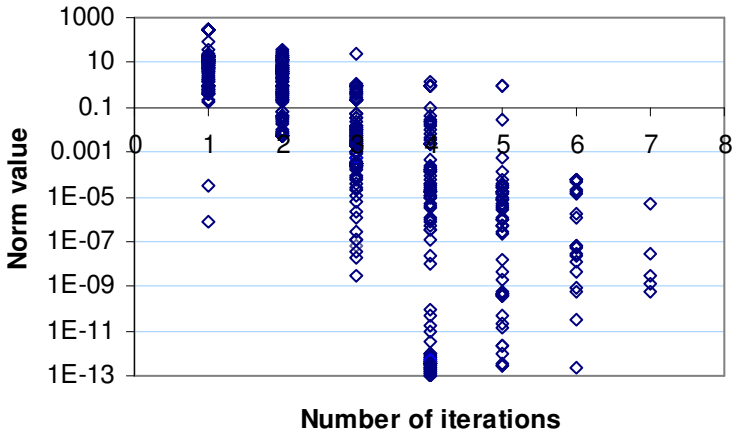

Figure 5.23 Norm value for each iteration

Table 5.6 reports the maximum and mean value of the norm at the last iteration of all simulations (both SHV and PC) executed for each network. It is worth clarifying that the norm values presented are the sum of both the mass and energy balance and are based on the imperial unit, i.e. cfs and ft for mass and energy balance respectively. This implies that corresponding values in SI units (m^3s^{-1} and m) would be much smaller. Results presented reinforce the evidence that EPANET-PDX is highly robust and reliable.

Table 5.6 Norm Value at the last iteration of the simulation

Network	Maximum (cfs and ft)	Mean (cfs and ft)
1	2.72550×10^{-9}	1.28297×10^{-9}
2	3.64349×10^{-5}	2.30958×10^{-6}
3	3.34541×10^{-5}	6.29189×10^{-6}
4	6.32202×10^{-5}	2.73626×10^{-5}
5	4.94513×10^{-6}	3.85161×10^{-7}
6	4.20527×10^{-6}	3.9964×10^{-5}

Values presented here are based on imperial unit, i.e. cfs and ft for mass balance and energy balance respectively. 1cfs = 0.02832 m^3s^{-1}, 1 ft = 0.3048 m

5.6 CONCLUSIONS

A wide ranging study on PDA and DDA involving a total of 1385 steady state simulations and 70 EPSs (24 hour duration) has been carried out. Results presented herein demonstrated that EPANET-PDX is robust and accurate in analyzing both normal and pressure deficient conditions. In terms of computational efficiency, the performance of EPANET-PDX compares very favourably to EPANET 2. With this said, one should bear in mind that EPANET 2 results are inaccurate, misleading or infeasible while analysing pressure deficient networks as demonstrated clearly in this chapter. As mentioned earlier in this chapter, aside from the simulations presented herein, another 46.1 million simulations have been carried out satisfactorily so far within the proposed Penalty-Free Multi-Objective Evolutionary Algorithm framework to solve renowned WDS benchmarks and also real life WDS.

This new EPANET-PDX model provides a fully equipped pressure dependent extended period simulation and is capable of simulating real world networks with tanks, pumps and valves. Evidence of its robustness includes the ability to produce realistic, hydraulically consistent results for the entire range of network demand satisfaction from zero to 100% without any convergence complications. Indeed in all of the cases attempted so far, there is no instance where the program failed to converge. The accuracy of the generated PDA results has been validated and verified using the hydraulic feasibility test and evaluation of the energy and mass balance

errors at the solution. Results presented demonstrated the drawbacks of DDA which include the exaggeration of pressure shortage and the inability to quantify the deficiency of the network performance.

From a numerical standpoint, the line search and backtracking procedure has proven to be effective in providing robustness and very efficient convergence to the hydraulic simulation model. Finally, the development of EPANET-PDX has enabled PDA to be used successfully in WDS optimization which will be presented in subsequent chapters.

CHAPTER SIX

PENALTY FREE MULTIOBJECTIVE EVOLUTIONARY APPROACH

6.1 INTRODUCTION

Evolutionary Algorithms (EAs) have been used in water distribution systems (WDSs) optimisation because of their ability to handle discrete design variables such as pipe diameters and deal with a population of solutions thus significantly increasing the chances of reaching a near-global optimum. Unlike traditional optimization techniques, the EA search is only based on the objective function information and not its continuity of derivatives. This enables EAs to perform well regardless of the complexity of the problem arising from discontinuous and non-differentiable functions.

A major limitation of the widely used EAs is their inability to handle constraints directly. Hydraulic constraints (i.e. mass balance and energy conservation) are normally satisfied externally using a hydraulic solver. The majority of the hydraulic solvers used in WDS optimization studies are conventional Demand Driven Analysis (DDA) based. Due to the assumption that all nodal demands are fully satisfied regardless of pressure, DDA is incapable of simulating pressure deficient conditions and yields very misleading results as demonstrated in the previous chapter. This presents a major problem as numerous solutions generated by stochastic natured EAs are highly pressure deficient and considered infeasible. An inaccurate performance assessment of solutions will potentially misguide the evolutionary search resulting in final solutions that are suboptimal.

To address the nodal pressure constraints, the most commonly adopted technique used is the penalty function methods. The cost objective function of an infeasible solution incurs an additional penalty cost based on its current state of deficiency. A highly infeasible solution will incur a high penalty cost. As such, the probability of it remaining in the subsequent generations will be low. The disadvantage of penalty function methods is that the parameters involved require great expertise in calibration with numerous time consuming trial runs. In addition, penalty parameters are case sensitive and do not necessarily steer the EA search toward the best solutions in every situation.

As reviewed earlier in Chapter 3, the self-adaptive penalty method proposed by Wu and Walski (2005) still utilizes parameters which require calibrations. Anomalies were observed in the tournament selection technique (Deb, 2000) as well as the self-adaptive fitness formulation (Farmani and Wright, 2003). The former selects an overly expensive design over a near feasible design which may well contain majority of the potential building blocks for the optimal solution where as the latter allows cheap infeasible solutions to be selected over expensive feasible ones.

The above-mentioned weaknesses have been eliminated in the proposed model. This chapter presents a new penalty-free multi-objective evolutionary approach (PFMOEA) for the optimization of water distribution systems (WDSs). The proposed approach utilizes pressure dependent analysis (PDA) to develop a multi-objective evolutionary search. PDA is able to simulate both normal and pressure deficient networks and provides the means to accurately and rapidly identify the feasible region of the solution space, effectively locating global or near global optimal solutions along its active constraint boundary. The significant advantage of this method over previous methods is that it eliminates the need for ad-hoc penalty functions, additional "boundary search" parameters, or special constraint handling procedures. Conceptually, the approach is downright straightforward and probably the simplest hitherto.

The PFMOEA has been applied to several WDS benchmarks to evaluate its search capability and computational performance. It is demonstrated that the approach is highly robust and efficient in locating optimal solutions. Superior results in terms of

the initial network construction cost and number of hydraulic simulations required were obtained. The improvements are demonstrated through comparisons with previously published solutions from the literature. The PFMOEA has also been applied to optimize the design of a real life WDS in the United Kingdom. This is an on-going research and early results demonstrated the model's robustness and practical capability to be applied to solve real life problems.

In the previous chapter, EPANET-PDX has been applied to hypothetical and real life networks to demonstrate its practicality and capability as a PDA hydraulic simulator. In this chapter, EPANET-PDX has been integrated within a multi-objective optimizer to evaluate the feasibility of solutions generated. This represents a true test of robustness as numerous hydraulic simulations are executed with every optimization run.

6.2 FORMULATION OF THE PENALTY-FREE BOUNDARY-CONVERGENT MULTI-OBJECTIVE OPTIMIZATION METHOD

The optimization of an engineering design involves multiple objectives which are often contradicting. For example, to maximise the available flow of the network and minimize its capital cost simultaneously are obviously opposing objectives. The presence of these objectives gives rise to a set of compromised solutions known as the Pareto-optimal or non-dominated solutions in which no one solution in this set can be deemed to be superior over the others. The goal in a multi-objective optimization is to find as many diverse Pareto-optimal solutions as possible after which a higher-level decision is required to select one of them for implementation.

The elitism preserving non-dominated sorting genetic algorithm (NSGA II) by Deb et al. (2002) was chosen as the multi-objective optimization method for this research. A basic NSGA II program in C++ language has been written and applied in the optimization work carried out in this research. This NSGA II model is binary coded and involves only simple GA operators such as single bit-wise mutation, single point

crossover and a simple tournament selection. The rationale of this is to enable the performance of the proposed penalty-free approach to be effectively gauged without involving any EA convergence enhancing operators.

The NSGA II procedure can be described as follows. First, a random parent population of size N is generated. Each member in the population is assigned a fitness level with regard to the defined objectives and then ranked on the basis of its non-domination level. The non-domination ranking is done as follows. For each solution p in the population, two entities are calculated, i.e. 1) n_p, the domination count which represents the number of solutions that dominate p, and 2) S_p, a set of solutions which is dominated by solution p. After these two entities are calculated for all solutions, solutions having a domination count of zero, i.e. $n_p = 0$ will be placed in the 1st non-dominated front (NDF) since they are not dominated by any other solutions. For each of the 1st NDF solutions, the domination count for each member, u residing in its S_p set is reduced by one. If the domination count for any member u becomes zero after the subtraction, this solution is placed in the 2nd NDF. The procedure is repeated for each non-dominated member of the 2nd front and the 3rd NDF is identified. The cycle continues until all solutions are allocated a front.

After the solutions are ranked, the crowding distance of each solution is calculated. This requires the solutions to be sorted in ascending order according to each objective considered. Solutions with the largest and smallest function values (for each objective) are assigned an infinite distance value. The distance values for intermediate solutions are then calculated as the absolute normalised difference in the function values of two adjacent solutions. The overall crowding distance for the solution is the sum of the individual distance corresponding to each objective. Hence, a solution having a high crowding distance indicates that it is residing in a less crowded area and is seen to be highly diverse compared to a solution with low crowding distance.

The selection operator follows next. The NSGA II employs a crowded tournament selection operator. During the tournament, the competitors will be compared from two aspects, i.e. their non-domination rank and crowding distance value. Consider two solutions, S1 and S2. S1 is considered the winner of the tournament if the following conditions are satisfied: 1) S1 has a higher non-domination rank than S2; 2) both have

the same non-domination rank but S1 has a larger crowding distance than S2. The first condition ensures that the chosen solution has a better non-domination rank while the second condition resolves the tie by favouring the solution with higher diversity. Recombination operators such as crossover and mutation are then carried out to create a child population of size *N*.

Both parent and child populations are combined to form a population of size 2*N* before being sorted once again using the non-domination ranking algorithm. Doing so ensures that elites from both child and parent populations are preserved and brought forth to the next generation. The new population of size *N* is formed by first including solutions belonging to the best non-dominated front of the combined population, and then subsequent non-dominated fronts in the order of their ranking. The last accepted front may contain more solutions than required to achieve a population of size *N*. If this occurs, the last front is sorted using a crowding distance operator. Solutions with high diversity are favoured and chosen to fill in the remaining slots. This whole procedure is repeated until a pre-specified number of generations are reached.

The proposed PFMOEA involves two primary objectives. The first objective is to minimise the network capital cost. The second objective is to ensure all nodal demands are satisfied. This is achieved by maximizing the total available flow of the most critical node in the network. Network costs normally fall in the range of millions while nodal outflow values are comparatively much smaller and may vary depending on the size of the network and mathematical units used. Due to the vast difference between the objective function values, directly applying both the network cost and the available flow as objective functions may yield technical hitches during the crowding distance comparison sorting stage of the NSGA II. This can potentially result in a biased judgement of distance for the solutions. To overcome this, both objective functions are normalised.

Also, a new efficient boundary search technique was introduced to focus the PFMOEA search on near feasible solutions. This is done by exponentiating the 1st and 2nd objective functions as shown in Eqs. 6.1 and 6.2 respectively. It is important to note that the exponent values remain the same throughout the optimization search. Hence, the objective functions for the PFMOEA are formulated as:

Minimise $F_1 = (CR)^2$ (6.1)

Maximise $F_2 = (DSR_{crit})^4$ (6.2)

where F_1 and F_2 represent the first and second objective functions respectively; CR represents the cost ratio which can be expressed as:

$$CR = \frac{C_{net}}{C_{net}^{\max}} \tag{6.3}$$

where C_{net} and $C_{net}^{\max}$ are the network cost and the maximum network cost in the population respectively. DSR_{crit} represents the demand satisfaction ratio of the most critical node, i.e. the node with the lowest residual pressure head and can be expressed as:

$$DSR_{crit} = \frac{Qn_{i_{crit}}}{Qn_{i_{crit}}^{req}} \tag{6.4}$$

where $Qn_{i_{crit}}$ and $Qn_{i_{crit}}^{req}$ are the actual flow and demand for the critical node i_{crit}. This way, both objective functions are normalised and have values between 0 and 1.0.

Fig. 6.1a and Fig. 6.1b show typical Pareto-optimal fronts of the PFMOEA with and without the implementation of the boundary search respectively. It is worth observing that the former possesses a more enhanced front that is denser with solutions near the boundary region compared to the latter which has quite a uniform spread of diverse solutions encompassing a wider range of DSR and contains a much higher proportion of infeasible solutions. The boundary search approach applied here is only at its preliminary phase. More work is required to further develop the method (See "Suggestions for Future Works" in section 9.3).

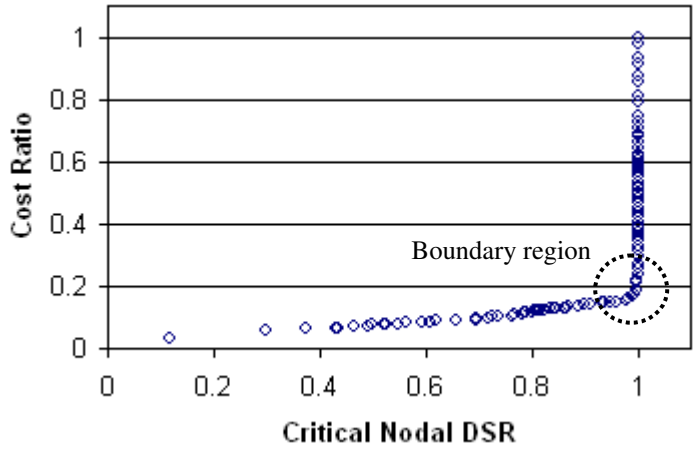

Figure 6.1a Pareto optimal front with boundary search

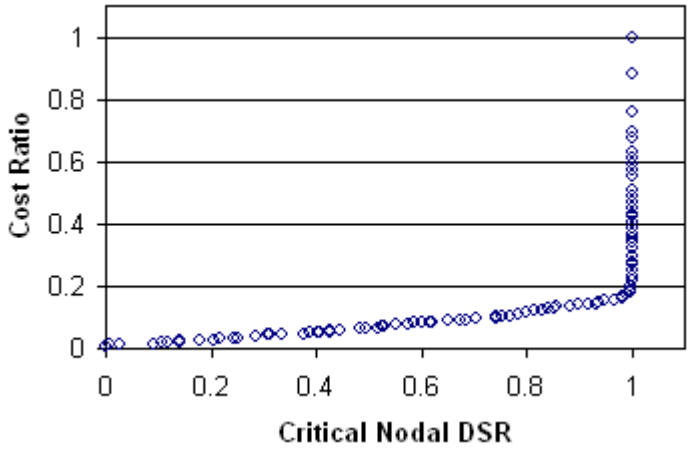

Figure 6.1b Pareto optimal front without boundary search

In the advance stages of the evolutionary process, after merging the parent and child populations (each of which has size *N*), the number of solutions belonging to the Pareto-optimal front (best non-dominated front) may exceed the number of solutions required to maintain a population of size *N*. Since all solutions residing in the same front are assumed (by NSGA II) to have the same quality, to select exactly *N* population members, these solutions are sorted using the crowding distance operator and solutions with the lowest crowding distance (i.e. solutions located in crowded regions) are eliminated. This will result in a front with a uniform spread of diverse solutions consisting of numerous highly infeasible solutions on one hand and numerous highly redundant solutions on the other hand. This approach totally

contradicts the desirable effect of the boundary search strategy (i.e. a Pareto-optimal front with solutions highly concentrated near the boundary of the feasible region as shown in Fig. 6.1a) and potentially leads to the elimination of some of the best solutions.

In the PFMOEA approach, 30% of the population consisting of the best (i.e. the least-cost feasible) solutions in each generation are retained by assigning them each with an extremely high crowding distance value. The remaining solutions are subjected to the crowding distance operator for selection to fill the remaining population slots. In this way, feasible solutions near the boundary region are preserved and diversity amongst the population members is still maintained to a certain extent. For example, consider a hypothetical PFMOEA search with a fixed population size of 100 and a set of 120 solutions in the best non-dominated front at the end of a generation. If there are 50 feasible solutions available, the cheapest 30 (i.e. 30% of 100) will be retained. 70 solutions out of the remaining 90 will then be selected based on their crowding distance to be combined with the 30 best solutions retained, forming a population size of 100 to be carried forward to the next generation.

The procedure of the NSGA II used in the PFMOEA is illustrated in Fig. 6.2.

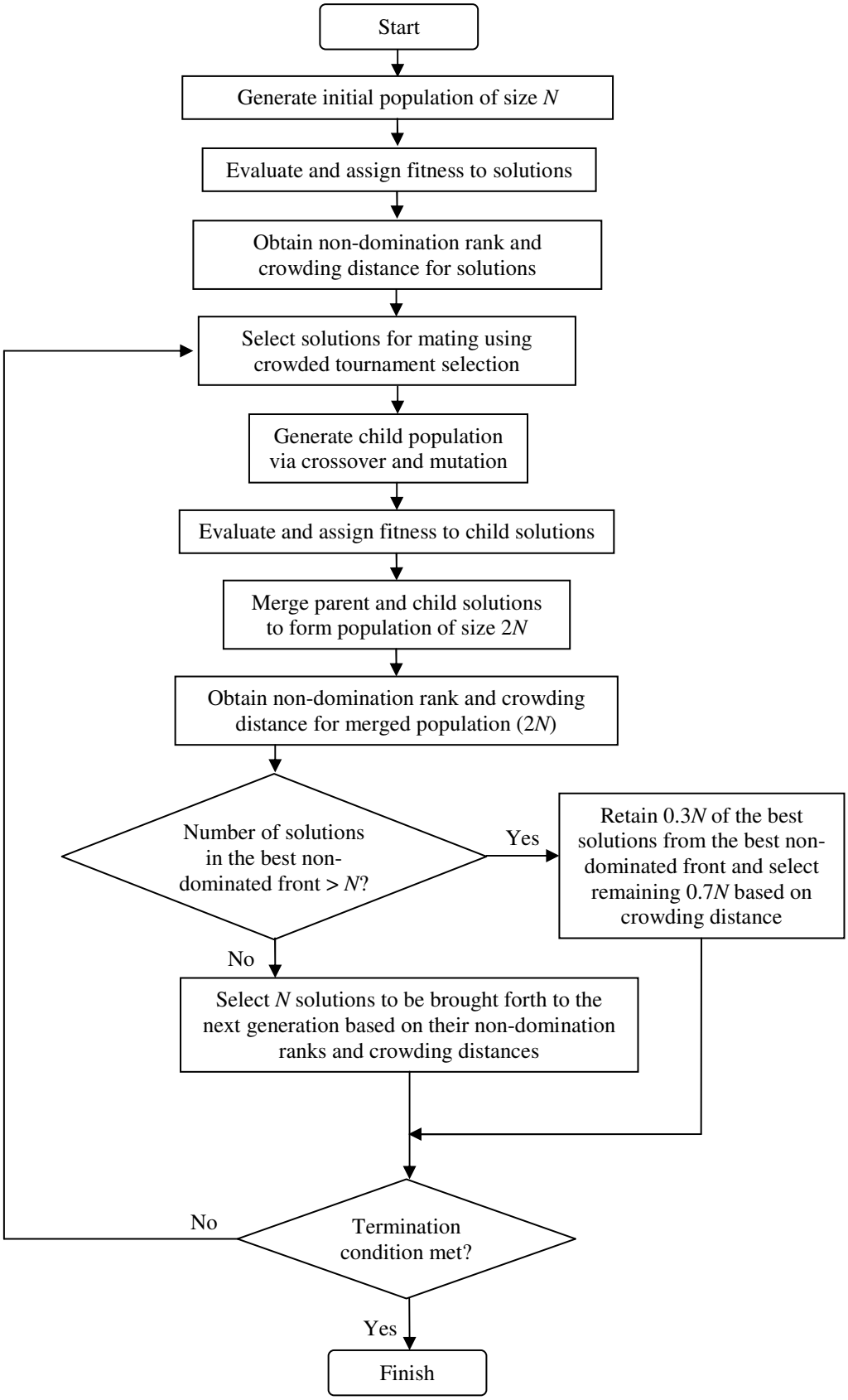

Figure 6.2 Flowchart of the NSGA II operation

In hydraulic analysis, two basic constraints need to be simultaneously satisfied, namely the mass conservation and the energy conservation constraints (Eq. 2.6 and Eq. 2.9 respectively as presented in Chapter 2). The mass conservation constraint requires that the sum of flows at each node must be zero. The energy conservation constraint requires that the total head loss along a path should be equal to the difference in head between its starting and ending nodes. Herein, the Hazen-Williams (HW) equation is used to approximate the head loss and can be described as:

$$h_j = \omega L_j \left(\frac{Qp_j}{C_j} \right)^{1.852} \frac{1}{D_j^{4.87}} \tag{6.5}$$

in which ω is a dimensionless conversion factor whose numerical value depends on the units used; h_j, L_j, Qp_j, C_j and D_j represent the head loss, length, flow rate, HW coefficient and internal diameter for pipe j respectively.

Several researchers use different conversion factors ω. Similarly to Savic and Walters (1997), with the purpose of covering the range of published values and enabling a rigorous comparison of optimal solutions obtained by other researchers in the literature, results presented in this chapter are based on two ω values i.e. 10.5088 and 10.9031.

6.3 APPLICATION OF THE PENALTY-FREE MULTI-OBJECTIVE OPTIMIZATION APPROACH

The PFMOEA is applied to three well-known optimization problems, i.e. the design of the Two-Loop and Hanoi WDSs, and the expansion of the New York Tunnels (Fig. 6.3a, Fig. 6.3b and Fig. 6.3c respectively). It is no doubt that the three benchmarks are simple and do not fully depict the actual problems of real-world WDSs. However, these networks have been extensively analyzed by numerous researchers using various methods and hence, the comparison of the PFMOEA results to the best

optimum solutions obtained from the literature would serve as a good ground in gauging and demonstrating the effectiveness of the proposed optimization approach. An Intel Core 2 Duo CPU 2.66 GHz, 3.23 GB RAM personal computer was used for this study. Since different researchers used computers with different specifications and capacity, a good way to fairly compare the PFMOEA's performance and efficiency with the other algorithms in the literature is by evaluating the number of function evaluations required in obtaining the best solution.

It is worth clarifying that no attempt was made to optimize the mutation rate herein. For the three examples presented, the mutation rates applied vary from 0.005 to 0.02 based on typical values obtained from the literature.

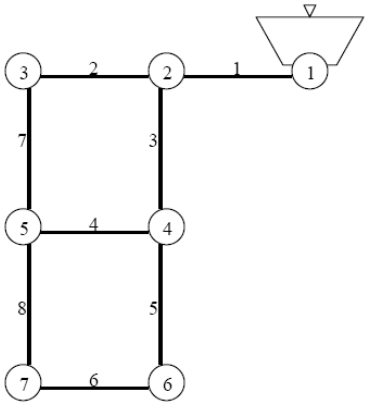

Figure 6.3a Layout of Two-Loop network

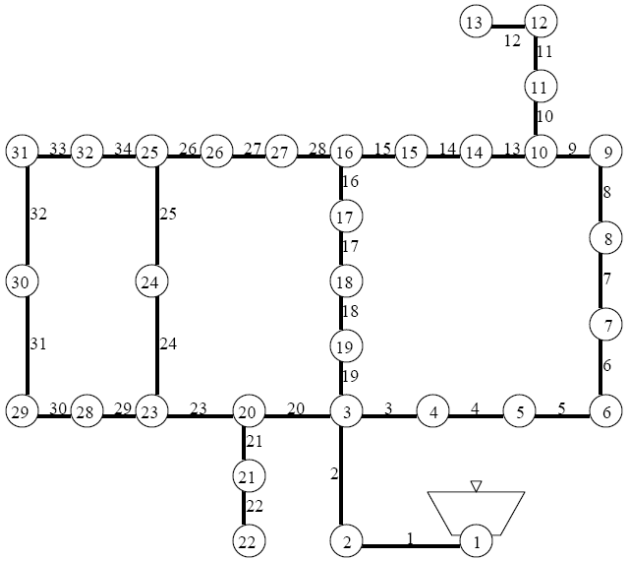

Figure 6.3b Layout of Hanoi network

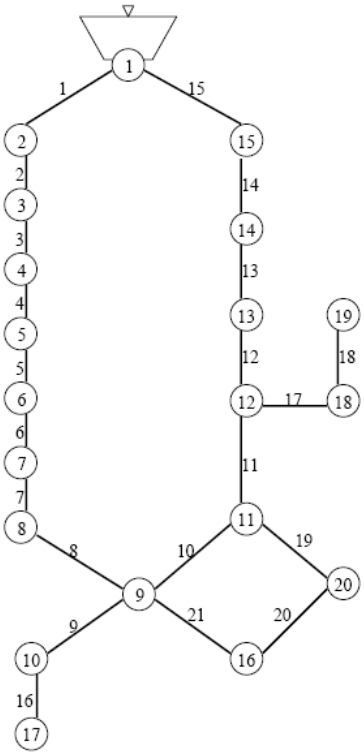

Figure 6.3c Layout of New York Tunnels

6.3.1 Two-Loop Network

Fig. 6.3a shows the layout of the Two-Loop network taken from Alperovits and Shamir (1977). This single source network consists of eight pipes of length 1000m and six demand nodes. The minimum pressure requirement for all nodes is defined as 30m. A Hazen-Williams roughness coefficient of 130 is used for new pipes. A set of 14 commercial pipe diameters is used in this design optimization problem. The diameters and costs of these pipes and node data can be found in Appendix C (section C-2).

Table 6.1 Solutions of the Two-Loop network

Pipe	Diameter (in)						
	ω = 10.5088					ω = 10.9031	
	Savic & Walters (1997)	Cunha & Sousa (1999)	Wu et al. (2001)	Eusuff & Lansey (2003)	PFMOEA	Savic & Walters (1997)	PFMOEA
1	18	18	18	18	18	20	20
2	10	10	10	10	10	10	10
3	16	16	16	16	16	16	16
4	4	4	4	4	4	1	1
5	16	16	16	16	16	14	14
6	10	10	10	10	10	10	10
7	10	10	10	10	10	10	10
8	1	1	1	1	1	1	1
Method	GA	SA	GA	SFLA	GA	GA	GA
Cost ($)	419,000	419,000	419,000	419,000	419,000	420,000	420,000
Eval.	250,000	25,000	7,467	11,323	2,200	250,000	2,600

SA represents simulated annealing.
SFLA represents shuffled frog leaping algorithm.

The best solutions found in previous studies in terms of the initial capital cost and number of function evaluations are presented in Table 6.1. Results, i.e. pipe diameters are presented in imperial units to enable an easy comparison. Savic and Walters (1997) were probably the only researchers who reported the solution with ω=10.9031; their least cost solution of $420,000 was obtained within a total of 250,000 function evaluations.

For this small network, 10 random runs were carried out, each for ω=10.5088 and ω=10.9031. A maximum of 10,000 function evaluations were allowed per run. The probability of crossover and mutation were set to 1.0 and 0.005 respectively. The PFMOEA identified both optimum solutions of $419,000 within 2,200 function evaluations and $420,000 within 2,600 function evaluations which respectively represent small fractions of 1.49×10^{-4}% and 1.76×10^{-4}% of the entire solution space (i.e. 14^8). Compared to the algorithms with the smallest numbers of function evaluations in the literature, the proposed approach required significantly less computational effort in obtaining the least cost feasible solution, i.e. 29.5% of that required by Wu et al. (2001) for ω=10.5088 (7,467 function evaluations) and only

1.04% of that required by Savic and Walters (1997) for ω=10.9031 (250,000 function evaluations).

Fig. 6.4 shows the rate of improvement of the best PFMOEA runs. The overall performances of the PFMOEA were rather similar for both ω=10.5088 and ω=10.9031 cases. Though the former began with an initial population of solutions with much higher costs, the algorithm progressed rapidly within the first six generations and still succeeded in locating the optimal solution within an impressively low function evaluations count. Fig. 6.5 shows the pareto-optimal fronts generated for the two ω values (for the 10 random runs). All the fronts are virtually the same suggesting that the PFMOEA is robust and exhibits a consistent performance. The number of function evaluations and computational time required in obtaining the cheapest solution for each PFMOEA run are presented in Appendix C (section C-2).

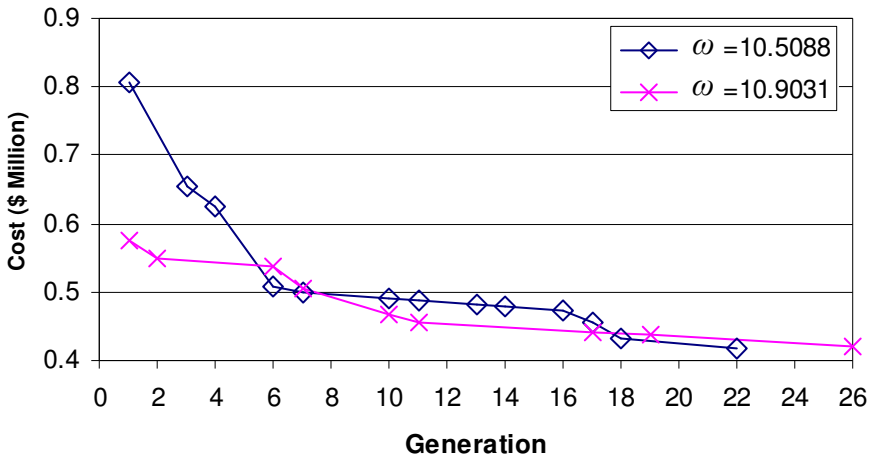

Figure 6.4 Progress of the best PFMOEA runs for the Two-Loop network

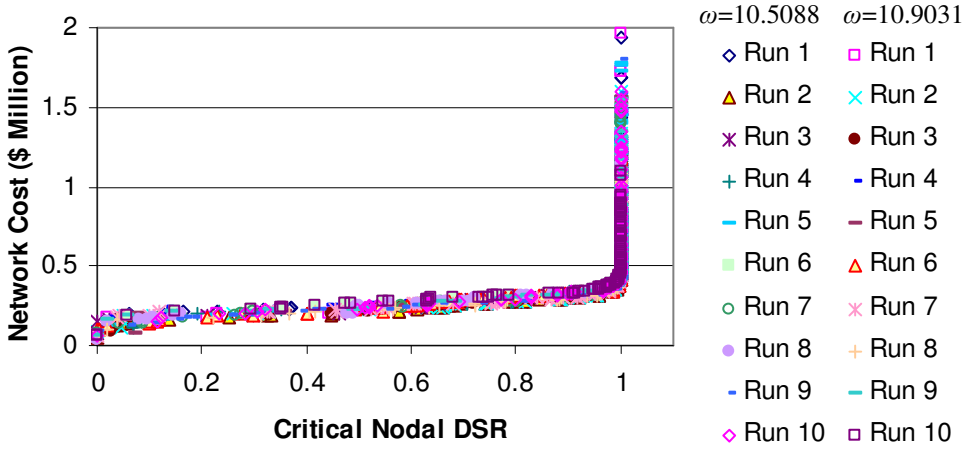

Figure 6.5 Pareto-optimal fronts for the Two-loop network

6.3.2 Hanoi Network

The Hanoi network (Fig. 6.3b), taken from Fujiwara and Khang (1990) consists of 34 pipes, 32 nodes and a single source of elevation 100m. The minimum head at all demand nodes is fixed at 30m. A set of six commercially available pipe diameters (12, 16, 20, 24, 30 and 40 in.) is utilised in the design optimization of the system with the cost of each pipe calculated based on the cost function $Cost_i=1.1\times L_i\times D_i^{1.5}$, where *Cost* ($), *L* (m) and *D* (in) are the cost, length and diameter of commercial pipe *i* respectively. All new pipes are assumed to have a HW roughness coefficient of 130. The network input data can be found in Appendix C (section C-3).

Solutions achieved by other researchers are presented in Table 6.2. Cunha and Sousa (1999) identified the solution of $6.056 million for ω=10.5088 while Wu et al. (2001) reported the solution with capital cost of $6.182 million for ω=10.9031. These solutions are perhaps the cheapest feasible solutions obtained (from EA searches which involve the entire solution space) within the lowest numbers of function evaluations in the literature hitherto. Kadu (2008) achieved the solutions of $6.056 million ($\omega$=10.5088) and $6.190 million ($\omega$=10.9031) both within a low function evaluation of 18,000. However, it is essential to highlight that a search space reduction technique was implemented and only selective candidate pipe diameters

(from the 6 commercial pipe sizes) were used. Hence, the GA search only involved 2.351×10^{19} possible solutions which is approximately 8.2×10^{-6} % of the entire solution space (i.e. $6^{34} = 2.865\times10^{26}$).

For this network, 60 runs each starting from a different initial population (randomly generated) were conducted for each ω value. A total of 200,000 function evaluations were permitted per run. The crossover probability was fixed to 1.0 and the range of mutation probability used was between 0.005 and 0.02. The PFMOEA succeeded in identifying the least cost feasible solutions for both ω values with 51,000 function evaluations for the solution of \$6.056 million (for ω=10.5088) and 100,000 function evaluations for the solution of \$6.182 million (for ω=10.9031) which respectively are equivalent to 1.78×10^{-20} % and 3.49×10^{-20} % of the entire search space. These values are lower than what was achieved by Kadu et al. (2008), i.e. 7.656×10^{-14} % of the reduced solution space. Compared to the 53,000 function evaluations by Cunha and Sousa (1999) and 113,626 function evaluations by Wu et al. (2001), this represents an approximate improvement of 3.77% and 12% for ω=10.5088 and ω=10.9031 respectively. It is worth mentioning that the PFMOEA also obtained the solution of \$6.19021 million which is a similar design to the \$6.190 million solution by Kadu et al. (2008) for ω=10.9031 (all pipe diameters are identical to Kadu et al. (2008) except for pipe 27 which is 16in) with 49,700 function evaluations. This solution has not been obtained by any other researchers or published in the literature.

Table 6.2 Solutions of the Hanoi Network

Pipe	Diameter (in)								
	ω = 10.5088						ω = 10.9031		
	Cunha & Sousa (1999)	Vairava-moorthy & Ali (2000)	Wu & Walski (2005)	Geem (2006)	*Kadu et al. (2008)	PFMOEA	Wu et al. (2001)	†*Kadu et al. (2008)	PFMOEA
1 - 8	40	40	40	40	40	40	40	40	40
9	40	40	40	40	40	40	40	30	40
10	30	30	30	30	30	30	30	30	30
11	24	24	24	24	24	24	24	30	24
12	24	24	24	24	24	24	24	24	24
13	20	20	20	20	20	20	16	16	16
14	16	16	16	16	16	16	12	12	12
15	12	12	12	12	12	12	12	12	12
16	12	12	12	12	12	12	12	16	12
17	16	16	16	16	16	16	20	20	20
18 - 19	20	20	20	20	20	20	24	24	24
20	40	40	40	40	40	40	40	40	40
21	20	20	20	20	20	20	20	20	20
22	12	12	12	12	12	12	12	12	12
23	40	40	40	40	40	40	40	40	40
24 - 25	30	30	30	30	30	30	30	30	30
26	20	20	20	20	20	20	24	20	24
27 - 28	12	12	12	12	12	12	12	12	12
29	16	16	16	16	16	16	16	16	16
30	12	12	12	12	12	12	16	12	16
31	12	12	12	12	12	12	12	12	12
32	16	16	16	16	16	16	16	16	16
33	16	16	16	16	16	16	16	20	16
34	24	24	24	24	24	24	24	24	24
Method	SA	GA	GA	HS	GA	GA	GA	GA	GA
Cost ($M)	6.056	6.056	6.056	6.056	6.056	6.056	6.182	6.190	6.182
Eval.	53,000	160,000	150,000	200,000	18,000	51,000	113,626	18,000	100,000

HS and SA represent harmony search and simulated annealing evolutionary algorithm respectively.
* Selective diameters used (not the full set of 6 commercial pipe sizes).
† Infeasible solution.

The least cost solutions presented by Kadu et al. (2008) and the PFMOEA were simulated using both EPANET-PDX and EPANET 2 to confirm the nodal pressure heads. Pressure heads for the four most critical nodes are presented in Table 6.3. For the solution with ω=10.9031 by Kadu et al. (2008), it was observed (Table 6.3) that the head at node 27 slightly violates the minimum nodal pressure requirement. All optimum solutions identified by PFMOEA were feasible in that all nodal heads (generated by EPANET-PDX and EPANET 2) were above the minimum pressure requirement.

Table 6.3 Critical node pressure heads for the Hanoi network

Node	Head (m)			
	ω = 10.5088	ω = 10.9031		
	PFMOEA and Kadu et al. (2008)	Kadu et al. (2008)	PFMOEA	
27	30.207 (30.170)	*29.984 (29.944)	30.331 (30.291)	30.413 (30.377)
29	30.260 (30.220)	30.186 (30.146)	30.088 (30.046)	30.681 (30.646)
30	30.521 (30.483)	30.703 (30.664)	30.596 (30.556)	30.225 (30.188)
31	30.802 (30.764)	31.019 (30.981)	30.912 (30.872)	30.376 (30.339)
Cost ($ Million)	6.056	6.190	6.19021	6.182

* Infeasible solution i.e. $Hn_i < 30$ m
Critical node heads generated by EPANET 2 are shown in parentheses

Table 6.4 shows the least cost solutions of the ten best PFMOEA runs for each of the two ω values used here. The critical nodal pressure heads presented confirm that all solutions meet the minimum required pressure and are fully feasible. The PFMOEA succeeded in locating the optimal solution seven times for ω=10.5088 and four times ω=10.9031. The costs of the other solutions obtained (as shown in Table 6.4) were only slightly higher (difference of less than 1%) compared to the lowest cost solutions reported in the literature. This along with the low number of function evaluations (Table 6.4) demonstrates that the PFMOEA is highly capable of locating near optimal solutions very quickly. The cheapest feasible designs obtained from the best five runs are presented in Appendix C (section C-3).

Table 6.4 Solutions from the best ten PFMOEA runs for the Hanoi Network out of 60 random runs within 200K FEs

Best Runs	ω =10.5088			ω =10.9031		
	Costs ($ Million)	Function Evaluations	Critical Nodal Heads (m)	Costs ($ Million)	Function Evaluations	Critical Nodal Heads
1	6.056	51,000	30.207	6.182	100,000	30.225
2	6.056	75,400	30.207	6.182	100,100	30.225
3	6.056	80,700	30.207	6.182	111,400	30.225
4	6.056	87,000	30.207	6.182	136,700	30.225
5	6.056	105,100	30.207	6.188	78,600	30.018
6	6.056	106,400	30.207	6.188	116,700	30.018
7	6.056	167,400	30.207	6.188	164,900	30.018
8	6.065	59,200	30.156	6.188	193,900	30.018
9	6.065	164,000	30.156	6.190	49,700	30.046
10	6.073	46,200	30.271	6.190	55200	30.046

The pareto-optimal fronts of the best 10 PFMOEA runs for each ω value are illustrated in Fig. 6.6. The PFMOEA performance is once again demonstrated to be consistent in that all the fronts are virtually identical.

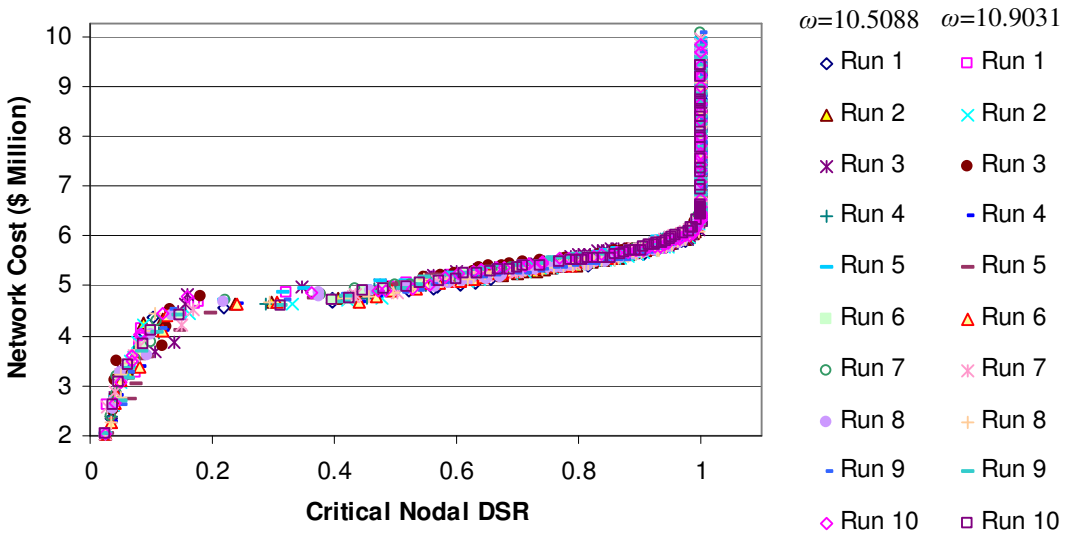

Figure 6.6 Pareto-optimal fronts of the best 10 PFMOEA runs for the Hanoi network

6.3.3 New York Tunnels

Fig. 6.3c shows the layout of the New York Tunnels. The network is fed from a single fixed-head source providing a head of 91.44m (300 ft) and consists of 20 demand nodes and 21 pipes the details of which can be found in Appendix C (section C-4). The objective of this optimization problem is to expand the existing tunnels by means of pipe paralleling so that the projected demands and pressure requirements can be met. The minimum head constraints are 79.248 m (260 ft) for node 16, 83.149 m (272 ft) for node 17 and 77.724 m (255 ft) for the remaining 18 nodes. There are 15 available diameters (36, 48, 60, 72, 84, 96, 108, 120, 132, 144, 156, 168, 180, 192 and 204 in) to be considered and the "do nothing" option, forming a total solution space of $16^{21}=1.93\times10^{25}$ possible network designs. The cost of each pipe calculated based on the cost function $Cost_i=1.1\times L_i\times D_i^{1.24}$, where *Cost* ($), *L* (ft) and *D* (in) are the cost, length and diameter of commercial pipe *i* respectively.

The best solutions reported in the literature by other authors using GA with various constraint handling methods are presented in Table 6.5. Vairavamoorthy and Ali (2000) reported a solution with a low cost of $37.10 million. However, the pipe diameter of 100in. used in this solution is not in the set of commercial pipe sizes allocated for this optimization problem. Savic and Walters (1997) reported the least cost solutions in the literature hitherto, i.e. $37.13 million for ω=10.5088 and $40.42 million for ω=10.9031. The solution of $37.13 million was also identified by Farmani et al. (2005b) within the lowest reported number of function evaluations so far. To the knowledge of the author, besides Savic and Walters (1997), no other previous studies in the literature reported solutions using ω=10.9031.

Table 6.5 Solutions of the New York Tunnels

Pipe	Diameter (in)								
	ω = 10.5088				ω =10.6792			ω =10.9031	
	Savic & Walters (1997)	Vaira-vamoor-thy & Ali (2000)	Farm-ani et al. (2005b)	PFMOEA	Monte-sinos et al. (1999)	Afshar & Marino (2007)	Wu & Simp-son (2002)	Savic & Walters (1997)	PFMOEA
7	108	96	96	108	-	144	-	-	-
15	-	-	-	-	120	-	120	144	144
16	96	*100	96	96	84	96	84	84	84
17	96	96	96	96	96	96	96	96	96
18	84	84	84	84	84	84	84	84	84
19	72	72	72	72	72	72	72	72	72
21	72	72	72	72	72	72	72	72	72
Cost ($M)	37.13	37.10	37.13	37.13	38.80	38.65	38.80	40.42	40.42
Eval.	1,000,000	80,000	26,340	7,200	18,300	13,420	22,500	1,000,000	17,800

* Pipe diameter 100in is not in the set of commercial pipe sizes allocated in this optimization problem
The dash (-) represents the do-nothing option. Pipe sizes not shown were unchanged, corresponding to the do-nothing option.

The solution space of the New York Tunnels problem is approximately one order of magnitude smaller than that of the Hanoi network. Hence, only 30 runs were conducted for each ω value. A total of 100,000 function evaluations were permitted per run. The crossover probability was fixed to 1.0 and the mutation probability used was between 0.005 and 0.01. For this example, the PFMOEA succeeded in locating the optimal solutions (identical to that of Savic and Walters (1997)) but with remarkably fewer function evaluations in comparison to the rest of the algorithms presented, i.e. 7,200 for ω=10.5088 and 17,800 for ω =10.9031. These respectively represent extremely small fractions of 3.73×10^{-22} % and 9.22×10^{-22} % of the total number of pipe size combinations (16^{21}). In comparison to the algorithms with the smallest numbers of function evaluations, the computational effort (function evaluations) required by the PFMOEA was only 27.33% of that required by Farmani et al. (2005b) for ω=10.5088 and 1.78% of that required by Savic and Walters (1997) for ω=10.9031.

It is also worth highlighting that within the 30 random runs executed, the optimum solutions of \$37.13 million (for ω=10.5088) and \$40.42 million (for ω=10.9031) were located seven and three times respectively. Details such as the required number of

function evaluations and CPU time in locating the cheapest solution in each run can be found in Appendix C (section C-4).

Both optimal solutions obtained by the PFMOEA (i.e. solutions of \$37.13 million and \$40.42 million) were simulated by EPANET-PDX and EPANET 2 to reconfirm their feasibility. Results (critical node pressure heads) are presented in imperial units to enable an easy comparison. It can be concluded from Table 6.6 that all nodal pressure heads meet the minimum pressure requirement.

Table 6.6 Critical node pressure heads for the New York Tunnels

Node	Minimum Required Head (ft)	ω = 10.5088		ω = 10.9031	
		EPANET Head (ft)	EPANET-PDX Head (ft)	EPANET Head (ft)	EPANET-PDX Head (ft)
16	260.0	260.161	260.212	260.282	260.332
17	272.8	272.861	272.89	272.882	272.912
19	255.0	255.206	255.266	255.398	255.458

Fig. 6.7 shows the pareto-optimal fronts of the best 10 PFMOEA runs for each ω value. Similar to the previous two benchmark networks optimized, all pareto-optimal fronts are effectively the same, further confirming the consistency of the PFMOEA performance. Table 6.7 shows the cost of five best feasible solutions generated from the best PFMOEA run for this network for ω=10.5088 and ω=10.9031. Details of these solutions (i.e. existing pipes to be paralleled and diameter of the new pipes) can be found in Appendix C (section C-4). The costs of these solutions were very close to the least cost solutions reported in the literature. This suggests that the PFMOEA is capable of obtaining a Pareto-optimal front consisting of non-dominated solutions which are highly comparable to the best (least cost) solution. A good range of solutions is therefore provided allowing for flexibility in choosing the final design for implementation during a higher level decision making stage which may involve other measures such as reliability. The cheapest feasible designs obtained from the best five runs are presented in Appendix C (section C-4).

Table 6.7 Solutions from the best PFMOEA run for the New York Tunnels

Solution	ω =10.5088			ω =10.9031		
	Cost ($ Million)	Critical Node	Head (m)	Cost ($ Million)	Critical Node	Head (m)
1	37.13*	17	83.1769	40.42*	17	83.1836
2	37.62	17	83.2101	41.12	17	83.1866
3	38.13	17	83.2391	41.13	17	83.1896
4	38.80	17	83.2412	41.29	17	83.2719
5	38.94	16	79.3455	41.96	17	83.2750

* Least cost solution reported in the literature.
Required head for node 17 is 83.149m.
Required Head for node 16 is 79.248m.

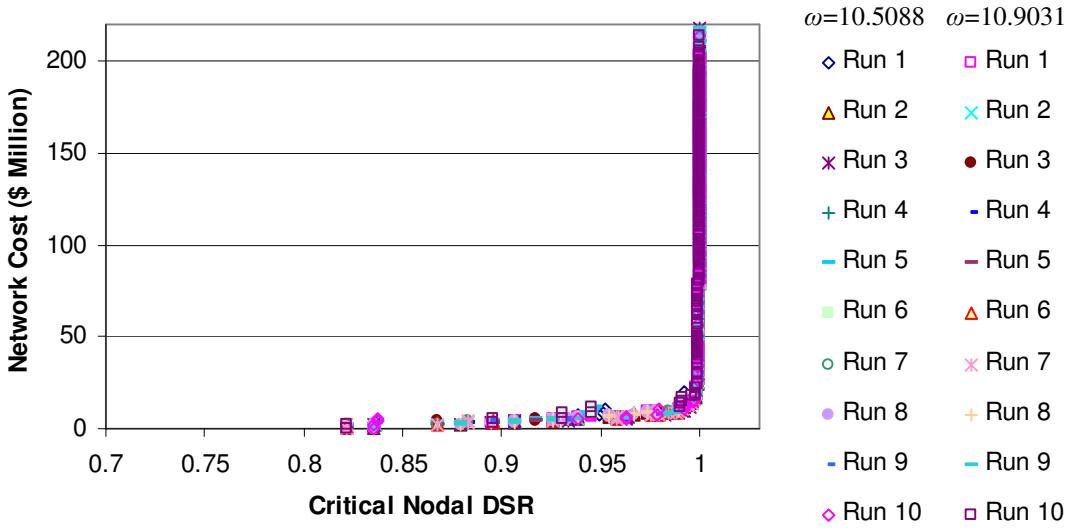

Figure 6.7 Pareto-optimal fronts of the best 10 PFMOEA runs for the New York Tunnels

The CPU times required by the PFMOEA to obtain the best reported solutions for all the three benchmark networks are presented in Table 6.8. To further quantify the overall performance of the PFMOEA, the maximum and mean costs of the cheapest feasible solution from the total runs are summarised in Table 6.9. It can be observed that the mean values of the cheapest feasible solutions are close to the cost of the best solutions (difference of less than 6%). In addition, the maximum cost of the cheapest solution (i.e. the solution obtained by the worst performing run) is not excessively higher than the cost of the optimum design for all of the cases. This shows that the PFMOEA is highly capable of locating cheap feasible solutions. The computational

time and function evaluations required for all PFMOEA runs are detailed in Appendix C (section C-4).

Table 6.8 Computational time required by the PFMOEA to obtain the best reported solutions

Network	Computational time (seconds)	
	ω =10.5088	ω =10.9031
Two Loops	19.2	22.8
Hanoi	352.1	703.4
New York Tunnels	59.2	143.7

Table 6.9 Overall performance of the PFMOEA

Network	ω	Best solution	Total number of runs	Number of times best solution found	Mean cost of cheapest feasible solution from the total runs	Maximum cost of cheapest feasible solution among the total runs
Two-Loop	10.5088	\$419,000	10	1	\$431,300	\$453,000
	10.9031	\$420,000	10	3	\$442,500	\$465,000
Hanoi	10.5088	$\$6.056\times10^6$	60	7	$\$6.156\times10^6$	$\$6.314\times10^6$
	10.9031	$\$6.182\times10^6$	60	4	$\$6.277\times10^6$	$\$6.548\times10^6$
New York Tunnels	10.5088	$\$37.13\times10^6$	30	7	$\$37.889\times10^6$	$\$39.940\times10^6$
	10.9031	$\$40.42\times10^6$	30	3	$\$41.834\times10^6$	$\$44.016\times10^6$

To further analyse the efficiency and robustness of the approach, the PFMOEA was also formulated with the second objective function being the network DSR to be maximized. Table 6.10 compares the performance of the PFMOEA with two different 2nd objective functions, i.e. maximizing the critical (i.e. smallest) nodal DSR and maximizing the network DSR. For the latter, the PFMOEA succeeded in locating all the least cost designs in the literature as well but at a much higher computational cost.

Table 6.10 Performance of the PFMOEA with different 2nd objective functions

Network	ω	Cost ($)	Number of Function Evaluations	
			Maximise critical nodal DSR	Maximize network DSR
Two-Loop	10.5088	4.190×10^5	2,200	20,300
	10.9031	4.200×10^5	2,600	4,800
Hanoi	10.5088	6.056×10^6	51,000	258,200
	10.9031	6.182×10^6	100,000	336,300
New York Tunnels	10.5088	37.13×10^6	7,200	554,400
	10.9031	40.42×10^6	17,800	28,200

The difference in both formulations lies in the fact that for solutions near the feasibility boundary, the ultimate deciding factor concerning the feasibility of a solution is based on the performance of the critical node, i.e. the worst performing node. The network DSR only represents the average performance of all nodes taken together. Most of the time, the performance of the critical node is overshadowed by other better performing nodes. For example, for a hypothetical network containing 100 nodes, consider a hypothetical solution which is made up of 99 fully satisfied nodes (i.e. DSR = 1) and 1 node with no outflow (i.e. DSR = 0). Though quite infeasible, this solution has an overall network DSR of 0.99 and would be ranked highly in terms of the network DSR. On the other hand, by utilizing the critical node DSR, the worst performing node is perceptibly distinguished amongst other nodes and any solution that has very poor nodal performances will incur a low fitness value. This way the algorithm is better able to identify quickly intermediate solutions that are potentially viable. This distinction (of the worst performing node) may not be particularly significant in the early phase of the evolution process. However, it becomes increasingly vital as solutions evolve through generations (especially near the end of the optimization run) and when the population pool begins to be dense with

near-feasible near-optimal solutions. Normally, this is shown by a noticeable plateau in the graph depicting the progress of the algorithm. For example, the progress of the best runs for the Two-loop network (ω =10.5088) using both formulations were compared in detail as shown in Fig. 6.8a. The PFMOEA based on the critical node DSR formulation will be referred to as PFMOEA 1; the PFMOEA based on the network DSR formulation will be referred to as PFMOEA 2.

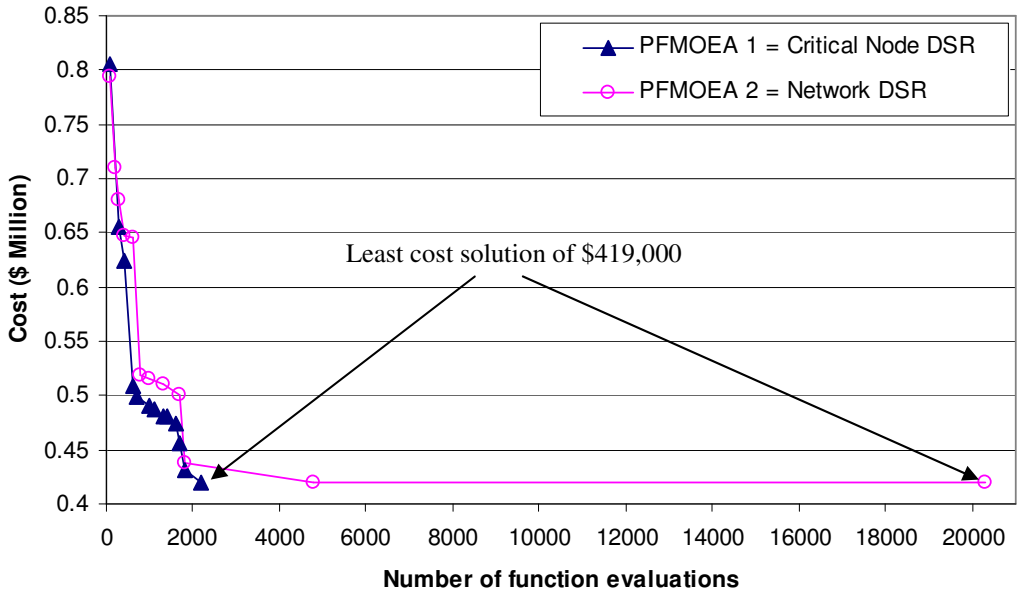

Figure 6.8a Progress of the PFMOEA using different formulations for the Two-Loop Network (ω =10.5088)

Both PFMOEA 1 and 2 started off with similar solutions and experienced rapid improvements (reduction in network cost) in the early phase of the evolution. It is worth observing that even at the early evolution stage the progress made by PFMOEA 1 is superior to that of PFMOEA 2. The point which marked the significant difference between formulations began shortly after 1,800 function evaluations where PFMOEA 1 continued to progress and obtained the optimal solution at 2,200 function evaluations while PFMOEA 2 was trapped in a plateau for a further 18,500 function evaluations before locating the optimal solution. The computational effort using the former was only 10.83% of the latter. This clearly shows that the critical node DSR is a better criterion in the decision process as it enforces more pressure on the search to stay close to the boundary as defined by the active constraints where "just feasible"

solutions are located, i.e. solutions with low or zero redundancy. The same outcome is observed for both the Hanoi WDS and New York tunnels examples, with the progress graphs as shown in Fig. 6.9a, Fig. 6.9b, Fig. 6.10a and Fig. 6.10b. Nevertheless, the fact that both PFMOEA formulations succeeded in locating the least cost designs for all networks demonstrates that the approach is highly robust.

It is worth highlighting that the PFMOEA has not only proven to be robust and efficient, but also its concept is extremely simple and straightforward to implement compared to other constraint handling techniques published in the literature. Not only does it not involve case-sensitive and/or network-specific parameters that require time-consuming calibration, the proposed algorithm does not require any complicated mechanisms. The fitness of each solution is essentially represented by the PDA which by itself serves as an accurate performance indicator of the solution. Infeasible solutions are assigned with accurate fitness and are allowed to compete fairly in the evolutionary process. With the accurate performance evaluation of both feasible and infeasible solutions, the active constraint boundaries can be precisely determined with literally no additional computational effort, enabling the feasibility boundary convergent strategy to function effectively.

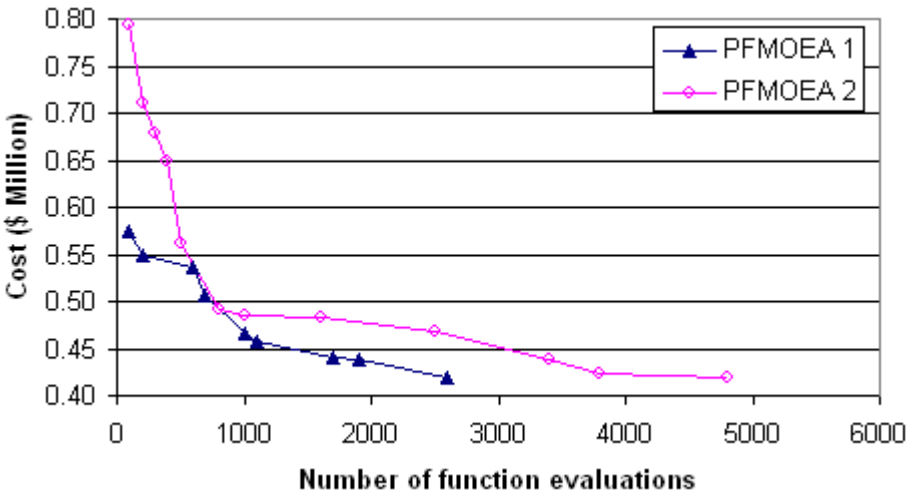

Figure 6.8b Progress of PFMOEA for Two-Loop network (ω = 10.9031)

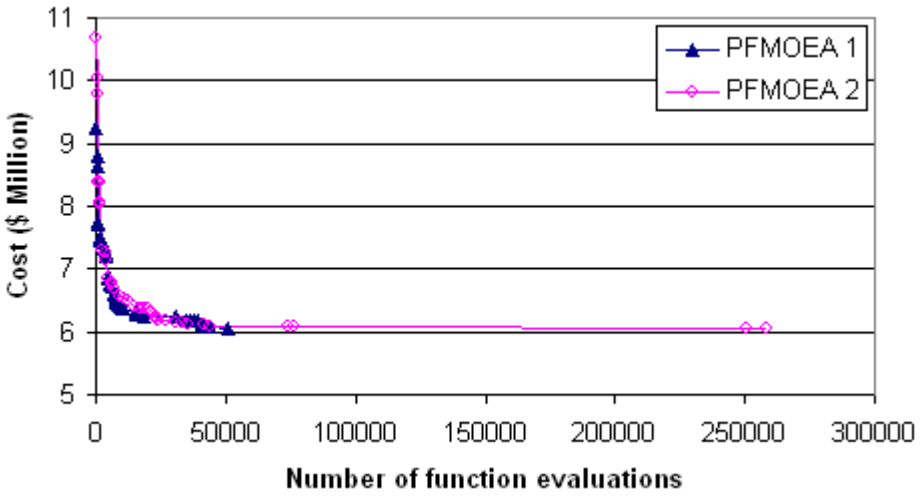

Figure 6.9a Progress of PFMOEA for Hanoi network (ω = 10.5088)

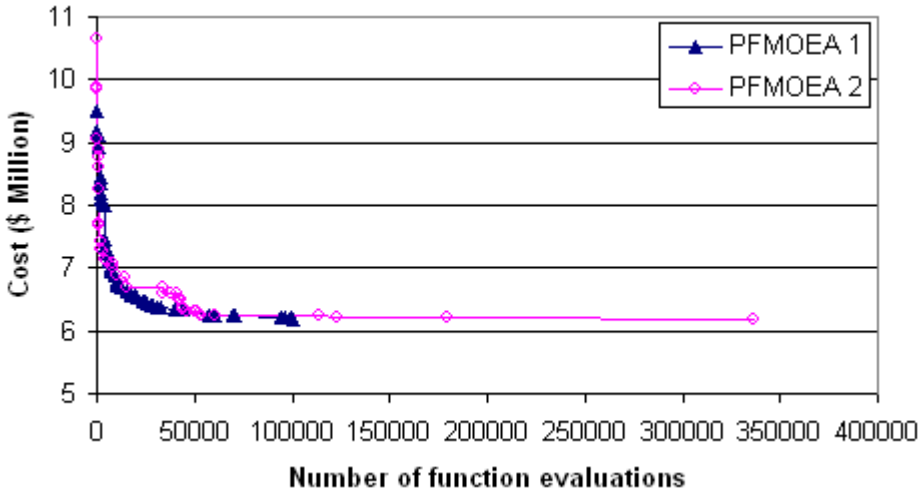

Figure 6.9b Progress of PFMOEA for Hanoi network (ω = 10.9031)

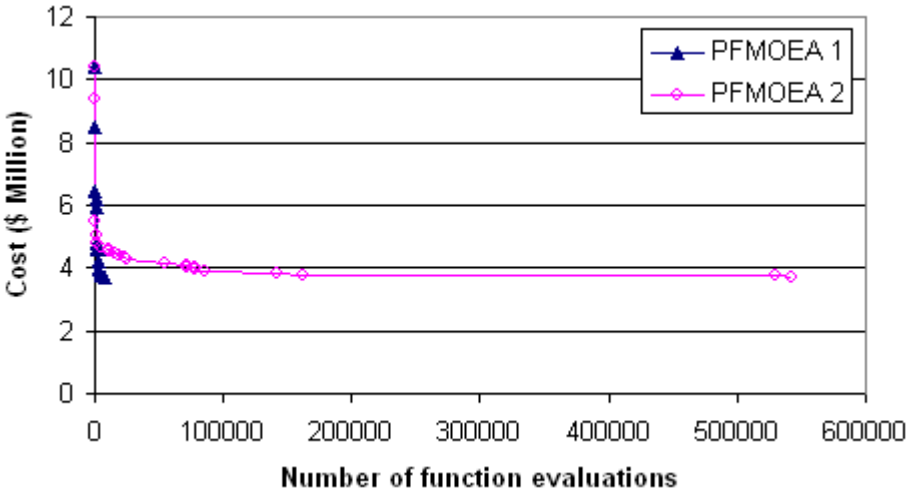

Figure 6.10a Progress of PFMOEA for New York Tunnels (ω = 10.5088)

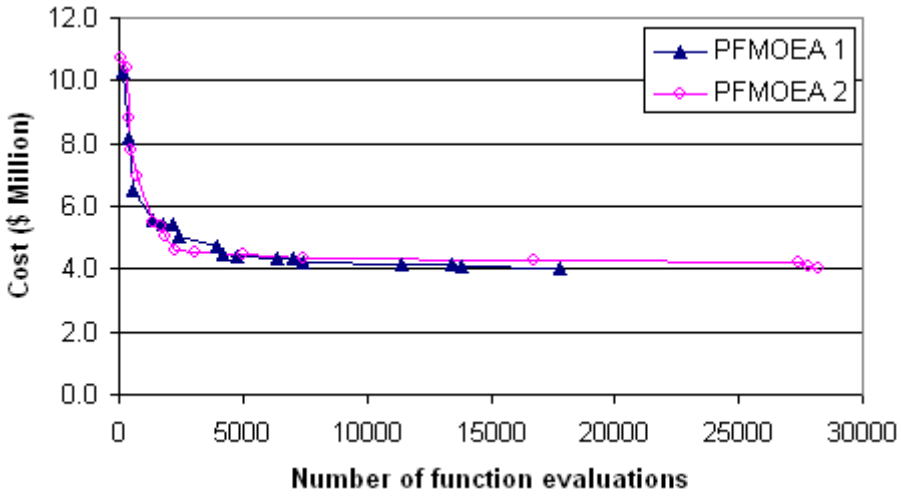

Figure 6.10b Progress of PFMOEA for New York Tunnels (ω = 10.9031)

6.4 CONCLUSIONS

In this chapter, the formulation of a new penalty-free multi-objective evolutionary optimization approach for water distribution systems (WDSs) has been presented. The described Penalty-Free Multi-Objective Evolutionary Approach (PFMOEA) combines a multi-objective evolutionary algorithm with pressure dependent analysis (PDA). PDA is capable of simulating infeasible solutions accurately, providing the means to quickly and accurately identify the feasible region of the solution space without the need for penalty functions or other special constraint handling techniques. The PFMOEA not only solves benchmark problems from the literature but also real life WDSs.

The algorithm has been applied to three benchmark networks and the results have been compared in detail with those obtained using other constraint handling algorithms from the literature. It was demonstrated that the algorithm is exceedingly efficient and robust with the capability of finding the least cost solutions reported in the literature with considerably fewer function evaluations. In addition, to evaluate the practical application of the PFMOEA, a real life network has been used as a case study. The least cost design obtained by the PFMOEA satisfied all the system requirements and was significantly lower in cost compared to the existing design.

The computational efficiency of the algorithm is due to the accurate performance evaluation of solutions. Infeasible solutions are accurately simulated and this enhances the boundary search techniques applied including the ability to focus the search around the active constraints. The significant advantage of this method over previous methods is that it eliminates the need for ad-hoc penalty functions or additional “boundary search” parameters. Hence there is no need for any parameter fine tuning or trial and error runs. Therefore, conceptually, the proposed formulation is the simplest by far.

EPANET-PDX has been used to evaluate solutions generated by the GA. An enormous amount of hydraulic simulations (a total of approximately 46.1 million simulations for all four examples) were involved since populations of new solutions

were constantly generated for every generation. This indeed has served as an extensive evaluation of the simulator's robustness and reliability. Once again EPANET-PDX demonstrated to be highly robust and reliable in that no convergence failure was encountered throughout this study.

CHAPTER SEVEN

APPLICATION OF THE PENALTY-FREE MULTI-OBJECTIVE EVOLUTIONARY ALGORITHM TO THE OPTIMAL LONG TERM DESIGN AND REHABILITATION MODEL

7.1 INTRODUCTION

Rehabilitation can be defined as reinstating and restoring the capacity and functional service of an existing water distribution system (WDS). All WDSs would need to be rehabilitated and upgraded at some point of their service span in order to continue supplying water to customers at a satisfactory level of service. The traditional "do nothing until a system component fails" approach would not only lead to customer complains but worst still incur higher replacement and repair costs. As the deterioration of aging WDSs is inevitable, there is a growing urge for methods that can assist in determining good economic strategy for progressive system rehabilitation and expansion.

The major question then is which components should be rehabilitated? Other important decisions to make would involve the type of rehabilitation/ upgrade options to be implemented, the timing and the magnitude of the rehabilitation/ upgrade to be carried out. There exists in the literature several optimal rehabilitation and upgrading models based on diverse approaches. A literature review on these models has been presented in Chapter 3. These models can be generalised into three categories. The first category is based predominantly on network economics that identify optimum water pricing and capacity expansion policies for water supply (e.g. the model by Dandy et al., 1985) but do not address the structural and hydraulic integrity. The

second category consists of individual asset-based models (e.g. Shamir and Howard, 1979; Walski and Pelliccia, 1982) that impart rehabilitation and upgrading decisions for individual components without considering network hydraulics. Models under the third category are known as the system-wide models (e.g. Halhal et al., 1997; Dandy and Engelhardt, 2001) that incorporate budget constraints and consider network hydraulics and performance explicitly. However, these models are still lacking in terms of addressing the deterioration of hydraulic capacity of pipes and the timing of rehabilitation explicitly.

Tanyimboh and Kalungi (2008, 2009) were probably the first to develop a holistic model for the optimal long term upgrading of water distribution networks that includes network performance, reliability, economic, social and environmental issues. The model explicitly considers pipe deterioration over time in terms of structural integrity and hydraulic capacity and allows for the direct and indirect failure costs. The basic formulation of the model is based on the segmental pipe approach developed by Alperovits and Shamir (1977) and linear programming (LP) is used to optimize the cost for design and rehabilitation of the water distribution network. Final results obtained have the property that a pipe may contain more than one pipe segment. This is undesirable for reasons of practicality. In addition, the LP formulation limits the model to networks with pipes only as the presence of pumps and valves introduces non-linearity to the main hydraulic constraints. Thus the model is not capable of optimizing all aspects of WDS design and operation.

This chapter expands the scope of the work by Tanyimboh and Kalungi (2008, 2009) by effectively eliminating the limitations imposed by the use of the conventional LP as the optimization model. The penalty-free boundary-convergent multi-objective evolutionary algorithm (PFMOEA) is applied in the rehabilitation and upgrading optimization framework in place of the LP. Since the evolutionary algorithm (EA) search is based on objective functions, its utilization provides the opportunity to include aspects such as operating costs, variations in demands, extended period simulation etc into the optimization model without significantly increasing the mathematical complexity.

The PFMOEA effectively handles node pressure constraints by involving pressure dependent analysis (PDA). It is extremely straightforward and efficient, and based on well-known benchmarks in the literature has proven to be capable of effectively steering the EA search to obtain least cost solutions (Chapter 6). Herein, the PFMOEA approach is applied to obtain the optimal design, rehabilitation and upgrading strategy for a real-world WDS in Wobulenzi, Uganda. The scope of this optimization problem is significantly wide as explained in the next section. This problem has been successfully solved previously using the linear programming model by Tanyimboh and Kalungi (2008, 2009) and its solution is used here as a yardstick to gauge the efficiency and efficacy of the PFMOEA.

7.2 FORMULATION OF THE LONG-TERM DESIGN, REHABILITATION AND UPGRADING MODEL

The long-term design, rehabilitation and upgrading model presented herein provides assistance in multi-criteria decision making for a staged network design, rehabilitation and upgrading. The overall optimization horizon was taken as 20 years and is divided into two phases. A two phase strategy is self-evidently more economical and provides added flexibility in dealing with any uncertainties or changes that arise during the first phase such as population and demand growth forecasts and changes in assumed pipe failure rates etc. The first phase involves optimizing the design of a new network while the second phase deals with upgrading and rehabilitating the network. The upgrading options considered are replacement and paralleling of pipes. However, it is worth highlighting that other rehabilitation options such as cleaning and relining can be easily implemented in the formulation. For an existing WDS, the initial design (i.e. Phase I) does not apply. In such a situation only the rehabilitation and upgrading part of the model (i.e. Phase II) is deployed.

7.2.1 Details of Various Costs Involved

The aim of the optimization is to minimize the total cost of a two-phase design and upgrading sequence while simultaneously ensuring that minimum service pressures at the demand nodes are met. The Tanyimboh and Kalungi (2008, 2009) model is quite complex and thus only the main equations are summarized here. The overall cost can be formulated as

$$Cost = \sum_{\tau=1}^{2} \beta_\tau C_\tau(s_\tau, r_\tau)(1+b)^{(d-v)} \tag{7.1}$$

where

$$C_\tau(s_\tau, r_\tau) = f1 + f2 + f3 \tag{7.2}$$

in which $C_\tau(s_\tau,r_\tau)$ is the cost of adding capacity r_τ in each design phase τ. This cost is a function of the added capacity along with the existing capacity s_τ at the beginning of the optimization phase. $f1$ represents the cost of pipelines including pipe installation, paralleling, replacement and repair costs. $f2$ is the indirect cost of setting up construction plant and machinery and is assumed to be incurred at the start of each phase. $f3$ is for the costs that vary depending on the magnitude of the capacity installed. $(1+b)^{(d-v)}$ is the compound factor in which v=0 when τ=1; v=$T1$, …, $T2$ when τ=2; $T1$ and $T2$ are the minimum and maximum duration (years) for Phase I. b is the annual compound interest rate for the capital borrowed that has to be paid back after d years. β_τ is a product of a discount factor $(1+r)^{-v}$ and price increase factor $(1+c)^{v}$ where r and c are the discount and the inflation rates in construction cost respectively. Both r and c were assumed to be equal.

The pipeline costs can be represented as

$$f1 = f1_a + f1_b + f1_c \tag{7.3}$$

where $f1_a$ and $f1_b$ represent the costs of new and parallel pipelines respectively and are assumed to be equal. $f1_c$ is the cost of replacing pipes and is assumed to be approximately 5% higher than paralleling. These costs are represented below in detail.

$$f1_a = f1_b = \sum_{ij \in IJ} \left(\gamma_p * \exp(c_p * D_{ij}) * l_{ij} + REP_{ij} \right) \tag{7.4}$$

$$f1_c = \sum_{ij \in IJ} \left(\gamma_r * \exp(c_r * D_{ij}) * l_{ij} + REP_{ij} \right) \tag{7.5}$$

where D_{ij} and l_{ij} are the diameter and length of pipe ij respectively. IJ represents the set of pipes in the WDS. γ_p, γ_r, c_p and c_r are user specified empirical coefficients; REP_{ij} are the repair costs of these new pipes which can be expressed as

$$REP_{ij} = \sum_{t=tb}^{tr} \frac{J_{ij}(t) * CB_{ij} * FCF(LU_{ij}) * l_{ij}}{(1+r)^{t-ts+1}}; \quad \forall ij \tag{7.6}$$

where r is the discount rate, ts and tr are the first and the last year of a given design phase respectively; tb is the time from which a pipe starts to incur repair costs. $FCF(LU_{ij})$ is the failure cost factor for land use, LU_{ij}, for pipe ij. The failure cost factors include indirect costs caused by pipe failures, e.g. disruption to traffic and damage incurred by third parties. CB_{ij} is the repair cost per break and is taken as

$$CB_{ij} = \gamma_{br} (D_{ij} * 1000)^{\Phi}; \quad \forall ij \tag{7.7}$$

where γ_{br} and Φ are user specified coefficients. $J(t)_{ij}$ is the break rate (breaks/km/year) in year t. The break rate was taken as

$$J_{ij}(t) = 0.001974 * \exp(-0.00974 * D_{ij}) * age_{ij}^{1.808}); \quad \forall ij \tag{7.8}$$

where age_{ij} is the number of years since installation of pipe ij.

Other miscellaneous costs associated with the volume of water supplied e.g. expansion of sewerage system were allowed for as follows.

$$f3 = VC * Q_{inst}^{VE} \tag{7.9}$$

where Q_{inst} is the installed capacity in a design phase in *l/s*; *VC* and *VE* are user specified coefficients.

7.2.2 Main Constraints

In the hydraulic analysis of WDSs, two basic constraints need to be simultaneously satisfied, namely the energy and mass conservation constraints. The energy conservation constraint requires that the total head loss along a path should be equal to the difference in head between its starting and ending nodes. Herein, the Hazen-Williams (HW) equation is used to approximate the head loss and can be described as:

$$h_{ij} = \omega l_{ij} \left(\frac{Qp_{ij}}{C_{ij}} \right)^{1.852} \frac{1}{D_{ij}^{4.87}} \tag{7.10}$$

in which h_{ij}, l_{ij} , Qp_{ij}, C_{ij} and D_{ij} represent the head loss, length, flow rate, roughness coefficient and internal diameter for pipe ij respectively; ω is a dimensionless conversion factor and a value of 10.67 (S.I. units) is used herein.

The roughness of pipes increases as the WDS ages and deteriorates. The effect of ageing on the carrying capacity of pipes is modelled using the Sharp and Walski (1988) equation as follows

$$C_{ij}(t) = 18.0 - 37.2 \log \left[\frac{e_{0ij} + a_{ij}(age_{ij})}{D_{ij}} \right]; \qquad \forall ij \tag{7.11}$$

where $C_{ij}(t)$ is the Hazen-Williams roughness coefficient in year t, e_{0ij} is the initial roughness (mm) at time of installation, a_{ij} is the roughness growth rate (mm/ year).

The mass conservation constraint requires that the sum of flows at each node must be zero. The nodal demand value Qn_j^{req} used herein is the demand (for node *j*) at the end of the relevant design phase. This is obtained by forecasting the nodal base demands from the first year of the design phase to the end of the relevant design period as follows.

$$Qn_j^{req} = Q_{0j}^{req}(1 + DGR/100)^t; \qquad \forall j \tag{7.12}$$

where Q_{0j}^{req} is the base demand for node *j*, *DGR* is the percentage annual rate of increase of the base demand and *t* is the number of years.

7.2.3 Optimization Problem Formulation

The PFMOEA formulation for the long term design, rehabilitation and upgrading problem involves two primary objectives. The first objective is to minimise the overall cost related to Phase I and Phase II. The second objective is to ensure all nodal demands are satisfied. This is achieved by minimizing any shortfall in the total available flow of the network. The objective functions are mathematically formulated as

Minimise $\qquad F_1 = (CR)^2$ (7.13)

Maximise $\qquad F_2 = (DSR)^4$ (7.14)

where F_1 and F_2 represent the first and second objective functions respectively. The exponentiation of both objectives enhances the preferential selection of the cheapest feasible and near-feasible solutions for crossover. *CR* represents the cost ratio which can be expressed as:

$$CR = \frac{Cost}{Cost^{\max}} \tag{7.15}$$

where $Cost$ and $Cost^{max}$ are the overall cost and the highest overall cost in the population respectively for the particular phase being optimized. DSR represents the demand satisfaction ratio of the network and can be expressed as:

$$DSR = \frac{Qn}{Qn^{req}} \tag{7.16}$$

where Qn and Qn^{req} are the total actual flow and demand for the network. It is worth reiterating that he term DSR represents the ratio of the available flow to the demand and takes values between 0 and 1. A solution having DSR value of less than 1 simply means it violates the minimum node pressure requirements and is deemed as infeasible. This is how the model distinguishes between feasible and infeasible solutions. Details on the PFMOEA procedure have been presented in Chapter 6. The overall methodology can be summarized as in Fig. 7.1.

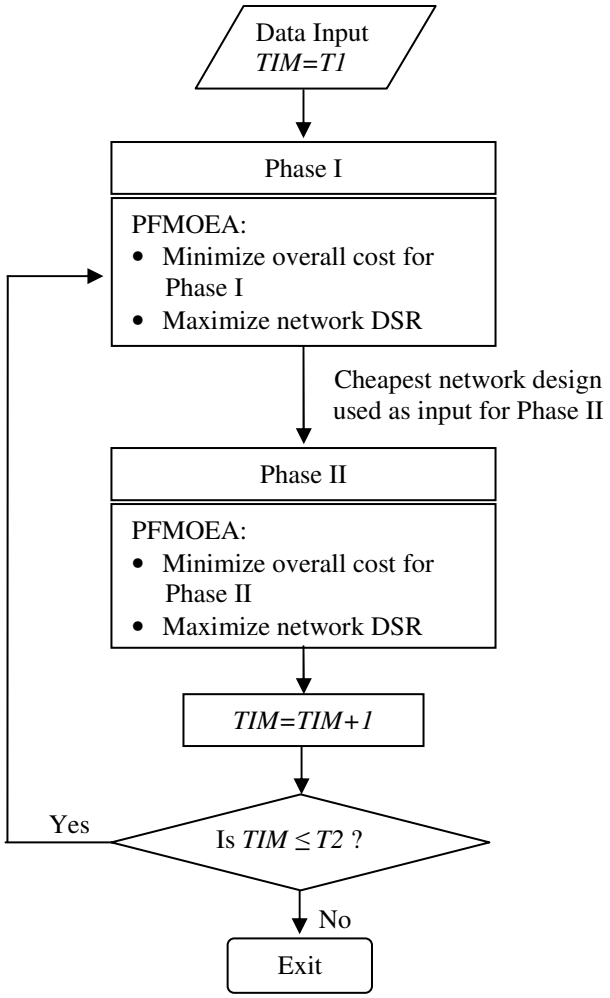

Figure 7.1 Flow diagram for the overall methodology

7.2.4 An Efficient Approach for Including Reliability in the Optimization

A comprehensive explanation of the concepts and formulations of reliability and failure tolerance has been presented in Chapter 2. As seen from Eq. 2.73, the calculation of reliability is extremely expensive computationally to be incorporated directly into an EA optimization process as it involves many pipe failure simulations. In this research, a strategy proposed by Tanyimboh and Sheahan (2002) has been adopted. The approach improves the efficiency of the reliability calculations by using the statistical entropy (Eqs. 2.78 to 2.81) as a means of screening out a very large proportion of candidate solutions. By taking the overall cost of both Phase I and II as

the principal criterion, the trade-offs between cost, entropy, reliability and redundancy are examined sequentially in priority order as follows:

1) Carry out a PFMOEA optimization.
2) Obtain the entropy value (Eq. 2.78) for each candidate design provided by PFMOEA.
3) Using the cost and entropy values, identify the cost-entropy non-dominated (CEND) designs and discard the rest of the designs.
4) Obtain the hydraulic reliability (Eq. 2.73) and failure tolerance (Eq. 2.74) for the retained (CEND) designs.
5) Using the cost and reliability values, identify the cost-reliability non-dominated (CRND) designs and discard the rest of the designs.
6) Using the cost and failure tolerance values, identify the cost-failure tolerance non-dominated (CFND) designs and discard the rest of the designs.

Only the reliability and failure tolerance of solutions belonging to the CEND set will be evaluated. The remaining bulk of the designs that do not belong to the CEND set would not be evaluated. The ultimate objective is to identify a set of cost-reliability non-dominated solutions whilst escaping the laborious effort of assessing the reliability of each solution. This technique is based on the proven concept that entropy is a robust surrogate for the hydraulic reliability measure (Tanyimboh and Templeman, 2000).

Compared to the effort involved in evaluating the hydraulic reliability of a design, the calculation of entropy value is a relatively simple exercise. It is straightforward and does not involve any hydraulic simulations let alone the multiple simulations for the reliability calculation in Eq. 2.73 (i.e. at least M+1 simulations for every candidate design; or a significantly larger number than M+1, literally orders of magnitude more, if multiple pipe failures are included). In addition, since reliability is not formulated as an additional objective, the complexity and computational effort of the optimization problem is enormously lessened as intergenerational reliability evaluations are obviated. In other words, reliability values need not be evaluated and compared for each solution in each generation (from the GA point of view). These aspects contribute to a significant reduction of the overall computational effort and time (as

will be demonstrated later in the results and discussion section) making this approach highly practical to be implemented in real world networks which may consist of hundreds of pipes and where extended period simulations are required to simulate the variation in diurnal demands and energy consumption.

7.3 MODEL APPLICATION TO A REAL-LIFE NETWORK

7.3.1 Description of the Network and Design Data

The PFMOEA was applied to the real life Wobulenzi (Uganda) WDS used in Tanyimboh and Kalungi (2008). Wobulenzi is a small town situated approximately 57 km (by road) to the North of Kampala city, the capital of Uganda. The population of the town was 10,640 in 1995 (when the network data were collected). The skeletonised network as shown in Fig. 7.2 consists of a reservoir, 17 nodes and 21 pipes. All the input data used herein are taken from Tanyimboh and Kalungi (2008). The minimum desired pressure head for full demand satisfaction was taken as 15 m. A set of eight available pipe diameters (80, 100, 150, 200, 250, 300, 350, 400 mm) were utilized in the design optimization. The costs of these pipes can be found in Appendix D. An annual demand growth rate (DGR) of 4% was assumed. A peak hour factor of 2.0 was used and a fire demand (25% of node demand) was added at node 4. These demands were then projected over the design period to obtain the overall design demands.

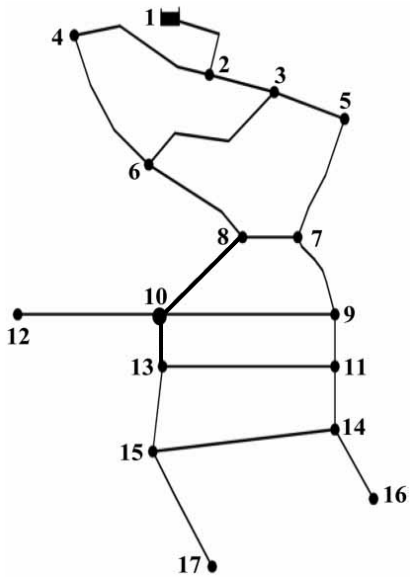

Figure 7.2 Layout of the Wobulenzi WDS

The rest of the data are also taken from Tanyimboh and Kalungi (2008) and are as follows. Compound interest rate b=8% and discount rate r=8%. The lower limit for the end of Phase I is $T1$=7 years and the upper limit is $T2$=14 years. Pipe-failure cost factors associated with the various land uses are as shown later in the results section. Pipe cost coefficients are γ_p=32.093, c_p=c_r=3.7, γ_r=33.928, γ_{br}=108.87 and Φ=0.6067. tb was taken as 6 years for new, replaced and parallel pipes. The setting-up cost at the beginning of each design phase is $f3$=\$100,000; installed capacity coefficients are VC=130 and VE=1.6; initial pipe roughness e_{0ij}=0.0021 mm; roughness growth rate a_{ij}=0.025 mm/year. Pipe and node data of the network can be found in Appendix D.

10 PFMOEA optimization runs (with different random initial populations) were found to be sufficient for this network in demonstrating the overall efficacy of the proposed approach. However, more runs can be carried out to further ensure that the best (optimal or near optimal) solutions are obtained. It is worth clarifying that each single PFMOEA run comprises of 8 separate runs with 8 different Phase I durations (i.e. the Phase I duration of 7, 8, 9, 10, 11, 12, 13 and 14). For each "Phase I duration" run,

10,000 function evaluations (i.e. a population of size 100 for 100 generations) were allocated for each phase (i.e. 10,000 function evaluations for Phase I and 10,000 function evaluations for Phase II). The probability of crossover and mutation were fixed as 1 and 0.005 respectively for all runs.

7.3.2 Results and Discussions

This section consists of two parts. In the first part, with the purpose of demonstrating the performance of the proposed approach, the cheapest solutions obtained by the PFMOEA are presented and compared to that of the LP formulation (Tanyimboh and Kalungi, 2008). Based on these solutions, the effects of delaying the rehabilitation and upgrading time on the overall design cost are analysed and discussed. The optimization process is then taken a step further (in the second part) where both reliability and failure tolerance measures are considered in the decision making.

It is worth mentioning that three alternative designs presented in Tanyimboh and Kalungi (2008). The first design was based on the shortest path flow distribution method. The layout of the network for this design was different to that illustrated in Fig. 2 in that it did not contain links connecting node 8 to node 10, and node 10 to node 13. Both the second and third designs were based on the maximum entropy flow distribution method. The layouts for these designs were identical to that of Fig. 2. A water pricing policy was enforced in the third design, but not for the second design. As explained in Chapter 3, the price elasticity of water demand is not zero. An increase in the price of water will result in a reduction of water demand. As such, the demands for the third design were lower than the second design. Interested readers may refer to Tanyimboh and Kalungi (2008) for more details of all three designs. The scope of this thesis does not cover water pricing management. Hence, to enable a fair comparison, the study herein only involves comparing the PFMOEA solutions to the second design of Tanyimboh and Kalungi (2008).

The average CPU (central processing unit) time required for a PFMOEA run in this study is 2.58 hours. A single PFMOEA run consist a total of 160,000 function evaluations. Hence, a single function evaluation only requires 0.058s. This

demonstrates the computational efficiency of the PFMOEA. The CPU time for each of the 10 runs executed can be found in Appendix D.

7.3.2.1 Comparison of Least Cost Solution between PFMOEA and Linear Programming

Fig. 7.3 shows the lowest overall infrastructure construction, maintenance and failure costs obtained for different Phase I durations for both the PFMOEA and LP models. For the PFMOEA model, the total cost decreases initially and attains a minimum at the end of Phase I duration of 9 years after which it increases. For the LP model, the minimum total cost corresponds to a Phase I duration of 11 years. Similar trends were exhibited by solutions from all 10 PFMOEA runs, strongly suggesting that the chosen range of Phase I durations, i.e. 7 to 14 years is appropriate in obtaining the cheapest solution. It should be noted that all solutions presented herein are fully feasible, i.e. the network demand is met in full and the minimum pressure constraint for all demand nodes is satisfied.

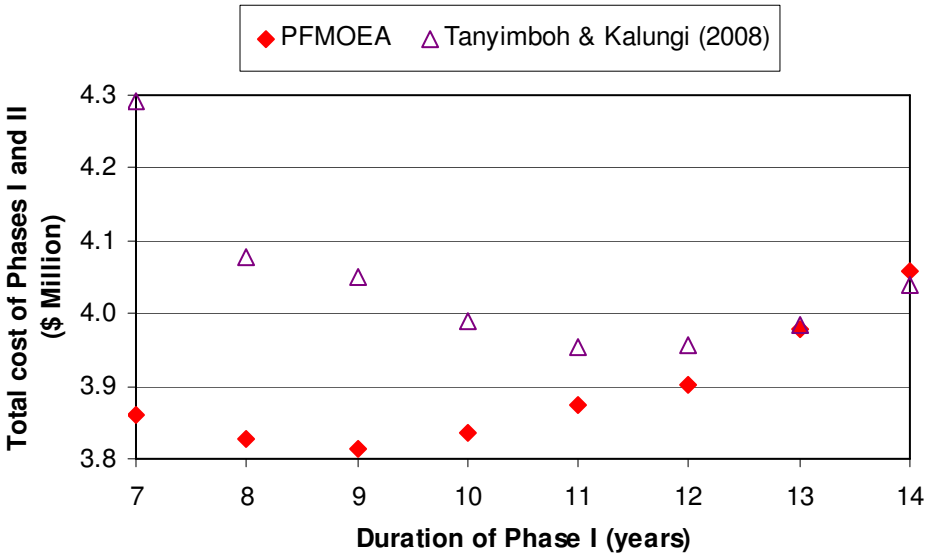

Figure 7.3 Total cost of the cheapest solutions

Fig. 7.4 shows a detailed breakdown of the total design, rehabilitation and upgrading costs for various Phase I durations. One can see the trend of each different cost

element and how it varies with the Phase I duration. The repair costs from Phases I and II contributed the lowest percentage to the total cost. The new network design and *f3* costs (i.e. additional sewerage and other costs) in Phase I are the major contributors to the total cost of all solutions. These costs along with the repair cost escalate significantly with the delay in rehabilitation and upgrading time (i.e. from a total of approximately 61% for Phase I duration=7 years to 80% for Phase I duration=14 years). Hence, based on the results shown in Fig. 7.3 and Fig. 7.4, similarly to Tanyimboh and Kalungi (2008), it can be inferred that a strategy of designing the network for a very long design horizon (or single phase design) would inevitably be much higher in cost due to the increasing repair costs with time and more so the initial surplus capacity allocated to cater for the relatively high demands at the end of the long design horizon (20 years in this case).

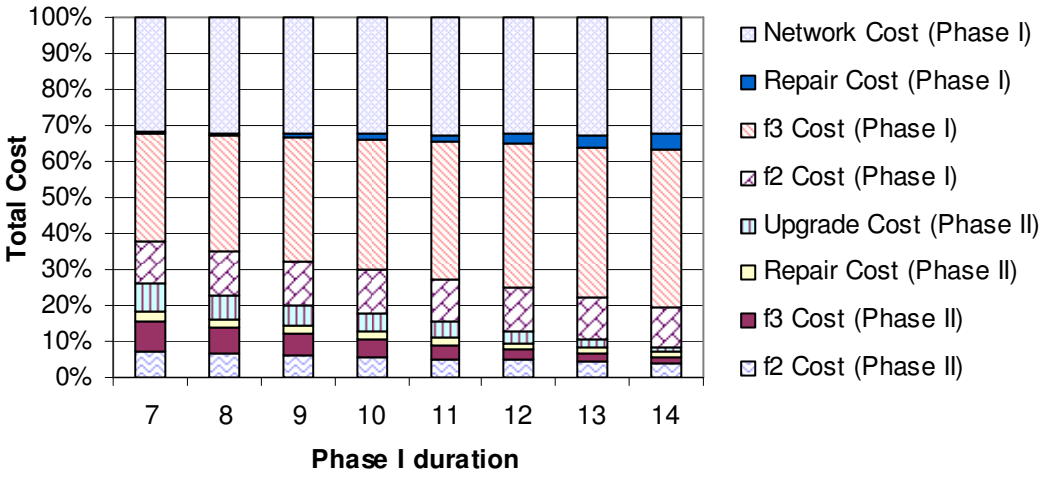

Figure 7.4 Percentage of cost elements for optimal solutions generated by PFMOEA

Table 7.1 shows the number of pipes paralleled and replaced in Phase II for the cheapest solutions obtained by the PFMOEA with different Phase I durations. The results generally reinforce Tanyimboh and Kalungi (2008) and suggest that in general paralleling is preferred to replacement. Therefore, subject to the structural integrity of the existing pipe, by retaining the existing capacity, it is obvious that the additional capacity installed (by paralleling) to achieve the desired capacity would be smaller thus presenting a cheaper rehabilitation option compared to the pipe replacement.

Table 7.1 Rehabilitation and upgrading decisions for optimal solutions of PFMOEA

Phase I duration (years)	No. of paralleled pipes	No. of replaced pipes
7	6	1
8	4	3
9	3	3
10	4	2
11	3	3
12	2	3
13	1	4
14	3	1

Table 7.2 presents the overall infrastructure construction, maintenance and failure costs for both the proposed and LP model (Tanyimboh and Kalungi, 2008). The cheapest solution obtained by the PFMOEA (details of solution are presented in Table 7.3) has a value of $3,814,298 and is to install a capacity for a 9-year demand in Phase I and then upgrade the network to the 20-year demand capacity in Phase II. In Tanyimboh and Kalungi (2008), the cheapest scheme reported has a value of $3,953,663 which is approximately 3.5% higher than the cheapest PFMOEA solution. This entails installing a capacity for an 11-year demand in Phase I and then upgrading to the 20-year demand capacity in Phase II. Based on the results obtained by both models herein, it seems that implementing the rehabilitation and upgrading phase more or less near the middle of the design horizon is probably the most economic strategy in terms of timing.

Table 7.2 Costs for the optimal designs for PFMOEA and LP

Phase I duration	PFMOEA Cost ($ Million)			PFMOEA Reliability[b]	LP Cost ($ Million)		
(years)	Phase I	Phase II	Total		Phase I	Phase II	Total
7	2.862	0.998	3.860	0.999010	2.907	1.386	4.293
8	2.950	0.877	3.827	0.999116	3.006	1.071	4.077
9	3.047	0.768	3.814[a]	0.999017	3.084	0.966	4.050
10	3.148	0.689	3.837	0.999106	3.200	0.789	3.989
11	3.281	0.593	3.873	0.998867	3.315	0.639	3.954[a]
12	3.399	0.504	3.902	0.998869	3.414	0.544	3.958
13	3.565	0.415	3.980	0.998919	3.523	0.461	3.984
14	3.725	0.334	4.059	0.998834	3.631	0.409	4.040

[a] Represents the cheapest solution
[b] The reliability value for the cheapest solution generated by the LP model is 0.999197

In general, designs based on segmental pipes (obtained via LP) will tend to be lower in cost compared to designs with uniform diameter pipes. However, it can be observed (from Fig. 7.3 and Table 7.2) that apart from the solution with a Phase I duration of 14 years, the proposed model succeeded in locating solutions with lower overall costs compared to those of the LP. The main reason is that unlike the LP model, the PFMOEA search is not restricted to solutions with maximum entropy flows and hence encompasses a wider solution space. This increases the probability of the search obtaining the global minimum cost solution.

The LP model used pre-specified maximum entropy flows which result in the selection of more uniform pipe diameters. Demand nodes linked with more equally sized supply paths can therefore be expected to cope better during critical operating conditions such as a pipe failure event. Hence, though higher in cost, the maximum entropy designs are generally more reliable. This can be seen in Table 7.2 where all PFMOEA solutions have lower hydraulic reliability values compared to the cheapest solution by Tanyimboh and Kalungi (2008) which has a hydraulic reliability of 0.999197. It is worth clarifying that the hydraulic reliability value presented herein for each solution represents the reliability of the network for its most deteriorated condition at the end of Phase II with the projected design demand of 20 years.

Table 7.3 Optimal diameters for the cheapest solution obtained by PFMOEA

Link	Failure Cost Factor[c]	Phase I	Phase II	
		Diameter (mm)	Upgrade option	Diameter (mm)
1-2	1.5	250	Paralleling	350
2-3	1.5	200	Paralleling	300
2-4	1.5	150	-	-
3-5	1.5	200	Replacement	350
3-6	1.5	80	-	-
4-6	3.0	80	-	-
5-7	3.0	200	-	-
6-8	3.0	80	-	-
7-8	3.0	80	Replacement	300
7-9	3.0	150	-	-
8-10	3.0	80	Paralleling	200
9-10	3.0	80	-	-
9-11	5.0	200	-	-
10-12	3.0	80	-	-
10-13	5.0	80	-	-
11-13	3.0	80	-	-
11-14	3.0	100	-	-
13-15	3.0	80	Replacement	150
14-15	3.0	80	-	-
14-16	3.0	80	-	-
15-17	1.0	100	-	-

[c] Values taken from Tanyimboh and Kalungi (2008). Cost factors are largely predetermined by land use.

7.3.2.2 Final Design Options based on Cost, Reliability and Failure Tolerance

Each PFMOEA run generates eight different sets of Pareto-Optimal solutions; each set corresponds to a particular Phase I duration (7 to 14 years). The cheapest feasible solution from each Pareto-Optimal set is chosen to be analysed for its reliability. Fig. 7.5 shows the plot of cost against entropy value for all of the cheapest feasible solutions (80 designs) generated by the 10 PFMOEA runs.

It is interesting to observe that the solutions fall in a very narrow range of entropy values (i.e. between 2.65 to 3.0). This is due to several reasons. Firstly, the PFMOEA approach is effectively a single objective optimization problem (i.e. cost minimization) solved using a multi-objective formulation. The second objective, i.e. maximizing the network DSR is essentially a means of handling the node pressure constraints. Hence the final solutions obtained are quite similar in terms of hydraulic performance (least cost feasible design). Furthermore, entropy was not formulated as an objective in the optimization process. Thus, it is not at all surprising that these solutions do not come from a wide range of entropy values and a vast number of them are not non-dominated.

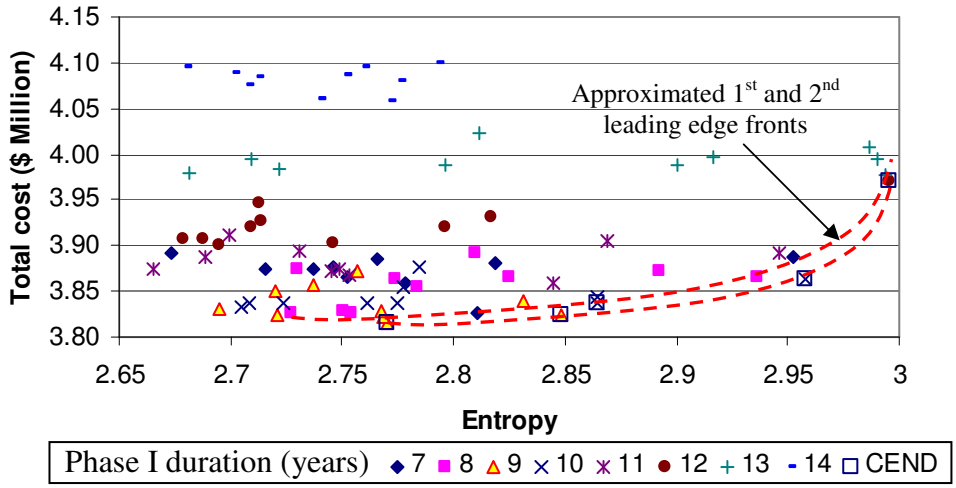

Figure 7.5 Cost versus entropy for all designs

There are only five cost-entropy non-dominated (CEND) solutions in Fig. 7.5 as shown. Thus only five reliability evaluations (Eq. 2.73) which involve a total of 110 hydraulic simulations (i.e. 5 CEND designs × 22 pipe configurations corresponding to different pipe failure scenarios) are carried out when using the proposed approach. This merely represents 6.25% of the 1,760 hydraulic simulations (80 available designs × 22 pipe configurations corresponding to different pipe failure scenarios) required for the reliability assessment of all the solutions. Also, the abovementioned 110 hydraulic simulations are an extremely small fraction (0.0025%) of the 4.4 million hydraulic simulations required (10 PFMOEA runs × 2 phases × 10,000 function evaluations per phase× 22 different pipe failure scenarios) for the reliability assessment if the reliability measure were to be incorporated as an objective in the EA optimization. Hence, it is clearly demonstrated that the filtering significantly

contributes to the efficiency of the method and provides a huge saving in computational time.

The plot of cost against hydraulic reliability was then generated using the five CEND solutions (extracted from Fig. 7.5) as shown in Fig. 7.6. Using Fig. 7.6, the cost-reliability non-dominated (CRND) solutions were identified. The four CRND solutions were then assessed and the cost-failure tolerance non-dominated (CFND) solutions were obtained as shown in Fig. 7.7.

Only three solutions which were non-dominated from both aspects (cost vs. reliability and cost vs. failure tolerance) remain to choose from. A multi-criteria decision making algorithm such as the analytic hierarchy process can then be easily applied to help select one option from the three final alternative design options based on the relative importance of the decision criteria considered. The AHP has been successfully applied in this area of work and the detailed description can be found in Tanyimboh and Kalungi (2009).

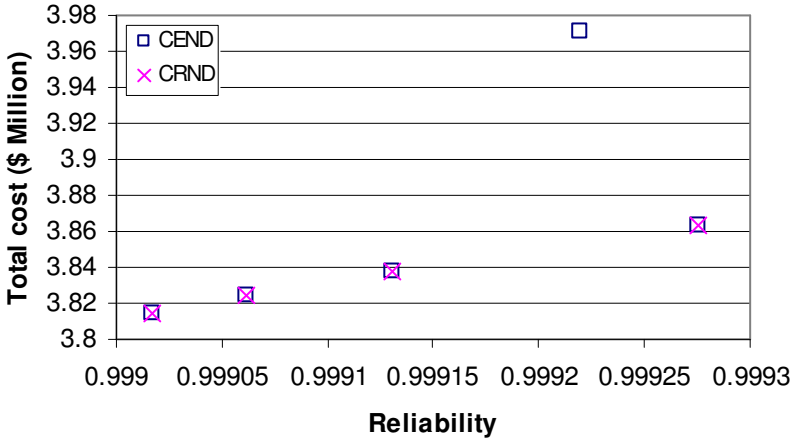

Figure 7.6 Cost versus hydraulic reliability for cost-entropy non-dominated designs

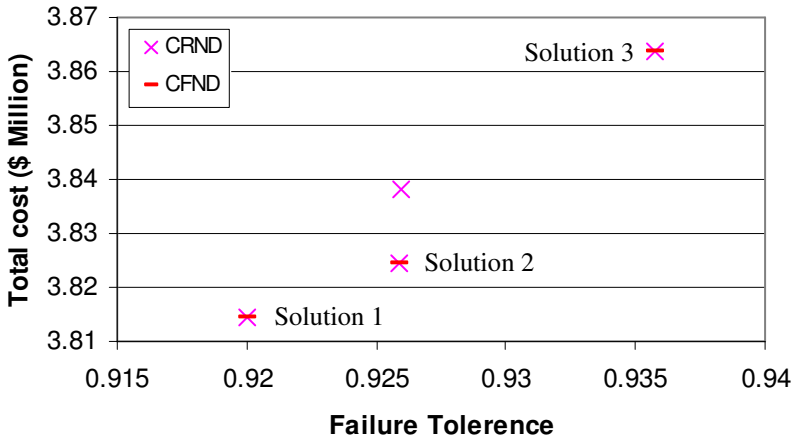

Figure 7.7 Cost versus failure tolerance for cost-reliability non-dominated designs

Table 7.4 shows the phasing periods, costs, reliability and failure tolerance values of the best solutions by both models. It is worth mentioning that Solution 1 (under the PFMOEA column) is the cheapest solution presented in the earlier part of the "Result and Discussions" section. Pipe diameters, rehabilitation and upgrading details corresponding to Solutions 2 and 3 can be found in Appendix D. All three solutions obtained by the PFMOEA are not only lower in cost but also have virtually the same hydraulic reliability and failure tolerance as the LP. PFMOEA Solution 3 dominates the best LP solution in all three aspects considered (cost, reliability and failure tolerance).

Table 7.4 Details of the final solutions for PFMOEA and LP

Solution	LP solution	PFMOEA solutions		
		1	2	3
Phase I duration (years)	11	9	9	10
Cost ($ Million)	3.954	3.814	3.824	3.864
Reliability	0.999197	0.999017	0.999062	0.999275
Failure Tolerance	0.924534	0.920000	0.925883	0.935727

To validate the robustness of the proposed "entropy screening" approach, the hydraulic reliability and failure tolerance values were obtained for all solutions as in

Tanyimboh and Setiadi (2008b). Fig. 7.8 and Fig. 7.9 show the plots of cost versus hydraulic reliability and cost versus failure tolerance respectively for all the PFMOEA solutions. It can be observed that though a large number of PFMOEA designs had lower costs, only four and nine solutions, respectively, dominated the best LP solution in the aspects of reliability and failure tolerance. Four PFMOEA solutions dominated the LP in both reliability and failure tolerance.

In Fig. 7.8, four of the five CRND designs are CEND. In Fig. 7.9, three out of the five CFND solutions are CEND solutions. The plots in both Fig. 7.8 and Fig. 7.9 are in good agreement. This reinforces Tanyimboh and Setiadi (2008a) and strongly implies that the entropy values serve as an excellent reliability surrogate and the approach used is highly robust and computationally efficient. It is essential to mention that CRND and CFND solutions that were not CEND were situated in the 2nd cost-entropy leading edge front. Hence, to further ascertain that all best designs (CRND and CFND) are included, more solutions from the first few leading edge fronts should be analysed as appropriate, particularly in situations where the non-dominated fronts have only a few solutions each.

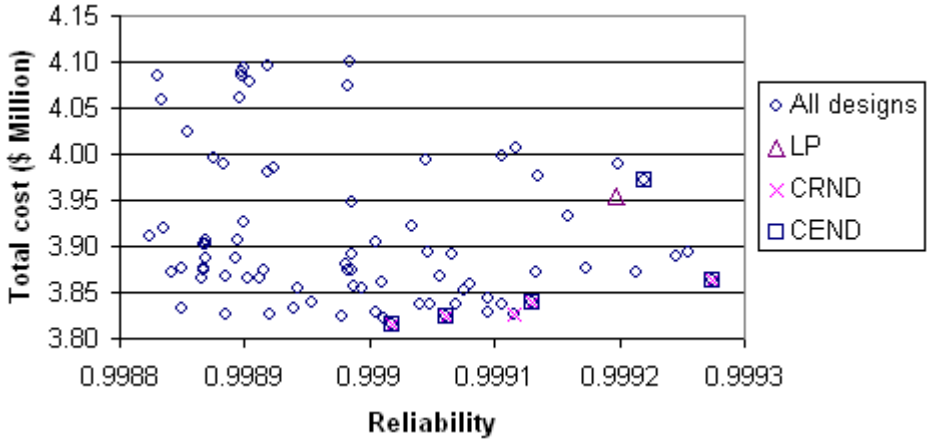

Figure 7.8 Cost versus hydraulic reliability for all designs

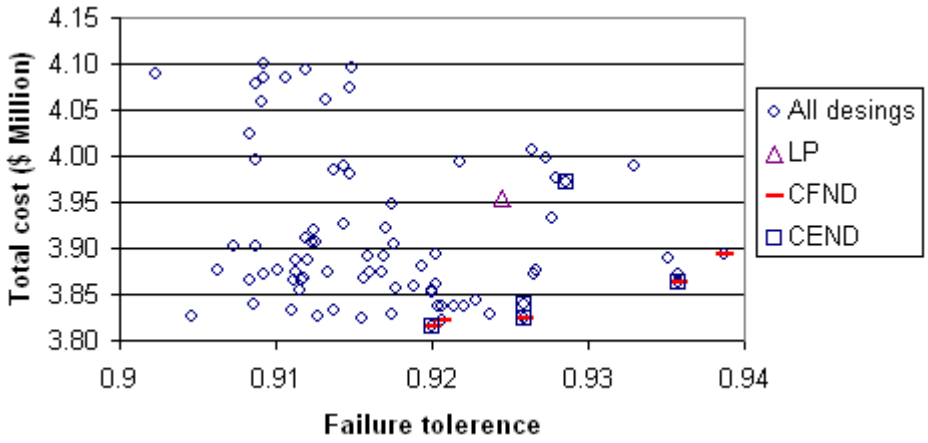

Figure 7.9 Cost versus failure tolerance for all designs

For additional justification of the filtering approach, the entropy values were plotted against the reliability and failure tolerance for solutions taken from the two leading edge fronts (Fig. 7.10). These solutions were chosen for the validation as they represent the best designs i.e. the most cost-efficient designs. For comparison purposes, the resilience index (RI) by Todini (2000) was computed as well for these solutions and its effectiveness as a reliability surrogate was evaluated. The positive correlations between entropy vs. reliabilty and failure tolerance appear to be reasonably strong as depicted in Fig. 7.11 and Fig. 7.12. Conversely, the correlations achieved by the resilience index were observed to be relatively weak (Fig. 7.11 and Fig. 7.12). This demonstrates that entropy is capable of performing well and consistently as a reliability measure surrogate. As expected, reliability correlated well with failure tolerance (Fig. 7.13).

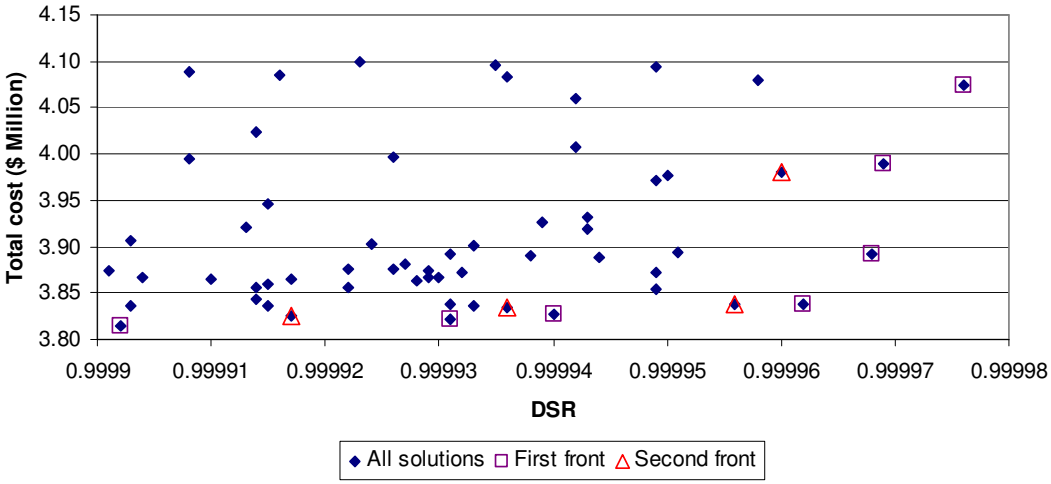

Figure 7.10 First and second Cost-DSR non-dominated fronts

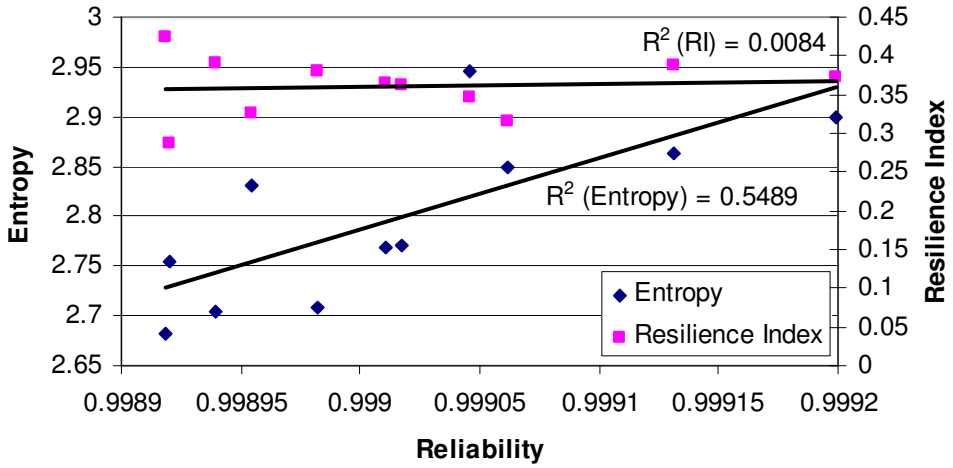

Figure 7.11 Plot of entropy and resilience index against reliability for solutions from the first and second Cost-DSR non-dominated fronts

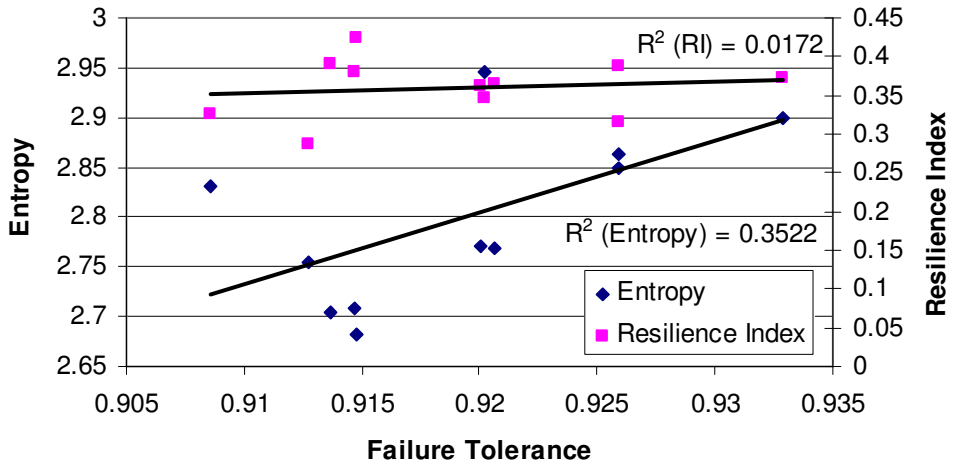

Figure 7.12 Plot of entropy and resilience index against failure tolerance for solutions from the first and second Cost-DSR non-dominated fronts

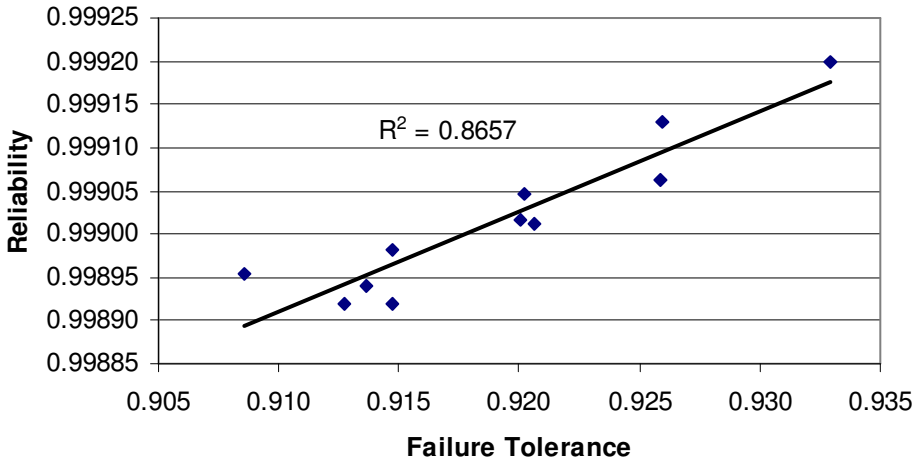

Figure 7.13 Correlation between failure tolerance and reliability of solutions from the first and second Cost-DSR non-dominated fronts

7.4 CONCLUSIONS

The penalty-free multi-objective evolutionary approach (PFMOEA) has been applied for cost-effective long-term design, rehabilitation and upgrading of a real life WDS. The use of penalty functions and/or constraint-violation tournaments is obviated by involving the pressure dependent analysis (PDA) in developing a multi-objective evolutionary search. PDA can simulate both feasible and non-feasible solutions accurately, enabling a more realistic hydraulic performance assessment of all solutions. In addition, the use of PDA in the reliability calculations adds to the accuracy in identifying the cost-reliability Pareto-Optimal front.

The PFMOEA yields several advantages over the linear programming (LP) approach by Tanyimboh and Kalungi (2008, 2009). Firstly, the final solutions have single segment pipes of constant diameter which are practical for real life implementation. Unlike conventional optimization techniques which only yield one final solution, the PFMOEA model yields multiple non-dominated solutions, providing greater flexibility during the final decision making process especially when compromises are necessary due to budget constraints. Since the PFMOEA search is only based on the objective functions and does not involve any mathematical gradient formulation, the proposed model provides the opportunity to extend the Tanyimboh and Kalungi (2008, 2009) formulation to networks with pumps, valves and other hydraulic components including tanks.

The long-term design, rehabilitation and upgrading model developed herein explicitly takes into consideration the deterioration over time of both the structural integrity and hydraulic capacity of every pipe. Both direct and indirect failure costs were taken into account. It simultaneously considers the upgrading options of paralleling and replacement of pipes, as well as the timing. Capital, rehabilitation and upgrading costs and hydraulic reliability were considered explicitly while selecting the final design options. The simplicity, robustness and high computational efficiency of the overall approach has been demonstrated.

CHAPTER EIGHT

NOVEL FORMULATIONS FOR OPTIMAL PUMP SCHEDULING, TANK LOCATION AND SIZING FOR WATER DISTRIBUTION SYSTEMS

8.1 INTRODUCTION

The literature is overwhelmed with a variety of water distribution system (WDS) optimization models with a large proportion of them focusing on networks consisting of pipes alone. Very few published works simultaneously incorporate the sizing and operation of tanks and pumps, the multiple operating conditions and the demand variation which are all typical features of the real world WDSs. This is mainly attributed to the significant increase in the optimization complexity which stems from the additional design variables (e.g. tank size and location, pump status) and operational constraints required to ensure that every operation criterion can be satisfied (e.g. the volume of water pumped must be sufficient to satisfy the system's daily demand, tank water level should fully recover by the end of the day etc). Consequently, it is more difficult for an optimization model to converge to feasible solutions, let alone obtain a cost effective solution. In addition, the accurate simulation of the WDS over an extended period in response to the demand variation is extremely time consuming to be implemented, particularly in an evolutionary algorithm optimization model which requires evaluation of large numbers of trial designs.

The "Anytown" network is probably the only benchmark available in the literature which involves multiple loadings and multiple storage tanks and pumps. A brief review on the works carried out on this network is presented. This network is a

hypothetical water distribution system set up by Walski et al. (1987) as a realistic benchmark to be optimized and solved by participants at the battle of the network models workshop. Participants used various classical optimization techniques such as linear programming, partial enumeration and non-linear programming techniques to rehabilitate the piping system while tank sizes and locations were manually selected based on engineering judgement and experience. Most of the models only optimized the system for a single loading (peak flow) which resulted in solutions that were able to perform satisfactorily during peak hours but lack the capacity to refill the tanks during off-peak loading. Details of these solutions can be found in Walski et al. (1987).

Murphy et al. (1994) were probably the first to apply evolutionary algorithm (EA) in solving the "Anytown" problem. The flexibility of the standard genetic algorithm used enabled the sizing and siting of tanks as well as pumping operation to be handled as additional design variables in the optimization process. A single objective approach was implemented and constraint violations (e.g. pressure deficiency, unbalanced flows in tanks) were included as penalties in the cost objective functions by applying weightings for each constraint violation. The selection of appropriate weightings required trial runs.

Walters et al. (1999) then solved the "Anytown" WDS in a multi-objective manner with minimum cost and maximum benefit as objectives. The benefit objective function was taken as the difference of the accumulated shortfalls between solutions before and after rehabilitation which included nodal pressure shortfalls, storage capacity differences and tank operating level differences. Similar to the penalty approach, dimensional weightings were required to convert these deficiency measures to a common basis. Though not mentioned in the paper, it can be deduced that these weightings require calibration and trial runs before they can be effectively incorporated into the optimization model.

Vamvakeridou-Lyroudia et al. (2005) also posed the "Anytown" problem as a multi-objective one and used fuzzy reasoning for the benefit evaluation. A fuzzy set was defined by its membership function which was used to rate each benefit aspect (e.g. pressure deficiency) relative to the deviation from the defined acceptable bounds.

Determining appropriate membership functions is generally problem specific. Different shape parameters were used to adopt various levels of stringency for the criteria. For each network element (e.g. node, link, tank), constraint and loading scenario, a fuzzy set was formed. Aggregators, which are essentially weightings, were then applied to the membership functions which governed the various different constraints to combine them together before the solution was evaluated as a whole. Many trial runs were conducted using different shape parameters and aggregation operators as each had a different degree of influence on the final result obtained. As a whole, the approach was rather complicated as its performance is heavily dependent on the many parameters and operators used. The approach required expertise to be effectively applied for solving optimization problems.

Several researchers took the problem further by incorporating the aspect of reliability in the optimization process. Farmani et al. (2005a) incorporated the resilience index as a second objective to increase the availability of water during pipe failures. Farmani et al. (2006) then extended the work to incorporate water quality by including water age as an additional objective. Farmani et al. (2005a, 2006) adopted the same constraint handling method as Walters et al. (1999). In Prasad and Tanyimboh (2008), the results from two approaches using different surrogate reliability measures i.e. statistical entropy and resilience index were examined. It was demonstrated that the use of statistical entropy as a reliability surrogate alleviated the shortcomings of the resilience index. This chapter will not delve into these aspects as they are not considered in the present research.

As observed, the constraint handling methods utilised by most researchers in their EA models require either penalty parameters or some form of weightings to standardize different constraint violation measures. Prasad and Tanyimboh (2008) and Prasad (2010) adopted the "penalty-free" constraint handling method which is essentially a tournament selection proposed by Deb (2000). This approach can potentially lead to anomalies in that it chooses expensive feasible solution over cost-effective borderline infeasible solution which may still be acceptable in practice and carry the overwhelming majority of the good genes. Detail explanations have been provided in Chapter 3.

In this chapter, the PFMOEA is applied to solve the design and rehabilitation problem of the "Anytown" WDS. Constraints are rigorously and effectively handled without the need for any other special constraint-handling technique, ad-hoc penalty functions or weightings. When tested on gravity-fed benchmark networks (i.e. Two looped network, Hanoi network, and New York Tunnels) as presented in Chapter 6, this optimization model proved to be exceedingly efficient and robust, being highly capable of finding the least cost solutions reported in the literature within considerably fewer function evaluations. The model also succeeded in finding optimal strategies for the long-term rehabilitation and upgrading of a real life network as presented in Chapter 7. Herein, this work is extended to optimize problems involving pump operation, energy consumption costs, tank sizing and location. Fully automated pump scheduling and tank sizing and siting were seamlessly incorporated into the optimization without manual intervention. The proposed formulation generated many novel solutions which are not only fully feasible, satisfying both pressure and operational constraints, but also cheaper than the best solution in the literature.

8.2 METHODOLOGY

8.2.1 Problem Variables

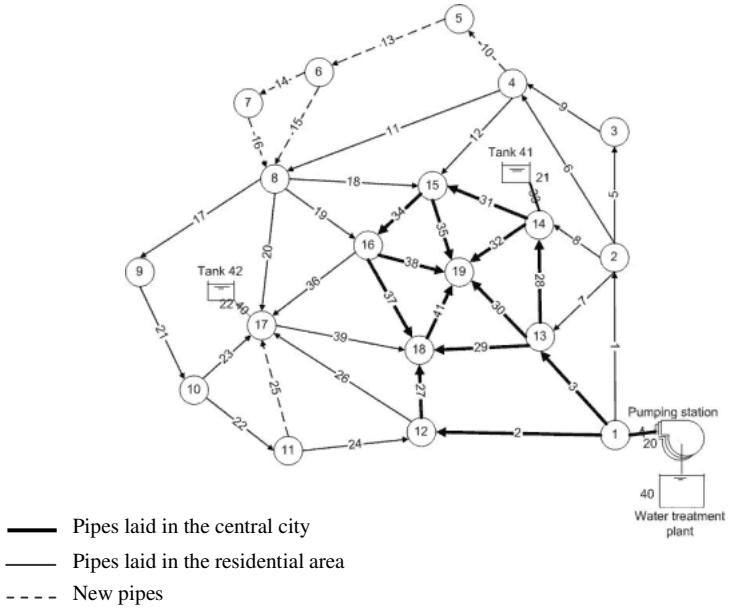

Figure 8.1 "Anytown" network layout

The layout of the "Anytown" network is shown in Fig. 8.1. A brief summary of the network is presented here for completeness. Other pipe and node information can be found in Appendix E. The water source of the network is a water treatment plant located at node 10 and is maintained at a fixed water level of 3.05 m (10 ft). Water is pumped from the plant into the system via three identical pumps operating in parallel. There are two existing storage tanks located at nodes 14 and 17 both with operating water levels between 68.58 m and 76.20 m. The volume of water below the level 68.58 m and above 65.53 m is retained for emergency purposes.

A minimum pressure of 28.12 m (40 psi) must be provided at all nodes at average day flow (duration of 24 hours) as well as instantaneous peak flow, which is 1.8 times the average day flow. The system is subjected to three different critical fire flow conditions under which it must supply water at a minimum pressure of 14.06 m (20 psi). With one pump being out of service and all tanks starting at their lowest operating levels, the emergency volume of each tank must be sufficient for the 2 hour fire and at the same time supply peak flow demands of 1.3 times the average day flow. Details of these fire flow conditions are given in Appendix E.

35 existing pipes are considered for paralleling (which includes sizing of the parallel pipe) or cleaning and lining. In addition, there are six additional new pipes to be considered. A maximum of two new tanks can be added in the improved design. Potential tank locations can be any of the 16 available nodes which are not connected directly to the existing tanks. Tanks are connected to a node by a riser of known length i.e. 30.7848 m (101 ft) but of variable diameter, further giving two additional diameter decision variables.

New pumping stations are not considered but an upgrade of the existing pumping station (which consists of three identical pumps connected in parallel) is allowed through the addition of a maximum of two new pumps with identical characteristics as the existing ones. Given 8 average day demand factors (one each for the eight 3-hour durations within 24 hours), 8 ON-OFF status control variables are used for the operation of a single pump. As such, each status control variable will correspond to a

demand factor. This enables the pump scheduling to be optimized for the different demand periods.

8.2.2 Tank Siting and Sizing

Herein, tank siting and sizing is directly and seamlessly incorporated into the optimization model without the need for any extraneous methodology or manual intervention at any point of the optimization process. With the accurate PDA simulation of nodal flows and pressures, the operation and status changes of tanks are precisely represented. No additional constraints are needed to prevent tanks from overfilling or dropping below emergency operating levels as the limits of the operational levels are explicitly recognised by the hydraulic simulator during the EPS as standard. This approach is straightforward as it avoids the problems of tank flow imbalance resulting from the mismatch between tank heads and corresponding water levels (Murphy et al., 1994; Walters et al., 1999). Independent research by Prasad (2010) led to more or less the same strategy. The approach can be summarized in the following steps:

1) A new tank is added to a node (tank parameters and new location are determined by the optimization model).
2) A snapshot simulation is executed at the beginning of the hydraulic time step.
3) The system is checked for status changes during the hydraulic time step. If the tank water level reaches the minimum level before the end of the time step, corresponding tank riser will be temporarily closed.
4) An additional snapshot analysis is performed taking care of the changed system state.
5) Steps 2 to 4 are repeated for the entire duration of the EPS (e.g. 24 hours herein).

It is worth mentioning that steps 2 to 4 are essentially the standard EPS procedure carried out using EPANET-PDX (which is conceptually the same as EPANET 2). Tank designs obtained at the end of the optimization process are final and no further tank adjustments (e.g. trimming the tank shape as in Vamvakeridou-Lyroudia et al., 2005) are required.

New tanks are assumed to be of cylindrical shape. Four sizing variables for the new tank are used: i.e. the total volume (*V*), ratio between diameter and height (*D/H*), ratio between emergency volume and total volume (*v/V*) and the bottom tank level (which represents the tank elevation). The *D/H* and *v/V* ratios are necessary in preventing the optimization algorithm from resulting in solutions with extremely wide or high tank designs which are unrealistic for real life implementation though perfectly feasible theoretically. For example, stand pipes are often associated with poorer water quality. The ranges of the values used were adopted from Prasad (2010). All nodes in the network are considered as possible locations for new tanks (except those already connected directly to existing ones). Table 8.1 summarizes the variables involved the problem formulation.

Table 8.1 Summary of decision variables involved

Variables	Explanations
Existing pipes	35 pipes to be considered for paralleling (including sizing of the parallel pipe) or cleaning and relining
New pipes	6 pipes to be sized
Existing tanks (operation)	Operation of 2 tanks to be optimized
New tanks (construction and operation)	Up to 2 tanks to be sized, located and operated optimally
New tank risers	Tank risers to be sized for the new tanks
Tank sizing parameters (new tanks)	*V*, *D/H*, *v/V* and elevation
Existing pumps (operation)	Operation of 3 pumps to be optimized
New pumps (construction and operation)	Up to 2 pumps to be added to the station and their operation optimized
Pump status (all pumps)	8 ON-OFF control variables per pump

The range of tank volumes and costs utilised in this work was taken from Walski et al. (1987) and can be found in Appendix E. Intermediate tank sizes are considered in the proposed approach and corresponding costs are interpolated linearly according to the standard volumes and costs provided. Since the NSGA II model employed herein is

binary coded, the values for candidates of each tank design variable are "discretized". Eight candidates were used for each design variable to avoid any redundant binary codes (a 3-bit binary string can represent $2^3 = 8$ discrete values). The values used are listed in Table 8.2. It is worth clarifying that the tank's total volume, elevation, *D/H* and *v/V* ratios are variables independent of each other. Hence the design of a new tank alone involves a total of 32 variables.

Table 8.2 Candidates for tank design variables

Total volume (m^3)	Cost ($)	Elevation (m)	*D/H*	*v/V*
227.279	115000	54.864	0.75	0.25
454.558	145000	57.912	0.85	0.3
909.117	265000	60.960	0.95	0.35
1136.396	325000	64.008	1.05	0.4
1590.954	365000	67.056	1.25	0.45
2272.792	425000	70.104	1.35	0.5
3409.188	512500	73.152	1.4	0.55
4545.584	600000	76.200	1.5	0.6

Note: Conversion factors used herein are identical to that of Walski et al. (1987) i.e. 1 gal = 0.004545584 m^3; and 1 ft = 0.3048 m.

8.2.3 PFMOEA Formulation to Solve the "Anytown" Network

The optimization problem is to upgrade and rehabilitate the system to meet future demands and pressure requirement in the most economic way, taking into consideration both capital expenditure and operational costs. The proposed approach involves two primary objectives. The first objective is to minimise the total cost which includes the capital and operating costs. The second objective is to maximize the network benefit resulting from the solution. The network benefit is essentially an overall performance measure of the solution which includes the aspects of hydraulics and tank operations. This measure also determines the feasibility of the solutions as explained below. The boundary search technique introduced earlier in Chapter 6 was used here also, to focus the PFMOEA search on the binding constraints. This is done by exponentiating the 1st and 2nd objective functions as shown in Eqs. 8.1 and 8.2 respectively. The problem can be mathematically formulated as follows:

Minimise $F_1 = \left(CR(i)\right)^2$ (8.1)

Maximise $F_2 = \left(Benefit(i)\right)^4$ (8.2)

where F_1 and F_2 represent the first and second objective functions respectively. *CR(i)* represents the cost ratio of solution *i* which can be expressed as:

$$CR(i) = \frac{C_{total}(i)}{C_{total}^{\max}} \tag{8.3}$$

where $C_{total}(i)$ is the total cost which includes the cost of the paralleling or cleaning and lining the pipes, additional pumps and tanks as well as the energy consumed by the pumps. The present worth of energy costs is based on an interest rate of 12% and an amortisation period of 20 years. Details of costs for pipe paralleling, cleaning and lining, pump operation and tanks can be found in Appendix E. $C_{total}^{\max}$ is the cost of the most expensive solution in the population. *Benefit(i)* corresponds to the network benefit resulting from solution *i* and can be expressed as:

$$Benefit(i) = \frac{1}{2}\left(\frac{\sum_{l=1}^{NL} \overline{DSR_l}}{NL} + \frac{\sum_{k=1}^{NT} TRR_k}{NT} \right) \tag{8.4}$$

where $\overline{DSR_l}$ represents the average network *DSR* for loading condition *l*. *DSR* which stands for demand satisfaction ratio is the ratio of the available flow to the demand. This result is available from PDA simulation. Maximizing the *DSR* of the network ensures all nodal demands are satisfied (Ackley et al., 2001). Handling the pressure constraints in this manner effectively eliminates the need for the penalty or tournament (e.g. Deb, 2000) methods. The average network DSR can be expressed as:

$$\overline{DSR_l} = \frac{\sum_{t=1}^{NS} DSR_t}{NS} \tag{8.5}$$

where DSR_t represents the network *DSR* for a single snap shot analysis for the t^{th} hydraulic time step and *NS* is the number of hydraulic time steps involved in the relevant loading condition. TRR_k stands for tank replenishment ratio and is essentially the ratio of the water level at the end of the last hour of the EPS to the maximum operational water level for tank *k*. Maximizing the *TRR* will ensure that tanks recover to their initial water level at the end of the 24 hour cycle. *NL* and *NT* are the number of loading conditions and tanks respectively. Both DSR_t and TRR_k take values between 0 and 1. Hence, the *Benefit(i)* is a normalised hydraulic performance and will reach a maximum value of 1 when all defined constraints have been met. Since all elements in the network benefit objective function represent necessary conditions and are normalised, no additional dimensional weightings are required and all benefit elements are treated with equal priority.

The network benefit objective formulation in Eq. 8.4 is only sufficient for achieving fully feasible designs but does not guarantee that solutions obtained fully utilize existing tank operational volumes during average day flow as will be demonstrated in the following section. Therefore, to improve the tank design methodology in this aspect, an additional term is incorporated into Eq. 8.4 as follows

$$Benefit(i) = \frac{1}{3}\left(\frac{\sum_{l=1}^{NL} \overline{DSR_l}}{NL} + \frac{\sum_{k=1}^{NT} TRR_k}{NT} + \frac{\sum_{k=1}^{NT} TUR_k}{NT} \right) \tag{8.6}$$

where TUR_k represents the tank utilisation ratio and is the ratio of the minimum operating water level of the tank (below which is the emergency storage for fire flows) to the lowest operating water level reached during the 24 hour EPS for tank *k*. Including this term in the network benefit objective would maximize the utilization of tank operational volumes. Solutions obtained by both network benefit formulations will be compared and discussed in the next section. The overall procedure of the PFMOEA for solving the "Anytown" network can be summarized as in Fig. 8.2.

Due to the numerous variables present in the optimization problem, a large population size of 200 was used. A total of fifteen optimization runs with different random seeds were conducted. Each run was executed for 5,000 generations. The probability of

crossover and mutation were fixed as 1 and 0.005. The inclusion of varying demand patterns, storage and pump operation scheduling requires the simulation of the network over an extended period. In this study, a hydraulic time step of 1 hour was used for the 24 hour average day flow loading condition. This greatly exceeds the accuracy of previous approaches in the literature where hydraulic time steps of 3 hours (Vamvakeridou-Lyroudia et al., 2005; Prasad, 2010) and 6 hours (Walters et al., 1999) had been applied.

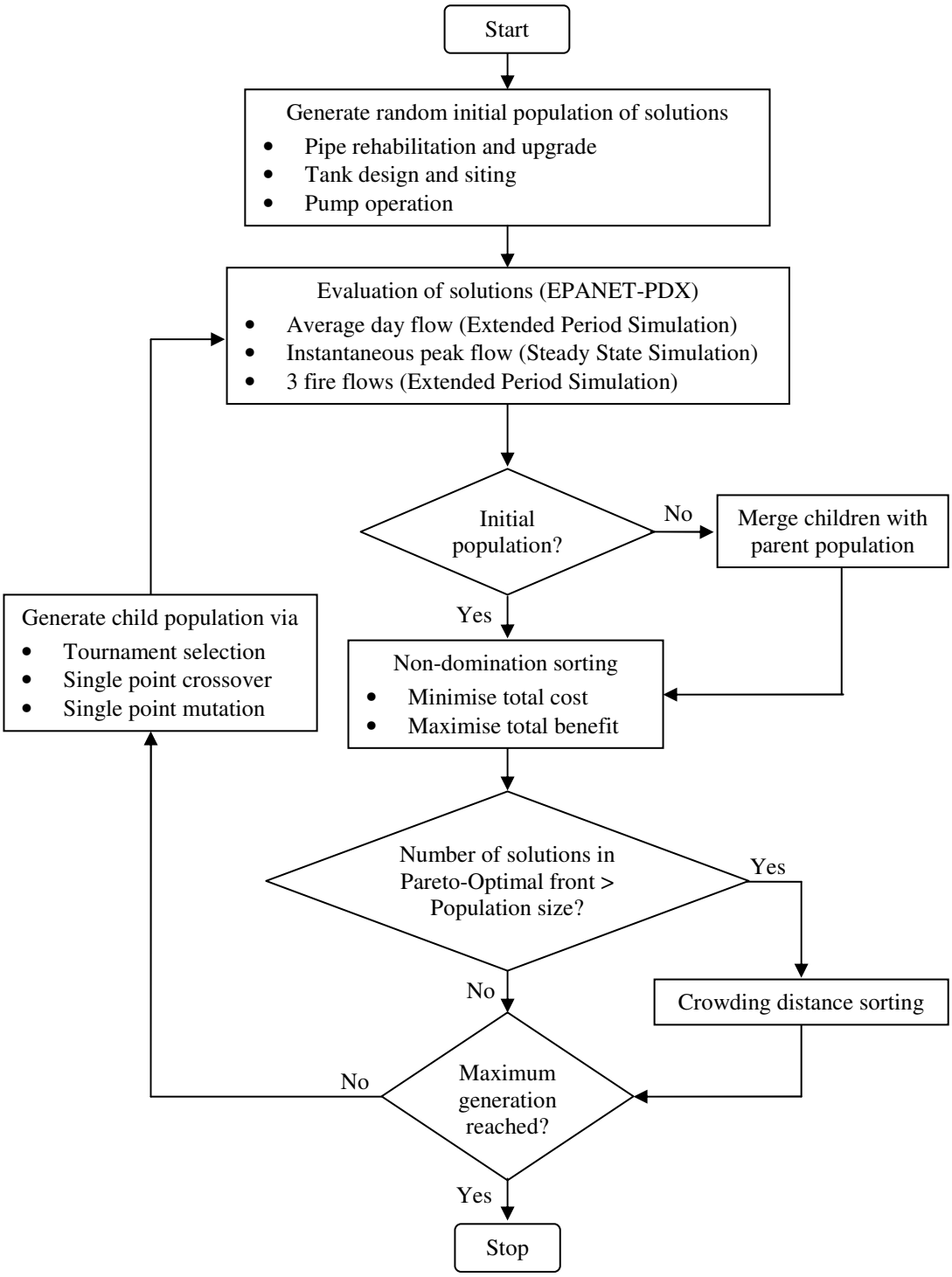

Figure 8.2 Overall procedure for PFMOEA

The use of steady state simulation during fire flows will tend to result in an overestimation of emergency volume. Hence, a hydraulic time step of 30 minutes was used for each fire flow event. In Vamvakeridou-Lyroudia et al. (2005), the minimum pressure limits were only checked for peak loading scenarios with the rationale that solutions which performed well for peak flows should also perform well for normal day loading. However, Prasad (2010) demonstrated that doing so was not sufficient to obtain final solutions that were fully feasible. Herein, the minimum pressure limits are considered explicitly for all five loading conditions.

8.3 RESULTS, DISCUSSIONS AND COMPARISON WITH OTHER OPTIMAL SOLUTIONS FROM THE LITERATURE

An Intel Core 2 Duo CPU 2.66 GHz, 3.23 GB RAM personal computer was used for this study. A typical PFMOEA run for solving the "Anytown" problem required on average 22.7 hours, a single generation on average required 16.36 s.

Two of the best solutions obtained by the PFMOEA are presented. These solutions are fully feasible as they do not violate any pressure constraints while operating under all five loading conditions and all tanks fully refilled at the end of the day (during the average day 24 hour cycle). Both solutions have been hydraulically simulated with a hydraulic time step of 1 minute to accurately confirm their feasibility. Table 8.3 presents a cost comparison of other best solutions published in the literature. The PFMOEA also obtained other cheaper solutions that though feasible with larger time steps (i.e. 30 and 60 minutes) were deemed infeasible when analysed with the overly stringent 1 minute time step EPS. These solutions (Solutions 3 and 4 which are both from different random runs) are also presented but will not be discussed in depth herein. Details of these and other solutions can be found in Appendix E. All PFMOEA solutions presented herein are lower in cost than the cheapest feasible solution reported in the literature to date, i.e. the solution by Prasad (2010) with a total cost of $10.59 million. PFMOEA Solutions 1, 2 and 4 achieved the lowest tank costs compared to previously published solutions.

Table 8.3 Cost Comparison with previous best solutions from the literature

Solutions	Costs ($ Millions)			
	Pipes	Energy	Tanks	Total
Murphy et al. (1994)	4.51	5.97	0.86	11.34
Walters et al. (1999)	4.10	5.90	0.90	10.90
Prasad (2010)	3.58	6.24	0.78	10.59
Vamvakeridou-Lyroudia et al. (2005)[a]	3.78	6.15	0.61	10.54
PFMOEA Solution 1	3.68	6.12	0.51	10.31
PFMOEA Solution 2[b]	3.68	6.22	0.51	10.41
PFMOEA Solution 3	3.58	6.22	0.54	10.34
PFMOEA Solution 4[b]	3.66	6.23	0.51	10.40

[a] Solution with "small pressure deficiencies" in two nodes, nodes 5 and 11.
[b] Solutions obtained using the benefit objective function with tank utilisation ratio, i.e. Eq. 8.6.

Pipe upgrade and rehabilitation details of the best two proposed solutions are summarized in Table 8.4. To avoid misunderstanding, it is worth mentioning that the original "Anytown" network problem was formulated based on imperial units. Hence, values of pipe diameters presented in Table 8.4 are after unit conversion (from inches to metres) and do not mean that continuous diameters were used. The results generally suggest that pipe paralleling is preferred over cleaning and lining as the rehabilitation option. In each of Solutions 1 and 2, only one pipe was selected for cleaning and lining (Table 8.4).

Table 8.4 Pipe upgrade and rehabilitation for Solutions 1 and 2

	Solution 1		Solution 2	
	Pipe ID	Diameter (m)	Pipe ID	Diameter (m)
PP	1	0.3556	2	0.6096
	2	0.6096	4	0.2032
	20	0.4064	17	0.2032
	23	0.3556	20	0.6096
	26	0.6096	26	0.6096
CL	40		3	
NP	10	0.3556	10	0.1524
	13	0.1524	13	0.254
	14	0.1524	14	0.2032
	15	0.254	15	0.4572
	16	0.3556	16	0.2032
	25	0.1524	25	0.2032
	Riser 7[a]	0.4064	Riser 6[a]	0.3048

1 in = 0.0254 m
PP = Pipe paralleling
CL = Pipe cleaning and lining
NP = New pipes
Risers 6[a] and 7[a] are risers for new tanks located at nodes 6 and 7 respectively.

The lowest cost solution, i.e. Solution 1, has a total cost of $10.31 million. Unlike most of the previous solutions with two tanks, a single new tank was added at node 7. No new pumps were added to the pumping station. Out of the three existing pumps, one operates during the peak demand hours from 9 am to the 6 pm and the remaining two operate for the entire 24 hours consuming a total energy of 18733.5 kWh per day as presented in Table 8.5. This operation strategy is somewhat different from other solutions published in the literature e.g. Walters et al. (1999) where the third pump is usually switched on during low demand period to fill up the tanks. Hence, for the Solution 1 design, additional required flows during the peak hours are supplied by both the new tank and the third pump. This could probably be the reason why the algorithm only allocated one new tank instead of two as in previous solutions in the literature (e.g. Prasad, 2010; Vamvakeridou-Lyroudia et al., 2005; and Murphy et al., 1994).

Table 8.5 Daily pumping operation for PFMOEA best solutions

Solutions	Number of pumps operating				Energy consumed (kWh/day)
	6-9h	9-15h	15-18h	18-6h	
1	2	3	3	2	18,733.50
2[a]	3	3	2	2	19,017.92

[a] Represents solution with tank draining strategy

Details of the newly added tank are presented in Table 8.6. Fig. 8.3 shows the tank operating levels over a cycle of 24 hours for the average day flow of Solution 1 obtained from an EPS with 1 minute hydraulic time step. The results show all tanks fully refilled at the end of the day. The newly added tank 7 and existing tank 41 drained rapidly in approximately 6 and 3 hours respectively. The water level in existing tank 42 fluctuated as the tank refilled partially and drained several times between the 9th to the 21st hour. As observed, this tank did not fully empty during the day (the dotted line in Fig. 3 represents the minimum operating level for the existing tanks, below which is the emergency storage). Only approximately 40% of the total operational volume was utilised. Hence, it is obvious that though cost effective, this design is undesirable from the standpoint of tank operation.

Table 8.6 Details and dimensions of new tanks

Properties	PFMOEA solutions	
	1	2
Maximum operating water level (m)	72.98	72.98
Minimum operating water level (m)	67.18	66.56
Top level (m)	74.31	74.31
Elevation (m)	60.96	60.96
Diameter (m)	18.67	18.67
Tank Location (Node ID)	7	6
V (m^3)	3409.188	3409.188
v/V	0.45	0.5
D/H	1.5	1.5

1 ft = 0.3048 m

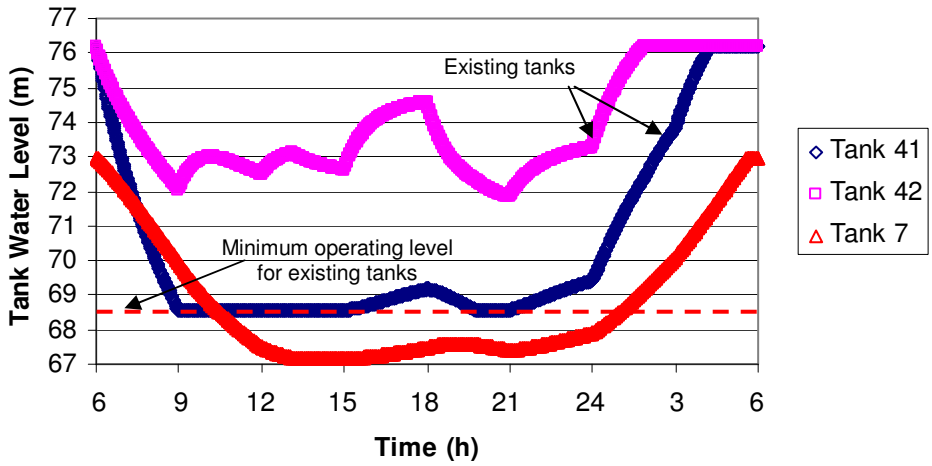

Figure 8.3 Tank operating water level for average day flow (Solution 1 by PFMOEA)

Fig. 8.4 shows the pump efficiency of Solution 1 over the 24 hour cycle (with 1 minute EPS time step). The performances of the three pumps were identical as all had the same efficiency curve. It can be observed that the pumps were operating consistently near their best efficiency point, i.e. 65% and did not fall below 60%. It is worth mentioning that aside from the additional variables implemented for pump scheduling (Table 8.1), no other operational constraints (e.g. constraint on pump operational capacity to meet daily demand variation as implemented in Prasad (2010) and Vamvakeridou-Lyroudia et al. (2005)) were applied. This further demonstrates the simplicity and superiority of the proposed approach.

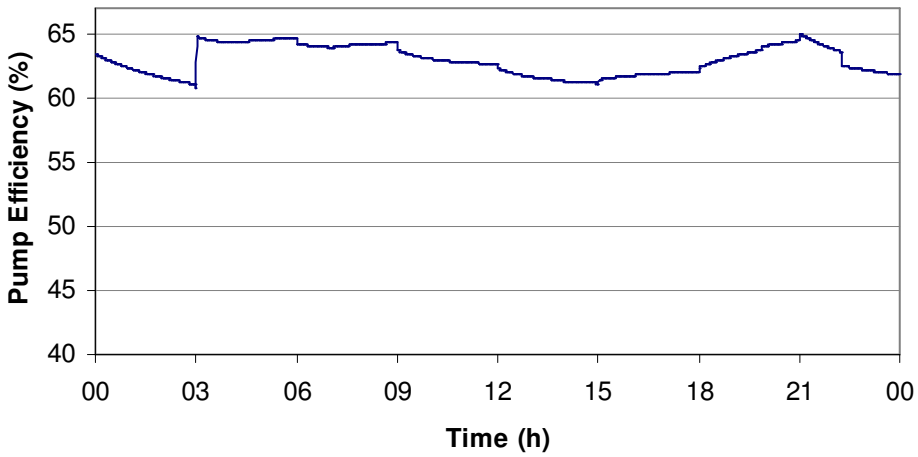

Figure 8.4 Pump efficiency for average day flow (Solution 1 by PFMOEA)

For comparison purposes, the tank operations from Prasad (2010) are presented in Fig. 8.5. As observed, both Solution 1 and Prasad (2010) had roughly similar tank operation patterns. Similarly, the capacity of existing Tank 42 was not fully utilised. The same scenario was also encountered by the best solution reported in Vamvakeridou-Lyroudia et al. (2005) during the average day and two fire flow loadings.

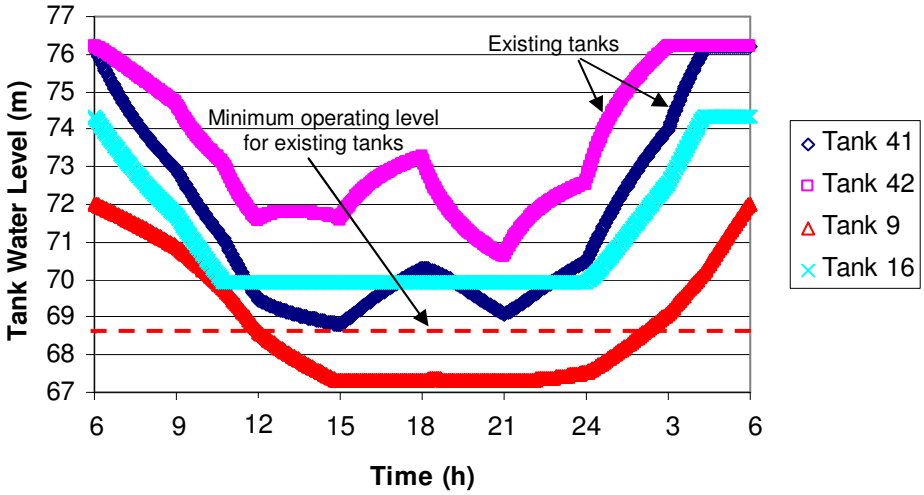

Figure 8.5 Tank operating water level for average day flow for the best solution obtained by Prasad (2010)

It is shown from the results of Solution 1 that the network benefit objective formulation (Eq. 8.4) applied is only sufficient for achieving fully feasible designs and does not guarantee that solutions obtained fully utilize tank operational volumes. Solution 2 was the cheapest feasible solution obtained from the PFMOEA run with the improved network benefit objective formulation (Eq. 8.6). The total cost achieved was $10.41 million. One new tank was added at node 6. No new pumps were added to the pumping station. The cost component for pumping is slightly higher than that of Solution 1.As in Solution 1, all three existing pumps operate during the peak demand hours while only two are required for the rest of the day (Table 8.5). Costs for the new tank and pipe rehabilitation were similar to that of the cheapest solution (i.e. Solution 1).

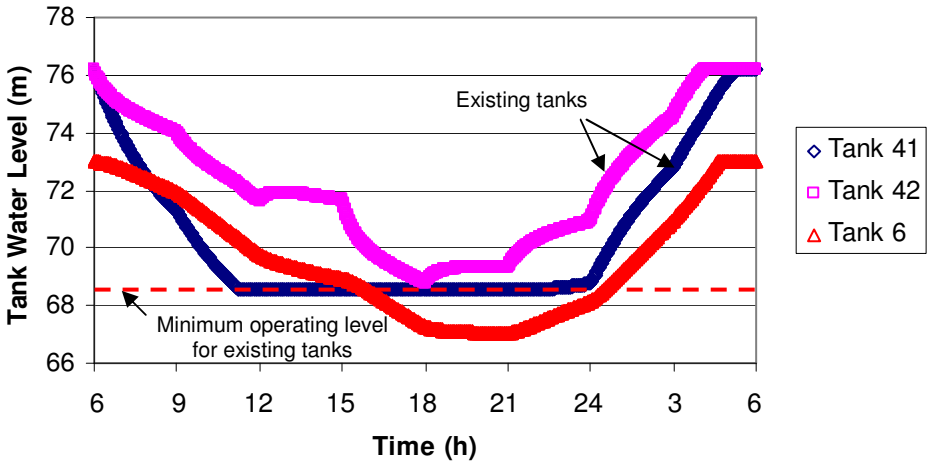

Figure 8.6 Tank operating water level for average day flow (Solution 2 by PFMOEA)

Fig. 8.6 summarizes the operation cycle of the tanks for the average day flow of Solution 2. The available operational volumes for all three tanks were effectively utilised during the cycle and recovered fully at the end of the day. Existing tanks 41 and 42 had significantly lower fluctuations in water levels. The new tank (at node 6) emptied gradually in 15 hours and filled up within approximately 7.67 hours during non-peak demand period. Though not completely depleted, water level in existing Tank 42 reached a minimum of 68.79 m, which was just 0.21 m above the minimum operating level at the 18th hour. This demonstrated that the enhanced network benefit formulation significantly improved the operating cycle of tanks. The water storage is efficiently used with tanks emptying and filling rather steadily throughout the day. Fig. 8.7a, Fig. 8.7b and Fig. 8.7c show the tank operations during the three fire flow loadings. The total emergency volumes provided by all tanks were more than sufficient to meet all the fire flows. Existing tanks 41 and 42 were fully drained at the end of all three fire flow scenarios. As for the most critical fire flow, i.e. fire flow 2, approximately 90% of the emergency volume of Tank 6 was used. Fig. 8.8 shows the pump efficiency of Solution 2 over the 24 hour cycle. Similar to Solution 1, the performances of the three pumps were highly efficient.

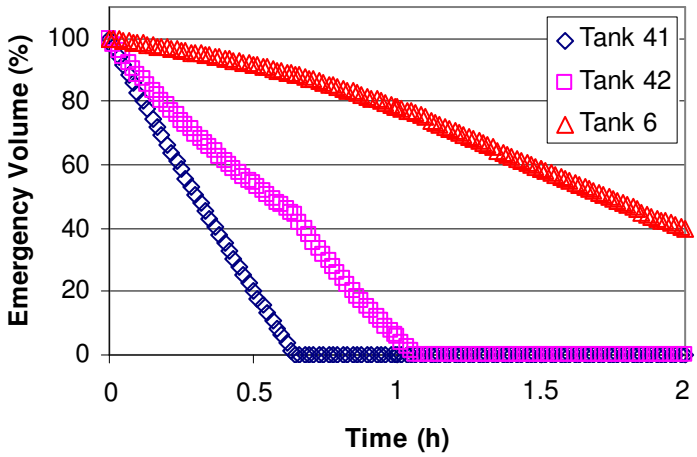

Figure 8.7a Tank operating water level for fire flow 1
(Solution 2 by PFMOEA)

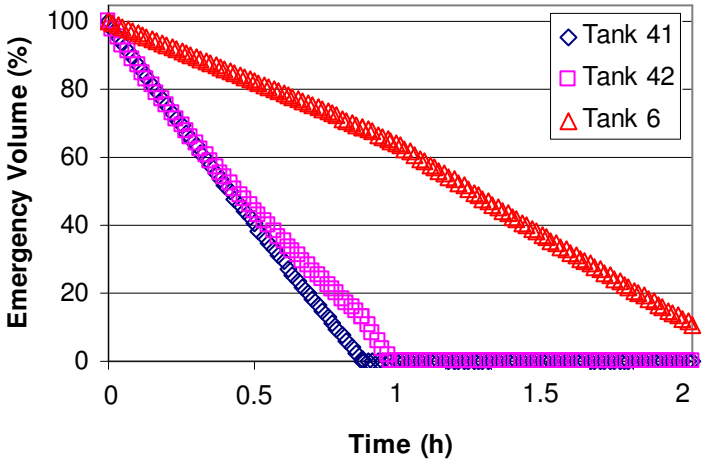

Figure 8.7b Tank operating water level for fire flow 2
(Solution 2 by PFMOEA)

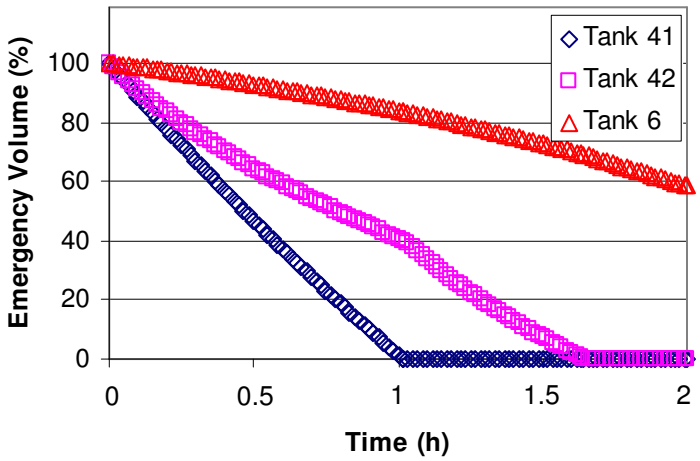

Figure 8.7c Tank operating water level for fire flow 3
(Solution 2 by PFMOEA)

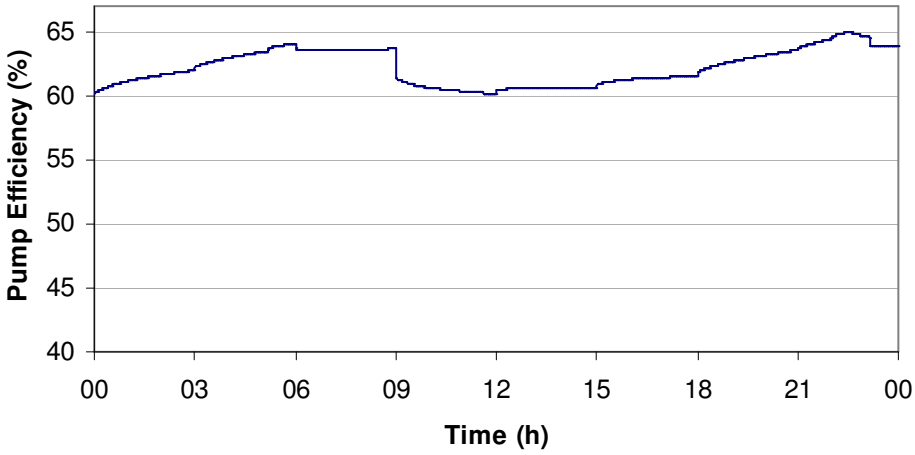

Figure 8.8 Pump efficiency for average day flow
(Solution 2 by PFMOEA)

Fig. 8.9 shows the Pareto optimal front out of which Solution 2 (preferred solution) was obtained. The trade-off characteristics between the network benefit and total cost objectives are clearly depicted. The multi-objective approach allows a range of non-dominated solutions to be produced with each solution delivering the maximum benefit for the cost involved. As observed, most of the solutions are concentrated in the feasible and near-feasible regions. This is the effect of focusing the EA search in both the feasible and infeasible regions close to the active constraint boundaries where

cost effective solutions are generally situated. Though the "Anytown" network posed a highly complex optimization problem, the PFMOEA still succeeded in finding multiple fully feasible designs. As observed in Fig. 8.9, aside from Solutions 2, there are many other fully feasible designs obtained as well within the same optimization run which are cheaper than the cheapest solution reported in the literature. This clearly demonstrates the effectiveness and robustness of the approach in locating feasible cost effective designs.

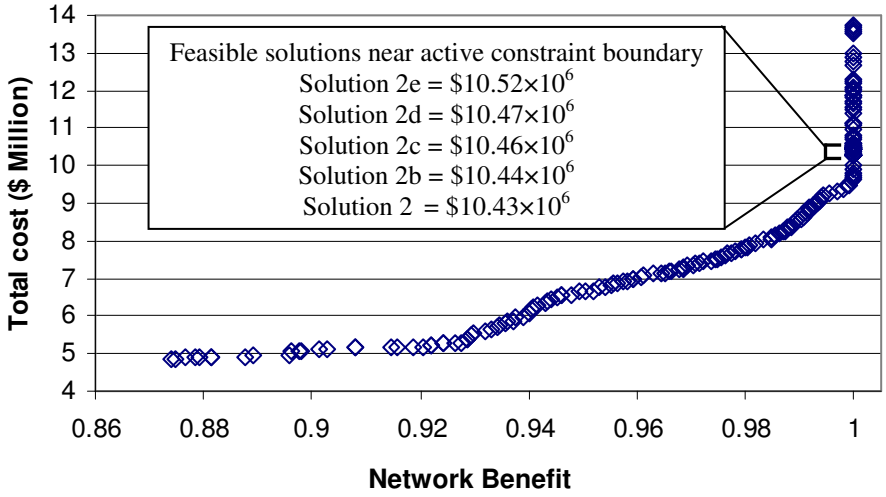

Figure 8.9 PFMOEA Pareto optimal front solutions

Table 8.7 gives the values of the pressures at the most critical nodes for various loading conditions for all the PFMOEA solutions presented. The results show that all solutions satisfied the pressure requirements specified for each design loading scenario. Results presented herein are based on steady state and extended period simulations (with hydraulic time step of 1 minute unless otherwise stated) performed with EPANET-PDX. It is worth mentioning that for a 24 hour EPS with a hydraulic time step of 1 minute, the average simulation time required by EPANET-PDX is only a fraction of a second, i.e. 0.843 seconds, exhibiting the computational efficiency of the hydraulic simulator.

Table 8.7 Minimum pressures for various loading conditions

Solutions	Critical nodal residual head (m)				
	Average day flow (24 hour EPS)	Instantaneous peak flow (SSS)	Fire flow 1 (2 hour EPS)	Fire flow 2 (2 hour EPS)	Fire flow 3 (2 hour EPS)
Solution 1	28.96 (16)	28.19 (9)	15.16 (16)	16.70 (16)	22.50 (11)
Solution 2	28.29 (16)	29.91 (9)	17.10 (16)	16.61 (7)	21.66 (9)
Solution 2b	28.27 (16)	30.89 (11)	16.73 (16)	15.78 (7)	18.30 (11)
Solution 2c	28.27 (16)	30.82 (11)	16.70 (16)	18.53 (5)	18.29 (11)
Solution 2d	28.27 (16)	30.85 (11)	16.69 (16)	18.53 (5)	18.28 (11)
Solution 2e[a]	28.31 (16)	31.12 (11)	17.43 (16)	16.89 (7)	19.34 (11)
Solution 3[a]	29.59 (16)	32.48 (16)	17.15 (16)	20.15 (16)	20.54 (9)
Solution 4[a]	28.99 (16)	31.44 (16)	15.37 (16)	16.92 (16)	20.75 (11)

1 psi = 0.703 m
The figures in parentheses represent the critical nodes
The required pressure is 28.12 m (40 psi) for average day and instantaneous peak flow; and 14.06 m (20 psi) for all fire flows
EPS - extended period simulation
SSS - single snapshot simulation
[a] Represents solutions simulated using 1 hour EPS time step

To further verify the feasibility of the solutions as well as the accuracy of EPANET-PDX, simulations using EPANET 2 (Rossman, 2002) were carried out as well. Fig. 8.10 shows a comparison of results of Solution 2 for the average day flow (24 hour EPS with 1 minute time step), all three fire flows (2 hour EPS with 1 minute time step) and the instantaneous peak flow simulated using both hydraulic simulators. A virtually perfect correlation of $1\text{-}R^2 = 7.5\times10^{-9}$ was achieved, further confirming the solution's feasibility as well as the accuracy of EPANET-PDX results. This is the same for the other PFMOEA solutions presented.

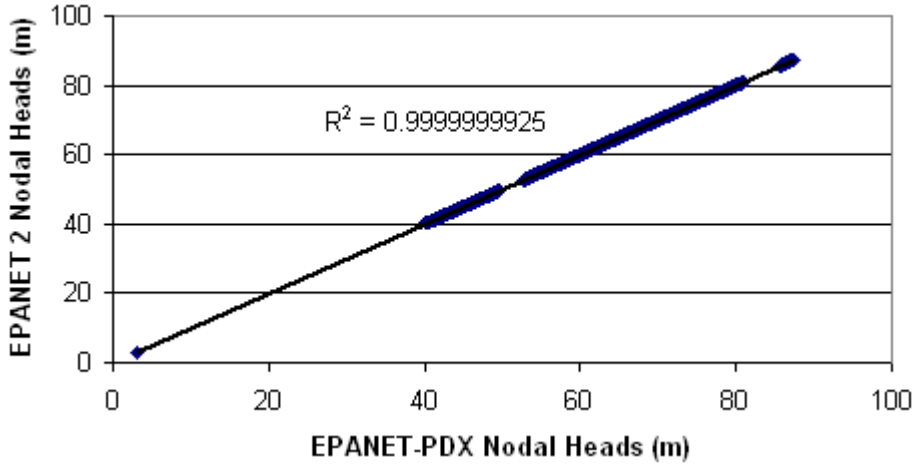

Figure 8.10 Correlation between nodal heads of EPANET-PDX and EPANET 2

In reality, high velocity flows in pipes would increase the rate of pipe internal erosion. Several authors implemented maximum flow velocity constraints while solving the "Anytown" network though not required in the original problem specification (Walski et al., 1987). These constraints are usually implemented indirectly in the optimization algorithm as a means of eliminating quickly designs with steep head loss gradients (Vamvakeridou-Lyroudia et al., 2005). The typical maximum flow velocity limit used is 2 m/s (Prasad, 2010). In this work, maximum velocity constraints were not implemented. However, it is worth mentioning that all PFMOEA solutions presented had average day flows with velocities less than 2m/s. This is probably due to the highly looped configuration of the "Anytown" layout. Take Solution 2 for instance, the maximum flow velocity was 1.51 m/s in pipe 4 (which connects node 1 to the pumping station) at the 10^{th} hour (where the demand factor was the highest i.e. 1.3).

8.4 CONCLUSIONS

The application of the penalty-free multi-objective evolutionary approach (PFMOEA) has been successfully extended to include optimal pump scheduling, energy consumption and the location and sizing of service reservoirs in an effective and straight forward manner. The problem was formulated as a multi-objective optimization problem with minimum cost and maximum network benefit as dual objectives. The significant advantage of this method over previous methods is that it is rigorous and entirely eliminates the need for ad-hoc penalty functions, tournament selection or any other complicated constraint handling methods. Hence, it does not require any parameter fine tuning or trial and error runs, saving a great deal of time.

With accurate PDA, the direct application of the standard extended period simulation enables pump scheduling and tank sizing and siting to be seamlessly incorporated into the optimization without the need for any extraneous methodology or manual intervention. Conceptually, the approach is straightforward and probably the simplest hitherto. The computational efficiency of the model was demonstrated to be high in which a single GA generation required 16.36s. It is worth reiterating that each solution entails the evaluation of 5 different loading conditions (of which 4 required extended period simulation).

The PFMOEA successfully solved the "Anytown" benchmark problem and the cheapest solution obtained was 2.6% cheaper than the least cost solution published in the literature. Solutions presented are fully feasible and satisfy both pressure and operational constraints for the various loading conditions involved. The tank siting and sizing methodology was proven to be effective. First and foremost, the solution (preferred) exhibited very efficient tank operating cycles whereby the capacity of existing and new tanks were not only fully utilized during peak hours but also completely refilled at the end of the day. Moreover, the performance of the pumps was consistently efficient throughout the day. The numerous cost effective solutions obtained demonstrate the effectiveness and robustness of this approach, indicating that the penalty-free approach can indeed enhance the evolutionary algorithm search in identifying cost effective solutions.

CHAPTER NINE

CONCLUSION

9.1 INTRODUCTION

Managing a water distribution system involves optimally designing the system to operate in a cost effective manner whilst meeting customers' demand at an acceptable service level. It also entails maintaining its service performance level for long term by periodically carrying out upgrades and/ or rehabilitation works to reinforce the network's structural integrity and expand its hydraulic capacity to cater for demand growth. These aspects are combinatory problems involving multiple criteria which are conflicting, leading to complications in choosing the most suitable option to be implemented. With the increase in expected water supply service level along with tighter budget constraints, the need for practical optimization tools to assist in decision making cannot be further stressed.

Evolutionary Algorithms (EAs) have been proven to be well suited for solving complex optimization problems but are incapable of directly handling constraints. Given that the WDS optimization problems are highly constrained, penalty methods are commonly used to convert these constrained solution spaces into unconstrained ones for the application of EAs. Penalty functions are formulated to penalize solutions that violate the pressure constraints and in doing, the search procedure is forced toward the region of feasible solutions. The optimal solution heavily depends on the penalty parameters. Users usually have to use trial and error to find the best value that would guide the search towards the feasible region. This may require extensive experimentation which are time consuming. Moreover, penalty parameters are often case sensitive in that they may perform well on some problems but not so well on

others. If poorly chosen, the penalty parameter can severely distort the objective function and affect the EAs performance.

Several researchers implemented "penalty-free" approaches in handling node pressure constraints. The approach of formulating each nodal pressure constraint as an objective is computationally prohibitive for large networks. Self-adaptive penalty methods in general still utilize parameters which require calibrations. Several anomalies were observed in some of the methods. The tournament selection technique will select an overly expensive design over a near feasible design which may well contain majority of the potential building blocks for the optimal solution. The self-adaptive fitness formulation allows cheap infeasible solutions to be selected over expensive feasible ones.

The goal of this research was to develop a versatile EA optimization tool which can be easily applied to various aspects of the water distribution system (WDS). The main challenge tackled was addressing the issue of constraint handling within the EA. This research has thoroughly investigated this problem and developed a rigorous and straightforward approach to handle pressure constraints without relying on ad-hoc penalty methods, special self-adaptive approaches or tournament selection techniques. As such, it does not involve any time consuming parameter calibration or trial runs and can be effectively implemented by a wide range of users/ engineers as it is user-friendly, i.e. no specialize skills or experience required for its application.

The model developed is referred to as the penalty-free multi-objective genetic algorithm (PFMOEA). The approach applied was to utilise a pressure dependent analysis (PDA) to accurately assess the performance of the generated solutions and in doing so efficiently guide the GA in locating optimal solutions. The PFMOEA has been successfully applied to solve optimization problems such as design, pump scheduling, tank sizing and siting, and long term rehabilitation and upgrading of the WDS, the methodologies as detailed in Chapter 6, 7 and 8. This chapter will focus on the overall summary and general conclusions of the work carried out followed by several recommendations for future works.

9.2 SUMMARY AND CONCLUSIONS

9.2.1 Design and Rehabilitation Optimization of WDS

The PFMOEA couples the EPANET-PDX simulator with the multi-objective NSGA II optimization model. The approach involves two objectives. The first objective is to minimize the network design cost while the second objective is to ensure that all nodal demands are fully satisfied. This is done by maximizing the demand satisfaction ratio of the most critical node. Doing so drives the search toward designs with fully satisfied demands which are essentially designs that satisfy all pressure constraints. As such, the pressure constraints are effectively handled without the need for any extraneous methods. The GA convergence properties were further enhanced by a "boundary search" technique in which the objective functions were exponentiated. This causes the search to favour solutions near the boundary between both feasible and infeasible region of the search space where optimal solutions are generally situated.

The PFMOEA has been applied to the three renowned benchmark networks as case studies, i.e. the Two-loop network, Hanoi network and New York Tunnels. In all three cases, the PFMOEA succeeded in obtaining designs identical to the cheapest solutions in the literature within considerably fewer function evaluations, demonstrating its efficiency in locating optimal solutions. The model converged to the optimal solutions whilst only having explored an extremely small fraction of the entire solution space. A sensitivity analysis was carried out to check the effect of using the maximization of network DSR as opposed to critical nodal DSR (as the objective) on the optimality of the final solutions. The PFMOEA still managed to obtain the least cost solutions using the former, however at a higher function evaluation count. Nevertheless, this further reinforces that the approach is highly robust and efficient.

In Chapter 8, the formulation of the PFMOEA was extended to include pumping cost and the design and locating of storage reservoirs. The problem was formulated as a multi-objective optimization problem with minimum cost and maximum network benefit as objectives. The network benefit is essentially the hydraulic performance

which includes the network demand satisfaction ratio along with both the tank replenishment and utilization ratios which govern the efficient operation of both the existing and newly added tanks. With accurate PDA, the direct application of the standard extended period simulation enables pump scheduling and tank sizing and siting to be seamlessly incorporated into the optimization without the need for any extraneous methodology or manual intervention.

The approach was applied to the "Anytown" benchmark network problem which involved the rehabilitation of pipes, pump scheduling, tank siting and sizing whilst considering multiple operating conditions and diurnal demand variation. The best PFMOEA solution obtained was cheaper compared to the lowest cost solution reported in the literature. The design was fully feasible in that it satisfied the pressure constraints for all loading conditions. Tanks depleted and refilled completely while pumps consistently exhibited efficient operation throughout the day. Many other good solutions which are fully feasible were obtained for this highly complex problem, once again indicating that the PFMOEA approach is highly robust and efficient in locating cost effective solutions.

9.2.2 Long-Term Design, Rehabilitation and Upgrading of WDS

The PFMOEA has been formulated to obtain the optimal long term rehabilitation and upgrading strategy for WDS in Chapter 7. The model approached the problem in a systematic and holistic manner. It explicitly takes into consideration the deterioration over time of both the structural integrity and hydraulic capacity of every pipe. Both direct and indirect failure costs were taken into account. The model directly addressed essential concerns of the rehabilitation and upgrading work such as the magnitude of upgrading along with the timing for implementation. The overall design horizon consists of two phases whose durations are sequentially optimized using simple dynamic programming approach. The first phase involves optimizing the design of a new network while the second phase optimally determines pipes for paralleling or replacement.

The PFMOEA model has been successfully applied to solve a real-life WDS to demonstrate its practical capability and efficiency. Comparing the results obtained by the PFMOEA to that of the earlier linear programming (LP) approach (Tanyimboh and Kalungi, 2008), it was demonstrated that that the former is more effective in finding cheaper solutions. The reasons behind this are 1) Evolutionary algorithms perform better in comparison to classical optimization techniques in locating near global optima and 2) The LP model used pre-specified pipe flows, i.e. maximum entropy flows, which resulted in the selection of more uniform pipes which are larger in the design of the network. Nevertheless, it was observed that a bulk of these cheaper PFMOEA solutions had lower reliability and failure tolerance measures, strengthening the evidence that designs carrying maximum entropy flows are generally more reliable than conventional designs. Two notable improvements of the PFMOEA approach from the earlier LP approach are: 1) PFMOEA designs obtained contain single segment pipes of constant diameter which are practical for real life implementation and 2) PFMOEA yields multiple non-dominated solutions and hence provides further flexibility during the final decision making process.

An efficient performance assessment module has been developed and incorporated in this work for two reasons, i.e. to explicitly address the reliability and failure tolerance of the WDS and to aid the final decision making process by eliminating a very large proportion of candidate solutions, the methodology as presented in Chapter 7. The approach essentially distinguishes solutions of the best cost-reliability trade-off front amongst the vast number of optimal solutions generated by several optimization runs. It involves using the statistical entropy as a preliminary hydraulic reliability filter which screens out a large proportion of designs before detailed reliability and failure tolerance analyses are carried out. Since reliability was not formulated as an additional objective, the complexity and computational effort of the optimization problem was enormously lessened as intergenerational reliability evaluations are obviated. This resulted in an enormous reduction of the overall computational effort, making this approach practical for the implementation of real world WDS. In addition, the proposed approach was validated in section which essentially improved the level of confidence in the results obtained as the outcome showed that entropy was highly correlated to the network reliability.

9.2.3 Pressure Dependent Analysis Hydraulic Simulator: EPANET-PDX

In water distribution systems (WDSs), the available flow at a demand node is dependent on the pressure at that node. When a network is lacking in pressure, not all consumer demands will be met in full. In this context, the assumption that all demands are fully satisfied regardless of the pressure in the system becomes unreasonable and represents the main limitation of the conventional demand driven analysis (DDA) approach to WDS modelling. A realistic depiction of the network performance can only be attained by considering demands to be pressure dependent. In the aspect of WDS optimization using EAs, accurate performance evaluation of solutions is exceedingly essential in order to efficiently guide the search toward the optimal solutions since these stochastic natured techniques generate large proportions of infeasible solutions.

In Chapter 5, an enhanced version of the EPANET 2 simulator that is extended to include PDA functionality has been developed. This extension is referred to as EPANET-PDX (pressure dependent extension). It integrates a head-flow relationship proposed by Tanyimboh and Templeman (2004) within the Global Gradient Method (Todini and Pilati, 1988) that constitutes the hydraulic engine of EPANET 2. The Tanyimboh and Templeman (2004) function is continuous in both its function and derivatives. As such, it has an advantage over other head flow relationships which are in general discontinuous in their derivatives at the transitions between zero and partial nodal flow and/or between partial and full demand satisfaction which can lead to convergence difficulties in the computational solution of systems of constitutive equations. The convergence of EPANET-PDX is further improved with the facilitation of a globally convergent strategy based on a line search and backtracking procedure. The line search and backtracking is a deterministic approach which optimizes the size of the Newton step taken at every iteration. This ensures both the head loss and flow continuity functions are progressively improved and avoids oscillations within the algorithm.

EPANET-PDX has been demonstrated to be robust, efficient and accurate in analyzing both normal and pressure deficient conditions. Simulations of real life networks consisting of multiple sources, pipes, valves and pumps were successfully

executed and results are presented. Evidence of its robustness includes the ability to produce realistic, hydraulically consistent results for the entire range of network demand satisfaction from zero to 100% with no convergence complications. EPANET-PDX has been successfully used in the application of the PFMOEA to solve complex optimization WDS problems involving pumps, allocation and sizing of storage reservoirs along with pump scheduling involving multiple operating conditions which requires the extended period simulations. Also, it accurately carried out pipe failure simulations for the reliability and failure tolerance calculation.

The accuracy of the generated PDA results (in terms of nodal pressure, pipe flow rates and nodal flows) has been validated and verified using PRAAWDS (Tanyimboh, 2008) and the hydraulic feasibility test (Ackley et al., 2001) which is a well established PDA result verification method. The comparison of both PDA and DDA results highlighted the fact that DDA results can be very misleading as they tend to underestimate the network performance under pressure deficient conditions. This was demonstrated in Chapter 5 where DDA nodal head results were negative though a huge proportion of demand was satisfied at the demand node. In terms of computational efficiency, the performance of both EPANET-PDX and EPANET 2 were compared comprehensively in terms of number of iterations required to converged and computational time. The results obtained have shown that EPANET-PDX compares favourably to the DDA based EPANET 2.

In a nutshell, the general conclusions are as follows:

1) The proposed penalty-free constraint handling approach indeed enhances the EA search in locating the optimal solutions in an effective and robust manner. Accurately assessing the performance of the solutions along with the simple boundary search method efficiently guides the search toward boundary solutions. The PFMOEA consistently performs well for WDS optimization problems of various levels of complexity.

2) The present research has proven that PDA is superior to DDA in analysing pressure deficient networks. PDA can calculate the actual outflow of demand nodes and realistically depicts the network deficiency. Conversely, DDA tends to exaggerate

the shortfall of the network, produces inaccurate nodal heads which are particularly misleading.

3) The inkling that PDA is much more computationally demanding than DDA has proven to be inaccurate. PDA is equally or at times even more efficient than DDA. EPANET-PDX has proven to be highly robust and performs consistently with high efficiency while analysing both normal and pressure deficient networks.

4) The evidence that statistical entropy is an appropriate performance measure for the WDS is further enhanced. The calculation of flow entropy is computationally trivial. As such, it provides a straight forward and rapid means of approximating the level of reliability in a WDS.

9.3 SUGGESTIONS FOR FUTURE WORKS

The research herein has solved a wide scope of the WDS optimization problem. There is, however, much room for further investigations and improvements to be done on the present work. Some of these issues are discussed next.

The complications involved in developing an optimal long term rehabilitation and upgrading strategy for a WDS have been demonstrated to be immense even for a network which only consists of pipes and a single reservoir. The PFMOEA has successfully obtained optimal designs for problems involving pumps and storage tanks. This strongly suggests that the time is ripe to widen the scope of the optimal long term upgrading problem to cover the entire supply system which includes components such as pumps, valves, treatment plants, multiple reservoirs etc. Another important aspect to be considered is water quality e.g. the minimization of water age. It can either be formulated as an objective by itself, or be incorporated as part of the 'benefit' objective. As detailed earlier, the PFMOEA employs the multi-objective NSGA II and EPANET-PDX which contains the full spectrum of hydraulic functionality including water quality analysis. Therefore, conceptually, these suggestions are highly feasible and no great difficulties are foreseen in implementing them.

Studies have shown the benefit of search space reduction on the convergence properties of the GA. Confining the number pipe diameters on the candidate list reduces the number of variables and hence effectively reducing the number of function evaluations required to locate the optimal solution. However, strategies to select appropriate candidate pipe sizes would have to be applied meticulously and wisely as limiting the search space may prevent the GA from exploring regions containing good prospective solutions, resulting in the final selection of suboptimal solutions.

A good suggestion would be to preselect feasible candidate diameters for each link based on the maximum entropy (ME) flow design. The ME design can be obtained at every specified generation, subsequently updating the candidate diameter list as the evolution progresses. Alternatively, the global ME design can be obtained separately as an individual optimization problem prior to solving the actual WDS optimization problem. Doing so will not significantly add to the overall computational burden of the GA since the calculation of maximum entropy is extremely straight forward and far less demanding compared to the 'pipe index' vector (Vairavamoorthy and Ali, 2005). Another positive outcome from doing so is that solutions obtained will inherently have higher reliability and failure tolerance values since the network has been designed to carry maximum entropy flows. Entropy based designs have been shown in studies to be not unduly expensive and hence cost effective solutions will still be obtained.

EPANET-PDX has been extensively used to run hydraulic analyses. However, the aspect of water quality analysis is still to be investigated. Since nodal heads generated by both analysis methods are different during pressure deficiency conditions, the pipe flow rates will well be different. Flow velocity inherently affects water quality parameters such as water age, the rate of chlorine decomposition, concentration of THM etc. The differences between PDA and DDA hydraulic models in simulating water quality could be another interesting topic of research. Using EPANET-PDX and EPANET 2 as PDA and DDA hydraulic models respectively would enable a like to like comparison. A study on how pressure deficiency affects the water quality of the WDS can be accurately carried out with the use of PDA.

Despite the profound advantages of PDA, the conventional DDA is still widely applied by practising engineers. One of the main reasons could probably be the unavailability of public domain PDA software. An effective way to increase the popularity of PDA is to release the EPANET-PDX source code to the public. Before doing so, several additional features could be incorporated into EPANET-PDX to make it more attractive to practising engineers. The hydraulic feasibility test could be implemented into EPANET-PDX as an option at the end of each simulation to increase confidence of the PDA results obtained. Another important feature to be considered is the inclusion of the reliability and failure tolerance calculations of the network or perhaps the statistical entropy since it is more computationally efficient. This will enable users to have a clear depiction of the reliability of the network analysed. In fact, since the developed NSGA II model was directly coded into the hydraulic simulator in this research, EPANET-PDX in reality has been transformed from functioning merely as a PDA hydraulic simulator to a powerful multi-feature optimization model which is capable of all the aspects carried out in this research e.g. pump scheduling, tank siting and sizing, optimal long term rehabilitation of WDS etc. However, more work needs to be done to systematically package this tool and make it more user-friendly in the aspect of the data input and presentation of results.

The penalty-free approach of constraint handling proposed here in has worked extremely well with the NSGA II. No doubt, theoretically the same outcome will be reaped if applied on other EAs. It will be really interesting though to see physical results to support this claim. Hence, studies on the application of this penalty-free constraint handling concept to other EAs e.g. shuffled frog leaping algorithm, harmony search to evaluate the improvement of the search performance is highly desirable.

The boundary search technique used in this research has proven to effectively focus the GAs exploration on boundary solutions as demonstrated in Chapter 6. Throughout the research work, fixed exponent values were used. A sensitivity analysis to analyse the effects of varying the values of the exponent should be carried out. Intuitively, a high exponent value for the DSR will post stricter bounds to the GA and may eliminate majority of the infeasible solutions at the early stage of the evolution,

potentially resulting in overly expensive final solutions. A heuristic could be developed to gradually increase these values with generations or perhaps, varying them based on the 'generational distance'. The generational distance measures the average distance between successive non-dominated solutions of the best Pareto-optimal front and represents the progress and improvement made by the algorithm.

The same applies for the NSGA II model developed herein where 30% of the best feasible solutions are assigned with high values of crowding distance to prevent them from being eliminated at latter stages of the evolution during the crowded tournament selection. The effects of varying the proportion of retained solutions on the optimality of final solutions have not been explicitly explored in this research. Similarly to the previous suggestion, a sensitivity analysis should be carried out to study the outcome of this variation and from analytical observation, develop a heuristic to manipulate this variable for the enhancement of the search.

The NSGA II used in this research utilized the most basic operators i.e. single point crossover and single bit wise mutation. Implementing other more advanced genetic operators such as simulated binary crossover, uniform crossover, non-uniform mutation, Gaussian mutation etc could further improve the exploration and exploitation properties of the PFMOEA. Also, the representation of solutions using real coding could lessen the computational burden since the decoding process is eliminated.

REFERENCES

Ackley, J. R. L., Tanyimboh, T. T., Tahar, B. and Templeman, A. B. (2001). "Head-driven analysis of water distribution systems." *Water Software Systems: Theory and Applications, Vol. 1*, Ulanicki, B., Coulbeck, B. and Rance, J. (eds.), Research Studies Press Ltd, England, ISBN 0863802745, Chapter 3:183-192.

Afshar, M. H., Marino, M. A. (2007). "A parameter-free self-adapting boundary genetic search for pipe network optimization." *Comput. Optim. Appl.*, 37, 83-102.

Alperovits, E., and Shamir, U. (1977). "Design of optimal water distribution systems." *Water Resource Research*, 13(6), 885-900.

Ang, W. H., Jowitt, P. W. (2006). "Solution for water distribution systems under pressure-deficient conditions." *Journal of Water Resources Planning and Management*, 132(3), 175-182.

Arulraj, G. P., and Suresh, H. R. (1995). "Concept of significance index for maintenance and design of pipe networks." *Journal of Hydraulic Engineering*, 121(11), 833-837.

Bäck, T., Hoffmeister, F., and Schwefel, H. P. (1991). "A survey of evolution strategies." R. K. Belew and L. B. Booker, eds., Proc. 4th Int. Conf. On Genetic Algorithms, Morgan Kaufmann, San Mateo, Calif., 2-9.

Bhave, P. R. (1991). "Analysis of Flow in Water Distribution Networks." Lancaster, PA: Technomic Publishing.

Chandapillai, J. (1991). "Realistic simulation of water distribution systems." *J. Transportation Engineering*, ASCE, 117 (2), 258-263.

Cullinane, M. J., Lansey, K. E. and Mays, L. W. (1992). "Optimization-availability-based design of water distribution networks." *J. Hydraul. Eng*., 118(3), 420-441

Cunha, M. C., and Ribeiro, L. (2004). "Tabu search algorithms for water network optimization." *European Journal of Operational Research*, 157, 746-758.

Cunha, M. C., Sousa, J. (1999). "Water distribution network design optimization: simulated annealing approach." *J. Water Resour. Plann. Manage. Div*., *Am. Soc. Civ. Eng.*, 125(4), 215-221

Cross, H. (1936). "Analysis of flow in networks of conduits or conductors." Bulletin No. 386, Engineering Experiment Station, University of Illinois, Urbana, I11., November.

Dandy, G. C., and Engelhardt, M. O. (2001). "Optimal scheduling of water pipe replacement using genetic algorithms." *Journal of Water Resources Planning and Management*, 127(4), 214-223.

Dandy, G. C., and Engelhardt, M. O. (2006). "Multi-objective trade-offs between cost and reliability in the replacement of water mains." *Journal of Water Resources Planning and Management*, 132(2), 79-88.

Dandy, G.C., McBean, E.A. and Hutchinson, B.G. (1985). "Pricing and expansion of a water supply system." *Journal of Water Resources Planning and Management*, 111(1), 24-41.

Dandy, G. C., Simpson A. R., Murphy L. J. (1996). "An improved genetic algorithm for pipe network optimization." *Water Resources Research*, 32(2), 449-458.

Deb, K. (2000). "An efficient constraint handling method for genetic algorithms." *Computer Methods in Applied Mechanics and Engineering*, 186(2), 311-338.

Deb, K. (2003). "Unveiling innovative design principles by means of multiple conflicting objectives." *Engineering Optimization*, 35(5), 445-470.

Deb, K., Pratap, A., Agarwal, S., and Meyarivan, T. (2002). "A fast and elitist multiobjective genetic algorithm: NSGA-II." *Evolutionary Computation*, IEEE Trans., 6(2), 182-197.

Eusuff, M. M., and Lansey, K. E. (2003). "Optimization of water distribution network design using the shuffled frog leaping algorithm." *Journal of Water Resources Planning and Management*, 129(3), 210-225.

Farmani, R., Walters, G. A. and Savic, D. A. (2005a). "Trade-off between total cost and reliability for Anytown water distribution network." *Journal of Water Resource Planning and Management*, 131(3), 161-171.

Farmani, R., Walters, G. A. and Savic, D. A. (2006). "Evolutionary multi-objective optimization of the design and operation of water distribution network: total cost vs. reliability vs. water quality." *Journal of hydroinformatics*, 8, 165-179.

Farmani, R., and Wright, J. A. (2003). "Self-adaptive fitness formulation for constrained optimization." *IEEE Trans. Evol. Comput*, 7(5), 445-455.

Farmani, R., Wright, J. A., Savic, D. A. and Walters, G. A. (2005b). "Self-adaptive fitness formulation for evolutionary constrained optimization of water systems." *Journal of Computing in Civil Engineering*, 19(2), 212-216.

Fujiwara, O., and Ganesharajah, T. (1993). "Reliability assessment of water supply systems with storage and distribution networks." *Water Resources Research*, 29(8), 2917-2924.

Fujiwara, O., and Khang, D. B. (1990). “A two-phase decomposition method for optimal design of looped water distribution networks.” *Water Resource Research*, 26(4), 539-549.

Geem, Z. W. (2006). "Optimal cost design of water distribution networks using harmony search**.**" *Engineering Optimization*, 38(3), 259-280.

Germanopoulos, G. (1985). “A technical note on the inclusion of pressure dependent demand and leakage terms in water supply network models.” *Civil Engineering Systems*, 2, 171-179

Gessler, J. (1985). “Pipe network optimization by enumeration.” *Proc., Spec. Conf., Comp. Applications for Water Resour.*, ASCE, New York, N.Y., 572-581.

Giustolisi, O., and Berardi, L. (2009). “Prioritizing pipe replacement: from multiobjective genetic algorithms to operational decision support.” *Journal of Water Resource Planning and Management*, 135(6), 484-492.

Giustolisi, O., Kapelan, Z., and Savic, D. A. (2008a). “Extended period simulation analysis considering valve shutdowns.” *Journal of Water Resource Planning and Management*, 134(6), 527-537.

Giustolisi, O., Savic, D. A., and Kapelan, Z. (2008b). “Pressure-driven demand and leakage simulation for water distribution networks.” *Journal of Water Resource Planning and Management*, 134(5), 626-635.

Goldberg, D. E., and Deb, K. (1991). “A comparison of selection schemes used in genetic algorithm.” *Proc., Foundations of Genetic Algorithms (FOGA)*, 69-93.

Goldberg, D. E., and Kuo, C. H. (1987). “Genetic algorithms in pipeline optimization.” *Journal of Computing in Civil Engineering*, ASCE, pp. 128-141.

Gupta, R., and Bhave, P. R. (1996). “Comparison of methods for predicting deficient network performance.” *Journal of Water Resource Planning and Management*, 122(3), 214-217.

Halhal, D., Walters, G. A., Ouazar, D., and Savic, D. A. (1997). “Water network rehabilitation with structured messy genetic algorithm.” *J. Water Res. Plan. and Management*, ASCE, 123(3), 137-147.

Harik, G. R., and Goldberg, D. E. (2000). “Linkage learning through probabilistic expression.” *Comput. Meth. Appl. Mech. Engng.*, 186(2-4), 295-310.

Holland, J. H. (1975). “Adaptation in natural and artificial systems.” *MIT Press*, Cambridge, Massachusetts, U.S.A.

Hopper, E., and Turton, B. C. H., (2001). “An empirical investigation of meta-heuristic and heuristic algorithms for a 2D packing problem.” *Eur. J. Oper. Res.*, 128, 34-57.

Jayaram, N., and Srinivasan, K. (2008). "Performance-based optimal design and rehabilitation of water distribution networks using life cycle costing." *Water Resour. Res.*, 44, W01417, doi:10.1029/2006WR005316.

Jeppson, R. W., Davis, A. (1976). "Pressure reducing valves in pipe network analyses." *Journal of Hydraulics Division*, 102(HY7), 987-1001.

Kadu, M. S., Gupta, R., and Bhave, P. R. (2008). "Optimal design of water networks using genetic algorithm with reduction in search space." *J. Water Resour. Plann. Manage.*, 134(2), 147-160.

Kalungi, P. (2003). A holistic approach to the optimal long-term upgrading of water distribution networks. PhD thesis. University of Liverpool.

Kalungi, P., and Tanyimboh, T. T. (2003). "Redundancy model for water distribution systems." *Reliability Engineering and System Safety*, 82(3), 275-286.

Keedwell, E., and Khu, S. T. (2006). "A novel evolutionary metaheuristic for the multi-objective optimization of real-world water distribution networks." *Engineering Optimization*, 38(3), 319-333.

Khu, S. T., and Keedwell, E. (2005). "Introducing choices (flexibility) in upgrading of water distribution network: the new york city tunnel network example." *Engineering Optimization*, 37(3), 291-305

Kleiner, Y., Adams, B. J., and Roger, S. J. (2001). "Water distribution network renewal planning." *J. Computing in Civil Engineering*, ASCE, 15(1), 15-26.

Lansey, K. E., Basnet, C., Mays, L. W., and Woodburn. J. (1992). "Optimal maintenance scheduling for water distribution systems." *Civil Engineering Systems*, 9, 211-226.

Lansey, K. E., and Mays, L. W. (1989). "Optimization model for design of water distribution systems." *Reliability analysis of water distribution system*, L. R. Mays, ed., ASCE, Reston, Va.

Loganathan, G. V., Park, S., and Sherali, H. D. (2002). "Threshold break rate for pipeline replacement in water distribution systems." *J. Water Resources Planning and Management*, 128(4), 271-279.

Loubser, B. F., and Gessler, J. (1990). "Computer-aided optimization of water distribution networks." *The Civ. Engr.* In South Africa, (Oct.), 413-422.

Maier, H. R., Simpson, A. R., Zecchin, A. C., Foong, W. K., Phang, K. Y., Seah, K. Y., and Tan, C. L. (2003). "Ant colony optimization for design of water distribution systems." *J. Water Resour. Plann. Manage.*, ASCE, 129(3), 200-209.

Martin, D. W., and Peters, G. (1963). "The application of Newton's method to network analysis by digital computer." *J. Institute of Water Engineers*, 17, 115-129.

Montesinos, P., Garcia-Guzman, A., Ayuso, J. L. (1999). "Water distribution network optimization using a modified genetic algorithm." *Water Resour. Res.*, 35(11), 3467-3473.

Munavalli, G. R., and Kumar, M. S. (2003). "Optimal scheduling of multiple chlorine sources in water distribution systems." *Journal of Water Resources Planning and Management*, ASCE, 129(6), 493-504.

Murphy, L. J., Dandy, G. C., and Simpson, A. R. (1994). "Optimum design and operation of pumped water distribution systems." *Proc., Conf. on Hydraulics in Civil Engineering*, Institution of Engineers, Brisbane, Australia, 149-155.

Murphy, L. J., Simpson, A. R., and Dandy, G. C. (1993). "Pipe network optimization using an improved genetic algorithm." Res. Rep. No. R109, Dept. Of Ci. and Envr. Eng., Univ. Of Adelaide, Australia.

OFWAT (2004). Levels of Service for the Water Industry in England and Wales. 2002-2003 Report. Ofwat Centre, 7 Hill Street, Birmingham B5 4UA, UK.

Prasad, T. D. (2010). "Design of pumped water distribution networks with storage." *J. Water Resour. Plann. Manage.*, 136(1), 129-132.

Prasad, T. D., and Park N. S. (2004). "Multiobjective genetic algorithms for design of water distribution networks." *J. Hydr. Engrg.*, ASCE 130(1),73-82.

Prasad, T. D., and Tanyimboh, T. T. (2008). "Entropy based design of "Anytown" water distribution network." In *Proceedings of the 10th Annual Water Distribution Systems Analysis Conference* , *J. E. Van Zyl, A. A. Ilemobade, and H. E. Jacobs* (eds.), August 17-20, Kruger National Park, South Africa.

Preis, A., and Ostfeld, A. (2008). "Multiobjective contaminant sensor network design for water distribution systems." *J. Water Resour. Plann. Manage.*, 134(4), 366-377.

Press, W. H., Teukolsky, S. A., Vetterling, W. T., Flannery, B. P. (1992). "Numerical Recipes in FORTRAN: The Art of Scientific Computing." *Cambridge University Press*, New York, USA.

Reddy, L. S., and Elango, K. (1989). "Analysis of water distribution networks with head dependent outlets." *Civil Engineering Systems*, 6(3), 102-110.

Rossman, L. A. (2002). EPANET 2 User's Manual, Water Supply and Water Resources Division, National Risk Management Research Laboratory, Cincinnati, OH45268.

Rossman, L. A. (2007). "Discussion of 'Solution for water distribution systems under pressure-deficient conditions'." *Journal of Water Resources Planning and Management*, 133(6), 566-567.

Salgado, R., Rojo, J., and Zepeda, S. (1993). “Extended gradient method for fully non-linear head and flow analysis in pipe networks.” *Integrated Computer Applications in Water Supply*-- Methods and Procedures for Systems Simulation and Control, 1, 49-60.

Savic, D. A., and Walters, G. A. (1997). “Genetic algorithms for least-cost design of water distribution networks.” *J. Water Resour. Plann. Manage.*, 123(2), 67-77.

Schaake, J. C., and Lai, D. (1969). “Linear programming and dynamic programming application to water distribution network design.” Report 116, Hydrodynamics Laboratory, Department of Civil Engineering, MIT, Cambridge, MA.

Setiadi, Y., Tanyimboh, T. T., and Templeman, A. B. (2005). “Modelling errors, entropy and the reliability of water distribution systems.” *Advances in Engineering Software*, 36(11-12), 780-788.

Seyoum, A. G., Tanyimboh, T. T., and Siew, C. (2011). “Comparison of demand driven and pressure dependent hydraulic approaches for modelling water quality in distribution networks.” *Computing and Control for the Water Industry 2011: Urban Water Management* - Challenges and Opportunities, Exeter, UK, 5-7 September 2011.

Shamir, U., and Howard, C. D. D. (1979). “An analytic approach to scheduling pipe replacement.” *J. AWWA*, 71(5), 248-258.

Shan, N. (2004). “Head dependent modelling of water distribution network.” MSc Dissertation, University of Liverpool, UK.

Sharp, W. W., and Walski, T. M. (1988). “Predicting internal roughness in water mains.” *Journal of the AWWA*, 80(9), 34-40.

Siew, C., and Tanyimboh, T. T. (2010). “Pressure-dependent EPANET extension: pressure-dependent demands.” *Proceedings of the 12th Annual Water Distribution Systems Analysis Conference*, WDSA 2010, September 12-15, Tucson, Arizona.

Siew, C., and Tanyimboh, T. T. (2011). “The computational efficiency of EPANET-PDX.” *Proceedings of the 13th Annual Water Distribution Systems Analysis Conference*, WDSA 2011, May 22-26, Palm Springs, California.

Su, Y. C., Mays, L. W., Duan, N., and Lansey, K. E. (1987). “Reliability-based optimization model for water distribution systems.” *J. Hydr. Engrg.*, 114(12), 1539-1556.

Tabesh, M. (1998). “Implications of Pressure Dependency of Outflows on Data Management, Mathematical Modelling and Reliability Assessment of Water Distribution Systems.” PhD thesis, University of Liverpool, England.

Tabesh, M., Tanyimboh, T. T., and Burrows, R. (2002). “Head driven simulation of water supply networks.” *Int. J. Eng., Transactions A: Basics*, 15(1), 11–22.

Tanyimboh, T. T. (2008). "Robust algorithm for head-dependent analysis of water distribution systems." *Proceedings of the 10th Annual Water Distribution Systems Analysis Conference*, WDSA 2008, August 17-20, Kruger National Park, South Africa.

Tanyimboh, T.T., Burd, R., Burrows, R., and Tabesh, M. (1999). "Modelling and realibility analysis of water distribution systems." *Water Science and Technology*, IWA, 39(4), 249-255.

Tanyimboh, T. T., and Kalungi, P. (2008). "Optimal long term design, rehabilitation and upgrading of water distribution networks." *Engineering Optimization*, 40(7), 637-654.

Tanyimboh, T. T., and Kalungi, P. (2009). "Multi-criteria assessment of optimal design, rehabilitation and upgrading schemes for water distribution networks." *Civil Engineering and Environmental Systems*, 26(2), 117-140.

Tanyimboh, T. T., Saleh, S., and Tietavainen, M. T. (2010). "Reliability assessment of water distribution systems with statistical entropy and other surrogate measures", *IWA World Water Congress*, 19-24 September, Montreal, Canada.

Tanyimboh, T. T., and Setiadi, Y., (2008a). "Joint layout, pipe size and hydraulic reliability optimization of water distribution systems." *Engineering Optimization*, 40(8), 729-747.

Tanyimboh, T. T., and Setiadi, Y. (2008b). "Sensitivity analysis of entropy-constrained designs of water distribution systems." *Engineering Optimization*, 40 (5), 439-457.

Tanyimboh, T. T., and Sheahan, C. (2002). "A maximum entropy based approach to the layout optimization of water distribution systems." *Civ. Eng. and Env. Syst.*, 19(3), 223-253.

Tanyimboh, T. T., and Tabesh, M. (1997). "Discussion of Comparison of methods for predicting deficient-network performance." *J. Water Resources Planning and Management*, 124 (6), 369-370.

Tanyimboh, T. T., Tabesh, M., and Burrows, R. (2001). "An appraisal of source head methods for calculating the reliability of water distribution networks." *J. Water Resources Planning and Management*, 127 (4), 206-213.

Tanyimboh, T. T., Tahar, B., and Templeman, A. B. (2003). "Pressure-driven modelling of water distribution systems." *Water Science and Technology Water Supply*, 3 (1-2), 255-262, 2003.

Tanyimboh, T. T., and Templeman, A. B. (1993). "Calculating maximum entropy flows in networks." *J. Operational Research Society*, 44(4), 383-396.

Tanyimboh, T. T., and Templeman, A. B. (1995). "A new method for calculating the reliability of single-source networks." *Developments in Computational Techniques for Civil Engineering, Topping BHV (ed.)*, Civil-Comp Press.

Tanyimboh, T. T., and Templeman, A. B. (1998). "Calculating the reliability of single source networks by source head method" *Advances in Engineering Software*, 29(7-9), 449-505.

Tanyimboh, T. T., and Templeman, A. B. (2000). "A quantified assessment of the relationship between the reliability and entropy of water distribution systems." *Engineering Optimization*, 33(2), 179-199.

Tanyimboh, T. T., and Templeman, A. B. (2004). "A new nodal outflow function for water distribution networks." *Proceedings of the 4th Int. Conf. on Engineering Computational Technology, BHV Topping and CA Mota Soares (Eds.)*, Civil-Comp Press, Stirling, UK, ISBN 0-948749-98-9, Paper 64, pp. 12, CD-ROM.

Tanyimboh, T.T., and Templeman, A.B. (2010). "Seamless pressure-deficient water distribution system model." *J. Water Management,* ICE, 163(8), 389-396.

Todini, E. (2000). "Looped water distribution networks design using a resilience index based heuristic approach." *Urban Water*, 2(3), 115-122.

Todini, E., and Pilati, S. (1988). "A gradient algorithm for the analysis of pipe networks." *Computer Applications in Water Supply*, Volume 1, Coulbeck, B., and Orr, C-H (eds.), Research Studies Press, England.

Udo, A., and Ozawa, T. (2001). "Steady-state flow analysis of pipe networks considering reduction of flow in the case of low water pressures." *Water Software Systems: Theory and Applications* (Ulanicki B, Coulbeck B and Rance J (eds.)). Research Studies Press, Taunton, UK, Vol. 1, 73-182.

Vairavamoorthy, K., and Ali, M. (2000). "Optimal design of water distribution systems using genetic algorithms." *Computer-aided Civil and Infrastructure Engineering*, 15, 374-382.

Vairavamoorthy, K., Ali, M. (2005). "Pipe index vector: a method to improve genetic-algorithm-based pipe optimization." *J. Hydr. Engrg.*, 131(12):1117-1125.

Vamvakeridou-Lyroudia, L. S., Walters, G. A., and Savic, D. A. (2005). "Fuzzy multiobjective optimization of water distribution networks." *J. Water Resour. Plann. Manage.*, 131(6), 467-476.

Vasan, A., and Simonovic, S. P. (2010). "Optimization of Water Distribution Network Design Using Differential Evolution." *J. Water Resour. Plann. Manage.*, ASCE, 136(2), 279-287.

Vitkovsky, J. P., and Simpson, A. R. (1997). "Calibration and leak detection in pipe networks using inverse transient analysis and genetic algorithms." Department of

Civil and Environmental Engineering, University of Adelaide: Adelaide, Australia, pp. 97.

Wagner, J. M., Shamir, U., Marks, D. H. (1988). "Water distribution reliability: simulation methods." *Journal of Water Resources Planning and Management*, 114(3), 276-294.

Walski, T. M. (1987) "Discussion of multi-objective optimization of water distribution networks." *Civ. Eng. Syst.*, 4(1), 215-217.

Walski, T. M., Brill, E. D., Gessler, J., Goulter, I. C., Jeppson, R. M., Lansey, K., Lee, H. L., Liebman, J. C., Mays, L., Morgan, D. R., and Ormsbee, L. (1987). "Battle of the network models: epilogue." *Journal of Water Resource Planning and Management*, 113(2), 191-203.

Walski, T. M., and Pelliccia, A. (1982). "Economic analysis of water main breaks." *Journal American Water Works Association*, 74(3), 140-147.

Walters, G. A., Halhal, D., Savic, D., and Ouazar, D. (1999). "Improved design of "Anytown" distribution network using structured messy genetic algorithms." *Urban Water*, 1(1), 23-38.

Wood, D., and Charles, C. (1972). "Hydraulic network analysis using linear theory." *Journal of Hydraulics Division*, vol. 98, no. HY7, 1157-1170.

Wu, Z. Y., Boulos, P. F., Orr, C. H., and Ro, J. J. (2001). "Using genetic algorithm to rehabilitate distribution systems." *Journal American Water Works Association*, 93(11), 74-85.

Wu, Z.Y., and Simpson, A.R. (2001). "Competent genetic-evolutionary optimisation of water distribution systems." *Journal of Computing in Civil Engineering*, 15(2), 89-101.

Wu, Z. Y., and Simpson, A. R. (2002). "A self-adaptive boundary search genetic algorithm and its application to water distribution systems." *J. Hydraul. Res.*, 40, 191-203.

Wu, Z. Y., and Walski, T. (2005). "Self-adaptive penalty approach compared with other constraint-handling techniques for pipeline optimization." *J. Water Resour. Plann. Manage.*, 131(3), 181-192.

Wu, Y. W., Wang, R. H., Walski, T. M., Yang, S. Y., Bowdler, D., and Baggett, C. C. (2009). "Extended global-gradient algorithm for pressure-dependent water distribution analysis." *Journal of Water Resource Planning and Management*, 135(1), 13-22.

Yates, D. F., Templeman, A. B., and Boffey, T. B. (1984). "The computational complexity of the problem of determining least capital cost designs for water supply networks." *Engineering Optimization*, 2, 142-155.

APPENDIX A

INPUT DATA FOR CASE STUDIES IN CHAPTER FOUR

A-1 Input Data for Network in Example 3

Table A-1.1 Node data for network in Example 3

Node No.	Elevation (m)	Demand (l/s)
1	63.4	0
2	56.4	2.15
3	18.9	0.6
4	21	3.1
5	60	0
6	14	0.4
7	9.6	0.19
8	7	1.72
9	25	0.86
10	7.2	0.77
11	25	0
12	23.4	1.69
13	22	1.72
14	64	0
15	22.9	0
16	64	0
17	66.8	0
18	65.6	0
19	73	0.13
20	89	0.25
21	103.9	0
22	85.5	4.55
23	48	0.01
24	28	0
25	28	0
26	28	0
27	28	0.23
28	28	0
29	28	0
30	23.9	0
31	24.5	0
32	24.5	0
33	24.5	0
34	28	1.07
35	32.6	1.4
36	28	0.75
37	28	1.2
38	28	0
39	27	0
40	24.9	0.93
41	37.7	1.63
42	20	1.1

43	20	0
44	26	3.73
45	24.2	2.55
46	17	0
47	18	1.12
48	44.6	0

Table A-1.2 Reservoir data for network in Example 3

Reservoir no.	Elevation (m)
49	50
50	78.9

Table A-1.3 Pipe data for network in Example 3

Pipe No.	Node1	Node2	Length (m)	Diameter (mm)	Roughness
1	1	2	1428	217	110
2	1	5	1428	166	120
3	1	50	162	166	120
4	2	5	5	217	100
5	2	14	185	154	120
6	2	26	1615	217	130
7	3	4	305	101	130
8	3	47	138	102	120
9	4	47	275	154	120
10	5	23	1130	166	100
11	6	7	290	178	110
12	6	43	180	178	130
13	7	8	385	202	115
14	7	8	385	202	110
15	7	42	470	229	130
16	8	9	810	102	120
17	8	11	845	145	110
18	9	10	520	102	130
19	10	11	155	145	130
20	10	12	545	154	130
21	12	13	204	102	115
22	12	48	340	77	120
23	14	16	10	154	100
24	14	18	10	152	110
25	15	39	2714	310	115
26	15	49	10	310	110
27	16	17	10	152	100
28	16	19	175	154	120
29	19	20	1410	154	110
30	20	21	1130	77	115
31	20	22	960	154	130
32	23	24	395	217	100
33	24	25	90	166	115
34	25	26	5	166	130

35	25	29	47	166	110
36	26	28	47	217	130
37	27	28	10	217	115
38	27	29	5	166	115
39	27	31	10	229	100
40	27	34	145	217	130
41	28	30	10	299	110
42	29	38	145	166	130
43	30	32	5	152	110
44	31	33	5	152	120
45	34	38	5	178	110
46	34	39	233	229	130
47	35	36	265	152	115
48	35	37	460	94	100
49	35	38	224	152	100
50	36	37	340	102	120
51	38	43	520	166	100
52	39	40	155	217	130
53	40	41	340	154	120
54	40	42	140	217	110
55	40	44	255	152	130
56	42	43	5	152	100
57	42	44	235	102	110
58	44	45	87	154	120
59	45	46	95	154	100
60	46	47	440	152	115
61	33	32	1	500	130

Table A-1.4 Pump data for network in Example 3

Pump No.	Node1	Node2	Flow (l/s)	Head (m)
62	18	17	500	65
63	31	30	500	25

A-2 Input Data for Network in Example 4

Table A-2.1 Node data for network in Example 4

Node No.	Elevation (m)	Demand (l/s)
1	100	16.203
2	100	0
3	100	0
4	100	0
5	100	0
6	100	0
7	100	0
8	100	0
9	100	254.629
10	100	23.148
11	100	0
12	100	0
13	100	0
14	100	17.361
15	100	0
16	100	0
17	100	162.037
18	100	0
19	100	0
20	100	0
21	100	74.074
22	100	0
23	100	0
24	100	0
25	100	104.166
26	100	0
27	100	0
28	100	0
29	100	0
30	100	12.731
31	100	196.759
32	100	92.592
33	100	0
34	100	0
35	100	0
36	100	0
37	100	138.888
38	100	0
39	100	0
40	100	0
41	100	0
42	100	0
43	100	0
44	100	0
45	100	1620.37
46	100	1620.37

Table A-2.2 Reservoir data for network in Example 4

Reservoir No.	Head (m)
47	138.9
48	91.4

Table A-2.3 Pipe data for network in Example 4

Pipe No.	Node1	Node2	Length (m)	Diameter (mm)	Roughness
1	2	47	240	950	120
2	33	34	60	900	110
3	31	48	1830	1450	130
4	43	48	3550	1150	135
5	41	9	1220	1450	130
6	9	31	640	1450	130
7	42	43	60	900	110
8	41	43	60	900	110
9	43	44	50	1000	110
10	42	48	3660	900	115
11	41	42	60	900	110
12	42	44	60	1000	110
13	40	42	800	900	115
14	37	41	3140	1450	130
15	38	43	3140	1150	130
16	39	44	3140	1650	135
17	36	38	60	900	110
18	38	39	60	1000	110
19	36	40	2300	800	115
20	37	38	60	900	110
21	35	38	4050	1150	130
22	36	37	60	900	110
23	33	36	4050	800	115
24	34	37	4050	1150	130
25	33	35	60	900	110
26	34	35	60	900	110
27	24	32	2150	800	110
28	32	33	180	800	110
29	23	34	2980	1450	135
30	25	35	2980	1450	135
31	30	46	12000	1650	135
32	22	24	670	950	110
33	28	29	60	1000	110
34	29	30	13400	1650	135
35	11	13	80	900	110
36	11	15	4290	950	120
37	12	14	4290	900	115
38	12	13	60	50	110
39	10	11	2590	950	120
40	11	12	60	50	110
41	6	12	2960	900	115
42	7	13	2960	1150	135

43	8	45	2280	1150	130
44	8	10	370	950	120
45	7	8	90	1000	130
46	6	7	60	50	110
47	5	6	1610	900	115
48	6	8	60	50	110
49	3	5	1350	950	115
50	4	8	2960	50	120
51	1	3	6530	950	120
52	3	4	60	900	110
53	2	1	230	950	120
54	2	4	7200	950	120
55	26	27	60	1000	110
56	27	29	3200	1150	135
57	25	26	4300	1450	135
58	26	28	3200	1150	135
59	22	23	80	800	115
60	23	25	90	750	130
61	18	23	2050	950	120
62	21	22	2380	800	115
63	20	23	3050	1150	135
64	19	21	670	50	115
65	18	19	60	50	110
66	19	20	60	50	110
67	17	19	1830	800	115
68	18	20	60	900	110
69	14	17	1950	800	115
70	15	18	3780	950	120
71	14	16	60	50	110
72	15	16	60	900	120
73	13	16	4290	1150	135
74	14	15	60	50	110

A-3 Input Data for Network in Example 5

Table A-3.1 Node data for network in Example 5

Node No.	Elevation (m)	Demand (l/s)
1	60	0
2	85	0
3	85	0
4	85	0
5	85	0
6	85	0
7	85	0
8	85	0
9	85	0
10	85	0
11	85	0

12	85	0
13	85	0
14	85	0
15	85	0
16	85	0
17	85	0
18	85	0
19	68	0
20	89	15.87
21	84	54.5
22	85	0
23	85	0.05
24	85	0
25	90	0.22
26	90	0.02
27	78.4	0
28	84	0
29	81.4	0
30	85	0
31	84	0
32	82.2	2.93
33	83	0
34	84	0
35	84	0
36	74	0
37	74	0
38	72.4	0.8
39	84.5	1.47
40	85	0
41	87	0
42	87	0
43	87	2.57
44	86	0
45	82.8	2.77
46	85	0
47	86	2.5
48	85.4	0
49	87	0
50	87	0
51	88.2	0
52	88	0
53	88	0.72
54	89	0
55	88	1.77
56	84	0
57	84	0
58	84	3.18
59	86	0
60	85	2.81
61	85.1	0
62	80	0
63	77	1.49
64	78	0
65	73	0.43

66	74.4	0
67	75.1	0
68	76	0
69	92	7.2
70	106	0.01
71	89	1.2
72	89	0
73	84	2.61
74	89.6	0
75	87	1.02
76	87	0
77	85	0
78	87	1.14
79	87	0
80	88	1.27
81	89	0
82	90	0
83	90	0.6
84	92	1.22
85	89	0
86	89.1	4.62
87	93	2.33
88	88	0
89	88	0
90	88	0
91	80	1.37
92	80	2.93
93	90.1	0
94	89.1	1.19
95	83.5	0.23
96	81.7	0
97	71	0
98	74.7	0.23
99	72.9	0.33
100	90	18.6
101	92	0.81
102	93.4	1.98
103	92.6	0
104	96	0
105	96	0
106	95	0
107	96.9	0
108	97	3.89
109	105.6	0
110	98	0
111	98	1.96
112	93	0
113	93	0
114	94	4.33
115	94	0
116	96	0
117	97	0
118	98	0
119	98	0

120	98	1.84
121	98.9	0
122	90	2.91
123	90	2.71
124	91.5	0.93
125	98	1.29
126	92	0
127	89	0
128	89	0
129	89	1.34
130	92	1.51
131	92.8	0
132	91	0.98
133	91	0
134	90	0.14
135	91	0
136	91	0
137	92	0
138	92	1.47
139	92.4	0
140	91	0
141	91.7	0
142	92.3	15.45
143	92	0
144	93	0
145	92.7	6.45
146	92.1	7.31
147	93	0
148	85.4	0.47
149	73	4.06
150	84	0
151	102	0
152	102	0
153	102	0
154	102	0
155	92	0.77
156	92	0.67
157	100.9	0
158	90	2.72
159	92	12.57

Table A-3.2 Reservoir data for network in Example 5

Reservoir No.	Elevation (m)
160	60.5
161	123
162	123
163	86
164	86

Table A-3.3 Pipe data for network in Example 5

Pipe No.	Node1	Node2	Length (m)	Diameter (mm)	Roughness
1	1	19	1510	200	100
2	2	163	40	450	115
3	3	6	20	450	130
4	4	164	45	600	100
5	5	6	30	600	110
6	6	7	10	600	100
7	7	8	10	600	115
8	7	150	20	600	110
9	8	18	20	300	100
10	8	21	35	600	120
11	9	17	10	75	110
12	10	18	5	300	115
13	11	16	5	300	130
14	12	18	5	300	100
15	13	16	5	300	115
16	14	18	5	300	130
17	15	16	5	300	110
18	16	17	30	300	130
19	17	22	2590	300	120
20	19	24	3220	150	130
21	19	24	2900	200	115
22	22	23	100	75	110
23	22	26	2420	300	115
24	24	25	150	75	110
25	24	27	700	300	120
26	26	27	350	150	130
27	26	27	350	200	110
28	26	29	550	300	130
29	26	100	10	150	120
30	27	28	100	100	130
31	27	29	400	225	130
32	28	39	580	100	130
33	29	30	80	300	130
34	30	41	470	300	110
35	30	42	470	225	120
36	31	32	220	100	130
37	31	40	470	75	110
38	32	33	350	100	130
39	32	45	380	100	120
40	33	35	140	100	120
41	34	35	65	75	130
42	34	47	320	75	110
43	35	55	870	150	130
44	36	37	100	175	115
45	36	65	1810	175	110
46	37	38	430	175	130
47	38	67	670	100	130
48	39	40	90	75	115
49	39	50	460	75	130
50	40	43	330	100	120

51	41	42	10	225	130
52	41	51	510	225	110
53	42	51	515	300	130
54	43	44	140	150	130
55	43	49	220	100	110
56	44	45	160	100	130
57	45	46	60	50	115
58	46	47	170	100	130
59	47	48	260	150	120
60	48	52	360	150	130
61	48	56	610	150	115
62	49	50	80	75	110
63	50	54	380	75	110
64	51	52	150	150	115
65	51	75	390	225	130
66	51	76	440	300	120
67	52	53	50	75	110
68	54	55	360	75	100
69	54	71	210	75	130
70	55	56	620	150	130
71	55	75	610	75	130
72	56	57	120	150	130
73	56	61	240	75	120
74	57	58	750	150	130
75	57	59	390	125	115
76	58	60	150	150	110
77	60	61	330	150	115
78	60	90	440	150	110
79	62	63	650	150	120
80	62	64	110	100	130
81	62	95	940	150	110
82	62	20	2	150	130
83	65	66	150	100	120
84	65	97	540	175	120
85	65	149	10	150	130
86	66	99	1250	75	110
87	67	68	80	100	130
88	68	99	1010	100	110
89	69	130	10	150	120
90	70	78	470	150	115
91	70	102	2015	150	130
92	71	72	70	75	120
93	72	73	90	150	120
94	72	74	110	150	130
95	74	76	190	450	115
96	74	77	130	125	110
97	74	83	300	75	120
98	74	113	920	450	120
99	75	85	315	225	100
100	77	78	190	125	120
101	77	80	340	100	115
102	78	79	135	150	130
103	80	81	230	100	115
104	81	82	90	100	100

105	81	84	285	225	130
106	81	113	200	225	130
107	82	112	135	75	120
108	82	130	335	75	100
109	83	84	210	75	110
110	84	85	685	150	115
111	84	87	240	150	120
112	85	90	160	225	100
113	86	89	430	100	130
114	86	90	410	150	100
115	86	92	390	150	110
116	87	88	185	100	130
117	87	125	290	100	120
118	87	126	725	150	115
119	87	130	210	100	100
120	88	89	135	100	120
121	88	123	230	100	120
122	89	122	190	100	110
123	90	91	320	225	110
124	91	92	310	150	130
125	91	93	580	225	115
126	93	94	100	100	110
127	93	134	840	225	115
128	95	96	690	175	115
129	95	147	1230	200	130
130	96	148	970	175	120
131	97	98	110	100	120
132	97	148	2440	175	130
133	102	103	30	150	115
134	102	112	430	150	110
135	103	105	160	100	120
136	104	115	220	225	120
137	105	106	140	100	100
138	105	107	150	100	120
139	106	114	140	100	130
140	107	108	50	100	130
141	107	118	460	100	120
142	108	116	70	100	120
143	108	117	90	100	100
144	109	110	55	450	110
145	109	153	290	450	130
146	110	111	245	100	115
147	110	121	150	450	110
148	111	120	310	450	130
149	112	114	165	75	115
150	113	114	165	225	120
151	113	120	740	450	100
152	114	115	65	225	110
153	114	119	410	100	115
154	115	116	160	100	115
155	116	117	70	100	100
156	117	118	165	100	120
157	118	119	50	100	100
158	119	120	145	100	115

159	120	121	30	450	120
160	121	127	980	300	130
161	122	123	100	100	130
162	122	124	340	100	100
163	123	124	330	100	115
164	124	126	235	100	120
165	125	155	1170	75	110
166	126	101	10	150	110
167	127	128	60	150	115
168	127	131	280	300	130
169	128	129	60	150	120
170	128	156	145	150	110
171	130	159	10	150	130
172	131	133	470	150	115
173	131	137	255	100	130
174	131	139	870	300	100
175	131	155	300	150	100
176	132	133	40	75	115
177	133	134	380	150	120
178	134	135	310	225	110
179	135	136	10	225	130
180	136	140	215	225	110
181	137	138	95	100	115
182	137	158	385	100	130
183	138	157	300	100	120
184	139	140	30	300	110
185	139	148	3010	300	130
186	140	141	65	300	130
187	141	142	55	200	130
188	141	143	45	200	115
189	143	144	370	200	120
190	144	145	210	150	100
191	144	147	450	150	110
192	145	146	400	150	115
193	146	147	140	150	115
194	151	162	250	450	100
195	152	153	190	450	130
196	154	161	80	450	115
197	156	157	145	150	120
198	157	158	110	150	120
199	3	2	1	500	100
200	153	154	1	500	100

Table A-3.4 Pump data for network in Example 5

Pump No.	Start Node	End Node
201	10	11
202	12	13
203	14	15
204	160	1

For Pump 201, Pump 202 and Pump 203, the hydraulic characteristics can be represented by $H_p = 40.0 - 1563Q_{pu}^2$, and for Pump 204 was $H_p = 66.67 - 1667\ Q_{pu}^2$, where the units of H_p (head lift of the pump) and Q_{pu} (flow delivered by the pump) are m and m^3/s respectively.

Table A-3.5 Valve data for network in Example 5

Valve No.	Node1	Node2	Diameter (mm)	Type	Maximum Flow Setting (l/s)
205	151	152	500	Flow Control Valve	30
206	4	5	500	Flow Control Valve	45

APPENDIX B

INPUT DATA AND ADDITIONAL RESULTS FOR CASE STUDIES IN CHAPTER FIVE

B-1 Input Data for Network in Example 2

Table B-1.1 Node data for network in Example 2

Node no.	Demand (m^3/s)	Elevation (m)	Desired Head (m)
1	0.001336	10	24
2	0.001336	10	24
3	0.001336	10	24
4	0.001336	10	24
5	0.001336	11.83	24
6	0.001336	11.83	24
7	0.001336	11.83	24
8	0.001336	11.83	24
9	0.001336	11.83	24
10	0.001336	11.83	24
11	0.001336	11.83	24
12	0.001336	11.83	24
13	0.001336	14.33	24
14	0.001336	14.33	24
15	0.001336	14.33	24
16	0.001336	14.33	24
17	0.001336	14.33	24
18	0.001336	14.33	24
19	0.001336	14.33	24
20	0.001336	14.33	24
21	0.001336	14.33	24
22	0.001336	14.33	24
23	0.001336	14.33	24
24	0.001336	14.33	24
25	0.001336	16.83	24
26	0.001336	16.83	24
27	0.001336	16.83	24
28	0.001336	16.83	24
29	0.001336	16.83	24
30	0.001336	16.83	24

31	0.001336	16.83	24
32	0.001336	16.83	24
33	0.001336	18.66	24
34	0.001336	18.66	24
35	0.001336	18.66	24
36	0.001336	18.66	24

Table B-1.2 Pipe data for network in Example 2

Pipe no.	Node 1	Node 2	Diameter (m)	Length (m)	Roughness
1	1	2	0.025	3.93	110
2	2	3	0.025	3.93	110
3	3	4	0.025	3.93	110
4	1	4	0.025	3.93	110
5	5	6	0.025	3.4	110
6	6	7	0.025	3.4	110
7	7	8	0.025	3.4	110
8	8	9	0.025	3.4	110
9	9	10	0.025	3.4	110
10	10	11	0.025	3.4	110
11	11	12	0.025	3.4	110
12	12	5	0.025	3.4	110
13	13	14	0.025	2.61	110
14	14	15	0.025	2.61	110
15	15	16	0.025	2.61	110
16	16	17	0.025	2.61	110
17	17	18	0.025	2.61	110
18	18	19	0.025	2.61	110
19	19	20	0.025	2.61	110
20	20	21	0.025	2.61	110
21	21	22	0.025	2.61	110
22	22	23	0.025	2.61	110
23	23	24	0.025	2.61	110
24	24	13	0.025	2.61	110
25	25	26	0.025	3.4	110
26	26	27	0.05	3.4	110
27	27	28	0.05	3.4	110
28	28	29	0.025	3.4	110
29	29	30	0.025	3.4	110
30	30	31	0.05	3.4	110

31	31	32	0.05	3.4	110
32	32	25	0.025	3.4	110
33	33	34	0.05	3.93	110
34	34	35	0.05	3.93	110
35	35	36	0.05	3.93	110
36	36	33	0.05	3.93	110
37	1	5	0.025	2.61	110
38	5	13	0.025	2.61	110
39	13	25	0.025	2.61	110
40	25	33	0.05	2.61	110
41	33	37	0.1	2.61	110
42	37	35	0.1	2.61	110
43	35	29	0.05	2.61	110
44	29	19	0.025	2.61	110
45	19	9	0.025	2.61	110
46	9	3	0.025	2.61	110
47	2	6	0.025	3.4	110
48	6	14	0.05	3.4	110
49	14	26	0.05	3.4	110
50	26	34	0.05	3.4	110
51	34	28	0.05	3.4	110
52	28	18	0.05	3.4	110
53	18	8	0.05	3.4	110
54	8	2	0.025	3.4	110
55	7	15	0.025	3.93	110
56	15	27	0.025	3.93	110
57	17	27	0.025	3.93	110
58	17	7	0.025	3.93	110
59	4	12	0.025	3.4	110
60	12	24	0.05	3.4	110
61	24	32	0.05	3.4	110
62	32	36	0.05	3.4	110
63	36	30	0.05	3.4	110
64	30	20	0.05	3.4	110
65	20	10	0.05	3.4	110
66	10	4	0.025	3.4	110
67	11	23	0.025	3.93	110
68	23	31	0.025	3.93	110
69	31	21	0.025	3.93	110
70	21	11	0.025	3.93	110

B-2 Detail results including Network DSR and Performance of EPANET-PDX and EPANET 2 for Source Head Variation and Pipe Closure Simulations

Note: The network DSR results are obtained from EPANET-PDX simulations.

Table B-2.1 Network DSR and performance of EPANET-PDX and EPANET 2 simulators for Source Head Variation simulations for Network 1

Source Head (m)	Network DSR	Average number of iterations		Average CPU time (s)	
		EPANET-PDX	EPANET 2	EPANET-PDX	EPANET 2
37	0.000	7	7	0.046	0.062
38	0.000	7	7	0.031	0.046
39	0.000	7	6	0.031	0.047
40	0.000	6	6	0.046	0.062
41	0.000	6	6	0.031	0.046
42	0.000	6	6	0.031	0.046
43	0.001	6	5	0.046	0.046
44	0.002	5	5	0.031	0.063
45	0.003	5	5	0.031	0.046
46	0.007	5	5	0.031	0.046
47	0.015	5	4	0.046	0.047
48	0.031	4	4	0.031	0.046
49	0.060	4	4	0.031	0.047
50	0.104	4	4	0.031	0.046
51	0.158	4	4	0.031	0.046
52	0.217	4	4	0.031	0.046
53	0.279	4	4	0.031	0.062
54	0.345	4	4	0.046	0.046
55	0.411	4	4	0.046	0.046
56	0.472	4	5	0.078	0.046
57	0.522	5	5	0.063	0.046

58	0.561	5	5	0.031	0.046
59	0.602	5	4	0.062	0.046
60	0.646	4	4	0.046	0.046
61	0.686	4	4	0.078	0.046
62	0.722	4	4	0.046	0.062
63	0.755	4	3	0.078	0.046
64	0.784	3	4	0.047	0.047
65	0.812	4	4	0.063	0.062
66	0.838	4	4	0.046	0.046
67	0.862	4	4	0.047	0.046
68	0.884	4	4	0.078	0.046
69	0.906	4	4	0.062	0.046
70	0.926	4	4	0.047	0.046
71	0.945	4	5	0.046	0.047
72	0.962	5	5	0.078	0.031
73	0.978	5	6	0.046	0.047
74	0.990	6	5	0.062	0.046
75	0.998	5	4	0.062	0.047
76	1.000	4	4	0.047	0.062
77	1.000	4	4	0.062	0.046
78	1.000	4	4	0.062	0.062
79	1.000	4	4	0.062	0.046
80	1.000	4	4	0.031	0.046
81	1.000	4	4	0.047	0.062
82	1.000	4	4	0.047	0.046
83	1.000	4	4	0.047	0.046
84	1.000	4	4	0.046	0.046
Average		5	5	0.048	0.049
Median		4	4	0.046	0.046

Table B-2.2 Performance of EPANET-PDX and EPANET 2 simulators for Pipe Closure simulations for Network 1

Simulation no.	Pipes Closed	Network DSR	Average number of iterations		Average CPU time (s)	
			EPANET-PDX	EPANET 2	EPANET-PDX	EPANET 2
1	2	0.841932	6	5	0.047	0.047
2	3	0.790333	4	5	0.047	0.031
3	4	0.925533	6	3	0.047	0.046
4	5	0.999999	3	3	0.062	0.046
5	6	0.870644	7	6	0.062	0.031
6	7	0.998617	4	5	0.062	0.046
7	8	0.86338	8	2	0.046	0.046
	Average		5.43	4.14	0.053	0.042
	Median		6	5	0.047	0.046

Table B-2.3 Network DSR and performance of EPANET-PDX and EPANET 2 simulators for Source Head Variation simulations for Network 2

Source Head (m)	Network DSR	Average number of iterations		Average CPU time (s)	
		EPANET-PDX	EPANET 2	EPANET-PDX	EPANET 2
5	0.000	5	5	0.063	0.063
6	0.000	5	5	0.062	0.063
7	0.000	6	6	0.062	0.063
8	0.000	5	5	0.062	0.062
9	0.001	5	5	0.063	0.078
10	0.002	5	5	0.062	0.062
11	0.004	5	5	0.062	0.062
12	0.008	4	4	0.063	0.062

13	0.019	4	4	0.062	0.063
14	0.040	4	5	0.062	0.062
15	0.079	4	5	0.062	0.078
16	0.137	4	4	0.063	0.078
17	0.212	4	4	0.062	0.062
18	0.298	4	4	0.062	0.078
19	0.393	4	4	0.062	0.063
20	0.502	4	4	0.062	0.063
21	0.629	5	5	0.062	0.078
22	0.749	5	4	0.078	0.062
23	0.841	5	4	0.063	0.062
24	0.908	4	4	0.062	0.062
25	0.953	4	4	0.062	0.062
26	0.979	4	4	0.062	0.063
27	0.992	4	4	0.062	0.063
28	0.997	4	4	0.062	0.062
29	0.999	4	4	0.062	0.063
30	1.000	4	4	0.062	0.063
31	1.000	4	4	0.062	0.078
32	1.000	4	4	0.078	0.078
33	1.000	4	4	0.062	0.063
34	1.000	4	4	0.062	0.093
35	1.000	4	4	0.062	0.063
36	1.000	4	4	0.093	0.062
37	1.000	4	4	0.062	0.078
38	1.000	4	4	0.063	0.062
39	1.000	4	4	0.063	0.062
40	1.000	4	4	0.062	0.062
Average		4.306	4.306	0.064	0.067
Median		4	4	0.062	0.063

Table B-2.4 Network DSR and performance of EPANET-PDX and EPANET 2 simulators for Pipe Closure simulations for Network 2

Simulation no.	Pipes Closed	Network DSR	Average number of iterations		Average CPU time (s)	
			EPANET-PDX	EPANET 2	EPANET-PDX	EPANET 2
1	1	1.000	4	4	0.11	0.047
2	10	1.000	4	4	0.078	0.062
3	20	1.000	4	4	0.078	0.109
4	30	1.000	4	4	0.093	0.046
5	40	1.000	4	4	0.063	0.046
6	50	1.000	4	4	0.078	0.062
7	60	1.000	4	4	0.062	0.062
8	70	1.000	4	4	0.078	0.046
9	2 & 3	1.000	4	4	0.062	0.062
10	6 & 7	1.000	4	4	0.093	0.062
11	11 & 12	1.000	4	4	0.078	0.046
12	16 & 17	1.000	4	4	0.062	0.062
13	21 & 22	0.972	6	6	0.078	0.047
14	26 & 27	1.000	4	4	0.062	0.047
15	31 & 32	1.000	4	4	0.062	0.343
16	36 & 37	1.000	4	4	0.062	0.046
17	41 & 42	0.000	5	1	0.078	0.063
18	46 & 47	1.000	4	4	0.062	0.047
19	51 & 52	1.000	4	4	0.062	0.046
20	56 & 57	1.000	4	4	0.062	0.062

21	61 & 62	1.000	4	4	0.062	0.046
22	66 & 67	1.000	4	4	0.062	0.046
23	1, 2 & 3	1.000	4	4	0.062	0.062
24	5, 6 & 7	1.000	4	4	0.078	0.046
25	11, 12 & 13	1.000	4	4	0.062	0.046
26	15, 16 & 17	0.972	6	6	0.078	0.046
27	21, 22 & 23	0.972	6	6	0.078	0.047
28	25, 26 & 27	1.000	4	4	0.046	0.047
29	31, 32 & 33	1.000	4	4	0.078	0.047
30	35, 36 & 37	0.996	4	4	0.063	0.047
31	41, 42 & 43	0.000	4	4	0.078	0.062
32	45, 46 & 47	1.000	4	4	0.062	0.047
33	51, 52 & 53	1.000	4	4	0.062	0.047
34	55, 56 & 57	1.000	4	4	0.078	0.047
35	61, 62 & 63	0.999	4	4	0.063	0.046
36	65, 66 & 67	1.000	4	4	0.094	0.046
37	1, 2, 3, 4 & 5	1.000	4	4	0.062	0.046
38	5, 6, 7, 8 & 9	1.000	4	4	0.062	0.062
39	11, 12, 13, 14 & 15	1.000	4	4	0.078	0.046
40	15, 16, 17, 18 & 19	0.972	6	6	0.062	0.062
41	21, 22, 23, 24 & 25	0.972	6	6	0.063	0.062
42	25, 26, 27, 28 & 29	1.000	4	6	0.062	0.062
43	31, 32, 33, 34 & 35	0.950	5	5	0.062	0.062
44	35, 36, 37, 38 & 39	0.974	5	5	0.062	0.047

45	41, 42, 43, 44 & 45	0.000	10	3	0.062	0.062
46	45, 46, 47, 48 & 49	1.000	4	4	0.062	0.046
47	51, 52, 53, 54 & 55	1.000	4	4	0.062	0.047
48	55, 56, 57, 58 & 59	1.000	4	4	0.062	0.047
49	61, 62, 63, 64 & 65	0.999	4	4	0.062	0.046
50	65, 66, 67, 68 & 69	1.000	4	4	0.063	0.046
51	1, 2, 3, 4, 5, 6, 7 & 8	1.000	4	4	0.062	0.062
52	11, 12, 13, 14, 15, 16, 17 & 18	0.972	6	4	0.078	0.062
53	21, 22, 23, 24, 25, 26, 27 & 28	0.972	6	6	0.063	0.062
54	31, 32, 33, 34, 35, 36, 37 & 38	0.590	7	7	0.062	0.062
55	41, 42, 43, 44, 45, 46, 47 & 48	0.000	9	9	0.062	0.047
56	51, 52, 53, 54, 55, 56, 57 & 58	1.000	6	4	0.062	0.047
57	61, 62, 63, 64, 65, 66, 67 & 68	0.997	4	4	0.078	0.046
	Average		4.38	4.2	0.069	0.058
	Median		4	4	0.062	0.047

Table B-2.5 Performance of EPANET-PDX and EPANET 2 simulators for Source Head Variation simulations for Network 3

Reservoir no.		Network DSR	Average number of iterations		Average CPU time (s)	
10	11		EPANET-PDX	EPANET 2	EPANET-PDX	EPANET 2
Head (m)						
14	94	0.000	5	5	0.046	0.047
16	96	0.000	5	5	0.047	0.047
18	98	0.000	5	5	0.062	0.062
20	100	0.000	5	5	0.062	0.062
22	102	0.000	5	5	0.046	0.047
24	104	0.000	5	5	0.062	0.062
26	106	0.001	5	5	0.062	0.047
28	108	0.003	6	6	0.062	0.046
30	110	0.007	6	6	0.047	0.046
32	112	0.015	6	6	0.047	0.062
34	114	0.027	6	6	0.062	0.062
36	116	0.042	6	6	0.078	0.062
38	118	0.059	6	6	0.078	0.062
40	120	0.078	6	6	0.046	0.047
42	122	0.100	5	5	0.062	0.078
44	124	0.123	4	4	0.062	0.062
46	126	0.145	5	5	0.062	0.062
48	128	0.169	5	5	0.047	0.046
50	130	0.193	5	5	0.047	0.062
52	132	0.219	5	5	0.046	0.062
54	134	0.248	5	5	0.062	0.046
56	136	0.283	5	5	0.062	0.062
58	138	0.314	5	5	0.046	0.046
60	140	0.342	5	5	0.062	0.046
62	142	0.367	5	5	0.078	0.046
64	144	0.391	5	5	0.063	0.062

66	146	0.414	5	5	0.072	0.062
68	148	0.435	5	5	0.07	0.062
70	150	0.455	5	5	0.072	0.046
72	152	0.475	5	5	0.07	0.078
74	154	0.494	5	5	0.072	0.046
76	156	0.512	5	5	0.109	0.062
78	158	0.530	5	5	0.047	0.046
80	160	0.547	5	5	0.046	0.062
82	162	0.565	5	5	0.078	0.062
84	164	0.583	5	5	0.031	0.046
86	166	0.603	5	5	0.047	0.062
88	168	0.626	7	7	0.047	0.046
90	170	0.650	7	7	0.047	0.046
92	172	0.676	7	7	0.062	0.046
94	174	0.701	6	6	0.047	0.063
96	176	0.725	5	6	0.078	0.046
98	178	0.747	6	5	0.047	0.046
100	180	0.766	6	6	0.046	0.047
102	182	0.782	6	6	0.046	0.062
104	184	0.797	6	6	0.046	0.078
106	186	0.810	6	6	0.047	0.062
108	188	0.823	6	6	0.046	0.062
110	190	0.835	6	6	0.031	0.046
112	192	0.847	6	6	0.046	0.046
114	194	0.860	6	6	0.046	0.062
116	196	0.872	3	3	0.063	0.046
118	198	0.885	4	4	0.046	0.062
120	200	0.898	5	5	0.046	0.046
122	202	0.911	6	5	0.047	0.047
124	204	0.924	5	5	0.047	0.062

126	206	0.936	10	10	0.063	0.063
128	208	0.948	10	10	0.046	0.046
130	210	0.959	10	10	0.047	0.046
132	212	0.969	10	10	0.062	0.046
134	214	0.979	10	10	0.046	0.063
136	216	0.992	9	9	0.046	0.046
138	218	0.997	8	8	0.125	0.046
140	220	0.999	7	7	0.063	0.046
142	222	0.999	7	7	0.047	0.047
144	224	1.000	5	5	0.046	0.046
146	226	1.000	4	4	0.046	0.046
148	228	1.000	4	4	0.046	0.062
150	230	1.000	4	4	0.046	0.046
152	232	1.000	4	4	0.078	0.047
154	234	1.000	4	4	0.062	0.062
156	236	1.000	4	4	0.078	0.062
158	238	1.000	4	4	0.078	0.047
	Average		5.575	5.562	0.059	0.054
	Median		5	5	0.047	0.047

Table B-2.6 Network DSR and performance of EPANET-PDX and EPANET 2 simulators for Pipe Closure simulations for Network 3

Simulation no.	Pipes Closed	Network DSR	Average number of iterations		Average CPU time (s)	
			EPANET-PDX	EPANET 2	EPANET-PDX	EPANET 2
1	1	1.000	4	4	0.062	0.062
2	2	0.554	4	4	0.046	0.046
3	3	0.806	1	1	0.062	0.062
4	4	1.000	3	3	0.062	0.046
5	5	1.000	7	7	0.047	0.047
6	6	1.000	4	4	0.062	0.046
7	7	1.000	3	3	0.047	0.046
8	8	0.998	4	4	0.047	0.046
9	9	0.966	6	6	0.046	0.046
10	1 & 3	0.806	5	5	0.046	0.062
11	2 & 4	0.488	4	4	0.047	0.062
12	6 & 7	1.000	3	3	0.046	0.046
13	5 & 9	0.903	7	7	0.078	0.062
14	3 & 8	0.821	5	5	0.078	0.047
15	4 & 9	0.730	9	9	0.063	0.047
16	1, 3 & 6	0.808	4	4	0.046	0.062
17	4, 7 & 9	0.699	12	12	0.062	0.062
18	4, 5 & 8	0.585	6	6	0.047	0.047
	Average		5.056	5.056	0.055	0.052
	Median		4	4	0.047	0.047

Table B-2.7 Network DSR and performance of EPANET-PDX and EPANET 2 simulators for Source Head Variation simulations for Network 4

Reservoir no.			Network DSR	Average number of iterations		Average CPU time (s)	
160	161, 162	163, 164		EPANET-PDX	EPANET 2	EPANET-PDX	EPANET 2
Head (m)							
5	35	65	0.000	5	5	0.385	0.182
7	37	67	0.000	5	5	0.172	0.172
9	39	69	0.000	5	5	0.165	0.179
11	41	71	0.000	5	5	0.179	0.178
13	43	73	0.000	5	5	0.16	0.181
15	45	75	0.000	5	5	0.163	0.154
17	47	77	0.000	5	5	0.169	0.157
19	49	79	0.000	5	5	0.161	0.175
21	51	81	0.000	5	5	0.16	0.173
23	53	83	0.005	5	5	0.165	0.183
25	55	85	0.005	5	5	0.159	0.156
27	57	87	0.022	5	5	0.168	0.162
29	59	89	0.076	5	5	0.161	0.163
31	61	91	0.165	5	5	0.161	0.162
33	63	93	0.223	5	5	0.175	0.176
35	65	95	0.241	5	5	0.165	0.178
37	67	97	0.246	5	5	0.165	0.166
39	69	99	0.247	5	5	0.165	0.177
41	71	101	0.247	5	5	0.164	0.159
43	73	103	0.248	5	5	0.176	0.163
45	75	105	0.253	5	5	0.166	0.16
47	77	107	0.265	5	5	0.169	0.161
49	79	109	0.287	5	5	0.16	0.178
51	81	111	0.317	5	5	0.159	0.157
53	83	113	0.354	5	5	0.16	0.176

55	85	115	0.390	5	5	0.162	0.171
57	87	117	0.423	6	6	0.164	0.166
59	89	119	0.454	6	6	0.165	0.16
61	91	121	0.488	6	6	0.162	0.159
63	93	123	0.531	6	6	0.184	0.163
65	95	125	0.590	6	6	0.163	0.165
67	97	127	0.661	6	6	0.162	0.167
69	99	129	0.736	8	8	0.163	0.161
71	101	131	0.806	5	5	0.167	0.167
73	103	133	0.864	5	5	0.167	0.164
75	105	135	0.908	7	7	0.178	0.167
77	107	137	0.937	6	6	0.158	0.181
79	109	139	0.955	6	6	0.163	0.161
81	111	141	0.968	6	6	0.161	0.177
83	113	143	0.979	6	6	0.168	0.161
85	115	145	0.987	6	6	0.159	0.158
87	117	147	0.993	6	6	0.166	0.167
89	119	149	0.997	6	6	0.157	0.161
91	121	151	0.999	6	6	0.158	0.169
93	123	153	1.000	6	6	0.163	0.158
95	125	155	1.000	6	6	0.174	0.161
97	127	157	1.000	6	6	0.181	0.156
99	129	159	1.000	6	6	0.162	0.164
101	131	161	1.000	6	6	0.158	0.161
103	133	163	1.000	7	7	0.168	0.158
	Average			5.52	5.52	0.169	0.167
	Median			5	5	0.164	0.164

Table B-2.8 Network DSR and performance of EPANET-PDX and EPANET 2 simulators for Pipe Closure simulations for Network 4

Simulation no.	Pipes Closed	Network DSR	Average number of iterations		Average CPU time (s)	
			EPANET-PDX	EPANET 2	EPANET-PDX	EPANET 2
1	7 & 9	0.736	6	6	0.266	0.265
2	26 & 27	0.916	7	7	0.125	0.093
3	36 & 38	1.000	6	6	0.109	0.109
4	60 & 61	1.000	7	7	0.109	0.109
5	81 & 84	1.000	6	6	0.125	0.109
6	97 & 108	1.000	6	6	0.125	0.109
7	113 & 122	0.987	6	6	0.11	0.109
8	126 & 128	1.000	6	6	0.109	0.109
9	170 & 175	0.996	6	6	0.11	0.109
10	194 & 198	1.000	4	4	0.125	0.094
12	25 & 48	1.000	5	5	0.266	0.25
11	1, 20 & 202	1.000	6	6	0.109	0.109
27	66,67 & 118	1.000	5	5	0.25	0.218
28	17, 106 & 159	1.000	5	5	0.256	0.25
29	141, 157 & 159	1.000	5	5	0.19	0.204
13	4, 5 & 204	1.000	6	6	0.109	0.109
14	14, 15 & 200	1.000	6	6	0.109	0.094
15	16, 17 & 201	1.000	6	6	0.109	0.109
16	19, 22 & 25	0.997	6	5	0.109	0.093
17	41, 63 & 69	0.994	6	6	0.125	0.109

18	52, 54 & 55	0.991	6	6	0.125	0.093
19	58, 59 & 62	1.000	6	6	0.109	0.109
20	99, 101 & 102	0.993	6	6	0.109	0.109
21	144, 146 & 149	0.927	6	6	0.11	0.109
22	151, 156 & 157	1.000	5	5	0.109	0.109
23	171, 179 & 181	0.999	6	6	0.109	0.109
24	184, 187 & 188	1.000	6	6	0.14	0.14
25	192, 193 & 203	0.998	6	6	0.125	0.109
45	67, 118, 148 & 159	1.000	5	5	0.268	0.266
49	13, 54, 66, 67 & 148,	0.995	5	5	0.261	0.258
26	1, 20, 24, 25 & 202	1.000	7	7	0.156	0.109
30	43, 81, 84, 85 & 86	0.986	1	1	0.156	0.157
31	52, 53, 60, 64 & 67	1.000	5	5	0.161	0.148
32	59, 70, 72, 74 & 76	0.988	10	10	0.169	0.144
33	89, 132, 135, 137 & 147	0.961	6	6	0.152	0.148
34	90, 91, 92, 96 & 149	0.966	6	6	0.152	0.143
35	97, 108, 109, 115 & 163	0.977	7	7	0.172	0.149
36	110, 111, 112, 121 & 122	0.977	8	8	0.207	0.144
37	142, 143, 192, 193 & 203	0.971	6	6	0.109	0.109

38	142, 144, 143, 194 & 198	0.926	5	5	0.11	0.109
39	158, 166, 170, 174 & 175	0.753	6	6	0.109	0.093
40	177, 178, 184, 186 & 187	1.000	2	2	0.181	0.153
41	5, 6, 7, 9, 10, 12, 14 & 16	1.000	8	8	0.96	0.142
42	32, 33, 49, 50, 51, 62, 63 & 64	0.976	7	7	0.149	0.138
43	66, 67, 68, 69, 70, 71, 72 & 73	1.000	6	6	0.142	0.139
44	74, 75, 76, 121, 122, 123, 124 & 125	0.916	6	6	0.105	0.143
46	21, 22, 25, 27, 28, 29, 47, 52, 53 & 60	0.915	7	7	0.53	0.144
47	17, 18, 19, 22, 25, 26, 27, 28, 29 & 31	0.915	8	8	0.149	0.139
48	34, 35, 36, 37, 38, 39, 40, 41, 42 & 43	1.000	8	8	0.145	0.138
50	186, 187, 188, 189, 190, 191, 192, 193, 194 & 195	0.936	6	6	0.21	0.233
	Average		5.96	5.94	0.173	0.139
	Median		6	6	0.125	0.109

Table B-2.9 Network DSR and performance of EPANET-PDX and EPANET 2 simulators for Source Head Variation simulations for Network 5

Head of Reservoirs 205 & 206 (m)	Network DSR	Average number of iterations		Average CPU time (s)	
		EPANET-PDX	EPANET 2	EPANET-PDX	EPANET 2
66	0.000	1	1	0.171	0.156
67	0.000	1	1	0.171	0.171
68	0.000	7	7	0.156	0.156
69	0.000	8	8	0.156	0.156
70	0.000	8	8	0.171	0.156
71	0.000	1	1	0.156	0.156
72	0.001	7	7	0.156	0.156
73	0.002	7	7	0.171	0.156
74	0.005	7	7	0.156	0.156
75	0.010	7	7	0.156	0.156
76	0.021	6	6	0.156	0.156
77	0.044	6	6	0.156	0.156
78	0.087	6	6	0.171	0.156
79	0.154	6	6	0.171	0.171
80	0.240	6	6	0.171	0.156
81	0.331	6	6	0.203	0.156
82	0.419	6	6	0.156	0.156
83	0.501	6	6	0.156	0.156
84	0.577	6	6	0.156	0.156
85	0.647	5	5	0.156	0.156
86	0.711	5	5	0.156	0.156
87	0.770	5	5	0.156	0.171
88	0.822	5	5	0.156	0.156
89	0.869	5	5	0.156	0.156
90	0.908	5	5	0.156	0.156
91	0.940	5	5	0.171	0.156

92	0.964	5	5	0.156	0.156
93	0.980	5	5	0.156	0.156
94	0.990	5	5	0.156	0.171
95	0.995	5	5	0.156	0.156
96	0.998	5	5	0.156	0.156
97	0.999	5	5	0.156	0.156
98	0.999	5	5	0.171	0.171
99	1.000	5	5	0.156	0.156
100	1.000	5	5	0.156	0.141
101	1.000	5	5	0.156	0.156
102	1.000	5	5	0.156	0.156
103	1.000	5	5	0.156	0.156
104	1.000	5	5	0.156	0.171
105	1.000	5	5	0.156	0.156
106	1.000	5	5	0.156	0.156
107	1.000	5	5	0.156	0.156
108	1.000	5	5	0.156	0.156
109	1.000	5	5	0.156	0.171
110	1.000	5	5	0.156	0.156
Average		5.289	5.289	0.157	0.158
Median		5	5	0.156	0.156

Table B-2.10 Performance of EPANET-PDX and EPANET 2 simulators for Pipe Closure simulations for Network 5

Note: The network DSR for all Pipe Closure simulations for this network are 1.00.

Simulation no.	Pipes Closed	Average number of iterations		Average CPU time (s)	
		EPANET-PDX	EPANET 2	EPANET-PDX	EPANET 2
1	549, 550, 551, 552 & 553	5	6	0.016	0.031
2	289, 290, 291, 292 & 293	5	6	0.047	0.015
3	152, 195, 238, 281 & 324	5	6	0.031	0.016
4	549, 550, 551, 552 & 553	5	6	0.047	0.031
5	527, 529, 531, 533 & 535	5	6	0.031	0.016
6	545, 546, 547, 548, 549, 550, 551 & 552	5	6	0.031	0.031
7	133, 178, 223, 268, 313, 358, 403 & 448	5	6	0.031	0.016
8	72, 124, 205, 234, 330, 415, 510 & 528	5	6	0.047	0.031
9	501, 502, 503, 504, 505, 506, 507 & 508	4	6	0.032	0.016
10	523, 524, 525, 526, 527, 528, 529 & 530	4	6	0.031	0.015
11	402, 403, 404, 443, 445, 449, 453, 484, 485 & 527	4	6	0.031	0.031
12	544, 545, 546, 547, 548, 549, 550, 551, 552 & 553	4	5	0.031	0.016

13	248, 268, 270, 289, 290, 291, 292, 311, 313 & 333	4	5	0.047	0.016
14	97, 140, 183, 226, 269, 312, 355, 398, 441 & 484	4	6	0.031	0.031
15	64, 107, 150, 193, 236, 279, 322, 365, 408 & 451	5	5	0.032	0.016
16	329, 330, 331, 332, 333, 334, 335, 336, 337 & 338	5	6	0.047	0.031
17	41, 86, 131, 176, 221, 266, 311, 356, 401 & 446	5	6	0.031	0.015
18	135, 180, 225, 270, 315, 360, 405, 450, 495 & 540	5	5	0.031	0.032
19	88, 133, 178, 223, 268, 313, 358, 403, 448 & 493	5	6	0.031	0.015
20	41, 42, 43, 44, 45, 46, 47, 48, 49 & 50	5	6	0.047	0.016
21	158, 159, 175, 177, 179, 201, 202, 220, 222 & 245	5	6	0.031	0.031
22	52, 95, 116, 117, 118, 119, 120, 138, 181 & 224	5	6	0.032	0.016
23	347, 349, 350, 373, 374, 391, 392, 393, 394 & 417	5	6	0.031	0.015
24	248, 249, 270, 272, 274, 292, 293, 317, 319 & 337	5	6	0.047	0.032

25	381, 406, 409, 423, 447, 450, 453, 491, 494 & 510	5	6	0.031	0.015
26	398, 436, 441, 481, 484, 526, 527, 546, 547 & 548	5	6	0.047	0.032
27	441, 443, 482, 484, 486, 525, 527, 529, 548 & 549	5	6	0.031	0.015
28	477, 479, 481, 484, 485, 522, 524, 526, 528 & 530	5	6	0.031	0.031
29	398, 439, 441,443, 482, 484, 486, 505, 506 & 527	5	6	0.032	0.016
30	294, 295, 296, 318, 324, 362, 367, 407, 410 & 425	5	5	0.047	0.031
31	354, 376, 397, 419, 440, 462, 483, 505, 526 & 548	5	6	0.015	0.016
32	403, 421, 422, 444, 464, 463, 485, 505, 506 & 526	5	5	0.047	0.016
33	365, 381, 406, 423, 447, 465, 488, 501, 529 & 549	5	6	0.031	0.031
34	17, 54, 76, 99, 142, 163, 187, 230, 250 & 275	5	6	0.047	0.015
35	18, 33, 55, 76, 98, 119, 141, 162, 184 & 205	5	6	0.031	0.032
36	17, 32, 52, 74, 93, 116, 134, 158, 175 & 200	5	6	0.032	0.015

37	17, 55, 56, 57, 101, 145, 146, 147, 191 & 209	5	6	0.031	0.016
38	115, 116, 119, 121, 123, 134, 135, 136, 138 & 139	5	6	0.047	0.031
39	140, 142, 143, 144, 146, 147, 148, 150, 151 & 152	5	6	0.031	0.016
40	290, 291, 292, 293, 294, 295, 296, 324, 328 & 329	5	5	0.031	0.031
41	330, 331, 332, 333, 334, 335, 336, 337, 338 & 339	5	6	0.032	0.016
42	379, 400, 403, 405, 406, 407, 444, 445, 446 & 447	5	6	0.046	0.031
43	382, 409, 411, 451, 455, 468, 486, 498, 511 & 512	5	6	0.032	0.016
	Average	4. 860	5.837	0.035	0.022
	Median	5	6	0.031	0.016

Table B-2.11 Performance of EPANET-PDX and EPANET 2 simulators for Source Head Variation simulations for Network 6

Head of tanks 41 & 42 (m)	Average number of iterations		Average CPU time (s)	
	EPANET-PDX	EPANET 2	EPANET-PDX	EPANET 2
150	4.148	3.037	0.046	0.031
155	4.296	3.148	0.046	0.031
160	3.891	3.189	0.046	0.031
165	4.111	3.000	0.046	0.031
170	4.002	2.858	0.046	0.046
175	4.111	3.074	0.046	0.031
180	4.407	3.222	0.046	0.031
185	4.519	3.296	0.046	0.031
190	4.222	3.519	0.046	0.031
195	4.185	3.556	0.046	0.046
200	4.259	3.481	0.046	0.031
205	3.963	3.148	0.047	0.046
210	4.259	3.185	0.047	0.031
215	4.185	3.148	0.046	0.031
220	3.852	3.185	0.046	0.031
225	3.889	3.259	0.046	0.031
230	3.852	2.926	0.046	0.031
235	4.074	3.148	0.046	0.031
240	3.963	3.111	0.046	0.031
245	3.852	2.926	0.046	0.031
Average	4.102	3.171	0.046	0.033
Median	4.111	3.148	0.046	0.031

Table B-2.12 Performance of EPANET-PDX and EPANET 2 simulators for Pipe Closure simulations for Network 6

Simulation no.	Pipes Closed	Average number of iterations		Average CPU time (s)	
		EPANET-PDX	EPANET 2	EPANET-PDX	EPANET 2
1	11 & 19	4.111	3.074	0.046	0.031
2	35 & 17	4.333	3.074	0.063	0.031
3	24,34 & 6	4.704	2.519	0.047	0.031
4	17,28 & 35	4.222	3.148	0.047	0.031
5	15,41,36 & 24	4.231	2.500	0.046	0.032
6	12,27,23 & 30	4.259	2.519	0.047	0.047
7	32,15,22,38 & 20	3.963	2.963	0.047	0.015
8	11,15,32,23 & 20	4.481	2.852	0.047	0.047
9	15,25,41,29 & 34	4.154	2.462	0.047	0.031
10	11,34,15,25 & 38	4.077	2.538	0.047	0.032
Average		4.260	2.792	0.0484	0.0328
Median		4.226	2.695	0.047	0.031

APPENDIX C

INPUT DATA AND ADDITIONAL RESULTS FOR CASE STUDIES IN CHAPTER SIX

C-2 Input data and additional PFMOEA results for the Two-Loop network

Table C-2.1 Commercial pipe sizes and corresponding costs for the Two-Loop network

Diameter (in)	Cost ($/ m)
1	2
2	5
3	8
4	11
6	16
8	23
10	32
12	50
14	60
16	90
18	130
20	170
22	300
24	550

Table C-2.2 Node data for the Two-Loop network

Node	Demand (m^3/h)	Elevation (m)
2	100	150
3	100	160
4	120	155
5	270	150
6	330	165
7	200	160

Table C-2.3 Reservoir data for the Two-Loop network

Reservoir	Head (m)
1	210

Table C-2.4 Performance of the PFMOEA in optimizing the Two-Loop network (ω =10.5088)

PFMOEA Run	Cost ($)	CPU time (s)	Function evaluations
1	419000	19.21	2200
2	422000	71.81	7400
3	424000	66.23	7500
4	424000	72.60	8600
5	426000	87.49	10000
6	427000	54.03	5900
7	428000	31.69	3800
8	442000	13.59	1600
9	448000	38.74	4000
10	453000	22.82	1900
Average	431300	47.82	5290

Table C-2.5 Performance of the PFMOEA in optimizing the Two-Loop network (ω =10.9031)

PFMOEA Run	Cost ($)	CPU time (s)	Function evaluations
1	420000	52.49	4600
2	420000	55.18	4700
3	420000	22.80	2600
4	441000	54.80	5000
5	447000	33.80	3200
6	448000	36.46	3200
7	450000	51.16	5000
8	452000	22.10	2200
9	462000	33.09	3100
10	465000	32.09	3200
Average	442500	39.39	3680

C-3 Input data and additional PFMOEA results for the Hanoi network

Table C-3.1 Node data for the Hanoi network

Node	Demand (m^3/h)	Elevation (m)
2	890	0
3	850	0
4	130	0
5	725	0
6	1,005	0
7	1,350	0
8	550	0
9	525	0
10	525	0
11	500	0
12	560	0
13	940	0
14	615	0
15	280	0
16	310	0
17	865	0
18	1,345	0
19	60	0
20	1,275	0
21	930	0
22	485	0
23	1,045	0
24	820	0
25	170	0
26	900	0
27	370	0
28	290	0
29	36	0
30	360	0
31	105	0
32	805	0

Table C-3.2 Reservoir data for the Hanoi network

Reservoir	Total Head (m)
1	100.0

Table C-3.3 Pipe data for the Hanoi network

Pipe	Start Node	End Node	Length (m)	HW Friction Factor
1	1	2	100	
2	2	3	1,350	130
3	3	4	900	130
4	4	5	1,150	130
5	5	6	1,450	130
6	6	7	450	130
7	7	8	850	130
8	8	9	850	130
9	9	10	800	130
10	10	11	950	130
11	11	12	1,200	130
12	12	13	3,500	130
13	10	14	800	130
14	14	15	500	130
15	15	16	550	130
16	17	16	2,730	130
17	18	17	1,750	130
18	19	18	800	130
19	3	19	400	130
20	3	20	2,200	130
21	20	21	1,500	130
22	21	22	500	130
23	20	23	2,650	130
24	23	24	1,230	130
25	24	25	1,300	130
26	26	25	850	130
27	27	26	300	130
28	16	27	750	130
29	23	28	1,500	130
30	28	29	2,000	130
31	29	30	1,600	130
32	30	31	150	130
33	32	31	860	130
34	25	32	950	130

Table C-3.4 Performance of the PFMOEA in optimizing the Hanoi network (ω =10.5088)

PFMOEA Run	Cost ($ 10^6)	CPU time (s)	Function evaluations
1	6.056	714.97	105100
2	6.056	692.38	80700
3	6.056	529.69	75400
4	6.056	352.10	51000
5	6.056	708.17	106400
6	6.056	595.81	87000
7	6.056	1352.67	167400
8	6.065	1416.12	186800
9	6.065	478.59	59200
10	6.065	1375.55	168700
11	6.065	1269.08	164100
12	6.069	429.81	65900
13	6.069	1048.56	139400
14	6.073	390.55	46200
15	6.077	1116.07	155900
16	6.081	1147.91	172400
17	6.081	1428.74	187400
18	6.081	1325.42	188000
19	6.083	838.96	132900
20	6.095	476.23	62500
21	6.095	501.95	62500
22	6.099	606.77	76400
23	6.106	1557.74	192200
24	6.126	1488.40	188500
25	6.130	541.28	70100
26	6.135	488.31	73300
27	6.142	657.20	76700
28	6.142	968.53	131200
29	6.142	1056.13	131200
30	6.151	834.87	109800
31	6.151	564.55	87600

32	6.165	420.90	56700
33	6.174	1154.74	165500
34	6.180	586.32	71800
35	6.186	702.53	103800
36	6.186	851.04	137400
37	6.186	1287.69	188100
38	6.204	916.96	105100
39	6.204	763.09	113500
40	6.205	1490.10	198600
41	6.207	1361.13	191700
42	6.207	1549.83	191700
43	6.208	572.81	79000
44	6.209	631.22	81000
45	6.213	928.38	122400
46	6.213	961.75	131900
47	6.222	837.48	101800
48	6.224	1308.65	174000
49	6.227	1388.45	186100
50	6.232	574.08	71400
51	6.232	789.74	110700
52	6.232	1568.88	185300
53	6.236	1107.11	154400
54	6.272	539.90	73300
55	6.272	1576.30	179700
56	6.272	556.92	69700
57	6.279	1421.99	172300
58	6.303	1383.77	197100
59	6.314	1138.64	185300
60	6.314	627.41	90600
Average	6.156	916.16	122868.33

Table C-3.5 Performance of the PFMOEA in optimizing the Hanoi network (ω =10.9031)

PFMOEA Run	Cost ($ 10^6)	CPU time (s)	Function evaluations
1	6.182	841.35	111400
2	6.182	1103.35	136700
3	6.182	703.40	100000
4	6.182	693.20	100100
5	6.188	1206.17	164900
6	6.188	1298.61	193900
7	6.188	764.80	116700
8	6.188	595.86	78600
9	6.190	565.09	87100
10	6.190	737.17	106400
11	6.190	463.64	55200
12	6.190	1545.26	193300
13	6.190	400.07	49700
14	6.190	420.98	49800
15	6.191	1249.05	188700
16	6.191	1180.86	171700
17	6.191	604.48	82000
18	6.193	1414.77	199200
19	6.196	1217.68	144100
20	6.196	774.09	105000
21	6.196	1386.52	166800
22	6.196	1173.81	128300
23	6.196	775.20	114300
24	6.197	397.89	53600
25	6.204	1056.66	130700
26	6.204	293.82	36500
27	6.206	1029.60	134300
28	6.206	1172.66	154600
29	6.210	939.69	129600
30	6.223	1475.13	174500
31	6.249	679.77	76700

32	6.249	616.00	76700
33	6.257	1285.73	173200
34	6.264	1493.23	181400
35	6.264	1374.94	187800
36	6.264	706.79	90100
37	6.278	1252.95	155000
38	6.294	685.85	90300
39	6.294	7.18	930
40	6.314	731.38	90600
41	6.331	532.08	67900
42	6.338	980.56	137100
43	6.338	740.35	92800
44	6.343	950.19	130400
45	6.343	355.28	46600
46	6.343	1284.69	178100
47	6.351	734.75	106100
48	6.351	1201.57	175800
49	6.358	1567.36	197400
50	6.372	1503.89	198600
51	6.393	548.86	72400
52	6.406	1619.86	173000
53	6.433	939.20	125400
54	6.440	568.01	76000
55	6.457	741.36	91700
56	6.465	898.71	104000
57	6.482	868.31	114500
58	6.482	1056.63	141400
59	6.526	1136.93	160500
60	6.548	1427.67	196900
Average	6.277	932.85	122783.33

Table C-3.6 The cheapest feasible solutions generated from the five best PFMOEA runs for the Hanoi network

Pipe	Diameter (in)									
	ω = 10.5088					ω = 10.9031				
1	40	40	40	40	40	40	40	40	40	40
2	40	40	40	40	40	40	40	40	40	40
3	40	40	40	40	40	40	40	40	40	40
4	40	40	40	40	40	40	40	40	40	40
5	40	40	40	40	40	40	40	40	40	40
6	40	40	40	40	40	40	40	40	40	40
7	40	40	40	40	40	40	40	40	40	40
8	40	40	40	40	40	40	40	40	40	40
9	40	30	30	30	30	40	40	30	40	40
10	30	30	30	30	30	30	30	30	30	30
11	24	30	30	30	30	24	30	30	30	30
12	24	24	24	24	24	24	24	24	24	24
13	20	20	20	20	20	16	20	16	20	20
14	16	16	16	16	12	12	16	12	16	20
15	12	12	12	12	12	12	16	12	12	12
16	12	12	12	12	12	12	12	16	12	12
17	16	16	16	16	16	20	16	20	16	16
18	20	24	20	24	24	24	24	24	24	24
19	20	20	24	20	24	24	20	24	24	24
20	40	40	40	40	40	40	40	40	40	40
21	20	20	20	20	20	20	20	20	20	20
22	12	12	12	16	12	12	12	12	12	12
23	40	23	40	40	40	40	40	40	40	40
24	30	30	30	30	30	30	30	30	30	30
25	30	30	30	30	30	30	30	30	30	30
26	20	20	20	20	20	24	20	20	20	20
27	12	12	12	12	12	12	16	16	16	12
28	12	12	12	12	12	12	12	12	12	12
29	16	16	16	16	16	16	16	16	16	16
30	12	12	16	12	16	16	12	12	12	12
31	12	12	12	12	12	12	12	12	12	12
32	16	16	12	16	12	16	16	16	20	16
33	16	16	16	16	16	16	20	20	20	20
34	24	24	20	24	20	24	24	24	24	24
Cost ($M)	6.056	6.065	6.068	6.077	6.081	6.182	6.188	6.190	6.191	6.193

C-4 Input data and additional PFMOEA results for the New York Tunnels

Table C-4.1 Node data for the New York Tunnels

Node	Demand (ft^3/s)	Elevation (ft)
2	92.4	0
3	92.4	0
4	88.2	0
5	88.2	0
6	88.2	0
7	88.2	0
8	88.2	0
9	170.0	0
10	1.0	0
11	170.0	0
12	117.1	0
13	117.1	0
14	92.4	0
15	92.4	0
16	170.0	0
17	57.5	0
18	117.1	0
19	117.1	0
20	170.0	0

Table C-4.2 Reservoir data for the New York Tunnels

Reservoir	Total Head (ft)
1	300.0

Table C-4.3 Pipe data for the New York Tunnels

Pipe	Start Node	End Node	Diameter (in)	Length (ft)	HW Friction Factor
1	1	2	180	11,600	100
2	2	3	180	19,800	100
3	3	4	180	7,300	100
4	4	5	180	8,300	100
5	5	6	180	8,600	100
6	6	7	180	19,100	100
7	7	8	132	9,600	100
8	8	9	132	12,500	100
9	9	10	180	9,600	100
10	11	9	204	11,200	100
11	12	11	204	14,500	100
12	13	12	204	12,200	100
13	14	13	204	24,100	100
14	15	14	204	21,100	100
15	1	15	204	15,500	100
16	10	17	72	26,400	100
17	12	18	72	31,200	100
18	18	19	60	24,000	100
19	11	20	60	14,400	100
20	20	16	60	38,400	100
21	9	16	72	26,400	100

Table C-4.4 Performance of the PFMOEA in optimizing the New York Tunnels (ω =10.5088)

PFMOEA Run	Cost ($ 10^6)	CPU time (s)	Function evaluations
1	37.139	59.20	7200
2	37.139	202.31	23800
3	37.139	311.98	36000
4	37.139	188.45	21600
5	37.139	67.42	8200
6	37.139	172.92	19000
7	37.139	125.40	13600
8	37.572	142.72	17400
9	37.572	186.96	21800
10	37.572	106.88	12400
11	37.572	471.04	53600
12	37.572	247.83	27400
13	37.572	72.93	8000
14	37.572	201.88	22000
15	37.725	522.76	58400
16	37.779	166.18	20400
17	37.779	655.73	78400
18	37.779	230.60	26800
19	37.871	367.85	43600
20	37.871	64.26	7200
21	37.871	242.55	26600
22	38.024	933.04	98800
23	38.211	541.97	59800
24	38.303	171.50	19400
25	38.451	204.21	24200
26	38.456	74.25	8200
27	38.922	546.02	60000
28	39.263	541.43	61200
29	39.440	845.56	98400
30	39.940	582.56	66400
Average	37.889	308.27	34993.33

Table C-4.5 Performance of the PFMOEA in optimizing the New York Tunnels (ω =10.9031)

PFMOEA Run	Cost ($ 10^6)	CPU time (s)	Function evaluations
1	40.42	143.70	17800
2	40.42	383.40	47200
3	40.42	281.05	33400
4	40.884	563.25	68600
5	40.884	71.95	8800
6	40.884	689.27	81400
7	40.896	329.69	40400
8	40.896	575.00	67600
9	40.896	462.93	53200
10	41.296	506.36	63800
11	41.328	540.99	62400
12	41.469	384.92	46000
13	41.481	143.79	17800
14	41.728	506.86	64400
15	41.728	659.37	84000
16	41.728	565.21	68000
17	41.802	422.28	52600
18	41.826	214.41	27200
19	41.826	558.76	64800
20	42.156	638.52	81600
21	42.234	325.12	41200
22	42.234	771.91	98200
23	42.691	513.47	65400
24	42.691	185.57	23400
25	42.806	758.01	93400
26	42.819	559.99	69200
27	43.377	75.98	9000
28	43.379	482.56	58000
29	43.790	628.13	74200
30	44.016	137.27	16400
Average	41.834	435.99	53313.33

Table C-4.6 Five best feasible solutions generated from the best PFMOEA run for the New York Tunnels

Pipe	Diameter (in)									
	ω = 10.5088					ω =10.9031				
3	-	-	-	-	-	-	-	36	-	-
7	108	120	132	132	120	-	-	-	-	-
15	-	-	-	-	-	144	144	144	156	156
16	96	96	96	96	108	84	84	84	84	84
17	96	96	96	96	96	96	96	96	96	96
18	84	84	84	84	84	84	84	84	84	84
19	72	72	72	84	72	72	84	72	72	84
21	72	72	72	72	72	72	72	72	72	72
Cost ($M)	37.13	37.62	38.13	38.80	38.94	40.42	41.12	41.13	41.29	41.96

The dash (-) represents the do-nothing option. Pipe sizes not shown were unchanged, corresponding to the do-nothing option.

Table C-4.7 The cheapest feasible solutions generated from the five best PFMOEA runs for the New York Tunnels

Pipe	Diameter (in)									
	ω = 10.5088					ω =10.9031				
1	-		-	-	108	-	-	-	-	-
3	-		-	-	-	-	-	-	-	-
7	108	108	108	-	-	-	-	-	-	-
15	-		-	84	-	144	144	132	156	132
16	96	96	96	96	96	84	84	96	84	96
17	96	108	96	96	96	96	108	96	96	108
18	84	72	84	84	84	84	72	84	84	72
19	72	72	60	72	72	72	72	72	72	72
21	72	72	84	72	72	72	72	72	72	72
Cost ($M)	37.13	37.57	37.72	37.78	37.87	40.42	40.88	40.89	41.29	41.33

The dash (-) represents the do-nothing option. Pipe sizes not shown were unchanged, corresponding to the do-nothing option.

APPENDIX D

INPUT DATA AND ADDITONAL RESULTS FOR THE WOBULENZI WATER DISTRIBUTION SYSTEM CASE STUDY IN CHAPTER SEVEN

Table D-1 Node data for the Wobulenzi network

Node No.	Elevation (m)	Demand (l/s)
2	1042.2	0
3	1020	1.59
4	1032	5.07
5	1002	8.09
6	1003.4	1.59
7	1000	4.15
8	1000	4.47
9	998	1.92
10	997	0
11	998	1.6
12	990	1.69
13	997	2.18
14	997	1.57
15	995	2.69
16	993	1.8
17	990	2.5

Table D-2 Reservoir data for the Wobulenzi network

Reservoir No.	Elevation (m)
1	1064.5

Table D-3 Pipe data for the Wobulenzi network

Pipe No.	Node1	Node2	Length (m)	Roughness
1	1	2	117	130
2	2	3	235.5	130
3	2	4	435	130
4	3	5	190.2	130
5	3	6	486.5	130
6	4	6	613	130
7	5	7	460.1	130
8	6	8	241	130
9	7	8	30	130
10	7	9	252.9	130

11	8	10	250	130
12	9	10	216	130
13	9	11	20	130
14	10	12	484	130
15	10	13	20	130
16	11	13	216	130
17	11	14	106	130
18	13	15	173.5	130
19	14	15	273	130
20	14	16	136.8	130
21	15	17	337	130

Table D-4 Cost data for pipes for the Wobulenzi network

Diameter (mm)	Pipe cost ($/m)
80	42
100	48
150	56
200	70
250	80
300	100
350	115
400	140

Table D-5 CPU time required by PFMOEA to solve the Wobulenzi network problem

PFMOEA runs	CPU time (hour)
1	2.39
2	2.50
3	2.53
4	2.49
5	2.45
6	2.52
7	2.43
8	2.91
9	3.07
10	2.47
Average	2.58

Table D-6 Optimal diameters for PFMOEA solutions 2 and 3

	Phase I		Phase II			
	Diameter (mm)		Solution 2		Solution 3	
Link	Solution 2	Solution 3	Upgrade option	Diameter (mm)	Upgrade option	Diameter (mm)
1-2	250	250	Paralleling	250	Paralleling	300
2-3	200	250	Paralleling	300	-	-
2-4	150	150	-	-	-	-
3-5	150	100	-	-	Paralleling	300
3-6	200	200	-	-	-	-
4-6	80	80	-	-	-	-
5-7	100	80	-	-	Paralleling	250
6-8	150	200	Replacement	300	-	-
7-8	80	80	-	-	Replacement	200
7-9	100	100	-	-	-	-
8-10	150	200	Replacement	250	-	-
9-10	80	80	-	-	-	-
9-11	80	80	-	-	-	-
10-12	80	80	-	-	-	-
10-13	150	150	-	-	Replacement	250
11-13	80	80	-	-	-	-
11-14	100	150	-	-	-	-
13-15	100	80	Paralleling	150	Replacement	200
14-15	80	80	-	-	-	-
14-16	80	80	-	-	-	-
15-17	100	80	-	-	-	-

APPENDIX E

INPUT DATA AND ADDITIONAL RESULTS FOR THE "ANYTOWN" NETWORK CASE STUDY IN CHAPTER EIGHT

Table E-1 Node data and loading conditions for the "Anytown" network

Node	Elevation (ft)	Average day demand (gpm)	Instantaneous peak (gpm)	Fire 1 (gpm)	Fire 2 (gpm)	Fire 3 (gpm)
1	20	500	900	650	650	650
2	50	200	360	260	260	260
3	50	200	360	260	260	260
4	50	600	1080	780	780	780
5	80	600	1080	780	*1500*	780
6	80	600	1080	780	*1500*	780
7	80	600	1080	780	*1500*	780
8	80	400	720	520	520	520
9	120	400	720	520	520	520
10	120	400	720	520	520	520
11	120	400	720	520	520	*1000*
12	50	500	900	650	650	650
13	50	500	900	650	650	650
14	50	500	900	650	650	650
15	50	500	900	650	650	650
16	120	400	720	520	520	520
17	120	1000	1800	1300	1300	*1000*
18	50	500	900	650	650	650
19	50	1000	1800	*2500*	1300	1300

Table E-2 Pipe data for the "Anytown" network

Pipe no.	Start node	End node	Length (m)	Diameter (m)	Roughness	Location
1	1	2	12000	12	120	Residential
2	1	12	12000	12	70	City
3	1	13	12000	16	70	City
4	1	20	100	30	130	City
5	2	3	6000	10	120	Residential
6	2	4	9000	10	120	Residential
7	2	13	9000	12	70	Residential
8	2	14	6000	10	120	Residential
9	3	4	6000	10	120	Residential

11	4	8	12000	8	120	Residential
12	4	15	6000	10	120	Residential
17	8	9	12000	8	120	Residential
18	8	15	6000	10	120	Residential
19	8	16	6000	8	120	Residential
20	8	17	6000	8	120	Residential
21	9	10	6000	8	120	Residential
22	10	11	6000	8	120	Residential
23	10	17	6000	10	120	Residential
24	11	12	6000	8	120	Residential
26	12	17	6000	10	120	Residential
27	12	18	6000	8	70	City
28	13	14	6000	12	70	City
29	13	18	6000	12	70	City
30	13	19	6000	10	70	City
31	14	15	6000	12	70	City
32	14	19	6000	10	70	City
33	14	21	100	12	120	City
34	15	16	6000	10	70	City
35	15	19	6000	10	70	City
36	16	17	6000	8	120	Residential
37	16	18	6000	12	70	City
38	16	19	6000	10	70	City
39	17	18	6000	8	120	Residential
40	17	22	100	12	120	Residential
41	18	19	6000	10	70	City
142	21	41	1	12	120	City
143	22	42	1	12	120	Residential
110	4	5	6000	-	130	New
113	5	6	6000	-	130	New
114	6	7	6000	-	130	New
115	6	8	6000	-	130	New
116	7	8	6000	-	130	New
125	11	17	9000	-	130	New

Table E-3 Pipe rehabilitation alternative costs for the "Anytown" network

Pipe diameter (in)	New pipes ($/ft)	Duplicating existing pipes ($/ft)		Clean and line existing pipes ($/ft)	
		City	Residential	City	Residential
6	12.8	26.2	14.2	17.0	12.0
8	17.8	27.8	19.8	17.0	12.0
10	22.5	34.1	25.1	17.0	12.0
12	29.2	41.4	32.4	17.0	13.0
14	36.2	50.2	40.2	18.2	14.2
16	43.6	58.5	48.5	19.8	15.5
18	51.5	66.2	57.2	21.6	17.1
20	60.1	76.8	66.8	23.5	20.2
24	77.0	109.2	85.5	30.1	-
30	105.5	142.5	116.1	41.3	-

Table E-4 Pump characteristic for the "Anytown" network

Discharge (gpm)	Pump head (ft)	Efficiency (%) (wire to water)
0	300	0
2000	292	50
4000	270	65
6000	230	55
8000	181	40

Table E-5 New tank costs for the "Anytown" network

Tank volume (gal)	Cost ($)
50000	115000
100000	145000
250000	325000
500000	425000
1000000	600000

OTHER PFMOEA SOLUTIONS FOR THE "ANYTOWN" NETWORK PROBLEM

Table E-6 Pipe Upgrade and Rehabilitation for Solutions 3 and 4

	Solution 3		Solution 4	
	Pipe ID	Diameter (m)	Pipe ID	Diameter (m)
PP	2	0.762	2	0.6096
	4	0.1524	17	0.2032
	20	0.6096	20	0.2032
	26	0.696	26	0.6096
				0.6096
CL	18		3	
NP	10	0.1524	10	0.254
	13	0.2540	13	0.254
	14	0.2032	14	0.2032
	15	0.3556	15	0.3048
	16	0.2032	16	0.254
	25	0.1524	25	0.1524
	Riser 10[a]	0.3556	Riser 6[a]	0.3048
	Riser 6[a]	0.4572		

1 in = 0.0254 m
PP = Pipe paralleling
CL = Pipe cleaning and lining
NP = New pipes
Risers 6[a] and 10[a] are risers for new tanks located at nodes 6 and 7 respectively.

Table E-7 Pipe Upgrade and Rehabilitation for Solutions 2[b] and 2[c]

	Solution 2[b]		Solution 2[c]	
	Pipe ID	Diameter (m)	Pipe ID	Diameter (m)
PP	2	0.6096	2	0.6096
	4	0.254	4	0.254
	17	0.254	17	0.254
	20	0.6096	20	0.6096
	26	0.6096	26	0.6096
CL	3		3	
NP	10	0.1524	10	0.1524
	13	0.254	13	0.254
	14	0.2032	14	0.2032
	15	0.4572	15	0.4572
	16	0.2032	16	0.254
	25	0.1524	25	0.1524
	Riser 6[a]	0.254	Riser 6[a]	0.254

1 in = 0.0254 m
PP = Pipe paralleling
CL = Pipe cleaning and lining
NP = New pipes
Riser 6[a] is the riser for the new tank located at node 6.

Table E-8 Pipe Upgrade and Rehabilitation Solutions 2^d and 2^e

	Solution 2^d		Solution 2^e	
	Pipe ID	Diameter (m)	Pipe ID	Diameter (m)
PP	2	0.6096	2	0.6096
	4	0.254	4	0.254
	17	0.254	17	0.254
	20	0.6096	20	0.6096
	26	0.6096	26	0.6096
CL	3		3	
	143			
NP	10	0.1524	10	0.1524
	13	0.254	13	0.254
	14	0.2032	14	0.2032
	15	0.4572	15	0.4572
	16	0.2032	16	0.2032
	25	0.1524	25	0.1524
	Riser 6[a]	0.254	Riser 6[a]	0.254

1 in = 0.0254 m
PP = Pipe paralleling
CL = Pipe cleaning and lining
NP = New pipes
Riser 6[a] is the riser for the new tank located at node 6.

Table E-9 Daily Pumping Operation for Solutions 3, 4, 2^b, 2^c, 2^d and 2^e

Solution	Number of pumps operating							
	6-9h	9-12h	12-15h	15-18h	18-21h	21-24h	24-3h	3-6h
3	3	3	3	3	2	2	2	2
4[a]	3	3	3	3	2	2	2	2
2^b	3	3	3	2	2	2	2	2
2^c	3	3	3	2	2	2	2	2
2^d	3	3	3	2	2	2	2	2
2^e	3	3	3	2	2	2	2	2

[a] Represents solution with tank draining strategy

Table E-10 Details and dimensions of new tanks for Solutions 3, 4, 2^b, 2^c, 2^d and 2^e

Properties	PFMOEA solutions						
	3		4	2^b	2^c	2^d	2^e
	Tank 1	Tank 2					
Maximum operating water level (m)	81.30	75.856	71.48	72.98	72.98	72.98	74.19
Minimum operating water level (m)	79.11	66.91	65.64	66.56	66.56	66.56	67.13
Top level (m)	81.49	76.28	71.97	73.41	73.41	73.41	74.66
Bottom level (m)	76.20	64.0	57.91	60.96	60.96	60.96	60.96
Diameter (m)	7.4	15.35	17.57	18.67	18.67	18.67	20.55
Tank Location (Node ID)	10	6	6	6	6	6	6

1 ft = 0.3048 m

LIST OF PUBLICATIONS

CONFERENCE PAPERS

Siew, C., and Tanyimboh T. T. (2009). "Augmented gradient method for head dependent modelling of water distribution networks." In *Proceeding of the 11th Annual Water Distribution Systems Analysis Symposium, S. Starrett* (ed.), May 17-21, Kansas City.

Siew, C., and Tanyimboh T. T. (2009). "Assessment of the head dependent gradient method with reference to PRAAWDS." In *Integrating Water Systems: Proceedings of the 10th International Conference on Computing and Control for the Water Industry, J. Boxall and C. Maksimovic* (eds.), September 1-3, Sheffield, UK.

Siew, C., and Tanyimboh, T.T. (2010). "Practical application of the head dependent gradient method." *Proceedings of the International Water Association World Water Congres,* 19-24 September, Montreal, Canada.

Siew, C., and Tanyimboh, T.T. (2010). "Pressure-dependent EPANET extension: pressure-dependent demands." *Proceedings of the 12th Annual Water Distribution Systems Analysis Conference, WDSA 2010*, September 12-15, Tucson, Arizona.

Siew, C., and Tanyimboh, T.T. (2010). "Pressure-dependent EPANET extension: extended period simulation." *Proceedings of the 12th Annual Water Distribution Systems Analysis Conference, WDSA 2010*, September 12-15, Tucson, Arizona.

Siew, C., and Tanyimboh, T.T. (2010). "Penalty-Free Multi-Objective Evolutionary Optimization of Water Distribution Systems." *Proceedings of the 12th Annual Water Distribution Systems Analysis Conference, WDSA 2010*, September 12-15, Tucson, Arizona.

Siew, C., and Tanyimboh, T.T. (2011). "The computational efficiency of EPANET-PDX." *Proceedings of the 13th Annual Water Distribution Systems Analysis Conference, WDSA 2011*, May 22-26, Palm Springs, California.

Siew, C., and Tanyimboh, T.T. (2011). "Penalty-free evolutionary algorithm optimization for the long term rehabilitation and upgrading of water distribution systems." *Proceedings of the 13th Annual Water Distribution Systems Analysis Conference, WDSA 2011*, May 22-26, Palm Springs, California.

Siew, C., and Tanyimboh, T.T. (2011). "Design of the "Anytown" network using the penalty-free multi-objective evolutionary optimization approach." *Proceedings of the 13th Annual Water Distribution Systems Analysis Conference, WDSA 2011*, May 22-26, Palm Springs, California.

Seyoum, A. G., Tanyimboh, T. T., and **Siew, C.** (2011). "Comparison of demand driven and pressure dependent hydraulic approaches for modelling water quality in distribution networks." *Computing and Control for the Water Industry 2011: Urban Water Management* - Challenges and Opportunities, 5-7 September 2011, Exeter, UK.

Phan, D. T., Lim, J. B. P., **Siew, C.**, Tanyimboh, T. T., Issa, H., and Sha, W. (2011). "Optimization of cold-formed steel portal frame topography using real coded genetic algorithm." The 12th East Asia-Pacific Conference on Structural Engineering and Construction, EASEC-12, January 26-28, Hong Kong SAR, China.

JOURNALS PUBLISHED

Siew, C., and Tanyimboh, T. T. (2011). "Practical application of the head dependent gradient method for water distribution networks." *Water Science and Technology- Water Supply*, 11(4), 444-450.

JOURNALS ACCEPTED FOR PUBLICATION

Siew, C., and Tanyimboh, T.T. (2011). "Pressure-dependent EPANET extension." *Water Resources Management.*

Phan, D. T., Lim, J. B. P., Sha, W., **Siew, C.**, Tanyimboh, T. T., Issa, H., and Mohammad, F. A. (2011) "Design optimization of cold-formed steel portal frames taking into account the effect of topography." *Engineering Optimization.*

JOURNALS SUBMITTED

Siew, C., and Tanyimboh, T.T. (2011). "Penalty-free feasibility boundary convergent multi-objective evolutionary algorithm for the optimization of water distribution systems." *Water Resources Management (submitted).*

Siew, C., and Tanyimboh, T.T. (2011). "Efficient evolutionary algorithm optimization for the long term rehabilitation and upgrading of water distribution systems." *Reliability Engineering & System Safety (submitted).*

Siew, C., and Tanyimboh, T.T. (2011). "New improved multiobjective genetic algorithm design optimization of the "Anytown" water distribution network." *Water Resources Research (submitted).*